Black holes and bubbled solutions in string theory

Giulio Pasini

NNT : 2016SACLS218

Thèse de doctorat de l'Université Paris-Saclay préparée à l'Université Paris-Sud

Institut de Physique Théorique - CEA/Saclay

Ecole doctorale n°564
Physique en Île-de-France
Spécialité de doctorat : Physique

par

M. Giulio Pasini

Black holes and bubbled solutions in String Theory

Thèse présentée et soutenue à l'Institut de Physique Théorique - CEA/Saclay, le 13 septembre 2016 :

Après avis des rapporteurs :

M.	Tomás Ortín	Professeur, IFT, Universidad Autónoma de Madrid
M.	Kostas Skenderis	Professeur, University of Southampton

Composition du Jury :

M.	Emilian Dudas	Professeur Ecole Polytechnique	(Président du jury)
M.	Tomás Ortín	Professeur IFT, Universidad Autónoma de Madrid	(Rapporteur)
M.	Iosif Bena	Professeur IPhT - CEA/Saclay	(Directeur de thèse)
M.	Nikolay Bobev	Maître assistant Katholieke Universiteit Leuven	(Examinateur)
Mme	Mariana Graña	Professeur IPhT - CEA/Saclay	(Examinatrice)

Black Holes and Bubbled Solutions in String Theory

Keywords: black holes, String Theory, smooth solutions, supergravity, microstates

Abstract

There exist many smooth solutions in String Theory characterized by a nontrivial topology threaded by fluxes and no localized sources. In this thesis we analyze some of the most important bubbled solutions along with the different purposes they are studied for.

Some smooth, eleven-dimensional solutions can be interpreted as BPS black hole microstates in the context of the Fuzzball proposal. One can promote these to be microstates for near-BPS black holes by placing probe supertubes at a metastable minimum inside these solutions. We show that these minima can lower their energy when the bubbles move in certain directions in the moduli space, which implies that these near-BPS microstates are in fact unstable. The decay of these solutions corresponds to Hawking radiation and we compare the emission rate and frequency to those of the corresponding black hole.

By modifying the asymptotic behavior of these microstates one could be able to construct microstates for five-dimensional BPS black rings with no electric charge. To do so one needs to find a new supergravity solution in five-dimensions whose Killing vector switches from timelike to null in some open regions. We construct explicit examples where the norm of the supersymmetric Killing vector is a real not-everywhere analytic function such that all its derivatives vanish at a point where the Killing vector becomes null.

In the Lin-Lunin-Maldacena solution we find a supersymmetry-breaking mechanism similar to that used for near-BPS microstates. We analyze the potential energy of M2 probes polarized into M5 brane shells. When the charges of the probe are parallel to those of the solution we find stable configurations, while when the charges are opposite we find metastable states that break supersymmetry and analyze the decay process to supersymmetric configurations.

We analyze also the Klebanov-Strassler solution and construct its T-dual in Type IIA. This is done by just reconstructing the solution expanded on a small region of the deformed conifold, after a thorough analysis to choose the most suitable isometry. Our construction is the first step in a program to test the stability of antibranes in Type IIA backgrounds.

Trous Noirs et Solutions Régulières en Théorie des Cordes

Mots clés: trous noirs, Théorie des Cordes, solutions régulières, supergravité, microétats

Résumé

Il existe des nombreuses solutions lisses dans le domaine de la thèorie des cordes, caractérisées par une topologie non triviale (bulles) et sans sources localisées. Dans cette thèse nous analysons quelques-unes parmi les solutions les plus importantes avec les différents objectifs pour lesquels ils sont étudiées.

Des solutions lisses en onze dimensions peuvent être interprétées comme microétats BPS de trou noir dans le cadre de la *Fuzzball proposal*. On peut promouvoir ces microétats à être quasi-BPS en plaçant de supertubes dans un minimum métastable à l'intérieur de ces solutions. Nous montrons que ces minima peuvent abaisser leur énergie lorsque les bulles se déplacent dans certaines directions dans l'espace des modules, ce qui implique que ces microétats quasi-BPS sont en fait instables. L'énergie dissipée par ces solutions correspond au rayonnement Hawking et on compare le taux d'émission et la fréquence à celles du trou noir correspondant.

En modifiant la géométrie asymptotique de ces microétats on pourrait construire des microétats pour des trous noirs BPS sans charge électrique en cinq dimensions. Il faut donc trouver une nouvelle solution de supergravité en cinq dimensions dont la norme du vecteur de Killing passe de positive à nulle dans certaines régions. Nous construisons des exemples explicites où la norme du vecteur de Killing supersymétrique est une fonction réelle non-analytique telle que tous ses dérivés sont nulles à un point où le vecteur de Killing devient nul.

Dans la solution de Lin-Lunin-Maldacena on trouve un mécanisme pour briser la supersymétrie similaire à celui utilisé pour les microétats quasi-BPS. Nous analysons l'énergie potentielle des branes M2 polarisées en branes M5. Lorsque les charges des M2 sont parallèles à ceux de la solution, nous trouvons des configurations stables. Lorsque les charges des M2 ne sont pas parallèles, nous trouvons des états métastables qui brisent la supersymétrie et nous analysons le processus de rayonnement d'énergie.

Nous analysons aussi la solution de Klebanov-Strassler et construisons sa version T-duale dans la supergravité de type IIA. Pour cela une analyse approfondie est nécessaire pour choisir l'isométrie la plus appropriée. Notre construction est la première étape d'un programme pour tester la stabilité des antibranes dans la supergravité de type IIA.

Publications

The original results presented in this thesis have been published in the following papers:

Les résultats originaux présentés dans cette thèse ont été publiés dans les articles suivants:

G. Pasini and C. S. Shahbazi, "Five-dimensional null and time-like supersymmetric geometries," Class. Quant. Grav. **33** (2016) no.17, 175003 doi:10.1088/0264-9381/33/17/175003 [arXiv:1512.02211 [hep-th]].

G. Pasini, "Type IIA Klebanov-Strassler: the hard way," JHEP **1603** (2016) 178 doi:10.1007/JHEP03(2016)178 [arXiv:1511.06686 [hep-th]].

I. Bena and G. Pasini, "Instabilities of microstate geometries with antibranes," JHEP **1604** (2016) 181 doi:10.1007/JHEP04(2016)181 [arXiv:1511.01895 [hep-th]].

S. Massai, G. Pasini and A. Puhm, "Metastability in Bubbling AdS Space," JHEP **1502** (2015) 138 doi:10.1007/JHEP02(2015)138 [arXiv:1407.6007 [hep-th]].

Non fronda verde, ma di color fosco;
non rami schietti, ma nodosi e 'nvolti;
non pomi v'eran, ma stecchi con tòsco:

non han sì aspri sterpi né sì folti
quelle fiere selvagge che 'n odio hanno
tra Cecina e Corneto i luoghi cólti.

Inferno, XIII - vv. 4-9

CONTENTS

INTRODUCTION

String Theory is today the most promising theoretical framework to unify the four fundamental forces of the Universe, naturally comprising quantum gravity. String Theory differs from other theories in Physics in that its building blocks are strings, namely one-dimensional manifolds, instead of point particles. The implications of having fundamental extended objects such as strings are enormous: on one side String Theory automatically needs supersymmetry to be consistent, while on the other side it requires ten dimensions to be coherently formulated. These two requirements seem hardly verifiable experimentally, but are of primary importance for the consistence of the theory and while it is somehow counter-intuitive they can lead to simple and beautiful physics.

Supersymmetry is a continuous symmetry that essentially consists in the exchanging bosonic and fermionic particles while keeping the theory invariant. Supersymmetry imposes strong constraints on the spectrum of the particles (there clearly has to be a one-to-one correspondence between fermionic states and bosonic states), on their masses and charges and on the possible interactions that can be considered in a lagrangian formulation of a theory. To date there is no experimental observation of supersymmetry, even if the last run at LHC has reached energies high enough to possibly reveal the existence of supersymmetric particles. However, within String Theory there exist numerous mechanisms and examples of supersymmetry breaking, that are of vital importance for the theory to make contact with the experimental results we have today. As we will see, supersymmetry breaking is used in String Theory to possibly explain many of the paradoxes for non-BPS black holes, or to create solutions that asymptote to de Sitter space and that hence comprise a positive cosmological constant, making contact with the modern experimental results.

The fact that String Theory lives in ten dimension is also not an issue. Even though there are no experimental results that more than four dimensions exist, we expect particle accelerators to be able to conduct viable experiments on extra dimensions in the next years.

It is important to stress that the energy needed to test the existence of extra dimensions depends on the chosen model and consequently some models will be tested earlier than others. Still, extra dimensions can be seen somehow as a mathematical requirement for the consistency of String Theory. Indeed, a mechanism known as *compactification* is used to reduce the ten-dimensional physics of String Theory to four dimensions (while often five-dimensional or three-dimensional physics are studied). In the simplest example, this operation is carried on by considering the extra dimensions as circles and by taking their radii to go to zero. More generally, one can consider the extra dimensions as a compact manifold that is shrinking to a point. While the physics of the compactification manifold is not directly accessible to the four remaining dimensions, some traces remain of the compactification process. Indeed, the moduli of the chosen manifold determine some of the characteristics of the spectrum of the four-dimensional theory. The richness of the physics arising from the compactification process explains why String Theory is able to predict the existence of many different universes, or why it is possible to explain the existence of black hole entropy.

There exists another mechanism for String Theory to make contact with the four-dimensional world: the AdS-CFT conjecture. This is a duality between four-dimensional conformal field theories and String Theory solutions that asymptote to an Anti de Sitter space. This duality is most intriguing as it connects a ten-dimensional theory with gravity to a four-dimensional well-known conformal field theory with no gravity. AdS-CFT contributed to make incredible progress on both sides of the duality and to date is still most used to give physical interpretation to the ten dimensional physics of String Theory. In the thesis we will often relate our results to the corresponding gauge theory results, but as AdS-CFT is never used explicitly and is not central for the proofs we will only refer to the literature without reviewing the gauge/gravity duality in great detail.

There exist different formulations of String Theory, that are all ten-dimensional. This means that the theory can be formulated in different theoretical frameworks, that are all physically equivalent as they are related by duality operations. Consequently, each physical configuration can be mapped from one framework to the other and one often chooses the best framework given the specific configuration to describe. We will only focus on Type IIA and Type IIB String Theory. More specifically, we will only consider the low energy limit of these two theories, which are Type IIA and Type IIB supergravity. While Supergravity was initially an independent field from String Theory, it soon turned out that some supergravities are nothing but low energy limits of the latter.

A major breakthrough took place in 1995, where the different formulations of String Theory were unified in a single eleven-dimensional theory, M-theory. While the full formulation of the latter remains an unreached goal still today, its low-energy limit is the well-known eleven-dimensional supergravity. In the thesis we will only work in eleven-dimensional, Type IIA and Type IIB supergravity and we will explain in detail the duality

transformation to pass from one frame to the other.

One of the most important characteristics of String Theory is that in the supergravity regime there exist many smooth nontrivial solutions. These solutions have no localized sources and are characterized by a nontrivial topology whose cycles are threaded by fluxes, giving rise to the charges and momenta. The fact that these solutions have no singularities and a rich topology makes them most intriguing and suitable to be used in all the main areas of String Theory. In this thesis we will explore some of the most famous smooth solutions in the different contexts of their applications. Our goal is hence two-fold: on one side we want to analyze and make progress in the specific research line a smooth solution is presently studied for, while on the other side we want to show the richness and complexity of the field by proposing four different research lines that apparently are not related to each other. We will hence analyze the Lin-Lunin-Maldacena (LLM) solution [1], the eleven-dimensional, three-charge smooth microstates of [2, 3], the Klebanov-Strassler (KS) solution [4] and a modification to the eleven-dimensional microstates.

The Lin-Lunin-Maldacena solution [1] is a family of smooth solutions originally found in Type IIB supergravity. We will study more closely its eleven-dimensional formulation as it represents the gravity dual of the M2 brane theory with a fermion mass turned on. In the thesis we compute the potential energy of probe M2-M5 branes in the LLM solution. We find two new results, depending on the charges of the probe. First of all, when the M2-M5 charges are parallel to those of the solution we find stable supersymmetric configurations for the probe. This means that, despite there being no localized sources in the LLM solution, it is as if this solution were sourced by branes identical to our probe, namely M2-M5, i.e. that the fluxes threading the nontrivial LLM geometry carry mixed M2 and M5 charges. Secondly, when the charges of the M2-M5 probe are opposite to those of the solution we find metastable configurations for the probes that break supersymmetry. Indeed, these minima have much more energy with respect to those of the first kind. We then study in detail the possible decay mechanism that leads to supersymmetric final configurations. Our findings hence suggest that metastable configurations that break supersymmetry also exist in the dual gauge theory, namely the mass-deformed M2 brane theory.

The smooth, eleven-dimensional, three charge microstates found in [2, 3] is the second family of solutions that will be analyzed. The geometry of these solutions is that of a long warped throat, that is capped-off at the end and has many different blown-up cycles at the bottom. In addition, six of the eleven coordinates are merely spectators, meaning that they do not play any role in the physics. Indeed, compactifying at no cost along the six coordinates, these solutions become similar to well-known black hole solutions

in five dimensions, but contrarily to the latter they are smooth and horizonless and are hence *black hole microstates*. Microstate geometries are smooth horizonless solutions that have the same charges and asymptotic behavior of that of a black hole. They are the most important piece of the Fuzzball proposal, a program that intends to explain black hole paradoxes interpreting solutions with a horizon as "thermodynamical" descriptions in terms of ensembles of microstate geometries.
Although many microstates are known for different types of BPS black holes, the world of near-BPS black holes remains quite unexplored. Recently, it has been found that one can promote the class of microstates we will examine to near-BPS microstates by placing an anti-supertube at a metastable location, using a similar mechanism to the one that breaks supersymmetry in LLM. In the thesis we will construct such near-BPS microstates. We will also show that they are in fact unstable once one considers all the degrees of freedom of the system. Hence the introduction of a metastable supertube triggers a motion of the bubbles at the bottom of the throat that induces radiation emission, so that the microstates evolve towards extremality. We will claim that this corresponds to Hawking radiation, an expected feature characterizing near-BPS microstates. We compute its energy rate and its frequency and compare the results with the exact one known for the corresponding black hole. Expecting the microstate to be part of a thermodynamical ensemble - the fuzzball - we claim that the microstate we built is not typical in the ensemble, estimate the departure from typicality and suggest possible explanations.

In this thesis it will also be shown that the microstates found in [2, 3] can be suitably modified to possibly construct microstates for five-dimensional black holes with no electric charge. One necessary step to construct electrically-neutral microstates is to have solutions of five-dimensional supergravity where the Killing spinor passes from timelike to null. While this is not a new phenomenon in general, solutions where this happens on open sets of the spacetime manifold are yet unknown and would be of primary importance to construct the new microstates. We find explicit examples that satisfy a condition that is close to the desired one: we manage to have the Killing vector along with all its derivatives vanish at a point. Our construction is based on the fact that the microstates of [2, 3] are completely determined once one fixes the poles and residues of some harmonic functions. One can then have the Killing vector to vanish at a point together with an arbitrary number of its derivatives by suitably arranging a sufficient number of poles and tuning the residues. Consequently, to set all the derivatives to zero one has to arrange an infinite number of poles. We find many examples where the conserved charges become infinite in the limit, but we also construct valid solutions where the charges remain finite and that asymptote $AdS_3 \times S_2$.

The last smooth solution we examine is the one found by Klebanov and Strassler (KS) [4]. This has a D3 brane charge and dielectric D5 brane charge and the six-dimensional external space is a deformed conifold. The importance of this solution relies

on the fact that it is the gravity dual of confining vacua and that it is also a model for a region of high warping inside a flux compactification. This is why KS is the most suitable known solution to apply the KKLT uplift mechanism, that allows to find (meta)stable dS vacua in String Theory, which hence makes contact with the cosmological observations about the positivity of the cosmological constant. The core step of the KKLT mechanism applied to KS is the insertion of metastable anti-D3 branes. Recently, it has been observed that the backreaction of the antibranes might cause singularities in the KS solutions, which might affect the effectiveness of the KKLT uplift mechanism. In this thesis we construct the T-dual version of the KS solution, in view of testing the stability of antibranes in the unexplored regime of parameters of Type IIA supergravity. To do so we first identify a suitable isometry that would lead to a well-known brane configuration in Type IIA. In particular, we require an NS5 brane to arise as a consequence of T-duality and to wrap a specific holomorphic curve that is well-known in the literature. To avoid clutter we then reconstruct only a small region of the T-dual solution, that corresponds to the region where the anti-D3 branes are inserted in the original version. We perform many consistency checks about our construction. Lastly, we construct the T-dual solution of KS with backreacted D3 branes. This is made possible by reconstructing a small region only, which avoids prohibitive computations for the backreacted branes.

This thesis is divided into two parts. Part I is a review of fundamental well-known results in the literature that are necessary to understand Part II, which presents original analysis about smooth solutions in String Theory.

Part I consists of two chapters. In Chapter 1 we introduce eleven-dimensional, Type IIB and Type IIA supergravities along with dimensional reductions and T-duality, which are the duality transformations that allow to switch among these theories. We also present some standard solutions in eleven-dimensional supergravity and the standard D-brane solution in ten dimensions. We introduce the probe brane action and perform two explicit computations of probe potential. In Chapter 2 we explain how smooth bubbled solutions arise in String Theory via geometric transitions. We then introduce the three main smooth solutions that will be analyzed: the Lin-Lunin-Maldacena solution, the Klebanov-Strassler solution and the eleven-dimensional, three charge microstates. Particular emphasis is given to the computations of physically relevant parameters such as conserved charges and to the description of the nontrivial cycles that support the fluxes.

Part II consists of four chapters, each of them dedicated to the analysis the four different research directions involving the smooth solutions mentioned above. The structure of these chapters is similar: they start with a technical introduction to the research direction in question, then a detailed analysis of original results is presented and finally some

possible developments are illustrated.

In Chapter 3 we show the existence of metastable vacua that break supersymmetry in LLM and analyze their properties. Chapter 4 is dedicated to showing the instability of near-BPS microstates and to analyzing their energy emission rate. Chapter 5 is devoted to the construction of the T-dual solution to KS, along with the geometrical analysis necessary to pick the right isometry and the numerous consistency checks that validate our procedure. In Chapter 6 we describe the construction of solutions to five-dimensional supergravity where the Killing vector vanishes at a point together with all its derivative. To date, this is as close as we can get to constructing five-dimensional solutions with timelike and null killing vector on open sets.

Additional details are presented in the Appendices. In particular, Appendix A presents some complementary details and calculations about Chapter 3, while Appendix B gives additional insight into the T-duality of Chapter 5. Finally, in Appendix C we present an alternative construction to that described in Chapter 6.

INTRODUCTION (FRANÇAIS)

La théorie des cordes est aujourd'hui le cadre théorique le plus complet pour unifier les quatre forces fondamentales de l'Univers, comprenant naturellement la gravité quantique. La théorie des cordes se distingue des autres théories en physique parce que des cordes jouent le rôle des particules élémentaires. Les conséquences d'avoir des cordes comme objets fondamentaux sont énormes: la théorie des cordes d'un côté exige automatiquement la supersymétrie pour être cohérent et de l'autre côté il peut être formulée seulement en dix dimensions. Ces deux conditions ne semblent pas vérifiables expérimentalement, mais sont essentiels pour la cohérence de la théorie et ils peuvent conduire à des modèles simples et complexes au même temps.

La supersymétrie est une symétrie continue qui essentiellement échange bosons et fermions tout en gardant la théorie inchangée. La supersymétrie impose des contraintes fortes sur le spectre des particules (il doit y avoir une correspondance biunivoque entre états fermioniques et états bosoniques), sur leurs masses et charges et sur les interactions possibles qui peuvent être considérés dans le lagrangien de la théorie. à ce jour, il n'y a pas d'observation expérimentale de la supersymétrie, même si la dernière expérience à LHC a atteint des énergies suffisamment élevées pour révéler l'existence de particules supersymétriques. Cependant, dans la théorie des cordes il existe des nombreux mécanismes et exemples où la supersymétrie est brisée, qui sont d'une importance vitale afin que la théorie reproduise les résultats expérimentaux que nous avons aujourd'hui. Le fait que la supersymétrie peut être brisée est utilisé dans la théorie des cordes pour expliquer plusieurs paradoxes autour les trous noirs, ou pour créer des solutions dont la géométrie asymptotique est un espace de type de Sitter, ce qui implique l'existence d'une constante cosmologique positive en reproduisant tous les résultats expérimentaux modernes.

Le fait que la théorie des cordes est formulée en dix dimension n'est pas un problème. Même si il n'y a pas des résultats expérimentaux qui confirment que plus de quatre dimensions existent, dans les prochaines années il y aura des accélérateurs de partic-

ules caractérisés par une énergie suffisamment haute pour vérifier l'existence de dimensions supplémentaires. Pourtant, les dimensions supplémentaires peuvent être considérés en quelque sorte comme une exigence mathématique pour la cohérence de la théorie des cordes. En effet, un mécanisme connu sous le nom de *compactification* est utilisé pour réduire la physique en dix dimensions de la théorie des cordes à quatre dimensions (bien que la physique en cinq dimensions ou en trois dimensions soit souvent étudiée). Dans l'exemple le plus simple, cette opération est réalisée en considérant les dimensions supplémentaires comme des cercles et en prenant la limite des leur rayons à zéro. Plus généralement, on peut considérer les dimensions supplémentaires comme une variété compacte qui se rétrécit à un point. Alors que la physique de la variété de compactification ne soit pas directement accessible aux quatre dimensions restantes, le processus de compactification laisse certaines traces. En effet, les modules de la variété choisie déterminent les caractéristiques du spectre de la théorie à quatre dimensions. La richesse de la physique dérivant du processus de compactification explique pourquoi la théorie des cordes est capable de prédire l'existence de nombreux univers différents, ou pourquoi il est possible d'associer une entropie aux trous noirs.

Il existe un autre mécanisme qui connecte la théorie des cordes au monde à quatre dimensions: la conjecture AdS-CFT. Ceci est une dualité entre les théories conformes à quatre dimensions et des solutions de la théorie des cordes qui asymptote à un espace de Anti de Sitter. Cette dualité est la plus intrigante car elle relie une théorie de dix dimensions avec gravité à une théorie de jauge conforme à quatre dimensions sans gravité. La conjecture AdS-CFT a contribué à progresser de façon incroyable dans les deux côtés de la dualité et à ce jour est encore utilisé pour donner une interprétation intuitive à la physique à dix dimensions de la théorie des cordes. Dans la thèse, nous allons souvent rapporter nos résultats à ceux de la théorie de jauge correspondante, mais comme la conjecture AdS-CFT n'est jamais utilisée explicitement et n'est pas nécessaire pour les démonstrations nous allons nous référer à la littérature sans examiner cette dualité en détail.

Il existe plusieurs formulations de la théorie des cordes, qui demandent dix dimensions. Cela signifie que la théorie peut être formulée dans différents cadres théoriques, qui sont tous physiquement équivalents car ils sont liés par des opérations de dualité. Par conséquence, chaque configuration physique peut être transformée d'un cadre à l'autre et on choisit souvent le meilleur cadre pour décrire chaque configuration spécifique. Nous allons seulement nous concentrer sur la théorie de type IIA et la théorie de type IIB. Plus précisément, nous ne considérons que les limites de basse d'énergie de ces deux théories, qui sont les supergravités de type IIA et IIB. Alors que la supergravité était initialement un domaine indépendant de la théorie des cordes, il est vite apparu que certains supergravités ne sont que des limites de baisse énergie de ce dernière.

Une révolution dans la physique théorique a eu lieu en 1995, où les différentes formu-

lations de la théorie des cordes ont été unifiées en une seule théorie en onze dimensions, la *théorie M*. Alors que la formulation complète de ce dernière reste un objectif encore non atteint, sa limite de basse énergie est une supergravité à onze dimensions que est bien connue. Dans la thèse, nous allons examiner seulement la supergravité à onze dimensions et les supergravités de type IIA et IIB et nous allons expliquer en détail les transformations de la dualité pour passer d'un cadre à l'autre.

Une parmi les caractéristiques les plus importantes de la théorie des cordes est le fait que dans le régime supergravité il existe de nombreuses solutions régulières et non banales. Ces solutions n'ont pas de sources localisées et sont caractérisées par une topologie non triviale dont les cycles sont supportés par de flux qui est à la base des charges et moments conservées. Le fait que ces solutions n'ont pas des singularités et présentent une topologie riche les rend plus intrigantes et aptes à être utilisés dans tous les principaux domaines de la théorie des cordes. Dans cette thèse, nous allons explorer trois parmi les solutions régulières les plus célèbres dans les différents contextes de leurs applications. Notre objectif est donc double: d'un côté, nous voulons analyser et expliquer notre progrès dans chaque domaine de recherche spécifique dans lequel chaque solution régulière est actuellement étudié, tandis que de l'autre côté nous voulons montrer la richesse et la complexité de la théorie des cordes en proposant quatre domaines de recherche différents qui, apparemment, ne sont pas liés. Nous allons donc analyser la solution de Lin-Lunin-Maldacena (LLM) [1], les microétats correspondantes à des trous noirs avec trois charges en onze dimensions [2, 3], la solution de Klebanov-Strassler (KS) [4] et une modification des microétats en onze dimensions.

La solution de Lin-Lunin-Maldacena [1] est en effet une famille de solutions régulières trouvé en origine dans la supergravité de type IIB. Nous allons étudier en détail sa formulation en onze dimensions, car elle représente la théorie duale avec gravité de celle qui est supportée par des branes M2 en présence d'un flux transversal supplémentaire. Dans la thèse, nous calculons l'énergie potentielle des branes M2-M5 dans la solution de LLM. Nous trouvons deux nouveaux résultats, en fonction des charges des branes. Lorsque les charges M2-M5 sont parallèles à celles de la solution, nous trouvons des configurations supersymétriques stables pour les branes. Cela signifie que, en absence de sources localisées dans la solution de LLM, les flux de cette solution supportent des charges de type M2 et M5 . D'autre part, lorsque les charges M2-M5 sont opposées à celles de la solution, nous trouvons des configurations métastables pour les branes qui brisent la supersymétrie. En effet, ces minima ont beaucoup plus d'énergie par rapport à ceux du premier type. Ensuite, nous étudions en détail un possible mécanisme de rayonnement qui conduit ces minima métastables à des configurations finales supersymétriques. Nos résultats suggèrent donc que les configurations métastables qui brisent la supersymétrie existent aussi dans la

théorie de jauge duale, c'est à dire une théorie des branes M2 avec des flux supplémentaires.

Les microétats régulières avec trois charges trouvés en [2, 3] sont la deuxième famille de solutions qui sera analysée. La géométrie de ces solutions est celle d'une longue gorge AdS déformé, qui est plafonné à la fin et présente beaucoup de cycles non triviales. Six des onze coordonnées ne sont que des spectateurs et ils ne jouent aucun rôle dans la physique. En effet, on peut compactifier sans difficultés ces six cordonnées. Ces solutions deviennent donc semblables à des solutions de trou noir bien connues en cinq dimensions, mais contrairement à ces derniers, ils sont régulières et sans horizon et sont donc appelées *microétats de trou noir*. Les microétats sont des solutions régulières qui ont les mêmes charges et la même géométrie asymptotique de ceux d'un trou noir. Ils sont l'ingrédient le plus important de la *Fuzzball proposal*, un programme qui a l'objectif d'expliquer les paradoxes des trous noires en interprétant ces derniers comme le résultat effectif d'un ensemble de microétats.
Bien que nombreux microétats sont connus pour différents types de trous noirs supersymétriques, le monde des trous noirs quasi-BPS reste assez inexploré. Récemment, on a trouvé qu'on peut promouvoir la famille de microétats que nous examinerons à des microétats quasi-BPS en plaçant un anti-supertube dans ces solutions, grâce à un mécanisme similaire à celui qui brise la supersymétrie dans la solution LLM. Dans la thèse, nous allons construire ces microétats quasi-BPS. Nous allons également montrer qu'ils sont en fait instables une fois qu'on considère tous les degrés de liberté du système. Par conséquence, l'introduction d'un anti-supertube métastable déclenche un mouvement des cycles au fond de la gorge AdS qui induit un rayonnement d'énergie qui fait évoluer les microétats quasi-BPS vers des états supersymétriques. Nous allons affirmer que cela correspond à un rayonnement de Hawking, qui est une caractéristique des microétats quasi-BPS. Nous calculons le taux d'émission d'énergie et la fréquence de ce rayonnements et comparons les résultats avec ceux du trou noir correspondant. Enfin, le microstate que nous avons construit n'est pas typique dans l'ensemble prévu dans la *Fuzzball proposal*, et nous suggérons des explications possibles.

Dans cette thèse, il sera également démontré que les microétats trouvés en [2, 3] peuvent être convenablement modifiés pour construire des microétats pour des trous noirs en cinq dimensions non chargés. Une étape nécessaire pour cela est d'avoir des solutions de supergravité en cinq dimensions où le vecteur de Killing passe de type temps à type nul. Bien que ce ne soit pas un phénomène nouveau en général, des solutions où cela se produit sur des ensembles ouverts de la variété d'espace-temps sont encore inconnus et seraient d'une importance vitale pour construire les nouveaux microétats. Nous trouvons des exemples explicites qui satisfont une condition très proche de celle désirée: on construit des solutions où le vecteur de Killing et tous son dérivés sont zéro à un point. Notre construction est basée sur le fait que les microétats de [2, 3] sont complètement déterminés une fois que l'on fixe les pôles et les résidus de certaines fonctions harmoniques. On peut alors

fixer à zéro le vecteur de Killing avec un nombre arbitraire de ses dérivés en disposant convenablement un nombre suffisant de pôles et en réglant leur résidus. Par conséquence, pour fixer tous les dérivés à zéro on doit disposer d'un nombre infini de pôles. Nous trouvons de nombreux exemples où les charges conservées deviennent infinies dans la limite, mais nous construisons également des solutions valides où les charges restent finies et que asymptote $AdS_3 \times S_2$. Nos résultats sont une première étape vers la construction d'un solution de supergravité en cinq dimensions avec un vecteur de Killing de type mixte sur des ensembles ouverts de la variété d'espace-temps.

La dernière solution régulière que nous examinons est celle trouvée par Klebanov et Strassler (KS) [4]. Cette solution de type IIB préserve une charge de type D3 et une charge diélectrique de type D5 et l'espace extérieur de dimension six est une conifold déformée. L'importance de cette solution se trouve dans le fait qu'il est le principal contexte d'application du mécanisme KKLT, qui permet de trouver de solutions (méta)stables de type de Sitter en théorie des cordes, permettant à ce dernière de reproduire les résultats des observations cosmologiques sur la positivité de la constante cosmologique. L'étape de base du mécanisme KKLT appliqué à la solution KS est l'insertion de branes métastables de type anti-D3 dans la géométrie. Récemment, il a été observé que la backreaction des antibranes pourrait causer des singularités dans la solution KS, ce qui pourrait avoir une incidence négative sur l'efficacité du mécanisme KKLT. Dans cette thèse, nous construisons la version T-duale de la solution KS, en vue de tester la stabilité des antibranes dans le régime de paramètres inexploré de la supergravité de type IIA. Nous identifions d'abord une isométrie appropriée qui conduirait à une configuration des branes bien connue dans la supergravité de type IIA. Dans la version de type IIA une nouvelle brane de type NS5 apparaît en conséquence de la T-dualité: elle enveloppe une courbe holomorphe spécifique qui est bien connue dans la littérature. Pour éviter des calculs très complexes nous reconstruisons seulement une petite région de la solution T-duale, qui correspond à la région où les branes anti-D3 sont insérés dans la version originale. Nous effectuons beaucoup de vérifications sur notre construction. Enfin, nous construisons la solution T-duale de celle de KS avec l'insertion de branes D3. Ceci est rendu possible grâce à la reconstruction d'une petite région seulement, ce qui évite des calculs insolubles pour la backreaction.

Cette thèse est divisée en deux parties. Dans la Partie I on présente une description des résultats fondamentaux bien connus dans la littérature qui sont nécessaires pour comprendre la Partie II, qui présente une analyse originale des solutions régulières dans la théorie des cordes. La Partie I est composée par deux chapitres. Dans le Chapitre 1 nous introduisons la supergravité en onze dimensions et les supergravités de Type IIA et IIB ainsi que les transformations de réduction dimensionnelle et de T-dualité, qui permettent de passer

d'une théorie à l'autre. Nous présentons également quelques solutions standard dans la supergravité en onze dimensions et la solution standard de D-branes en dix dimensions. L'action pour les branes est introduite et deux calculs explicites d'énergie potentielle sont effectués. Dans le Chapitre 2 nous expliquons comment la théorie des cordes rend possible l'existence des solutions régulières grâce au mécanisme de la *transition géométrique*. Nous introduisons ensuite les trois principales solutions régulières qui seront analysés: celle de Lin-Lunin-Maldacena, celle de Klebanov- Strassler et les microétats en onze dimensions avec trois charges. Une importance particulière est accordée aux calculs des paramètres physiques comme les charges conservés et à la description des cycles non triviales dans la topologie.

La Partie II se compose de quatre chapitres, dédiés à l'analyse des quatre domaines de recherche relatifs aux solutions régulières mentionnés ci-dessus. La structure de ces chapitres est similaire: ils commencent par une introduction technique au domaine de recherche en question, puis une analyse détaillée des résultats originaux est présentée et, enfin, certains développements possibles sont illustrés. Dans le Chapitre 3, nous montrons l'existence d'états métastables qui brisent la supersymétrie dans la solution LLM et nous analysons leurs propriétés. Le Chapitre 4 est consacré à la démonstration de l'instabilité des microétats quasi-BPS et à l'analyse de leur taux d'émission d'énergie. Le Chapitre 5 est consacré à la construction de la solution T-duale à celle de KS, ainsi qu'à l'analyse géométrique nécessaire pour choisir l'isométrie et aux nombreux vérifications qui valident notre procédure. Dans le Chapitre 6, nous décrivons la construction de solutions de supergravité en cinq dimensions où le vecteur de Killing devient nul à un point avec l'ensemble de son dérivé.

Des détails supplémentaires sont présentés dans les annexes. En particulier, l'Annexe A présente quelques détails complémentaires et des calculs au sujet du Chapitre 3, tandis que l'Annexe B donne des informations supplémentaires sur la T-dualité du Chapitre 5. Enfin, dans l'Annexe C, nous présentons une construction alternative à celle décrite dans le Chapitre 6.

Part I

Review of supergravity and smooth solutions

CHAPTER 1

ELEVEN-DIMENSIONAL, TYPE IIA AND TYPE IIB SUPERGRAVITIES

1.1 Eleven-dimensional Supergravity

The so-called "Second Superstring Revolution" started in 1995 with a series of papers regarding an eleven-dimensional theory that was supposed to unify all the different known formulations of String Theory into a single coherent mathematical framework. This theory was given the name of M-theory and opened many fascinating perspectives on the nature of String Theory, Supersymmetry and Quantum Field Theories. Although large parts of this unifying framework are still unknown, for the purposes of this thesis it is sufficient to restrict to the low-energy limit of M-Theory, namely eleven-dimensional supergravity.
Eleven-dimensional supergravity [5] is a supersymmetric theory of gravity formulated in eleven-dimensions. It contains extended objects such as M2 branes and M5 branes that are interacting in a self-consistent fashion both electromagnetically and gravitationally. The bosonic field content of eleven-dimensional supergravity is indeed extremely simple and consists of:

- a metric $g_{\mu\nu}$ $(\mu, \nu = 0, ...10)$, that can locally be expressed as a standard eleven-dimensional minkowskian metric $\eta_{\mu\nu} = diag(-1, 1...1)$. The metric tensor describes the geometry of spacetime and the gravitational interaction.

- A three-form potential A_3 that gives rise to a four-form field-strength:

$$G_4 = dA_3 \tag{1.1}$$

  In the following the geometric language will be employed as much as possible and

the indexes of the forms will remain implicit. This allows to write more compact formulas making the geometrical meaning clear. For instance, equation (1.1) can be rewritten specifying all the indexes as

$$G_4 \equiv G_{\mu\nu\rho\sigma}\, dx^\mu \wedge dx^\nu \wedge dx^\rho \wedge dx^\sigma \qquad G_{\mu\nu\rho\sigma} = 4!\partial_{[\mu} A_{\nu\rho\sigma]} \tag{1.2}$$

where the square-brackets mean anti-symmetrization.
The three form potential A_3 and the associated field-strength are just a generalization of the so-called vector potential A_μ and the related field strenght $F_{\mu\nu}$ of the four-dimensional theories. Indeed, A_3 encodes the electric and magnetic fields suitably generalized for an eleven-dimensional background.

The dynamics of the background in eleven-dimensional supergravity is specified by the following action:

$$S_{11} = \frac{1}{2k_{11}^2}\left(\int d^{11}x\,\sqrt{-g}R - \int \frac{1}{2}G_4 \wedge \star G_4 + \frac{1}{6}A_3 \wedge G_4 \wedge G_4\right) \tag{1.3}$$

where

$$2k_{11}^2 = 16\pi G_{11} = (2\pi)^8 l_P^9 \tag{1.4}$$

and G_{11} is the Newton constant in eleven dimensions and l_P is the Planck length. In (1.3) g is the determinant of the metric $g_{\mu\nu}$, R is the associated Ricci scalar and the Hodge star maps a n-form G_n to a $(11-n)$-form G_{11-n} whose components are given by:

$$\star\,(G)_{j_1\ldots j_{11-n}} = \sqrt{-g}G_{a_1\ldots a_n}g^{a_1 i_1}\cdots g^{a_n i_n}\epsilon_{i_1,\ldots i_n, j_1\ldots j_{11-n}} \tag{1.5}$$

where ϵ denotes the Levi-Civita tensor and the upper indexes for g denote the inverse metric tensor.
It is straightforward to give a physical interpretation to the action (1.3). The first integral is the well-known Einstein-Hilbert action that describes how the metric is specified by eventual sources or fields. The second integral describes the dynamics of the electric and magnetic fields interacting with gravity, while the third term in (1.3) is a Chern-Simons term that is required in order to preserve supersymmetry.
The action (1.3) specifies the dynamics of the background fields in eleven-dimensional supergravity. There exist only two fundamental (extended) objects in eleven-dimensional supergravity: M2 branes and M5 branes.

- M2 branes are conventionally considered electric objects. They can be thought as a sort of extension of the electron to eleven dimensional supergravity. Note that M2 branes are extended objects, indeed they are two-dimensional manifolds that sweep a three-dimensional worldvolume if one takes time evolution into account. Similarly, an electron is a point-like object that sweeps a one-dimensional worldline in four

dimensions. By definition, M2 branes couple electrically to A_3:

$$S_{M2} = Q_{M2} \int d^3\sigma \hat{A}_3 \tag{1.6}$$

where $\hat{A}_3$ is the pullback of A_3 on the M2 brane worldvolume described by the coordinates $\sigma^0, \sigma^1, \sigma^2$ and Q_2 is the M2 brane charge. The latter is measured by the dual-field strength:

$$Q_{M2} = \int_{S_7} \star G_4 \tag{1.7}$$

where S_7 is a seven-sphere surrounding the brane in the eight-dimensional transversal space. This is exactly as for the charge of an electron, which is defined as the integral of the electric field across a two-sphere surrounding the electron.

- M5 branes are magnetic objects that can be thought as the generalization of a four-dimensional magnetic monopole. M5 branes, as the name suggests, are 5-dimensional manifolds that sweep a six-dimensional worldvolume. Their charge is measured by

$$Q_{M5} = \int_{S_4} G_4 \tag{1.8}$$

where S_4 is a four-sphere surrounding the M5 in the six-dimensional transverse space.

M2 branes and M5 branes are BPS objects, meaning that in suitable units their mass is equal to their charge. This is a requirement in order to obtain a supersymmetry-preserving solution.

1.2 Standard solutions of eleven-dimensional supergravity

Varying the action (1.3) with respect to $g_{\mu\nu}$ and A_3 one gets the equations of motion for these fields. Notice that the equation for the metric is nothing but a generalization of the famous Einstein's equation to eleven dimensions.
A supergravity background is specified once one solves the equations of motion. This section is dedicated to some of the simplest supergravity solutions in eleven-dimensions, that arise from M2 and/or M5 branes at rest. While these solutions have a clear physical interpretation it is fundamental to stress that all these solutions are *singular*, as they are characterized by localized sources that are M2 and/or M5 branes. Note also that the singularities are extended loci, as they coincide with the branes.

1.2.1 The standard M2 brane solution

This is one of the simplest solutions possible, where the metric and three-form potential are sourced by N coinciding M2 branes extended along t, x^1, x^2 and localized at $x^i = 0$,

$i = 3, ..., 10$. Assuming that each M2 brane has unitary M2 charge and recalling that M2 branes are BPS objects, N specifies both the total charge and the total mass. By convention the coordinates wrapped by the branes, x^0, x^1, x^2, span the *external space*, while the remaining coordinates span the *internal space* or *transverse space*. This distinction is also used for more complex solutions and will be heavily used in the following.

The solution generated by the N M2 branes is given by:

$$\begin{aligned} ds_{11}^2 &= H_2^{-2/3}(-dt^2 + dx_1^2 + dx_2^2) + H_2^{1/3} ds_8^2 \\ A_{t12} &= (1 - H_2^{-1}) \end{aligned} \tag{1.9}$$

where ds_8^2 is a standard euclidean metric on the eight-dimensional transverse space, and H_2 is a harmonic function usually called *warp factor*:

$$H_2 = 1 + \frac{32\pi^2 N l_{11}^6}{r^6} \qquad r^2 = \sum_{i=1}^{8} x_{2+i}^2 \tag{1.10}$$

with N the number of M2 branes.
As anticipated, the solution (1.9) presents localized M2 branes at $r = 0$.

1.2.2 The standard M5 brane solution

The solution "dual" to that in equation (1.9) is sourced by N M5 branes wrapping $x_0, ...x_5$ and localized at $x_i = 0$ for $i = 6, ...10$. It is given by:

$$\begin{aligned} ds_{11}^2 &= H_5^{-1/3}(-dt^2 + dx_1^2 + ... + dx_5^5) + H_5^{2/3} ds_5^2 \\ G_{\alpha_1 ... \alpha_4} &= \frac{1}{2} \varepsilon_{\alpha_1, ..., \alpha_5} \partial_{\alpha_5} H_5 \end{aligned} \tag{1.11}$$

with the M5 brane warp factor H_5 given by

$$H_5 = 1 + \frac{a}{r^3} \qquad r^2 = \sum_{i=6}^{10} x_i^2 \tag{1.12}$$

Comparing (1.11) with (1.9) it is possible to get some intuition about the form of standard brane solutions and the connection between the analytic form of the metric and the physical object they describe:

- Both solutions are characterized by a warpfactor of the form $H \sim r^{-\alpha}$, where $\alpha = 6$ for M2 branes and $\alpha = 3$ for M5 branes (the constants represent a gauge choice that is physically meaningless). The fact that the warpfactors decay at infinity with different powers should not be surprising: indeed the warpfactor is computed by solving a standard harmonic equation in the transverse space, and as the dimensionality of this space changes between M2 and M5 branes so does α.

- The powers of the warpfactors in the metric tell important information about what coordinates the branes are wrapping and where they are localized. Indeed, as one moves from infinity to a region close to the branes the external space gets contracted, while the internal space gets infinitely redshifted. Consequently, in (1.9) and (1.11) the coordinates wrapped by the branes appear in the metric multiplied by a warpfactor with a *negative* power. Vice-versa, this power is positive for the external space.

1.2.3 Intersecting branes

Combining the M2 brane solution (1.9) with the M5 brane solution (1.11) one can obtain many different supersymmetric solution that contain M2 branes and M5 branes intersecting in a supersymmetric fashion [6]. We present here some of these solutions, using the two observations at the end of the previous section to determine the configuration and the nature of the brane that sources these solution. For the sake of clarity, we will omit all the physical quantities (such as the Planck length and Newton's constant) in the potentials and/or four-form field strength, reabsorbing them into proportionality constants.

The solution given by two different stacks of M2 branes, labelled by a and b, is given by:

$$\begin{aligned} ds_{11}^2 &= H_{2,a}^{-2/3} H_{2,b}^{-2/3}(-dt^2) + H_{2,a}^{-2/3} H_{2,b}^{1/3}(dx_1^2 + dx_2^2) + H_{2,b}^{-2/3} H_{2,a}^{1/3}(dx_3^2 + dx_4^2) \\ &\quad + H_{2,a}^{1/3} H_{2,b}^{1/3}(dx_5^2 + ... + dx_{10}^2) \\ G_{t12\alpha} &= \frac{1}{2}\frac{\partial_\alpha H_{2,a}}{H_{2,a}^2} \qquad G_{t34\alpha} = \frac{1}{2}\frac{\partial_\alpha H_{2,b}}{H_{2,b}^2} \qquad \alpha = 5, ..., 10 \end{aligned} \tag{1.13}$$

where

$$H_{2,a} = H_{2,a}(x_5, ..., x_{10}) \sim 1 + \frac{c_a}{r^4} \qquad r^2 = \sum_{i=5}^{10} x_i^2 \tag{1.14}$$

and an analogous equation holds for $H_{2,b}$. The solution (1.13) is sourced by two stacks of M2 branes, the a-stack wrapping t, x_1, x_2 and the b-stack wrapping t, x_3, x_4, as can be deduced by the warpfactors with power $-2/3$. Both stacks are smeared in the two directions that are wrapped by the other stack, so for instance branes of the stack a are smeared along x_3 and x_4. This is required by supersymmetry and by the fundamental request of getting a stable and static solution. The smearing process also explains why the nontrivial part of the warpfactors goes as r^{-4}, where r is the radius in the *common* transverse space: as the branes are smeared it is as if one needed to integrate the original warpfactor of (1.9) along two directions, getting a power of -4. Finally, we mention that this solution preserves eight supercharges, exactly half of those preserved by (1.9).

In the same spirit of (1.13) one can write the solution of three separate stacks of M2 branes, labelled by a, b, c:

$$\begin{aligned} ds_{11}^2 &= H_{2,a}^{-2/3} H_{2,b}^{-2/3} H_{2,c}^{-2/3}(-dt^2) + H_{2,a}^{-2/3} H_{2,b}^{1/3} H_{2,c}^{1/3}(dx_1^2 + dx_2^2) \\ &+ H_{2,b}^{-2/3} H_{2,a}^{1/3} H_{2,c}^{1/3}(dx_3^2 + dx_4^2) + H_{2,c}^{-2/3} H_{2,a}^{1/3} H_{2,b}^{1/3}(dx_5^2 + dx_6^2) \\ &+ H_{2,a}^{1/3} H_{2,b}^{1/3} H_{2,c}^{1/3}(dx_7^2 + ... + dx_{10}^2) \\ G_{t12\alpha} &= \frac{1}{2}\frac{\partial_\alpha H_{2,a}}{H_{2,a}^2} \qquad G_{t34\alpha} = \frac{1}{2}\frac{\partial_\alpha H_{2,b}}{H_{2,b}^2} \qquad G_{t56\alpha} = \frac{1}{2}\frac{\partial_\alpha H_{2,c}}{H_{2,c}^2} \qquad \alpha = 7, ..., 10 \end{aligned} \tag{1.15}$$

Tracking the exponents in the metric (1.15) it is clear that the a-stack wraps t, x_1, x_2, the b-stack wraps t, x_3, x_4 and the c-stack wraps t, x_5, x_6. The three stacks are smeared along the directions of the other two stacks, so for instance the M2 branes of the a-stack are smeared along x_3, x_4, x_5, x_6. The three warpfactors now only depend on the radius defined on the common transverse space, spanned by $x_7, ..., x_{10}$. This solution preserves four supercharges.

The solution sourced by a stack of M5 branes and a stack of M2 branes wrapping one common direction is given by:

$$\begin{aligned} ds_{11}^2 &= H_2^{-2/3} H_5^{-1/3}(-dt^2 + dx_1^2) + H_2^{-2/3} H_5^{2/3}(dx_2^2) + H_2^{1/3} H_5^{-1/3}(dx_3^2 + ... + dx_6^2) \\ &+ H_2^{1/3} H_5^{2/3}(dx_7^2 + ... + dx_{10}^2) \\ G_{t12\alpha} &= \frac{1}{2}\frac{\partial_\alpha H_2}{H_2^2} \qquad G_{6\alpha\beta\gamma} = \frac{1}{2}\varepsilon_{\alpha\beta\gamma\delta}\partial_\delta H_5 \qquad \alpha, \beta, \gamma, \delta = 7, ..., 10 \end{aligned} \tag{1.16}$$

The M2 branes wrap t, x_1, x_2, as emphasized by the fact that these coordinates are multiplied by $H_2^{-2/3}$ in the metric -compare with (1.9)- while the M5 branes wrap $t, x_1 x_3, x_4, x_5, x_6$, as one can see tracking the coefficient $H_5^{-1/3}$ in the metric. Both stacks are smeared along the direction wrapped by the other stack, so for instance the M2 branes are smeared along x_3, x_4, x_5, x_6. The two warpfactors now depend on the radius defined on the *common* transverse space x_7, x_8, x_9, x_{10}. Note also that the four-form is a sort of hybrid between that of the M2 brane solution (1.9) and that of the M5 brane solution (1.11). This solution preserves eight supercharges.

There are other possible solutions that belong to the class of intersecting branes, which can be easily derived by suitably mixing the solutions above. For instance, one can have a solution generated by two stacks of M5 branes having three directions in common, or a solution sourced by two separated M2 brane stacks having each one direction in common

with an M5 brane stack.

The importance of eleven-dimensional solutions relies on the fact that thanks to different dualities they can be related to brane solutions in different types of supergravities, namely Type IIA and Type IIB, which are ten-dimensional. Each of these supergravities has is own field content and branes, but as the different solution are related by duality transformations they are physically equivalent.

1.3 Type IIA Supergravity via dimensional reduction

Eleven-dimensional supergravity can be easily mapped to the ten-dimensional Type IIA supergravity upon compactifying a coordinate on a circle and shrinking the radius of the circle to zero [7, 8]. Type IIA Supergravity is the low-energy limit of Type IIA String Theory, one of the frameworks in which Superstring Theory can be formulated. The field content of Type IIA supergravity is presented in this section, together with the necessary formulas for the dimensional reduction that relates Type IIA and 11D supergravity.
According to the boundary conditions for open/closed strings in ten dimensions it is possible to obtain fields of different nature in Type IIA. There exist three Neveu-Schwarz Neveu-Schwarz fields (NS-NS) and four Ramond-Ramond (RR) fields.
The NS-NS sector consists of:

- the ten dimensional metric $g_{\mu\nu}$,
- an antisymmetric two-form field B_2. This should be considered as a two form potential and the physical field is its differential

$$H_3 \equiv dB_2$$

- A scalar field Φ, the dilaton.

The RR sector consists of:

- the potentials C_p, with $p = 1, 3, 5, 7$. These are not completely independent from each other, as we will see in the following. The charges related to these potentials are -as usual- measured by their field strengths. In the following, we will always deal with the *improved* field strengths:

$$F_{p+1} = dC_p + H_3 \wedge C_{p-2} \tag{1.17}$$

  The improved field strengths are related to each other by

$$F_8 = \star F_2 \qquad F_6 = \star F_4 \tag{1.18}$$

  which physically implies that F_8 (F_6) is the magnetic dual of F_2 (F_4).

There exist two categories of fundamental objects that source the fields of Type IIA. These couple either electrically or magnetically to the potentials.

- The Neveu-Schwarz (NS) branes interact with the NS-NS fields. These consist of the F1 string (a one-dimensional brane) that couples to B_2 electrically and the NS5 brane that couples to B_2 magnetically.
- The Dirichlet branes (D-branes) interact with the RR fields. These can be thought of a suitable generalization of the electron to the ten-dimensional theory, exactly as for M2 and M5 branes. Given the dimensions of the RR fields C_p, in Type IIA theory there exist D-branes with $D = 0, 2, 4, 6$. For instance, the D2 brane couples electrically to C_3 as in (1.6), while it couples magnetically to C_5. The situation is reversed for the D4-brane, that couples electrically to C_5 and magnetically to C_2. The object that couples electrically to C_1 is the D0 brane, which is essentially a point particle.

It was stated previously that the Type IIA theory with its fields and branes can be obtained via dimensional reduction from the eleven-dimensional supergravity. This procedure consists in compactifying one of the eleven coordinates on a circle considering the radius to be parametrically small. To fix the conventions, take x_{10} to be the coordinate to compactify. The eleven-dimensional metric is then rewritten as:

$$ds_{11}^2 = e^{4\Phi/3}\left[(dx_{10} + C_\mu dx^\mu)^2 + e^{-2\Phi} ds_{10}^2\right], \tag{1.19}$$

where ds_{10}^2 defines the Type IIA metric and $C_\mu dx^\mu \equiv C_1$ defines the 1-form RR potential, while Φ is the dilaton. The other Type IIA fields are specified after the dimensional reduction of the eleven-dimensional potential A_3:

$$\begin{aligned} (C_3)_{ijk} &= (A_3)_{ijk} \qquad i,j,k \neq 10 \\ (B_2)_{ij} &= (A_3)_{ij10} \end{aligned} \tag{1.20}$$

The compactification of an eleven-dimensional solutions also maps M2 branes and M5 branes to either D-branes or NS-branes in Type IIA according to the following rules:

- If the M2 brane is wrapping x_{10} it becomes an F1 string in Type IIA
- If the M2 brane is not wrapping x_{10} it becomes a D2 brane in Type IIA
- If the M5 brane is wrapping x_{10} it becomes a D4 brane in Type IIA
- If the M5 brane is not wrapping x_{10} it becomes a NS5 brane in Type IIA

Note that formulas (1.19) and (1.20) are valid both ways, meaning that one can equally *uplift* type IIA supergravity to 11D supergravity. This is because the two theories are dual

to each other, which means that physically they describe the same phenomena, but in two different theoretical framework. Indeed, our discussion here has ben limited to the low-energy limits of M-theory and Type IIA string theory, i.e. 11D and type IIA supergravities respectively. As M-theory unifies all the theoretical framework of string theory, its low-energy limit and the low-energy limit of Type IIA are physically equivalent. Hence one can choose the most convenient framework to perform calculations and the duality of the two theories guarantees that every result is valid regardless to the chosen setup. In Chapter 3 this duality will become of utmost importance. Indeed all the results of Chapter 3 will be derived in Type IIA supergravity, where the computations are much clearer, but thanks to the duality they will be extended to eleven-dimensional supergravity.

1.3.1 Probe branes, Dirac-Born-Infeld action and brane polarization

Once a Type IIA solution has been specified is it necessary to understand the dynamics of a brane in this background. According to the principles of general relativity, adding a brane to the background modifies the background itself (backreaction), and hence the dynamics of the brane is never independent from the dynamics of the metric and the potentials. While finding a static background can already be a demanding task, solving all the equations of motions for a brane interacting with the background becomes extremely involved. Hence here and in the following we only study the dynamics of probe branes, namely branes whose charge is much smaller than the background charges. As the mass of our branes is equal to their charge, we can assume that the whole background is not modified by the presence of our probe. We further assume that our probes stand in a fixed position in spacetime, namely that they do not move. Hence their action is by definition equivalent to their potential energy. We will see in subsequent chapters that the potential of a probe brane can reveal fundamental pieces of information about the solution itself.

A Dp brane action is given by:

$$S = -|T_{Dp}| \int d^{p+1}\sigma e^{-\Phi} \sqrt{-\det(\hat{g} + \hat{B}_2 + \mathcal{F}_2)} - T_{Dp} \int e^{\hat{B}_2 + \mathcal{F}_2} \wedge \oplus_n \hat{C}_n \tag{1.21}$$

where a hat above the fields denotes the pullback of a field over the brane worldvolume spanned by $\sigma^0, ..., \sigma^p$:

$$\hat{B}_{ab} \equiv B_{\mu\nu} \frac{\partial x^\mu}{\partial \sigma^a} \frac{\partial x^\nu}{\partial \sigma^b} \tag{1.22}$$

The field $\mathcal{F}_2$ is a two-form defined on the worldvolume of the brane and hence does not need pullbacks. The second integrand is intended to be the sum of all possible $p+1$-forms obtained exponentiating $(\hat{B}_2 + \mathcal{F}_2)$ and taking the wedge product with the available C_n RR fields. In (1.21) T_{Dp} is the D-brane charge density. By convention this is positive for D-branes and negative for anti-D-branes. As the mass of D-branes is equal to their charge, T_{Dp} appears as a prefactor for both integrals.

It is important to have some physical intuition about the action (1.21). The first integral encodes the gravitational interaction felt by the brane. Indeed, it includes the integral of the volume form on the brane (i.e. the pullback of the metric) which represents the gravitational interaction as from General Relativity. It also includes the field $\mathcal{F}_2$ that, being defined on the brane, interacts gravitationally, something that is again familiar from General relativity.
The second integral in (1.21) represents the electromagnetic interactions of the brane, again in the presence of gravity. Notice that also the field $\mathcal{F}$ interacts with the background.
A final explanation is needed for the field $\mathcal{F}_2$, which, contrarily to all the other quantities in (1.21), is defined only on the brane worldvolume. The field $\mathcal{F}_2$ is a two-form and, exactly as for B_2, it couples to F1 strings in Type IIA. The only exception is that this F1 string is contained in the brane we are considering. This can be seen as it is possible to associate to this F1 string a conserved charge. Hence when $\mathcal{F}_{01} \neq 0$ the brane that is embedded in the background is not exactly a pure brane, but really a higher dimensional brane containing a F1 string. In addition, if $\mathcal{F}_{ij} \neq 0$, also other lower-dimensional branes can be contained in the original probe.

1.3.2 An example: D2 probes in D2 brane backgrounds

This section is focused on a specific simple example: computing the potential for an M2 probe brane embedded in the M2 brane background (1.9).
The actions of the branes in 11D supergravity are usually quite involved and (1.21) is valid in Type IIA (or Type IIB) only. Therefore, instead of trying to uplift (1.21) to 11D, we use the results of Section (1.3) to dimensionally reduce the background (1.9) to type IIA. Notice that the potential calculated in Type IIA is valid also in 11D supergravity as the two theories are dual to each other.
Compactifying the standard M2 brane solution (1.9) along x_{10} one gets the D2 brane solution in Type IIA:

$$\begin{aligned} ds_{10}^2 &= H^{-1/2}(-dt^2 + dx_1^2 + dx_2^2) + H^{1/2} ds_7^2 \\ e^{2\Phi} &= H^{1/2} \qquad C_{t12} = (1 - H^{-1}) \end{aligned} \tag{1.23}$$

where the warpfactor now becomes:

$$H = 1 + \frac{c_2 g_s N l_p^5}{r^5} \tag{1.24}$$

and in the equations above c_2 is an unimportant intergation constant.
This solution is sourced by N D2 branes wrapped along x^0, x^1, x^2. Given the Type IIA background it is necessary to embed the probe D2 before determining the potential.
The D2 worldvolume is spanned by the coordinates $\sigma^0, \sigma^1, \sigma^2$, while it is embedded in

spacetime via ten functions $X^\mu(\sigma)$. String Theory incorporates General Relativity and hence all the equations are covariant under diffeomorphisms. This means that one can parametrize the embedding of the D2 brane choosing the *static gauge*, so that:

$$X^0(\sigma) = \sigma^0 \qquad X^1(\sigma) = \sigma^1 \qquad X^2(\sigma) = \sigma^2 \tag{1.25}$$

The probe approximation implies that the brane is placed in a particular position in spacetime and is kept fixed in that position, without considering its backreaction. This is mathematically expressed by:

$$\frac{\partial X^j}{\partial \sigma^i} = 0 \qquad j = 3, ..., 9 \quad i = 0, 1, 2 \tag{1.26}$$

which enormously simplifies all the pullbacks (1.22).
Now we are ready to compute the potential felt by a probe D2 brane in the background (1.23), for the D2 probe embedded as in (1.25) with $T_{D2} > 0$:

$$V = -T_{D2} H^{-1} - T_{D2}(1 - H^{-1}) = -T_{D2} \tag{1.27}$$

The probe brane feels no force as the potential is constant. This result is not surprising and can be easily explained in two (correlated) ways. Firs of all, the probe D2 is *parallel* to the N branes that source the solution and has the same charge. Hence it is subject to the attraction of the gravitational force and to the repulsion of the electromagnetic interaction. As the two forces depend on the same power of the radius and as the D2 mass in equal to its charge, the force has to be zero. Secondly, it is known that parallel branes of the same kind do not break any supersymmetry and as a consequence their potential has to be constant.
It is instructive to compute the potential for a probe brane embedded as in (1.25) but with *opposite* charge $-T_{D2}$ with respect to the background (i.e. and anti-D2):

$$V = -T_{D2} H^{-1} + T_{D2}(1 - H^{-1}) = -2T_{D2} H^{-1} + const \tag{1.28}$$

The electromagnetic force is now attractive and hence is summed up with the gravitational interaction. The force is given by $\partial_r V$ and it points radially towards the origin, as expected[1].
As a final remark notice that choosing a different orientation than (1.25) only the gravitational interaction would contribute to the potential and the force would be attractive. Therefore, the only stable configuration for the probe is the one in (1.25), i.e. the one that does not break supersymmetry.

[1] As the kinetic part in the action (1.21) is taken to be zero, what remains is by definition the potential with an overall minus sign

1.4 Type IIB supergravity via T-duality

Type IIB String Theory is often studied together with Type IIA String Theory. The two theories are related by a duality operation that is called T-duality [7, 8]. The latter can be heuristically explained as follows. One can expand the motion of a string wrapping a compact direction in Fourier series. As a string is an extended object, one obtains winding modes and momentum modes. If one performed the same operation for the motion of a particle along a compact direction one would obtain momentum modes only, hence the existence of winding modes are subject to the fact that strings are extended objects. T-duality consists in changing the radius of the compact direction from R to $1/R$, which exchanges winding modes and momentum modes, performing a duality transformation between Type IIA and Type IIB String Theory.

As Type IIA supergravity is the low-energy limit of Type IIA String Theory, a T-duality maps it into the low-energy limit of Type IIB String Theory, i.e. Type IIB supergravity. In the following we describe the field content of Type IIB supergravity along with the branes that live in this theory, then we present the formulas for T-duality that relate these two supergravities.

The field content of Type IIB supergravity consists of:

- Three NS-NS fields, namely the ten-dimensional metric, the two-form potential and the dilaton, exactly as in Section 1.3
- Five RR potentials C_p with $p = 0, 2, 4, 6, 8$, that once differentiated are combined with $H_3 = dB_2$ into the improved RR field strengths:

$$F_{p+1} = dC_p + H_3 \wedge C_{p-2} \tag{1.29}$$

The brane content can be inferred from the dimension of the potentials:

- Two NS-branes, namely the F1 brane and the NS5 brane, that couple to the NS-NS potential exactly as in Section 1.3
- Four Dp-branes, with $p = 1, 3, 5, 7$ that couple electrically with the C_p potential (note that a D9-brane cannot exist as it would completely fill the space). Dp-branes and potentials are related via electric-magnetic dualities in a similar fashion as in Section 1.3. Indeed, one has $F_p = \star F_{10-p}$ and at the same time the Dp brane that couples electrically to F_p is the magnetic dual of the D_{10-p} brane that couples electrically to F_{p-10}. In particular, note that the five-form field strength F_5 is self-dual as $F_5 = \star F_5$.

We now turn to the formulas of T-duality that relate Type IIA and Type IIB supergravity, also known as Buscher's rules. A fundamental ingredient to T-dualize a Type IIA solution to a Type IIB solution (and vice-versa) is to find a compact isometry direction y. Before performing the T-duality it is convenient to rewrite the fields as follows

$$\begin{aligned} ds^2 &= g_{yy}(dy + A_i dx^i)^2 + \widehat{g}_{ij} dx^i dx^j \\ B_2 &= B_{iy} dx^i \wedge (dy + A_i dx^i) + \widehat{B}_2 \\ C_p &= C^y_{p-1} \wedge (dy + B_{iy} dx^i) + \widehat{C}_p \end{aligned} \tag{1.30}$$

The T-dual solution is then given by

$$\begin{aligned} d\widetilde{s}^2 &= g_{yy}^{-1}(dy + B_{iy} dx^i)^2 + \widehat{g}_{ij} dx^i dx^j \\ e^{2\tilde{\Phi}} &= g_{yy}^{-1} e^{2\Phi} \\ \widetilde{B}_2 &= A_i dx^i \wedge dy + \widehat{B}_2 \\ \widetilde{C}_s &= \widehat{C}_{s-1} \wedge (dy + B_{iy} dx^i) + \widehat{C}^y_s \end{aligned} \tag{1.31}$$

If the RR potentials are not know it is possible to perform the T-duality directly on the field strengths. These should first be rewritten as:

$$F_p = F^y_{p-1} \wedge (dy + A_i dx^i) + \widehat{F}_p \tag{1.32}$$

and then transformed into:

$$\widetilde{F}_s = \widehat{F}^y_{s-1} \wedge (dy + B_{iy} dx^i) + F^y_s \tag{1.33}$$

Note that the formulas are valid in both ways, i.e. they can be used to map a Type IIA solution to a Type IIB one and vice-versa.

It is fundamental to understand what happens to a Type IIA D-brane when a T-duality is performed. There are two possible outcomes:

- If the isometry chosen for the T-duality is wrapped by the D-brane in Type IIA, then this brane gives rise to a (D-1)-brane in Type IIB
- If the isometry chosen for the T-duality is not wrapped by the D-brane in Type IIA then this brane generally has to be smeared along this direction (otherwise it would not be an isometry for the Type IIA solution). Consequently, the smeared D-branes in Type IIA give rise to a single (D+1)-brane in Type IIB

It is important to stress that the two outcomes stated above represent what happens most of the times and it is clearly possible to find complicated isometries or brane configurations where these rules do not apply. Notably, as T-duality perfectly works in both directions,

i.e. from Type IIA to Type IIB and vice-versa, the two observations above also apply in both ways.

1.4.1 The standard Dp-brane solution

After introducing Type IIA supergravity in Section 1.3 and TypeIIB supergravity in Section 1.4 it is now possible to write down the standard Dp brane solution. This is the general solution sourced by a single stack of Dp branes wrapping the time direction and the first p coordinates. Although these solution have a very similar form, it is important to stress that they live in Type IIA supergravity when p is even and in Type IIB supergravity when p is odd. They can be related to each other by repeatedly applying T-duality as introduced in Section 1.4 and all can be derived from the standard solutions of eleven-dimensional supergravity of Sections 1.2.1 and 1.2.2 by applying dimensional reduction and/or T-duality.

The standard Dp-brane solution is given by the following metric, dilaton and potential [9]:

$$\begin{aligned} ds_{10}^2 &= H_p^{-1/2}(-dt^2 + ... + dx_p^2) + H_p^{1/2}(dx_{p+1}^2 + ... + dx_9^2) \\ e^{\phi} &= H_p^{(3-p)/4} \\ C_{01...p} &\sim 1 - H_p^{-1} \end{aligned} \tag{1.34}$$

The warpfactor H_p depends only on the radius defined on the transverse space:

$$H_p = 1 + \frac{\alpha_p}{r^{7-p}} \tag{1.35}$$

where α_p is a dimensionful constant that depends on the number of D_p branes. The family of solutions (1.34) is the fundamental building block to construct more elaborate brane models, involving branes of different species or stacks of branes wrapping different directions.

1.4.2 T-duality in action: branes within branes

We now apply the formulas from T-duality (1.31) to pass from the Type IIA D2 brane solution revised in (1.23) to a Type IIB solution. We will then probe the obtained solution using the action (1.21), which remains essentially the same in Type IIB provided that one suitably adjusts the indices compatibly with the field content of this theory.

In the D2 brane solution (1.23) the D2 branes wrap t, x_1, x_2. Therefore according to the discussion of Section (1.4) one could T-dualize along x_2, obtaining a D1 brane solution, or along x_3, obtaining a D3 brane solution. Here we want do do something more general. We choose to T-dualize along an intermediate direction between x_2 and x_3. Suppose that this direction $\tilde{x}$ forms an angle α with x_2, so that one has $x_3 = \tilde{x}\sin\alpha$ and $x_2 = \tilde{x}\cos\alpha$.

Defining

$$c = \cos\alpha \qquad s = \sin\alpha \tag{1.36}$$

it is possible to T-dualize the D2 brane solution (1.23) along $\tilde{x}$ and then rewrite the new Type IIB solution using the old coordinates x_2 and x_3. The Type IIB solution is given by:

$$\begin{aligned}
ds^2 &= H^{-\frac{1}{2}}(-dx_0^2 + dx_1^2) + K^{-1}(dx_2^2 + dx_3^3) + H^{\frac{1}{2}}(dx_4^2 + ... + dx_9^2) \\
e^{\phi} &= K^{-\frac{1}{2}} H^{\frac{1}{4}} \\
B_2 &= -cs(H^{\frac{1}{2}} - H^{-\frac{1}{2}})K^{-1} dx_2 \wedge dx_3 \\
C_2 &= c(H^{-1} - 1) dx_0 \wedge dx_1 \\
C_4 &= s(H^{-1} - 1) H^{\frac{1}{2}} K^{-1} dx_0 \wedge dx_1 \wedge dx_2 \wedge dx_3
\end{aligned} \tag{1.37}$$

where we have defined

$$K = c^2 H^{-\frac{1}{2}} + s^2 H^{\frac{1}{2}} \tag{1.38}$$

In (1.37) we preferred to write the potentials B_2, C_2 and C_4 as full forms instead of directly writing their components for better clarity. The Type IIB solution (1.37) interpolates between a standard D1 brane solution and a standard D3 brane solution. Indeed, taking $\tilde{x} = x_2$ in Type IIA one can just substitute $s = 0$ and $c = 1$ in (1.37), ending up with a standard D1 brane solution. This confirmed by the fact that the T-duality direciton x_2 was wrapped by the D2 branes in Type IIA, that hence loose one dimension in Type IIB. In addition, one ends up just with a nontrivial C_2 potential, which is sourced precisely by D1 branes. Vice versa, taking $\tilde{x} = x_3$ one has to substitute $s = 1$ and $c = 0$ in (1.37), ending up with a nontrivial C_4 potential only, which is sourced by D3 brane. The hybrid solution (1.37) seems to be sourced by both D1 and D3 branes. To confirm this intuition it is useful to perform a probe calculation.

To prove that the solution (1.37) is sourced by D1 and D3 branes we need to take a mixed D1-D3 probe that is parallel to the sourced branes. We hence take a D3 probe wrapping t, x_1, x_2, x_3. To turn on a D1 charge inside the probe it is sufficient to turn on a constant potential F_2 on the probe worldvolume:

$$F_2 = f dx_2 \wedge dx_3 \tag{1.39}$$

where f is a constant. Using the action (1.21) it is possible to compute the potential energy V for the probe:

$$V = -K^{-\frac{1}{2}} H^{-\frac{3}{4}} \sqrt{1 + A^2} + C_{0123} + C_{01}(B_{01} + F_{01}) \tag{1.40}$$

where

$$A = K(F_{01} + B_{01}) = fK - cs(H^{\frac{1}{2}} - H^{-\frac{1}{2}}) \tag{1.41}$$

Now (1.41) can be rewritten as

$$A = H^{\frac{1}{2}} s(fs - c) + H^{-\frac{1}{2}} c(fc + s)$$

and therefore setting the constant f in (1.39)

$$f = \frac{c}{s} \tag{1.42}$$

one gets $A = H^{-\frac{1}{2}} c/s$ and $1 + A^2 = H^{-\frac{1}{2}} K/s^2$. Substituting these expressions in (1.40) and assuming $s \geq 0$ one has

$$V = \frac{1}{s} \tag{1.43}$$

Hence there is no force exerted by the D1-D3 background on the D1-D3 probe for $f = c/s$, the potential being constant.

As our D1-D3 probe is in equilibrium everywhere in the geometry defined by (1.37) and as the latter is a supersymmetric solution, one can safely conclude that this geometry is precisely sourced by D1-D3 branes. Aside from the properties of T-duality, this example also shows how powerful the probe computation is. Probes will be used extensively in the next chapters to provide checks and relevant information about the examined solution.

CHAPTER 2

BUBBLED SOLUTIONS

2.1 Geometric Transitions

The solutions presented explicitly in Chapter 1 are all singular. There exist different types of singularities in Supergravity and a priori singular doesn't mean physically meaningless. As an example, a curvature singularity that is cloaked by an horizon gives rise to a physically acceptable black-hole like solution. However one of the most prominent characteristics of String Theory is that it gives rise to many completely smooth solutions. Smooth solutions are particularly attractive for many reasons: for instance, they are widely used to explain some of the black hole paradoxes and to construct cosmological models that match modern observations within String Theory.

The mechanism that gives rise to smooth solutions as opposed to singular solutions is known as *geometric transition* [10, 11]. Consider for instance some localized branes wrapping a circle. At weak effective coupling these objects can be described by studying open strings that live on them. One can also estimate their number by integrating a suitable field strength over a cycle that is dual to the initial circle. Then, if one increases the coupling, the branes start to backreact on the geometry and the circle they wrap shrinks to zero size, as a consequence of the metric. The branes now have to be described by means of closed strings. At the same time, the dual gaussian cycle blows up and becomes topologically nontrivial. As the localized branes vanish, their charges remain dissolved into the fluxes that thread these cycles. The solutions obtained through this mechanism are smooth, where smoothness is obtained at the cost of a more complicated topology.

There is a nice simple example where one can get a mathematically friendly solution starting from an apparently simple one which is found in a domain as simple as classical

physics. Think of a charged point-particle at the center of empty space: this apparently trivial construction is mathematically extremely elaborate. Not only the potential is divergent at the location of the particle, but important quantities such as the charge densities are not even functions but distributions. If one "blows up " the charged point particle into a uniformly charged sphere the electric potential is now continuous (but not derivable at the radius of the sphere) and all the other quantities are much friendlier. Smoothness is hence added at the cost of blown-up cycles. This mechanism is somehow analogous to what happens in String Theory, where all the sophistications insured by a rigorous theoretical framework insure that the overall solution is smooth.

The rest of this chapter is dedicated to the presentation of some of the most famous smooth solutions in String Theory. These solutions are used to investigate different areas of String Theory and the following chapters will contribute to make progress in the different directions these solutions are analyzed for:

- In § 2.2 we present the smooth solution found by Lin, Lunin and Maldacena (LLM) in [1]. Chapter 3 is dedicated to further analyzing this solution and showing the existence of metastable states that break supersymmetry within this solution [12].

- In § 2.3 we describe the smooth geometries first constructed in [2, 3] that are used to construct three-charge, five-dimensional BPS black hole microstates. These ideas together with the proof of instability for similarly constructed microstates for near-BPS black holes are further discussed in Chapter 4, that illustrates the main results of [13].

- In § 2.4 the Klebanov-Strassler solution [4] is introduced. This solution is a fundamental tool to test the KKLT uplift mechanism [14] that aims at constructing stable dS spaces in String Theory, hence creating solutions with a positive cosmological constant as experimental observations require. Recent investigations underlined some possible issues to this construction and in Chapter 5 we present the T-dual solution of the KS solution as a first step to further test these issues in a different duality frame than the original [15].

- The smooth solutions of § 2.3 can have also other purposes than being black hole microstates. Indeed, by suitably modifying these solutions in Chapter 6 and reducing them to five dimensions they can be used to construct the first $\mathcal{N} = 1$ supergravity solution where the Killing spinor is timelike and spacelike in distinct open regions of the space [16]. These solutions hence nicely interpolates between the two different classes (timelike and spacelike) that were classified in [17].

2.2 The Lin-Lunin-Maldacena solution

In this Section we present the first example of bubbled solution, found by Lin, Lunin and Maldacena in [1] and that will be further explored in Chapter 3. Originally, this was found as a Type IIB solution, while here we present it in the eleven-dimensional duality frame obtained by applying a suitable T-duality and then uplifting - see § 1.4 and § 1.3. This operation is carried on in preparation of the analysis conducted in Chapter 3. The original Type IIB solution is presented in Appendix A.1.

The LLM solution essentially represents a smooth solution of M2 branes polarized into M5 branes where the brane charges are dissolved into flux instead of being polarized.
As recalled in § 1.1 a solution in eleven-dimensional supergravity consists of an eleven-dimensional metric and a four-form field strength. For the LLM solution these fields are given by[1]:

$$ds_{11}^2 = H^{-2/3}(-dt^2 + d\omega_1^2 + d\omega_2^2) + H^{1/3}\Big[h^2(dy^2 + dx^2) + ye^G d\Omega_3^2 + ye^{-G} d\tilde{\Omega}_3^2\Big] \tag{2.1}$$

$$\begin{aligned} G_4 = &-d(H^{-1}h^{-2}V) \wedge dt \wedge d\omega_1 \wedge d\omega_2 \\ &+ \big[d(y^2 e^{2G}V) - y^3 \star_2 dA\big] \wedge d\Omega_3 + \Big[d(y^2 e^{-2G}V) - y^3 \star_2 d\tilde{A}\Big] \wedge d\tilde{\Omega}_3 \end{aligned} \tag{2.2}$$

where the warp factor H is given by

$$H = e^{-2\Phi} = h^2 - V^2 h^{-2} \tag{2.3}$$

Comparing (2.1) with (1.9) one can see that the metric (2.1) describes a three-dimensional external space corresponding to the M2 brane worldvolume directions warped on an eight-dimensional transverse manifold that consists of a two-dimensional subspace spanned by the coordinates (y, x) and two three-spheres S^3 and $\tilde{S}^3$. The Hodge star $\star_2$ refers to the flat space spanned by (y, x). The functions $A, \tilde{A}, h, G, V$ are given by

$$A = \frac{z + \frac{1}{2}}{y^2} \quad \tilde{A} = \frac{z - \frac{1}{2}}{y^2} \tag{2.4}$$

$$h^{-2} = 2y \cosh G \quad G = \operatorname{arctanh}(2z) \tag{2.5}$$

$$y\partial_y V = \partial_x z \quad y\partial_x V = -\partial_y z \tag{2.6}$$

The full solution is determined in terms of a single master function $z(x, y)$ that obeys a linear equation:

$$\partial_x^2 z + y\partial_y\left(\frac{\partial_y z}{y}\right) = 0 \tag{2.7}$$

The coordinate y plays a special role since it is the product of the radii of the two three-spheres. At $y = 0$ at least one of the two three-spheres shrinks to zero size. For the

[1]Note that the four-form field strength as given in (2.35) of [1] is incorrect.

geometry to be smooth, the shrinking three-sphere and the radial direction should combine to form $\mathbb{R}^4$. This requires the function z to have a special behavior. The geometry is non-singular if the boundary values of equation (2.7) are $z = \pm\frac{1}{2}$ on the $y = 0$ line spanned by x. As long as $y \neq 0$ there are two non-vanishing three-spheres, S^3 and $\tilde{S}^3$. At the $y = 0$ line, S^3 shrinks to zero in a non-singular fashion if $z = -\frac{1}{2}$, while $\tilde{S}^3$ shrinks smoothly if $z = \frac{1}{2}$. Both spheres shrink at the boundary of these two regions where they combine to form $\mathbb{R}^8$.

One way to pictorially represent the boundary behavior of z in the $y = 0$ line is by drawing black and white strips according to the value of $z = \pm\frac{1}{2}$. We depict this black and white partitioning of the real line x in Figure 2.1.

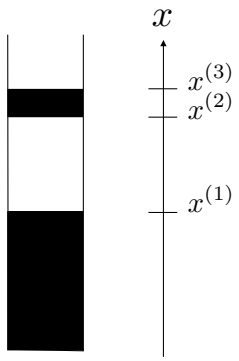

Figure 2.1: A general LLM solution in eleven-dimensional supergravity is defined by the boundary values of z on the $y = 0$ line spanned by x. The line is hence divided into segments (that are possibly semi-infinite), which are colored in white if $z = +\frac{1}{2}$ and in black if $z = -\frac{1}{2}$. A different partition of this line corresponds to a different solution of the LLM family.

2.2.1 The multi-strip solution

A general LLM smooth solution is determined by a superposition of solutions to (2.6) and (2.7) with the boundary value of z being $\pm 1/2$:

$$z_0(x, y) = \frac{1}{2}\frac{x}{\sqrt{x^2 + y^2}} \tag{2.8}$$

$$V_0(x, y) = -\frac{1}{2}\frac{1}{\sqrt{x^2 + y^2}} \tag{2.9}$$

For the metric (2.1) to asymptote to $AdS_4 \times S^7$, i.e. the standard M2 brane solution (1.9), the multi-strip solution must have a semi-infinite black region at one side of the $y = 0$ line and a semi-infinite white region on the other. The simplest non-trivial solution corresponds to a pair of finite-size white and black strips with adjacent semi-infinite black and white regions, represented in Figure 2.1. A general multi-strip solution is then obtained by

superposition:

$$z(x,y) = \sum_{i=1}^{2s+1} (-1)^{i+1} z_0(x - x^{(i)}, y) \tag{2.10}$$

$$V(x,y) = \sum_{i=1}^{2s+1} (-1)^{i+1} V_0(x - x^{(i)}, y) \tag{2.11}$$

where $x^{(i)}$ is the position of the ith boundary and s denotes the number of pairs of white and black strips. For odd i the boundary changes from black to white while for even i the boundary changes from white to black. This will be the general form of a smooth solution corresponding to dielectric vacua of the mass-deformed theory.

2.2.2 M2 and M5 charges

We now show that the metric (2.1) indeed asymptotes to the standard M2 brane solution (1.9) With the coordinate transformation

$$y = \frac{R^2}{2} \sin\alpha \qquad x = \frac{R^2}{2} \cos\alpha \tag{2.12}$$

the two three-spheres combine with the angle α to form a seven-sphere. For large radius R the warp factor H reduces to the warp factor of an M2 brane and we precisely recover (1.9). In § 1.1 it was recalled that the number of M2 branes N can be measured as:

$$N = \frac{1}{(2\pi l_p)^6} \int_{S^7_\infty} \star_{11} G_4 \tag{2.13}$$

where S^7_∞ is a seven-sphere in the asymptotic region that surrounds the M2 branes. From the expansion of the warp factor of the multi-strip solution introduced in the previous section we get:

$$R^6 H = 8 \sum_{i=1}^{s} \Big[(x^{(2i+1)} - x^{(2i)}) \sum_{j=1}^{i} (x^{(2j)} - x^{(2j-1)}) \Big] \equiv 8T \tag{2.14}$$

from which we get that the M2 charge of the solution is related to the strip widths as:

$$N = \frac{T}{4\pi^2 l_p^6} \tag{2.15}$$

As discussed in [1], a useful way to represent a LLM geometry is through the Young diagram corresponding to the momentum basis of free fermions. It is easy to see that T corresponds to the number of boxes of the Young diagram associated to the particular configuration. For a general multi-strip solution, the black and white regions map to the

vertical/horizontal edges of the Young diagram with the edge sizes corresponding to the sizes of the respective strips (see Figure 2.2 for an illustration).

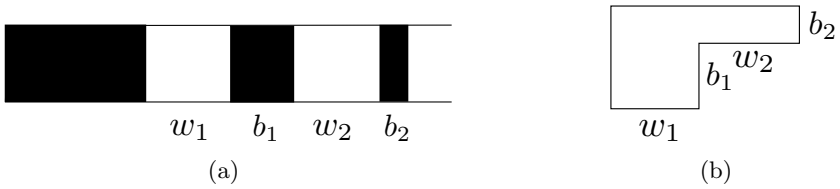

Figure 2.2: Correspondance between the partition of the real line that defines a general solution (a) and the Young diagram (b), illustrated for a two-strips solution.

However, even though the metric (2.1) asymptotes that of an M2 brane solution, the LLM solution as a whole does not asymptote to the M2 solution. Indeed, G_4 does not tend to the standard harmonic solution (1.9) (*i.e.* with legs along the M2 worldvolume only) as it also contains two additional transverse terms. These are the non-normalizable modes associated to the mass perturbation in the dual M2 brane theory. These transverse fluxes give rise to a M5 dipole charge:

$$M = \frac{1}{(2\pi l_p)^3} \int_{S^4} G_4 \tag{2.16}$$

There are various topological 4-cycles in the multi-strip solution. For example, we can consider an S^4 containing an S^3, which is obtained by fibering the S^3 on a curve ξ_w that encloses a white strip and whose boundary ends at $y = 0$ on a region where $z = -1/2$, *i.e.* where the S^3 smoothly shrinks to zero size, as illustrated in Figure 2.3.

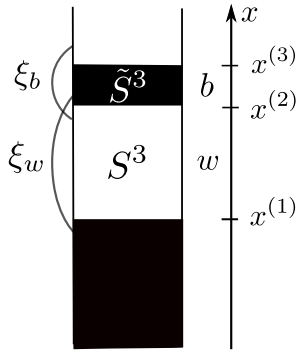

Figure 2.3: The M5 charge corresponding to a white (black) strip is obtained by integrating the four-form flux over a four-cycle obtained by fibering the S^3 ($\tilde{S}^3$) over the curve ξ_w (ξ_b) whose end points lie in a region where the S^3 ($\tilde{S}^3$) shrinks to zero size.

For definiteness, let us consider the first white strip of length $w = x^{(2)} - x^{(1)}$. We then

obtain, from (2.2):

$$(2\pi l_p)^3 M_w = 2\pi^2 \int_{\xi_w} \Big[d(y^2 e^{2G} V) - y^3 \star_2 dA \Big] \tag{2.17}$$

The function $y^2 e^{2G} V$ is smooth and globally well-defined and so the first term in (2.17) does not contribute to the integral via Stokes theorem. The second term in (2.17) satisfies the Laplace equation $d(y^3 \star_2 dA) = 0$. Hence we obtain:

$$(2\pi l_p)^3 M_w = 4\pi^2 \int_{x^{(1)}}^{x^{(2)}} dx \left(z + \frac{1}{2} \right) \Big|_{z=1/2} = 4\pi^2 \left(x^{(2)} - x^{(1)} \right) = 4\pi^2 w \tag{2.18}$$

We learn that the M5 charge corresponding to the four-form flux through the S^4 is proportional the size of the white strip w. Similarly, the M5 charge M_b, corresponding to four-form flux through an $\tilde{S}^4$ containing an $\tilde{S}^3$, obtained by fibering the $\tilde{S}^3$ on a curve ξ_b, is proportional to the size of the black strip b:

$$(2\pi l_p)^3 M_b = 4\pi^2 b \tag{2.19}$$

Clearly, the same result also applies for a general multi-strip solution, which contains various 4-cycles. From charge quantization, this result also gives the quantization condition for the length of the strips and it agrees with the result found in [18].

As a further check of our normalizations, we note that we can compute the M2 charge of the solution (2.13) from the IR data, using the transverse fluxes. We can do this by deforming the S^7 to the IR region $y \approx 0$, according to $S^7_\infty = \mathcal{D}_7 + \partial \mathcal{M}_8$, where $\mathcal{D}_7$ is a shrinking region with $y \approx 0$ and $\mathcal{M}_8$ is spanned by (y, x) and the two three-spheres. Since the geometry is smooth the integral over $\mathcal{D}_7$ vanishes and (2.13) reduces to

$$(2\pi l_p)^6 N = -\frac{1}{2} \int_{\mathcal{M}_8} G_4 \wedge G_4 \tag{2.20}$$

where we used the equation of motion $d \star_{11} G_4 = -\frac{1}{2} G_4 \wedge G_4$. The integral on the right hand side of (2.20) can be shown to factorize into products of M5 charges over the various four-spheres of a general multi-strip solution, given in (2.18) and (2.19). By taking into account the correct orientation of the fluxes, there are cancellations that lead precisely to the result (2.15), expressing N in terms of the number of blocks of the corresponding Young diagram. We note that for the solution corresponding to a single pair of finite-size black and white strips of length respectively w and b, the M2 charge is simply given by

$$N = \frac{wb}{4\pi^2 l_p^6} \tag{2.21}$$

which indeed corresponds to the number of boxes of a rectangular Young diagram after

taking into account the normalization (2.18).

In Chapter 3 we carry on a probe computation similar to that of § 1.4.2 to show that a mixed M2-M5 probe has a flat potential in the LLM solution. This shows that one can think of the LLM solution as being sourced by mixed M2-M5 branes, even though there are no localized sources and the whole solution is smooth. More interestingly, it will be shown that for some specific configurations of the probes M2-M5, these present metastable minima that break supersymmetry in the solution [12]. The study of this supersymmetry breaking is particularly interesting as in principle it can be linked to new black hole microstate geometries. In addition, the study of the metastable configuration can be paralleled with an analysis of supersymmetry breaking in the dual gauge theory.

2.3 Eleven-dimensional Microstate Geometries

In this section we review the construction of smooth eleven-dimensional, three-charge BPS microstate geometries. These are smooth eleven-dimensional solutions that once compactified to five dimensions are very similar to a class of three-charge black hole solutions, but contrarily to the latter they remain completely smooth. Therefore, these solutions have exactly the same charges and asymptotically the same metric as black hole solutions, but have no horizon and the would-be infinite black hole throat is capped-off to a finite length. At the bottom of the throat one can find the nontrivial topology that supports the flux necessary to justify the asymptotic charges. Smooth solutions that simulate black hole solutions are called *black hole microstates*. This notion will be further explained in Chapter 4 and we will focus on the construction of eleven-dimensional, three-charge microstate geometries in the meantime.

The solutions we are going to described were first found in [2, 3]. These preserve $\mathcal{N} = 4$ supercharges in 11D supergravity compactified on three tori. The metric and the three-form potential are given by[2]:

$$\begin{aligned} ds_{11}^2 &= -(Z_1 Z_2 Z_3)^{-\frac{2}{3}}(dt+k)^2 + (Z_1 Z_2 Z_3)^{\frac{1}{3}} ds_4^2 + (Z_1 Z_2 Z_3)^{\frac{1}{3}} \sum_{i=1}^{3} \frac{dx_{4+i}^2 + dx_{5+i}^2}{Z_i} \\ A^{(3)} &= A^1 \wedge dx^5 \wedge dx^6 + A^2 \wedge dx^7 \wedge dx^8 + A^3 \wedge dx^9 \wedge dx^{10} \end{aligned} \tag{2.22}$$

where k is the angular momentum vector, Z_i are the three warp factors associated to the electric conserved charges and $dx_{4+i}^2 + dx_{5+i}^2$ for $i = 1, 2, 3$ is the standard metric on a torus. Note that the structure of (2.22) is very similar to the solution sourced by three stacks of M2 branes (1.15), with the difference that (2.22) is completely smooth. Again, this is achieved via a nontrivial topology. The metric of the base space of this solution,

[2]While in Chapter 1 we used H to denote warpfactor, we use here the symbol Z to make contact with the notation that has become standard in the microstate literature. This notation will be maintained in Chapter 4.

ds_4^2, is chosen to be a multi-center Gibbons-Hawking/Taub-NUT metric:

$$ds_4^2 = V^{-1}(d\psi + \vec{A}\cdot d\vec{y})^2 + V(dy_1^2 + dy_2^2 + dy_3^2) \tag{2.23}$$

where

$$\vec{\nabla}\times\vec{A} = \vec{\nabla}V \tag{2.24}$$

and the Taub-NUT fiber ψ has period 4π. All the functions that appear in the solution (2.22) and in (2.23) depend on (y_1, y_2, y_3), and the full solution is completely determined by specifying four harmonic functions:

$$V = \sum_{j=1}^{N}\frac{v_j}{r_j} \qquad K^I = \sum_{j=1}^{N}\frac{k_j^I}{r_j} \qquad I = 1,...3 \qquad r_j = |\vec{y} - \vec{g}_j| \tag{2.25}$$

where N is the number of GH centers located at $\vec{g}_i$ and (v_j, k_j^I) are parameters to specify. Notice that one can potentially add some constants δV and δK^I to the functions in (2.25) so that the GH space asymptotes to $\mathbb{R}^3\times S_1$ and the δK^I generate some Wilson lines for the three form in (2.22). As we want the GH space to asymptote $\mathbb{R}^4$ these constants are taken to be zero.

Restricting to $v_j \in \mathbb{Z}$, the GH centers become benign orbifold singularities. The geometry in (2.23) asymptotes to flat $\mathbb{R}^4$ if one also requires

$$\sum_{j=1}^{N} v_j = 1 \tag{2.26}$$

The GH metric (2.23) is then ambipolar, meaning that its signature switches from $(+,+,+,+)$ to $(-,-,-,-)$. However, as shown in [19], this is not a problem for the full solution (2.22), which is everywhere smooth and has Lorentzian signature.

The warp factors Z_I of the solution are

$$Z_I = L_I + \frac{1}{2}C_{IJK}\frac{K^I K^J}{V} \tag{2.27}$$

where the L_I are harmonic functions in the GH space. Requiring the Z_I to be smooth at the GH centers and fixing their asymptotic value to 1 imply that

$$L_I = 1 - \frac{1}{2}C_{IJK}\sum_{j=1}^{N}\frac{k_j^I k_j^K}{v_j}\frac{1}{r_j} \tag{2.28}$$

where $C_{IJK} \equiv |\varepsilon_{IJK}|$. The BPS solution for the angular momentum vector k is written as

$$\vec{k} = \mu(d\psi + \vec{A}) + \vec{\omega} \tag{2.29}$$

where A is defined in (2.24) and μ is given by

$$\mu = \frac{C_{IJK}K^I K^J K^K}{6V^2} + \frac{K^I L_I}{2V} + M \tag{2.30}$$

with M another harmonic function. The vanishing of μ at the GH centers determines M as

$$M = m_0 + \frac{1}{12} C_{IJK} \sum_{j=1}^{N} \frac{k_j^I k_j^J k_j^K}{v_j^2} \frac{1}{r_j} \tag{2.31}$$

where m_0 is a constant whose value is found requiring that k vanishes at infinity:

$$m_0 = -\frac{1}{2} \sum_{j=1}^{N} \sum_{I} k_j^I \tag{2.32}$$

The last form to define in (6.21) is $\vec{\omega}$, which is given by:

$$\vec{\omega} = \frac{1}{24} C_{IJK} \sum_{i,j=1}^{N} v_i v_j \Pi_{ij}^I \Pi_{ij}^J \Pi_{ij}^K \vec{\omega}_{ij} \qquad \Pi_{ij}^I \equiv \frac{k_j^I}{v_j} - \frac{k_i^I}{v_i} \tag{2.33}$$

where, choosing a coordinate system with $\vec{y}^i = (0,0,a)$, $\vec{y}^j = (0,0,b)$ with $a > b$ and defining $\tan\phi = y_2/y_1$, one has:

$$\vec{\omega}_{ij} = -\frac{y_2^2 + y_1^2 + (y_3 - a + r_i)(y_3 - b - r_j)}{(a-b) r_i r_j} d\phi \tag{2.34}$$

To avoid the existence of closed-timelike-curves (CTCs) it is necessary that

$$Z_1 Z_2 Z_3 V - \mu^2 V^2 \geq 0 \tag{2.35}$$

holds everywhere in the GH space.

Furthermore, to avoid Dirac-Misner strings, the solution must satisfy the *bubble equations* that constrain the distances between the GH centers [20, 19, 3]:

$$\sum_{j=1\, j\neq i}^{N} \Pi_{ij}^{(1)} \Pi_{ij}^{(2)} \Pi_{ij}^{(3)} \frac{v_i v_j}{r_{ij}} = -2 \left(m_0\, v_i + \frac{1}{2} \sum_{I=1}^{3} k_i^I \right) \tag{2.36}$$

whith Π_{ij}^I as in (2.33). Only $N-1$ out of N bubble equations are independent: indeed summing the LHS of (2.36) over i one gets zero as the Π_{ij}^I are anti-symmetric in ij. For smooth microstate solutions this condition is equivalent to the vanishing of μ in (2.30) at every GH center [21]. Finally the electric three-form in (2.22) is specified by

$$dA^I = \Theta^I - d\left(\frac{dt + k}{Z_I} \right) \tag{2.37}$$

where Θ^I are the dipole field strengths

$$\Theta^I = -\sum_{a=1}^{3}[\partial_a(V^{-1}K^I)][(d\psi + A)\wedge dy^a + \frac{1}{2}V\varepsilon_{abc}\,dy^b\wedge dy^c] \tag{2.38}$$

In the formula above A is the three form computed in (2.24). In the next section we give a physical interpretation of some bubble solution and explain the role of the dipole field strengths.

2.3.1 Conserved charges and bubbles

Expanding the warp factors Z_I in (6.19) and the momentum vector of (6.21) it is possible to read the three electric charges Q_I and the two angular momenta J_1 and J_2 preserved by this solution. In particular, once the parameters (v_j, k_j^I) have been specified the charges Q_I, and the sum of the angular momenta are:

$$\begin{aligned} Q^I &= -2C^{IJK}\sum_{j=1}^{N} v_j^{-1}\tilde{k}_j^J\tilde{k}_j^K \\ J_1 + J_2 &= \frac{4}{3}C^{IJK}\sum_{j=1}^{N} v_j^{-2}\tilde{k}_j^I\tilde{k}_j^J\tilde{k}_j^K \end{aligned} \tag{2.39}$$

where

$$\tilde{k}_j^I \equiv k_j^I - v_j\sum_s k_s^I \tag{2.40}$$

The expression for the difference of the angular momenta depends also on the positions, $\vec{g}_i$, of the GH centers [3]:

$$J_1 - J_2 = 8|\vec{D}| \qquad \vec{D} = \sum_{I=1}^{3}\sum_{j=1}^{N}\tilde{k}_j^I\vec{g}_j \tag{2.41}$$

The three electric charges Q^I and the two angular momenta J_1 and J_2 are the only conserved charges of (2.22) and they can be seen from infinity. It is however useful to understand where the bubbled cycles are in the solution (2.22) and what kind of flux they are threaded by. Nontrivial cycles can be constructed by fibering the Gibbons-Hawking coordinate ψ of (2.23) on a line connecting two GH centers g_i and g_j. As it is clear from (2.23) the radius of the circle ψ vanishes at the location of a GH center and therefore this fibration creates two-dimensional surfaces in the GH space that are topologically equivalent to two-spheres S_2. The dipole field strengths introduced in (2.38) were introduced in the original construction of [2] precisely to measure the flux threading

these bubbles. Denoting Δ_{ij} the S_2 stretched from g_i to g_j one finds:

$$\int_{\Delta_{ij}} \Theta^I = \Pi^I_{ij} \tag{2.42}$$

where the fluxes Π^I_{ij} are precisely those defined in (2.33). These fluxes prevent the various two-cycles Δ_{ij} from collapsing. Indeed, being threaded by fluxes, the various Δ_{ij} should collapse under the effect of gravity. At the same time the shrinking of these cycles is opposed by a form of electrical repulsion and the balance between gravitational attraction and electrical repulsion is exactly what prevents these cycle from collapsing. The fluxes (2.42) are not visible from infinity and they do not constitute conserved charges in the rigorous sense, but they clearly contribute to the final conserved charges.

2.4 The Klebanov-Strassler Solution

The Klebanov-Strassler (KS) solution [4] is a Type IIB supergravity solution that preserves four supercharges and is completely smooth, as there are no localized sources but only fluxes threading a nontrivial topology. It can be thought of as the geometric transition of the singular Klebanov-Tseytlin solution [22]. The latter is similar to a standard D3 brane solution (1.34), where the six-dimensional external space is no longer euclidean, but is substituted by a manifold called *singular conifold*. This is essentially a cone whose base is topologically equivalent to an $S_2 \times S_3$, that being Ricci-flat solves theType IIB equations of motion. In the Klebanov-Tseytlin solution one further adds D5 branes parallel to the D3 branes and wrapping the S_2 within the singular conifold. As the S_2 shrinks at the tip of the cone so do the D5 branes, which hence cannot be seen from infinity and give rise to a dipole charge rather than a conserved charge. This solution is clearly singular at the location of the D3 branes and to make things even worse, this singularity cannot be cloaked by an horizon, which compromises the overall physical validity of the solution.

The geometric transition in KS replaces the branes with fluxes and at the same time puffs up some nontrivial cycles within the space transverse to the branes. Consequently, the overall KS metric looks like the standard D3 brane solution (1.34), with a four-dimensional warped Minkowski space and a (warped) six-dimensional internal space given by a *deformed conifold*. The latter is still a cone over a base that is topologically equivalent to an $S_2 \times S_3$, but as a result of the geometric transition the S_3 attains a finite radius at the tip of the cone and is threaded by constant fluxes, while the S_2 smoothly shrinks in this region.

To write the full KS solution it is first necessary to parameterize the deformed conifold and equip it with a Ricci-flat metric. In Chapter 5 we present three different coordinate systems for this manifold, each of them suitable to show some of its specific properties. Here it suffices to say that the base of the deformed conifold is a $T^{1,1}$ space, defined in [23]

as the quotient manifold

$$T^{1,1} = \frac{SU(2) \times SU(2)}{U(1)} \tag{2.43}$$

The $T^{1,1}$ space can be described by a combination of the Euler angles of the two $SU(2)$, consisting of two pairs of angles $\phi_i \in [0, 2\pi[$ and $\theta_i \in [0, \pi[$ with $i = 1, 2$ and a coordinate $\psi = \psi_1 + \psi_2 \in [0, 4\pi[$ arising from the quotient. These, together with a coordinate $\tau \geq 0$ for the radius of the cone, will be referred to as the *coset coordinates* for the deformed conifold. A standard basis of one-forms was found in [24]:

$$\begin{aligned} g^1 &= \frac{e^1 - e^3}{\sqrt{2}} & g^2 &= \frac{e^2 - e^4}{\sqrt{2}} & g^3 &= \frac{e^1 + e^3}{\sqrt{2}} \\ g^4 &= \frac{e^2 + e^4}{\sqrt{2}} & g^5 &= e^5 \end{aligned} \tag{2.44}$$

where

$$\begin{aligned} e^1 &= -\sin\theta_1\, d\phi_1 & e^2 &= d\theta_1 & e^3 &= \cos\psi \sin\theta_2\, d\phi_2 - \sin\psi\, d\theta_2 \\ e^4 &= \sin\psi \sin\theta_2\, d\psi_2 + \cos\psi\, d\theta_2 & e^5 &= d\psi + \cos\theta_1\, d\phi_1 + \cos\theta_2\, d\phi_2 \end{aligned} \tag{2.45}$$

Then the Ricci-flat Hyper-Kähler metric on the deformed conifold is [24]:

$$ds_6^2 = \frac{1}{2}\varepsilon^{\frac{4}{3}} K(\tau) \left[\frac{1}{3K^3(\tau)} [d\tau^2 + (g^5)^2] + \cosh^2\frac{\tau}{2}[(g^3)^2 + (g^4)^2] + \sinh^2\frac{\tau}{2}[(g^1)^2 + (g^2)^2] \right] \tag{2.46}$$

with

$$K(\tau) = \frac{(\sinh 2\tau - 2\tau)^{\frac{1}{3}}}{2^{\frac{1}{3}} \sinh\tau} \tag{2.47}$$

where ε is a deformation parameter. In particular, $K(\tau)$ is finite at the tip of the cone $\tau = 0$ and the metric (2.46) becomes the metric of a three-sphere whose radius depends on ε, as will be shown in Chapter 5.

It is now possible to write the full Klebanov-Strassler solution. The metrics looks like the standard D3 brane ansatz (1.34):

$$ds_{KS}^2 = h(\tau)^{-\frac{1}{2}}\, dx^i dx^i + h(\tau)^{\frac{1}{2}} ds_6^2 \tag{2.48}$$

where $dx^i dx^i$ is the standard four-dimensional Minkowski metric and ds_6^2 is as in (2.46). The warp factor $h(\tau)$ in (2.48) is given by:

$$h(\tau) = (g_s M \alpha')^2 \varepsilon^{-\frac{8}{3}} 2^{\frac{2}{3}} I(\tau) \qquad I(\tau) = \int_\tau^\infty dx\, \frac{x\coth x - 1}{\sinh^2 x} (\sinh 2x - 2x)^{\frac{1}{3}} \tag{2.49}$$

where $I(\tau)$ in (2.49) attains the value $a_0 \approx 0.71805$ for $\tau = 0$ so that the whole space-time (2.48) is smooth. The parameter M in (2.49) can be thought of as the quantized

number of D5 charge units preserved by this solution and measured by the three-form RR field strength. The RR and NS-NS fields are written in the canonical basis of one-forms on the deformed conifold (2.44):

$$B_2 = \frac{g_s M \alpha'}{2} \left[f(\tau) g^1 \wedge g^2 + k(\tau) g^3 \wedge g^4 \right] \tag{2.50}$$

$$F_3 = \frac{M \alpha'}{2} \left\{ g^5 \wedge g^3 \wedge g^4 + d[F(\tau)(g^1 \wedge g^3 + g^2 \wedge g^4)] \right\} \tag{2.51}$$

$$F_5 = \mathcal{F}_5 + \star \mathcal{F}_5 \tag{2.52}$$

$$\mathcal{F}_5 = B_2 \wedge F_3 = \frac{g_s M^2 (\alpha')^2}{4} \, \ell(\tau) \, g^1 \wedge g^2 \wedge g^3 \wedge g^4 \wedge g^5$$

$$\star \mathcal{F}_5 = 4 g_s M^2 (\alpha')^2 \varepsilon^{-\frac{8}{3}} \frac{\ell(\tau)}{K(\tau)^2 h^2 \sinh^2 \tau} \, dt \wedge dx^1 \wedge dx^2 \wedge dx^3 \wedge d\tau \tag{2.53}$$

where the functions f, k, F, l are given by:

$$f(\tau) = \frac{\tau \coth \tau - 1}{2 \sinh \tau} (\cosh \tau - 1) \qquad k(\tau) = \frac{\tau \coth \tau - 1}{2 \sinh \tau} (\cosh \tau + 1)$$

$$F(\tau) = \frac{\sinh \tau - \tau}{2 \sinh \tau} \qquad \ell(\tau) = \frac{\tau \coth \tau - 1}{4 \sinh^2 \tau} (\sinh 2\tau - 2\tau) \tag{2.54}$$

The fields B_2 in (2.50) and F_3 in (2.51) are nonzero at the tip, while F_5 smoothly vanishes there. Away from the tip, F_5 measures $N = kM$ units of fluxes threading the $T^{1,1}$ space, where k is an integer that jumps periodically with τ and is zero at the tip. Consequently, if one relates the cone coordinate τ with the energy scale of the dual gauge theory, each jump in the fluxes should represent a phase transition. Indeed, the KS solution is dual to the four dimensional $\mathcal{N} = 1$ $SU(N+M) \times SU(N)$ gauge theory. Each jump in the F_5 flux on the $T^{1,1}$ space corresponds to a Seiberg duality [25] between the $SU(N+M) \times SU(N)$ and the $SU(N+M) \times SU(N+2M)$ gauge theories. The puffing-up of the S_3 at the tip is due to the chiral symmetry breaking of the infrared physics of this gauge theory. These concepts will become more clear in Chapter 5, where the KS solution will be T-dualized to Type IIA following [15].

Part II

Black holes and smooth solutions

CHAPTER 3

METASTABILITY AND SUPERSYMMETRY BREAKING IN THE LIN-LUNIN-MALDACENA SOLUTION

3.1 Outline: metastable supersymmetry breaking

In this chapter we analyze the metastable supersymmetry breaking in the context of the LLM solution presented in Section 2.2. This is a smooth supergravity solution dual to the mass-deformed M2 brane theory. This in turn is part of a class of gauge theory that can in principle exhibit metastable supersymmetry breaking, namely that comprise metastable states that break supersymmetry. This phenomenon is of primary importance to have an insight into non-supersymmetric physics, possibly allowing to apply the technology of String Theory beyond one of its natural theoretical limits that seem nowadays incompatible with the real world, i.e. the fact that one is apparently constrained to study supersymmetric physics only. It is fundamental to stress that these non-supersymmetric states are not stable, but metastable. This means that they will decay to a stable supersymmetric state in a finite (but possibly very long) amount of time. Indeed, stable non-supersymmetric states cannot exist within a theory that is supersymmetric by construction. The fact that one compromises to study only a metastable supersymmetry breaking is of utmost importance, as supersymmetry allows to exactly solve a much simplified version of the equations of motion.

The existence of metastable non supersymmetric states in the mass-deformed M2 brane theory was already shown in [26], where the potential energy of these states was analyzed within the Polchinski - Strassler (PS) approximation [27]. In this chapter we will find the analogous dual metastable states in the gravity-dual theory, namely the LLM solution [1]. We will also thoroughly explain and made use of the PS approximation.

In addition to this, it will also be shown that the LLM solution in the eleven-dimensional duality frame consists of charges dissolved into flux of M2 branes polarized into M5 brane shells, whose complete backreaction was already caught in [28], even though these solutions are not smooth. This allows to give a better physical interpretation of the LLM solution and its gauge theory dual, stronger connecting the main physical entities on both sides of the gauge-gravity duality.

The strategy to show these results is to probe the LLM solution with M5 branes made of polarized M2 branes with positive or negative charge, wrapping contractible three-cycles.

- When the M2 charges have the same orientation as the background charges, we find that the M5 brane potential has global supersymmetric minima. These correspond to the dielectric vacua of the mass-deformed theory, and we will see that they are geometrized precisely by an LLM solution with an additional pair of black and white strips.

- Allowing the M5 brane probes to have M2 charge opposite to the charge dissolved in the background fluxes, we find that the M5 brane potential has a metastable minimum close to the North Pole of one of the four-spheres (i.e. near an LLM strip boundary), at least for some regime of parameters. This configuration decays via non-perturbative bubble nucleation toward one of the supersymmetric dielectric vacua corresponding to an LLM solution.

The polarized M2-M5 branes in question will be treated as probes, namely we do not take into account their backreaction on the geometry. While for the BPS probes we can easily identify the corresponding solution to be an LLM geometry with an additional strip, for non-BPS probes the backreaction is much more challenging.

The M2-M5 probe action in eleven dimensional supergravity is quite involved and while it is in principle possible to realize the program described above, the cumbersome formulas might make the physical interpretation of the results highly nontrivial. To overcome this trick it is much more convenient to work in the Type IIA duality frame by reducing the LLM solution as written in Section 2.2 along the coordinate ω_2 using then procedure delineated in Section 1.3. In this duality frame one can use D4-F1 probes instead, using the action (1.21) and computing the potential of the hybrid probe in a similar fashion as in Section 1.4.2 As the two frames are related by a duality transformation the results can be equivalently stated for the Type IIA frame with D4-F1 probes or for the eleven-dimensional frame with M2-M5 probes. In the following we will always describe our results talking about M2-M5 probes whenever no ambiguity is implied, even if the computations are always carried on in the dimensionally-reduced frame.

This chapter is organized as follows. In § 3.2 we show the IIA reduction of the LLM M-theory background and we use it to derive the Hamiltonian for a probe M5 brane with dissolved M2 charge in the worldvolume, wrapping a contractible 3-cycle. We also derive

a limit of the Hamiltonian describing a one-dimensional problem relevant to the study of its minima. In § 3.4 we study supersymmetric global minima of the probe Hamiltonian. We also show explicitly that such polarized supersymmetric probes are geometrized by an LLM solution with additional strips. In § 3.5 we show that the probe Hamiltonian admits metastable configurations and we obtain an analytic expression for the position of the minima using a Polchinski-Strassler – type approximation. We then discuss the decay process of these metastable probes to supersymmetric minima corresponding to dielectric vacua of the mass-deformed M2 brane theory. We illustrate the discussion of supersymmetric and metastable minima by plotting the Hamiltonian for a particular example in § 3.4 and § 3.5 respectively. We end with a discussion and a list of open problems in § 3.6. Some additional technical details about the computations can be found in Appendix A.3, A.2 and A.4.

3.2 The LLM solution in the Type IIA frame

To compute the potential for M2 branes polarizing into M5 branes it is convenient to work with the type IIA reduction of the M-theory solution (2.1)-(2.2) along ω_2. We relegate a detailed discussion of the type IIA solution to Appendix A.2 and summarize here the result. The metric and fluxes are:

$$ds^2_{IIA} = H^{-1}(-dt^2 + d\omega_1^2) + h^2(dy^2 + dx^2) + ye^G d\Omega_3^2 + ye^{-G} d\tilde{\Omega}_3^2 \tag{3.1}$$

$$B_2 = -H^{-1}h^{-2}V dt \wedge d\omega_1 \tag{3.2}$$

$$F_4 = \left[d(y^2 e^{2G}V) - y^3 \star_2 dA\right] \wedge d\Omega_3 + \left[d(y^2 e^{-2G}V) - y^3 \star_2 d\tilde{A}\right] \wedge d\tilde{\Omega}_3 \tag{3.3}$$

To compute the polarization potential in the next section we will also need the explicit expressions for the RR gauge potentials C_3 and C_5. Since $C_1 = 0$ we have $F_4 = dC_3$ and $\star F_4 = F_6 = dC_5 + H_3 \wedge C_3$. In the multi-strip solution (2.10)-(2.11) we can solve these equations analytically. For C_3 with legs on the S_3 we have

$$c_3(x,y) = \sum_{i=1}^{2s+1} (-1)^{i+1} \frac{2(x-x^{(i)})^2 + y^2}{2\sqrt{(x-x^{(i)})^2 + y^2}} + x + y^2 e^{2G(x,y)} V(x,y) + c \tag{3.4}$$

In the next section we will discuss in details the role of the constant c corresponding to a gauge choice for c_3. The RR five-form potential C_5 for the multi-strip solution with legs on the S_3 is

$$c_5(x,y) = \frac{2y^2}{1-2z(x,y)} - y^2 + \frac{c_3(x,y)V(x,y)}{H(x,y)h(x,y)^2} \tag{3.5}$$

Similar expressions are obtained for the RR forms with legs along $\tilde{S}_3$ (see Appendix A.2).

3.3 The probe action

We are interested in the potential for M5 branes carrying M2 charge in the M-theory solution discussed in § 2.2. The same potential is obtained from probe D4 branes carrying F1 charge placed in the dimensionally reduced IIA solution discussed in § 3.2. Hence we consider a D4 brane wrapped on a three-sphere of the internal space and which carries dissolved F1 charge along ω_1. The embedding is given by $t = \sigma^0$, $\omega_1 = \sigma^1$ and σ^2, σ^3, σ^4 along the three-sphere. The probe D4 brane action is computed by means of (1.21):

$$\begin{aligned} S_{D4} = -\mu_4 \int d^5\sigma e^{-\Phi} \Big[- \det \left(g_{ab} + 2\pi\alpha' \mathcal{F}_{ab} + B_{ab} \right) \Big]^{1/2} \\ + \mu_4 \int \Big[C_5 + (2\pi\alpha' \mathcal{F}_2 + B_2) \wedge C_3 \Big] \end{aligned} \tag{3.6}$$

where $\mathcal{F}_2$ is the induced worldvolume field strength on the brane

$$\mathcal{F}_2 = \mathcal{E} d\sigma^0 \wedge d\sigma^1 \tag{3.7}$$

and μ_4 is the D4 brane tension

$$\mu_4 = \frac{2\pi}{g_s (2\pi l_s)^5} = \frac{1}{(2\pi)^3 \mu_1 l_p^3} \tag{3.8}$$

where for future use we expressed this quantity in terms of the F1 string tension $\mu_1 = 2\pi\alpha'$ and the eleventh dimensional Planck length l_p. In the background (3.1), with RR gauge potentials given by (3.4) and (3.5), we obtain after integrating on the three-sphere S_3:

$$S_{D4} = \int d^2\sigma \mathcal{L}(\mathcal{E}) \tag{3.9}$$

with

$$\mathcal{L}(\mathcal{E}) = -\mu_4 V_{S_3} \Big[y^{3/2} e^{3G/2} H^{1/2} \sqrt{H^{-2} - (\mathcal{E} + B_2)} + c_5 + (\mathcal{E} + B_2) c_3 \Big] \tag{3.10}$$

where V_{S_3} is the volume of the three-sphere spanned by σ^2, σ^3 and σ^4 and we recall that the warp factor H is given by $H = h^2 - V^2 h^{-2}$. In order to compute the potential for the D4 brane we need to express the Lagrangian in terms of the F1 charge, which is proportional to the electric displacement [29, 30]:

$$n = \frac{\partial \mathcal{L}(\mathcal{E})}{\partial \mathcal{E}} \equiv \mu_1 V_{S_3} \mu_4 \, p \tag{3.11}$$

The Hamiltonian is obtained from the Legendre transformation:

$$\mathcal{H} = n\mathcal{E} - \mathcal{L}(\mathcal{E}) \tag{3.12}$$

This gives the potential for D4 branes with dissolved F1 charge or, equivalently, for M5 branes with dissolved M2 charge:

$$\mathcal{H} = \mu_4 V_{S_3}\Big[H^{-1}\sqrt{Hy^3e^{3G} + (p-c_3)^2} - pB_2 - c_5\Big] \tag{3.13}$$

In the subsequent sections we will study the dynamics of M2 branes polarizing into M5 brane probes as described by this Hamiltonian. Note that we can also consider polarization into multiple M5 branes. The Hamiltonian for m M5 branes is obtained multiplying (3.13) by an overall factor m and exchanging $p \to p/m$.

While we will focus on M5 branes wrapping the S_3 a similar analysis can be carried out for M5 branes wrapping the $\tilde{S}_3$. To obtain the Hamiltonian one just has to replace $G \to -G$ and $V_{S_3} \to V_{\tilde{S}_3}$ in (3.13) and substitute $\tilde{c}_3$ and $\tilde{c}_5$ for the RR fields whose expression is given in Appendix A.2.

To avoid clutter coming from the normalization (3.11), when normalizations are not needed we will often simply use p for the M2 charge.

3.3.1 One-dimensional Hamiltonian

To study the minima of the potential (3.13) of a probe M5 brane wrapping the S_3 of a multi-strip solution we substitute c_3 and c_5 with (3.4)-(3.5). To avoid clutter we drop the overall normalization factor in (3.13). It can be shown that the Hamiltonian minimizes on the $y = 0$ axis, when either one or both of the three-spheres shrink to zero size. We can thus reduce the problem to one dimension finding the explicit form of the Hamiltonian on the $y = 0$ line. Since we are considering an M5 brane wrapping the background S_3, the interesting dynamics will happen inside white strips where S_3 is of finite size. We will thus focus on the $y \to 0$ limit of the Hamiltonian in the region of the real line where the master function z takes the value $+1/2$. When approaching a white strip, the function z in (2.10) behaves as

$$z(x,y) = \frac{1}{2} - y^2\zeta_+^2(x) + \mathcal{O}(y^4) \tag{3.14}$$

which defines the function $\zeta_+^2(x)$. For a multi-strip solution (see § 2.2.1), this function is given by

$$\zeta_+(x) = \frac{1}{2}\sqrt{\sum_{i=1}^{2s+1}(-1)^{i+1}\frac{|x-x^{(i)}|}{(x-x^{(i)})^3}} \tag{3.15}$$

The function $V(x,y)$ then approaches $V_+(x)$:

$$V_+(x) = -\frac{1}{2}\sum_{i=1}^{2s+1}\frac{(-1)^{i+1}}{|x-x^{(i)}|} \tag{3.16}$$

The warp factor and the B-field can be expressed as follows:

$$H_+(x) = \frac{\zeta_+^2(x) - V_+^2(x)}{\zeta_+(x)} \qquad B_+(x) = -\frac{V_+(x)}{\zeta_+^2(x) - V_+^2(x)} \tag{3.17}$$

The three-form gauge potential approaches

$$c_3^+(x) = \sum_{i=1}^{2s+1} (-1)^{i+1} |x - x^{(i)}| + x + \frac{V_+(x)}{\zeta_+(x)^2} + c \tag{3.18}$$

and the five-form gauge potential approaches

$$c_5^+(x) = \frac{1}{\zeta_+^2(x)} - c_3^+(x) B_+(x) \tag{3.19}$$

We give the details of this derivation in Appendix A.3 and we will discuss in a moment the gauge choice for c. The Hamiltonian for a probe M5 brane wrapping the S_3 restricted to white strips on the $y = 0$ line is then given by

$$\mathcal{H}_+(x) = H_+(x)^{-1} \sqrt{\frac{H_+(x)}{\zeta_+^3(x)} + \left[p - c_3^+(x)\right]^2} - B_+(x)\left[p - c_3^+(x)\right] - \frac{1}{\zeta_+^2(x)} \tag{3.20}$$

In the following we study the global and local minima of this Hamiltonian for the multi-strip solution of § 2.2.1. We are most interested in probe M5 branes carrying M2 charge that polarize inside white strips at finite distance from the strip boundaries. This is illustrated for the simplest bubbling solution in Figure 3.1.

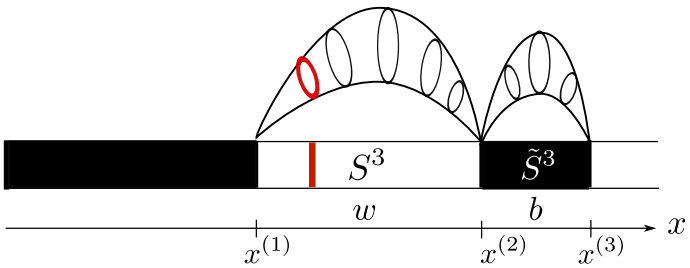

Figure 3.1: The topology of a single pair of finite-size white and black strips that are smoothly connected to a semi-infinite black strip on the left boundary and to a semi-infinite white strip on the right boundary. We consider (in red) probe M5 branes with dissolved M2 branes wrapping the S_3 that remains of finite size in the white strip region.

We note that one can also consider the $y \to 0$ limit of the Hamiltonian in the black region where the S_3 wrapped by the probe M5 brane shrinks to zero size. Naively one would expect the potential to vanish inside this region since the M5 brane has shrunk to zero size. Due to the non-trivial structure of supersymmetric M2 brane minima which we will discuss in § 3.4.1 this is not the case in general and we will study what happens inside

black strips in § 3.4.5.

3.4 Analysis of the supersymmetric minima of the probe potential

We now look for supersymmetric minima of the probe Hamiltonian (3.20) that describes M5 branes wrapping the S_3 and is restricted to the white strip regions of the real line $y = 0$. To satisfy $\mathcal{H}_+ = 0$ we have to impose

$$\left| c_3^+(x) - \frac{V_+(x)}{\zeta_+(x)^2} - p \right| \zeta_+(x) - \left(c_3^+(x) - \frac{V_+(x)}{\zeta_+(x)^2} - p \right) V_+(x) = 0 \tag{3.21}$$

As we will show, there are two different ways to solve (3.21). Correspondingly, there exist two different kinds of minima: those where the probe M5 brane shrinks to an M2 brane, and those where the M5 retains a finite-size. This second class of minima proves that the building blocks of the LLM solution are indeed M5 branes with dissolved M2 branes, dual to the dielectric vacua in the mass-deformed M2 brane theory and are the analogue of the ones found in [26].

3.4.1 Degenerate minima

To satisfy (3.21) we observe that

$$\lim_{x \to x^{(i)}} \frac{V_+(x)}{\zeta_+(x)} = (-1)^i \tag{3.22}$$

which means that the probe Hamiltonian can have supersymmetric minima located at the boundaries $x^{(i)}$ of the strips. This is as expected, since at these locations both S_3 and $\tilde{S}_3$ shrink to zero size, while our probe simply reduces to an M2 brane. As the background is maximally supersymmetric and sourced by dielectric M2 branes, a probe M2 would feel zero force if it preserves all the 16 supercharges, i.e. if it has the same orientation as the M2 sources. To fully solve (3.21) for $x = x^{(i)}$ we notice that $\frac{V_+}{\zeta_+^2} = 0$ at the boundaries. Hence defining the effective M2 charge

$$p_+^{eff}(x^{(i)}) = p - c_3^+(x^{(i)}) \tag{3.23}$$

we see that the Hamiltonian has a supersymmetric minimum at the boundary $x^{(i)}$ if

$$p_+^{eff}(x^{(i)}) > 0 \quad (i \text{ odd}) \qquad\qquad p_+^{eff}(x^{(i)}) < 0 \quad (\text{i even}) \tag{3.24}$$

The physical meaning of p_+^{eff} is clear: inserting the M5 probe in a white strip close to a boundary $x^{(i)}$, part of its M2 charge p is screened by the value of the potential $c_3^+(x^{(i)})$.

Indeed, from (3.20) we see that the effective M2 charge of the probe close to a boundary is p_+^{eff} rather than p.

Eq. (3.21) shows that M2 branes are BPS at odd boundaries, while anti-M2 branes are BPS at even boundaries. Another way to check this is to plot the potential for M2/anti-M2 probes which, using $G_4 = dA_3$, is given by

$$\mathcal{H}_{M2/anti-M2} = H^{-1} \mp A_{012} = (h^2 \mp V)^{-1} \tag{3.25}$$

This potential has indeed minima at the $y = 0$ line at odd or even boundaries respectively for $-$ or $+$. This is also confirmed by the analysis of the supersymmetry projector [18, 31].

3.4.2 Polarized minima and dielectric vacua

The second way to solve (3.21) is to require the expression inside the absolute value and the brackets to vanish. This yields for the location of the supersymmetric minima:

$$x_{susy} = \frac{1}{2}\left(p + x^{(1)} + \Sigma_b^l - \Sigma_b^r - c\right) \tag{3.26}$$

where Σ_b^l and Σ_b^r are the total size of the black strips that are respectively to the left and right of the white strip in which the probe M5 brane polarizes. In addition to the degenerate minima, we see from (3.26) that the Hamiltonian has minima located at a finite distance away from the boundaries. In the following, we will explicitly prove that these are the minima that correspond to vacua of the mass-deformed M2 brane theory. Depending on the value of the constant c in (3.26) such minima exist for positive as well as negative induced M2 charge p. The value of this constant corresponds to the gauge choice used to describe the physics at the supersymmetric minimum. We will come back to this gauge choice in detail in § 3.5.3 where we need to understand the effect on the probe brane when changing gauge. In the remainder of this section we will fix the gauge suitably to avoid cumbersome notation.

We mention that a result similar to (3.26) applies as well for M5 branes wrapping the $\tilde{S}_3$ which is non vanishing inside black strips. There are thus two channels into which a collection of (anti-) M2 branes can polarize: either into an M5 brane wrapping the S_3 or into an M5 brane wrapping the $\tilde{S}_3$. These are the different polarization channels that arise in the probe analysis [27, 26]. For simplicity, from now on we will focus on polarization inside the white strips. Polarization inside the black strips will be however important in § 3.5.3 to describe the final supersymmetric configuration metastable branes can decay to.

As a final remark, we stress that (3.26) holds even for the Hamiltonian with m M5 probe charge, provided that one replaces p with p/m.

The Polchinski-Strassler expansion

We now want to show that one can get the same result (3.26) expanding the Hamiltonian using the Polchinski-Strassler approximation [27]. The latter is a two-step expansion of the potential of a dielectric probe:

1. One first expands the potential for large distances from the sources and/or from the bubbled cycles supporting fluxes

2. Then one expands the potential in power series of the ratio of the probe charges, hence supposing that one charge is much smaller than the other

As explicitly shown in § 2.2, in this region the M-theory solution approaches the $AdS_4 \times S^7$ background perturbed by the four-form fluxes transverse to the M2 brane worldvolume directions, corresponding to the mass deformation in the dual M2 brane theory. The minimum we will find momentarily expanding the Hamiltonian in the geometry containing backreacted M5 branes is in agreement with the minimum found in [26] where the four-form fluxes were treated as perturbation of $AdS_4 \times S^7$. Note that in [26] the M5 potential was investigated directly using the Pasti-Sorokin-Tonin action [32], while here we are recovering the same result using the type IIA reduction.

Starting from the full Hamiltonian (3.13) it is convenient to first perform the coordinate change (2.12), expand the Hamiltonian at large R and then define

$$r^2 = R^2 \cos\left(\frac{\alpha}{2}\right) \qquad \tilde{r}^2 = R^2 \sin\left(\frac{\alpha}{2}\right) \tag{3.27}$$

where r is the radius of S_3 and $\tilde{r}$ is the radius of $\tilde{S}_3$. These are related to the original x and y coordinates as

$$y = r\tilde{r} \qquad 2x = r^2 - \tilde{r}^2 \tag{3.28}$$

In this way one can get an approximate expression for the Hamiltonian in the ultraviolet. As the probe is wrapping S_3, the Hamiltonian minimizes for $\tilde{r} = 0$, *i.e.* for $\alpha \to 0$, which coincides with the $y \to 0$ requirement of the previous section. Hence for r large and $\tilde{r} = 0$ one has for the metric functions appearing in (3.13)

$$H^{-1} \sim \frac{r^6}{N} + r^2 \qquad H y^3 e^{3G} \sim N \tag{3.29}$$

and for the form fields

$$B_2 \sim \frac{r^6}{N} + \frac{r^2}{2} \qquad c_3 \sim \frac{2N}{r^2} \qquad c_5 \sim -r^4 \tag{3.30}$$

where N is related to the M2 charge of the background given by (2.20). Inserting these

expansions into (3.13), the Hamiltonian reduces to:

$$\mathcal{H} \sim \left(\frac{r^6}{N} + r^2\right)\sqrt{N + \left(p - \frac{2N}{r^2}\right)^2} - \frac{pr^6}{N} - \frac{pr^2}{2} + r^4 \tag{3.31}$$

In [26] the probe is taken to have a much larger M2 charge than M5 charge. This reduces to the requirement $p >> \sqrt{N}$, which allows to Taylor expand the square root in (3.31) to get the final result[1]

$$\begin{aligned}\mathcal{H} &\sim \frac{pr^2}{2} - r^4 + \frac{r^6}{2p} \\ &= \frac{r^2}{2p}\left(r^2 - p\right)^2\end{aligned} \tag{3.32}$$

which is in perfect agreement with the result of [26]. Notice that the two higher order terms $\sim pr^6/N$ in (3.31) representing the M2 brane potential cancel out, and $\mathcal{H}$ is a perfect square as expected because of supersymmetry. The Hamiltonian (3.32) has a minimum for $r^2 = p$, which is nothing but (3.26) in the ultraviolet.

Restoring the correct mass dimension μ that comes with the four-form flux perturbation, one can check that the r^4 term is linear in μ, while the r^2 term has mass dimension μ^2 (see for example §4.2 of [33] for a simple review of the holographic origin of the polarization potential (3.32)). Note that this term cannot be explicitly computed in the Polchinski-Strassler – type analysis performed in [26], since in that case the background is computed only to first-order in the transverse flux perturbation and thus only at linear order in μ. However, it can be correctly guessed from supersymmetry just completing the square and our result confirms this rather explicitly.[2]

We can actually say much more. In the previous discussion we focused on the UV region and so we neglected the widths of the LLM strips in the IR. However, our analysis is not restricted to the asymptotic region. Firstly, the expression (3.32) also approximates the Hamiltonian for *small* x, *i.e.* near a strip boundary $x^{(i)}$, if we identify $2(x - x^{(i)}) \sim r^2$ in (3.20). The location of the minimum is then in agreement with (3.26). The reason why the probe potential is described by the same expression (3.32) inside finite-size strips is easy to understand. The r^6 term comes from the three-sphere the probe M5 is wrapping, and so this term is the same for both types of white strips. For the r^4 term things are much less obvious and naively this term seems to depend on the details of the backgrounds. However, by the magic noticed in [27, 26], this term only depends on the UV boundary conditions, since it comes from an expansion of a form which is both closed and co-closed. The r^2 term then is fixed by supersymmetry and hence is again the same for both types

[1] One can also directly get this result by expanding the Hamiltonian (3.20) for large x setting $2x \sim r^2$ and keeping only the leading terms in $1/p$.

[2] In type IIB, the $AdS_5 \times S^5$ background perturbed by three-form fluxes at second order has been computed in [34, 35], reproducing the PS result.

of strips. This is indeed the reason why one can safely compute the brane polarization by putting all the M2 branes at the origin: when they are puffed-up the probe will still feel the same potential. Again, since we are now probing the full geometry we can check this rather explicitly.

3.4.3 Backreaction of a supersymmetric probe configuration

Consider an arbitrary LLM solution with strips located at boundaries $x^{(1)}, \ldots, x^{(2s+1)}$, and let us focus on the asymptotic region very far from the strips, *i.e.* $x >> x^{(2s+1)}$. The analysis of the previous sections shows that a probe M5 brane with dipole charge m and with large M2 charge n, will polarize in this region at

$$x \approx \frac{n/m}{2\mu_1\mu_4 V_{S_3}} \tag{3.33}$$

where we wrote p in terms of the probe charge by using (3.11). What is the supergravity solution corresponding to this probe M5 brane? It is easy to show that this solution is found by adding an additional black strip carrying M5 charge $M_b = m$, precisely at the location (3.33). In fact, the M2 charge of such solutions is, using the relations (2.21), (2.19) and (3.8):

$$N \approx \frac{n/m}{2\mu_1\mu_4 V_{S_3}} \times \frac{M_b}{2\pi l_p^3} = n \tag{3.34}$$

which nicely matches the M2 charge of the probe. Hence, this explicitly confirms that the LLM solutions correctly geometrize the supersymmetric minimum found in the probe limit. A similar, though more involved, correspondence between DBI and SUGRA was studied for supertubes in bubbling backgrounds in [36, 37].

Repeating the same reasoning for the case of the supersymmetric minima (3.26) that arise inside the white strips is straightforward but more tedious. The backreaction of the probe sitting at those minima are again captured by an LLM solution with additional pair of white and black strip.

We stress that a completely similar analysis can be carried out for supersymmetric minima that arise for M5 brane probes wrapping the $\tilde{S}_3$ which is non-vanishing inside the black strips.

3.4.4 Example: LLM solution with a single pair of white and black strips - part I

We now specialize the previous discussion to a simple example. We focus on the simplest LLM geometry containing dielectric branes, namely the solution corresponding to a single pair of finite-size white and black strips and we consider the dynamics of probe M5 branes within the white strip, *i.e.* M5 branes wrapping three-cycles in the M-theory solution (2.1)-

(2.2). The white region of interest is smoothly connected to a semi-infinite black strip on the left boundary and by a finite-size black strip on the right boundary which smoothly connects to a semi-infinite white strip. We denote by $w = x^{(2)} - x^{(1)}$ and $b = x^{(3)} - x^{(2)}$, respectively, the widths of the finite-size white and black strip (see Figure 3.1). Without loss of generality we set $x^{(1)} = 0$ and we fix the gauge so that $c_3^+(0) = 0$.

We first discuss degenerate supersymmetric minima that arise at the boundary of the strips. On the left boundary of the white strip ($x = 0$) the Hamiltonian simplifies to

$$\mathcal{H}_+(0) = (|p| - p)\,\frac{w(w+b)}{b} \tag{3.35}$$

Hence for $p \geq 0$ the Hamiltonian has a supersymmetric minimum at the left boundary, where the S_3 the M5 brane is wrapping shrinks to zero size. On the right boundary of the white strip ($x = w$) the Hamiltonian simplifies to

$$\mathcal{H}_+(w) = [|2w - p| - (2w - p)]\,\frac{wb}{(w+b)} \tag{3.36}$$

and hence for $p \leq 2w$ the Hamiltonian has a supersymmetric minimum at the right boundary. Note that $c_3^+(0) = 0$ and $c_3^+(w) = 2w$ and so we have $p^{eff} = p$ on the left boundary and $p^{eff} = p - 2w$ on the right boundary. Hence, the conditions on p to have supersymmetric minima at the boundaries agree with the conditions that $p^{eff} > 0$ on the left boundary and $p^{eff} < 0$ on right boundary as discussed in § 3.4.1.

As we discussed in the previous section, we expect that the M2 branes sitting at the boundary of the white strip will polarize into BPS M5 branes, as illustrated in Figure 3.1. The backreaction of those probe branes is captured by an LLM geometry with an additional black and white pair of strips. The general result (3.26) for the position of such supersymmetric minima now simplifies to:

$$x_{susy} = \begin{cases} \dfrac{p}{2}\,, & \text{finite size white strip} \\ b + \dfrac{p}{2}\,, & \text{semi-infinite white strip} \end{cases} \tag{3.37}$$

We show the minimum in the asymptotic region and the minimum inside the white strip in Figure 3.2.

3.4.5 Wrapped Dirac strings

So far we have discussed the Hamiltonian of a probe M5 brane wrapping the S_3, which is of finite size inside white strips. The probe can polarize at a finite distance from a boundary inside a white strip or has degenerate minima at the boundaries of the strip where S_3 shrinks to zero size. Inside black strips the probe reduces to M2 branes and the Hamiltonian is thus determined by the dynamics of those M2 branes. In the following we

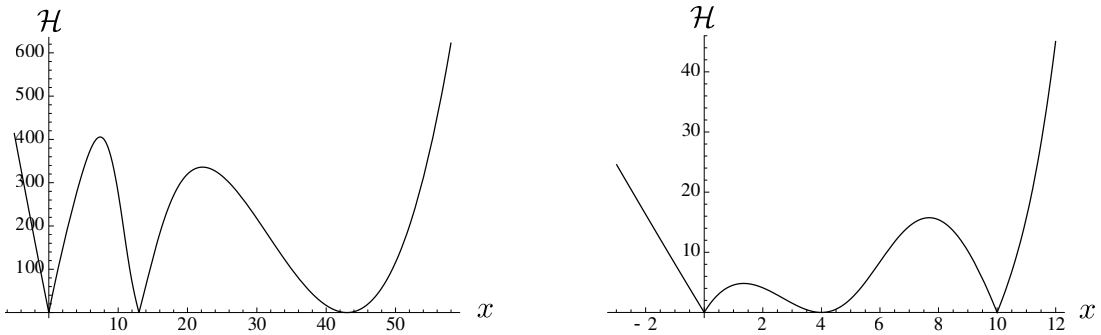

(a) $p = 80$. (b) $p = 8$.

Figure 3.2: Supersymmetric global minima of the probe potential, illustrated for a solution with $w = 10$ and $b = 3$: (a) A minimum in the semi-infinite white strip; the minima in this asymptotic region correspond to those found in [26]. (b) A minimum inside the white strip.

explain what happens inside black strips.

In an analogous way as for white strips we can take the $y \to 0$ limit of the Hamiltonian (3.13) for black strips, *i.e.* for regions where the master function z takes the value $-1/2$. We refer to Appendix A.3.2 for details and state here the result:

$$\mathcal{H}_-(x) = \frac{1}{\zeta_-(x)^2 - V_-(x)^2}\left[\zeta_-|p - c_3^-(x)| + V_-(x)(p - c_3^-(x))\right] \tag{3.38}$$

with $V_-(x) = V_+(x)$ and $\zeta_-(x)$ given by (A.34). The three-form potential reduces to

$$c_3^-(x) = \sum_{i=1}^{2s+1}(-1)^{1+i}|x - x^{(i)}| + x + c = x^{(1)} + 2\Sigma_w + \Sigma_b + c \tag{3.39}$$

where s is the number of pairs of finite-size white and black strips of the configuration, Σ_w is the total width of white strips to the left of the black strip in which we study the Hamiltonian and Σ_b is the total width of black strips in the solution. Note that the three-form potential is constant inside black strips.

The Hamiltonian (3.38) is considerably simpler than the Hamiltonian (3.20) because the M5 brane is of zero size in black strips and, hence, the Hamiltonian is dictated by the dynamics of the dissolved M2 branes. From (3.38) we see that the Hamiltonian vanishes inside a black strip if the M2 charge of the probe equals the value of the three-form potential inside that black strip. We can understand this as follows. The effective M2 charge $p_-^{eff}(x^{(i)}) = p - c_3^-(x^{(i)})$ corresponds to the M2 charge at the boundary $x^{(i)}$ of a black strip. Hence if $p_-^{eff}(x^{(i)}) = 0$ there are no (anti-) M2 branes at the boundary $x^{(i)}$ and the Hamiltonian (3.38) describing "nothing" vanishes everywhere inside that black strip.

If the effective M2 charge inside the black strip is non-zero, the situation is more

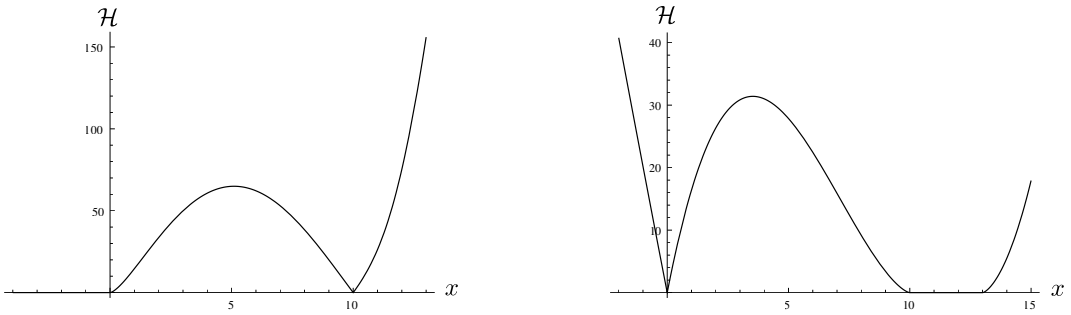

(a) $p = 0$. (b) $p = 20$.

Figure 3.3: The Hamiltonian in black strips describing "nothing". The Hamiltonian vanishes inside the semi-infinite black strip for $p = 0$ while it vanishes in the finite-size black strip for $p = 2w$.

involved. Recall from the discussion of degenerate minima of the Hamiltonian in § 3.4.1 that the M2 brane probe potential (3.25) has minima at the $y = 0$ line at odd or even strip boundaries depending on whether the effective M2 charge (3.23) is positive or negative. Hence, for non-zero values of the M2 charge, the Hamiltonian (3.25) vanishes only at one of the boundaries of the black strip. The Hamiltonian inside the black strip is then determined by the potential felt by M2/anti-M2 branes:

$$V_{M2/anti-M2} = |p_-^{eff}|\mathcal{H}_{M2/anti-M2} \tag{3.40}$$

One can indeed check that the Hamiltonian (3.38) coincides with the potential felt by M2 branes if $p_-^{eff} > 0$ while it coincides with the potential felt by anti-M2 branes if $p_-^{eff} < 0$.

We illustrate the flattening for the example of the single pair of white and black strip introduced in § 3.4.2. The semi-infinite black strip and the finite-size black strip are located respectively at $-\infty < x < 0$ and $w < x < w + b$ on the $y = 0$ axis (see Figure 3.1) where the three-form potential (3.39) takes the constant values $b + c$ and $2w + b + c$ respectively. Choosing $c = -b$ yields a gauge where $c_3^+(0) = 0$ and consequently $c_3^+(w) = 2w$. The M5 brane Hamiltonian then vanishes inside the semi-infinite black strip for $p^{eff}(x^{(1)}) = 0$ which implies $p = 0$. The Hamiltonian vanishes inside the finite-size black strip for $p^{eff}(x^{(2)}) = 0$ corresponding to $p = 2w$. We illustrate this for $w = 10$ and $b = 3$ in Figure 3.3.

3.5 Metastable supersymmetry-breaking minima

In this section we study local minima of the Hamiltonian (3.20) that are not supersymmetric. We will focus on the white strip $[x^{(2i-1)}, x^{(2i)}]$. As we will show, according to the value of p in (3.20) there can be metastable minima close to the left boundary $x^{(2i-1)}$ or

close to the right boundary $x^{(2i)}$ of the strip. In order to avoid clutter we will fix the gauge such that $c_3^+ = 0$ at the boundary of the strip we are expanding around which implies $p_+^{eff} = p$ at that boundary. For definiteness, we will focus on metastable minima close to $x^{(i)}$ with i odd and p negative, so that the probe is no longer BPS. We first derive analytic expressions that approximate well the location of such local minima, by using a Polchinski-Strassler–type of expansion. We then focus on the simple example of a single pair of white and black strip and we study the full Hamiltonian numerically. We end with a discussion of the decay process for the metastable probe.

3.5.1 Analytic results

In order to get analytic control over the M5 brane Hamiltonian, we would like to Taylor expand it around the boundary $x^{(i)}$, with i odd and p negative. While this expansion can be rather cumbersome, we should realize that for small enough $|p|$, many terms are actually subleading. Hence, it is sensible to keep only those terms that are of the leading order in p at the minimum. For $x^{(i)} < x < x^{(i)} + |p|$ the Hamiltonian (3.20) is well approximated by:

$$\mathcal{H}_+ \approx -p\left[B_+(x) + \frac{1}{H_+(x)}\right] + c_3^+(x)\left[B_+(x) + \frac{1}{H_+(x)}\right] - \frac{1}{\zeta_+^2(x)} - \frac{1}{p}\frac{1}{2\zeta_+^3(x)} \tag{3.41}$$

This is nothing but the familiar form of the potential for polarized branes [38]. The term that is linear in p is the force felt by probe anti-M2 branes in the background geometry, the term that is constant in p comes from the p-independent Wess-Zumino action and the p^{-1} term comes from the metric of the wrapped three-sphere. Starting from this expression, one can Taylor expand around $x^{(i)}$, keeping in mind that it is enough to keep only the leading terms. This can be easily achieved by noticing that

$$-\frac{1}{2\zeta_+^3(x)} = -4(x - x^{(i)})^3 + \mathcal{O}\left((x - x^{(i)})^5\right) \tag{3.42}$$

and

$$-\left[B_+(x) + \frac{1}{H_+(x)}\right] = a_1 + a_2(x - x^{(i)}) + \mathcal{O}\left((x - x^{(i)})^2\right) \tag{3.43}$$

where a_1 and a_2 are constants whose values depend on $x^{(i)}$:

$$\begin{aligned} a_1 &= 2\left(\sum_{j=1, j\neq i}^{2s+1} \frac{(-1)^j}{|x^{(i)} - x^{(j)}|}\right)^{-1} \\ a_2 &= \frac{3}{4}\left(\sum_{j=i+1}^{2s+1} \frac{(-1)^j}{(x^{(i)} - x^{(j)})^2} - \sum_{j=1}^{i-1} \frac{(-1)^j}{(x^{(i)} - x^{(j)})^2}\right)(a_1)^2 \end{aligned} \tag{3.44}$$

Writing $2(x-x^{(i)}) \approx r^2$, in terms of the radius r of the wrapped three-sphere S_3, we finally see that (3.20) is well-approximated for small r and small $|p|$ by:

$$\mathcal{H}_+ \approx p\, a_1 + p\, \frac{a_2}{2}\, r^2 - \frac{1}{2p} r^6 \tag{3.45}$$

If $a_2 > 0$ the Hamiltonian always has a metastable minimum at

$$r^2 = |p| \sqrt{\frac{a_2}{3}} \tag{3.46}$$

We can explicitly check that the terms of the potential (3.45) are detailed balanced, namely at the minimum the last two terms scale with the same power of p. One can also check that the omitted terms scale at the minimum with sub-leading power of $|p|$.

We would like to comment on an important difference between the metastable probe potential (3.45) and the supersymmetric potential (3.32). In the latter case, the minimum arise from a balance of r^2, r^4 and r^6 terms which combine to give a perfect square. In the present case, the r^4 term of the potential is missing, and the polarization is caused by the *negative* r^2 term. This term comes from the imperfect cancelation of gravitational attraction and electric repulsion that the anti-M2 probes feel in the background. In our case the term is negative since anti-M2s are repelled from the left boundary $x^{(i)}$, thus making the polarization more likely.

When $|p|$ grows, the approximation (3.45) breaks down and we would need to keep next-to-leading order pieces to study the behavior of the potential. While this can be done, the general result is rather cumbersome, so we will postpone the discussion to a particular example in the next section. We anticipate that by including the new terms, or by studying the full potential numerically as we will do in § 3.5.2, one can see that the metastable minimum will disappear above a critical value of the anti-M2 charge. Above that value the potential shows a perturbative instability toward one of the globally supersymmetric minima described in § 3.4, which are located at the right boundary of the strip.

The discussion regarding local minima in white strips close to even boundaries $x^{(2i)}$ is completely analogous but, as discussed in § 3.4.1, the role of M2 and anti-M2 branes are exchanged so that at even boundaries anti-M2 branes are BPS and the supersymmetry breaking polarized M5 brane contains M2 brane charge. One finds the same structure of metastable minima as before but now for small positive p. To show this, one can start with the analogue of (3.41), which is given by:

$$\mathcal{H}_+ \approx -p \left[B_+(x) - \frac{1}{H_+(x)} \right] + c_3^+(x) \left[B_+(x) - \frac{1}{H_+(x)} \right] - \frac{1}{\zeta_+^2(x)} + \frac{1}{p} \frac{1}{2\zeta_+^3(x)} \tag{3.47}$$

Expanding in $2(x^{(i)} - x) \sim r^2$ one gets

$$\mathcal{H}_+ \approx -p\, a_1 + p\, \frac{a_2}{2}\, r^2 + \frac{1}{2p} r^6 \tag{3.48}$$

If $a_2 < 0$ the above expression minimizes at $r^2 = p\sqrt{-\frac{a_2}{3}}$ and the discussion then proceeds as before.

3.5.2 Example: LLM solution with a single pair of white and black strips - part II

We now discuss the existence of metastable minima of the probe Hamiltonian in the example of the single pair of white and black strips introduced in § 3.4. We consider a probe M5 brane with induced anti-M2 charges close to the left boundary of the finite-size white strip at $x = 0$ (see Figure 3.1) and we expand the Hamiltonian for small values of x. The leading-order approximation (3.45) reduces to:

$$\mathcal{H}_+ \approx |p|\, \frac{2w(w+b)}{b} \;-\; |p|\, \frac{3(2w+b)}{b}\, x + \frac{4}{|p|}\, x^3 \tag{3.49}$$

It is easy to see that this potential has a metastable minimum at

$$x_{meta} = \frac{|p|}{2}\sqrt{1 + \frac{2w}{b}} \tag{3.50}$$

where the approximated potential (3.49) is

$$\mathcal{H}_+(x_{meta}) \approx\; |p|\, \frac{2w(w+b)}{b} - p^2 \left(1 + \frac{2w}{b}\right)^{3/2} \tag{3.51}$$

We note that the terms in the potential (3.49) are detailed balanced: at the minimum $x \sim |p|$ the last two terms scale like p^2. This approximates well the potential for small p and small x, as shown in Figure 3.4(a). When $|p|$ increases, the approximation breaks down and eventually the minimum disappears, see Figure 3.4(b). We also plot in Figure 3.5 the full Hamiltonian (3.13) by keeping the dependence both on x and y; one can easily see that the Hamiltonian indeed minimizes at $y = 0$.

To capture the transition from a metastable to an unstable configuration at the critical value $p^\star$ of the anti-M2 charge, one could include higher order terms in the expansion of the Hamiltonian. These are all the terms that, at the minimum, scale with the same next-to-leading power of p. We find however simpler to study directly the zeroes of the derivative of the potential numerically. We find that for the example $w = 10$, $b = 3$, the transition happens around $p^\star \approx -1.5$. We studied numerically the dependence of $p^\star$ on the widths of the strips for various examples. One can easily show in this way that increasing the width of the white strip in which the metastable M5 polarizes, i.e. increasing the

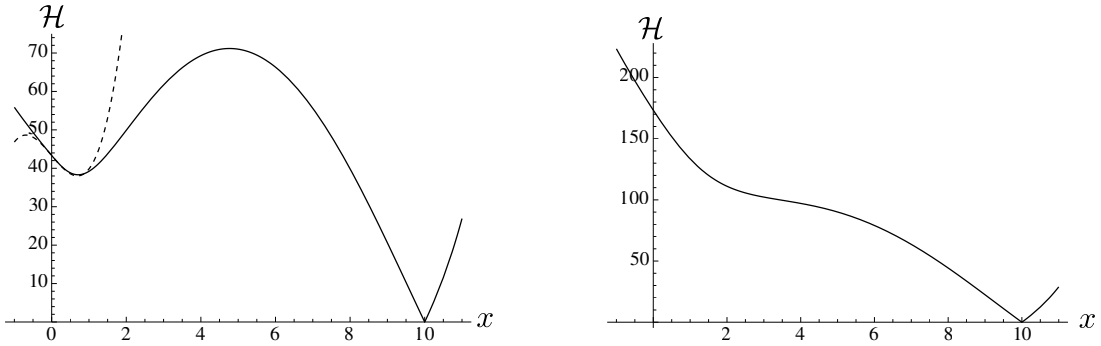

(a) $p = -1/2$. (b) $p = -2$.

Figure 3.4: (a) Metastable minimum for negative p. The dashed line is the leading order approximation of the Hamiltonian as given in (3.49). Below we give a Contour plot of (3.13) in the $x-y$ plane which shows that the Hamiltonian indeed minimizes on the $y = 0$ axis. (b) For larger $|p|$ the minimum disappears.

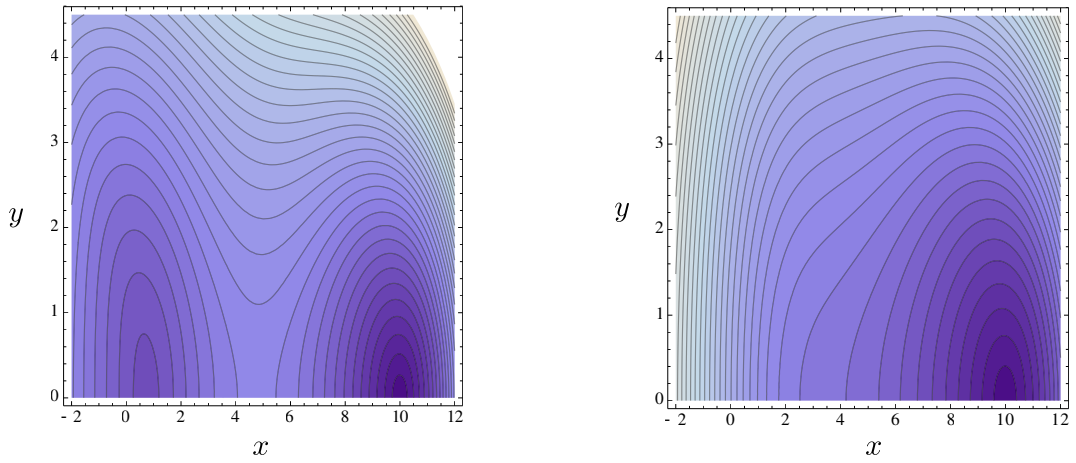

(a) $p = -1/2$. (b) $p = -2$.

Figure 3.5: Contour plots in the (x, y) plane of Figure 3.4. Darker colors mean lower energy. (a) The metastable minimum (on the left) and the supersymmetric minimum (on the right) are at $y = 0$. (b) The metastable minimum has disappeared and there is only the supersymmetric minimum (on the right) at $y = 0$.

four-form flux M_w on the S^4, $|p^\star|$ grows and hence one can have a metastable M5 brane with larger and larger number of anti-M2 branes dissolved in its worldvolume. This is quite similar to the metastable configuration in [39, 30].

However, we remark that even if $p < p^\star$, one can always find a metastable probe minimum just by considering polarization into multiple M5 branes, as discussed in § 3.3. In fact, one can divide the $|p|$ anti-M2 branes in m groups and make the single group polarize. One obtain a configuration with m M5 branes on top of each other, polarized at a radius proportional to p/m. Hence, we can bring $p/m > p^\star$ by a suitable choice of m.

3.5.3 Decay of metastable branes

We have seen that for induced anti-M2 charge, the probe M5 brane has locally stable minima at small but finite distance away from odd strip boundaries. These minima are classically stable since there is a non-perturbative barrier toward the global supersymmetric minimum close to the other strip boundary. Quantum mechanically, our probe will decay via bubble nucleation to this supersymmetric minimum. We now briefly describe how this process will take place. A similar mechanism was described in [39, 30], but in the present case there is some additional subtlety due to the presence of Dirac strings that we would like to clarify. While we will present the decay process for the example of the single pair of white and black strips it should be understood that the discussion carries over to the decay of metastable probes placed in any strip of a general multi-strip configuration.

The decay of the metastable M5 brane probe can be understood as brane-flux annihilation of its induced anti-M2 charge against the M2 charge dissolved in the background flux. Recall that the four-form flux through the four-sphere that stretches between the left and right boundary of the white strip, and which contains the S_3 the M5 brane is wrapping, is given by (see § 2.2.2)

$$(2\pi l_p)^3 M_w = \int_{x^{(1)}}^{x^{(2)}} dc_3^+ = c_3^+(x^{(2)}) - c_3^+(x^{(1)}) \tag{3.52}$$

The M5 brane couples magnetically to c_3^+ and so, when it sweeps out the four-sphere S^4 from the North Pole to the South Pole, the amount of four-form flux through the orthogonal four-sphere $\tilde{S}^4$ changes by one unit. Since we need at least two patches (the North Pole patch and the South Pole patch) to describe this process, we need to understand what happens to the probe when we change patch.

So far, we worked in a gauge where the three-form potential vanishes at the boundary of the strip that we are expanding around, which translates to fixing the constant c. This ensures that we work in a patch with no Dirac strings at that boundary and is thus the correct gauge in order to describe the physics of metastable minimum close to this boundary. When the metastable M5 brane tunnels to the stable minimum close to the other boundary, its quantized anti-M2 charge p stays the same, but its effective anti-M2 charge

$$p_+^{eff}(x^{(i)}) = p - c_3^+(x^{(i)}) \tag{3.53}$$

changes. Without loss of generality we consider metastable probes close to the boundary $x^{(1)}$ of the white strip and gauge fix $c_3^+(x^{(1)}) = 0$. In this patch "1" we denote by $p_1 \equiv p$ the quantized anti-M2 charge of the probe. The effective anti-M2 charge at the left boundary is $p_+^{eff}(x^{(1)}) = p_1 - c_3^+(x^{(1)}) = p$ while after the decay we have at right boundary $p^{eff}(x^{(2)}) = p - M_w$. Once the probe M5 brane has tunneled to the supersymmetric minimum close to the boundary $x^{(2)}$ we need to change patch in order

to correctly describe the physics at that minimum. The gauge transformation parameter when changing from patch "1" (no Dirac strings at $x^{(1)}$) to patch "2" (no Dirac strings at $x^{(2)}$) is

$$\gamma_{12} = c_3^+(x^{(1)}) - c_3^+(x^{(2)}) = -M_w \tag{3.54}$$

When changing patch the effective anti-M2 charge (3.53) stays the same while the quantized anti-M2 charge changes according to

$$p_2 = p_1 + \gamma_{12} = p - M_w \tag{3.55}$$

where p_2 denotes the quantized anti-M2 charge in the patch where there are no Dirac strings at the boundary $x^{(2)}$. Hence after the decay there are $|p_2| = |p^{eff}(x^{(2)})| = |p - M_w|$ anti-branes at the right boundary.

To summarize, in order to describe the vacuum structure and the dynamics of the probe one has to work in a fixed gauge and thus keep the quantized charges of the probe fixed. To describe the physics of the probe in a minimum close to the left/right boundary of a strip before and after the decay one has to work in a gauge where there are no Dirac strings at that boundary (North/South Pole of the four-sphere).

In the decay process the quantized anti-M2 charge of the metastable probe changes according to (3.55) by

$$\Delta p = p_2 - p_1 = -M_w \tag{3.56}$$

Furthermore, as we have explained above, when the probe sweeps out the four-sphere between the boundaries $x^{(1)}$ and $x^{(2)}$ it changes the four-form flux through the orthogonal four-sphere, given by M_b, by one unit. Hence, the initial M2 charge dissolved in the background flux as given by $N_1 = M_w M_b$ differs from the final M2 charge precisely by the amount (3.56). The final background M2 charge dissolved in flux is

$$N_2 = M_w(M_b + 1) \tag{3.57}$$

Note that the number of anti-branes actually *increases* during the decay and so does the amount of background flux. It is thus probably more suitable to call this decay process brane-flux *creation*.

One can easily check that this decay process conserves the total M2 charge of the background as measured in the UV:

$$N^{UV} = N^{IR} + N^{flux} \tag{3.58}$$

where N^{IR} denotes the the M2 charge due to the presence of the probe brane and N^{flux} denotes the M2 charge dissolved in the background fluxes. Before the decay $N_1^{UV} = p + M_w M_b$ while after the decay $N_2^{UV} = p - M_w + M_w(M_b + 1) = N_1^{UV}$.

When the metastable M5 brane probe close to the boundary $x^{(1)}$ decays to the degenerate supersymmetric minimum at the boundary $x^{(2)}$, the initial $|p|$ units of induced anti-M2 charge become $|p-M_w|$ anti-M2 branes located at $x^{(2)}$. At this boundary anti-M2 branes are supersymmetric. According to the discussion of § 3.4.2 the $|p-M_w|$ anti-M2 branes can polarize into a supersymmetric minimum inside the black strip adjacent to the boundary $x^{(2)}$. We can also consider the mirrored situation: probe M5 branes with small positive induced M2 charge p which are metastable close to the boundary $x^{(2)}$ and decay to the degenerate supersymmetric minimum at the boundary $x^{(1)}$. The $p+M_w$ M2-branes are supersymmetric at this boundary and can further polarize into a supersymmetric minimum inside the semi-infinite black strip.

While so far we have discussed polarization of multiple (anti-) M2 branes into a single M5 brane we can also consider polarization into multiple M5 branes both for the initial metastable as well as the final supersymmetric configuration. Polarizing $|p|$ anti-M2 into m_b metastable M5 branes wrapping the S_3 modifies the quantized anti-M2 charge after the decay to $p_2 = p - m_b M_w$. Likewise, the flux through the orthogonal sphere changes not by one but by m_b units so that the final M2 charged dissolved in the background flux is $N_2 = M_w(M_b + m_b)$. After the decay the $|p - m_b M_w|$ anti-M2 branes can further polarize into a single or multiple M5 branes. As discussed in § 3.4.2 polarization into m_w M5 branes wrapping the $\tilde{S}_3$ shifts the location of the supersymmetric minimum (3.26); hence one can always find a supersymmetric minimum inside the black strip by considering polarization into multiple M5 branes. This guarantees that metastable M5 branes, after decaying in the S_3 channel to a degenerate minimum, can always polarize into a smooth supersymmetric minimum in the $\tilde{S}_3$ channel. The decay process thus corresponds to the tunneling of metastable M5 branes carrying (anti-) M2 charge to a supersymmetric minimum dual to a dielectric vacuum of the mass-deformed M2 brane theory.

3.6 Future developments

The most interesting future development of our analysis would be finding the backreacted solution corresponding to the metastable M5 branes. Since the backgrounds we are probing correspond themselves to the backreaction of M5 branes with M2 charge dissolved in flux, we believe that it should be possible to extend some of the techniques recently used to study anti-branes backreaction in flux compactifcations (see for example [40, 41, 42]) to study the metastable M5 gravity solution. Only in this way we could explicitly check if the gravity solution is smooth and indeed corresponds to spontaneous supersymmetry breaking.

This would also be needed to understand the dynamics of the metastable M5 brane once its full backreaction is taken into account, along the lines of [33]. In particular, it is suggestive that in the probe approximation we detect a negative r^2 term in the polarization

potential. In a full backreacted regime, this implies that the throat created by the anti-branes repels a fellow anti-brane, thus signaling a tachyonic direction. If this happens for our metastable branes, this would point toward a more rich dynamics than the probe non-perturbative bubble nucleation picture would indicate.

Furthermore, since our result is quite similar to the metastable supertube found in [43, 44] in the probe approximation, finding the backreaction of our metastable M5 brane could give insight into the more challenging non-BPS supertube backreaction, and thus into the construction of large classes of non-extremal black hole microstate geometries in the context of the fuzzball proposal. In this context the study of the dynamics of non-BPS probes in a fully backreacted background would be crucial to understand black hole emission and to compare it with the semi-classical expectation.

CHAPTER 4

INSTABILITY OF NEAR-BPS MICROSTATE GEOMETRIES

4.1 From the black hole entropy paradox to the Fuzzball Proposal

4.1.1 The entropy puzzle for black holes

One of the most puzzling issues in modern theoretical physics concerns the information paradox in black holes. Black holes arose in the theoretical framework of General Relativity as early as 1916, when Schwarzschild found the first spherically-symmetric stationary solution to Einstein's equations. This solution exhibited new stunning and simple features: a singularity at the center of the space (we assume one uses spherical coordinates in 4d) screened by an event horizon at some fixed radius r_S. The event horizon is a spherical surface that separates spacetime in two distinct regions. In the inner region all causal curves have to terminate on the singularity, which pictorially corresponds to the notion that nothing can escape from a black hole. At the same time, the timelike Killing vector associated to time translation invariance becomes null on the event horizon and spacelike in the inner region. These new stunning features depend on core assumptions on general relativity, and during the next fifty years more complex black hole solutions were found, such as the Reissner-Nordström solution (an electrically charged black hole) in 1916-1918 and the Kerr solution (a spinning black hole) in 1963. The main features of these two nontrivial solution were joined in the Kerr-Newman solution in 1965, which describes the geometry of a rotating and electrically-charged black hole. Subsequently, many different black hole solutions were found in higher dimensions and lately in supersymmetric theories.

A major breakthrough in our understanding of black holes was made by Bekenstein and Hawking in 1973, where field theory computations in the proximity of a black hole

event horizon led to the conclusion that an entropy can be associated to black holes, which for a simple Schwarzschild black hole is given by:

$$S_{BH} = \frac{kA}{4l_P^2} \qquad l_P = \sqrt{\frac{G\hbar}{c^3}} \tag{4.1}$$

where k is the Boltzmann constant, A is the area of the event horizon and l_P is the planck length. Remarkably, the very same structure remains valid for charged and spinning black holes (with some modifications for the expression of A) and in higher dimension (where one just needs to adjust l_P). Aside from the notable fact that an object as stunning as a black hole possesses an entropy, the importance of (4.1) relies on the quantities that determine it. To date, the Bekenstein-Hawking formula remains the only rigorously derived formula that involves the characteristic constants of the main branches of physics: thermodynamics (via the Boltzmann constant), gravity (via the Newton constant G), relativity (via the speed of light constant c) and quantum mechanics (via $\hbar$). Therefore, the study of black holes can really connect these fundamental branches of modern physics and shed some light on their connections.

As the study of black holes progressed, many theorems were established in the sixties and seventies that constrained the form of a black hole solution. Most notably, it was proved that a black hole solution in General Relativity is uniquely determined by the conserved charges of the black hole. At the same time, the fact that an entropy of the form (4.1) can be associated to a black hole, led to the conclusion that black hole are perfectly valid thermodynamic systems, that are prone to be studied by a statistical approach. Hence, given the entropy S_{BH} for a black hole, thermodynamics establishes that this system is composed by a number of states proportional to $e^{S_{BH}}$. However, it is not clear what these states are and where they come from, since given the conserved charges only one solution exists to Einstein's equations. Clearly the theorem about black hole solutions and the thermodynamical interpretation of black holes cannot coexist together.

A possible resolution of the tension between General Relativity and thermodynamics was searched in the fundamental principles these two branches are constructed on. On one side, the validity and generality of thermodynamics was not to be questioned, as its results were proven and established since the late nineteenth century. On the other side, the experimental results of General Relativity confirmed the scientific value of this theory precisely while the black hole entropy mystery was discovered.

For quite some time people tried to explicitly construct the black hole microstates to match the expectations from S_{BH} by inserting additional structures in the region of black hole horizons. However, this strategy proved to be unsuccessful, as any structure added in the proximity of the horizon is unstable by definition (which is also the physical explanation of the theorem that states that black hole solutions are uniquely determined by the conserved charges of the system).

It was not until 1996 that a possible explanation about the mysterious black hole entropy was found, thanks to String Theory.

4.1.2 The fuzzball proposal

In 1996 Strominger and Vafa [45] studied a BPS brane system that upon compactification leads to a black hole solution. While in ten dimensions many systems of the same kind can be constructed, these all lead to the *same* black hole once one reduces to five dimensions. Strominger and Vafa managed to count the number of possible different states in ten dimensions, which matched *exactly* the expectations from the Bekenstein - Hawking formula. The computation was carried on in a regime of parameters where gravity was completed turned off, and it was subsequently possible to extend this result to every possible regime of parameters thanks to supersymmetry. String Theory made it possible to shed light onto a paradox that remained completely unsolved for more twenty years.

To date, one of the most promising theoretical frameworks that aims at solving black hole paradoxes in the contest of String Theory is the *Fuzzball Proposal* [46, 47], which we are going to briefly summarize. We stress that this is still a conjecture and some work is still to be done to prove its full validity.

According to the Fuzzball proposal, General Relativity is a valid description for a black hole only up to the horizon scale. Beyond the horizon the notions of space and time break down and General Relativity loses its physical meaning. The inner region beyond the event horizon is to be replaced by a quantum superposition of *black hole microstates*, namely geometries that are similar to the would-be black hole, each of them being smooth. At the same time, the event horizon only becomes a length scale that marks the transition from the General Relativity description to the Fuzzball description. Each microstate is inaccessible from far away, meaning that from the point of view of General Relativity one cannot distinguish among them, but if one could zoom in one would be able to see that microstates are all slightly different from one another. The number of microstates that are superimposed quantum mechanically should match the predictions from the Bekenstein-Hawking entropy (4.1).

Given a specific black hole solution in General Relativity, it is fundamental to understand what a microstate looks like. It turns out that a microstate is a solution of Einstein's equations that simulates a black hole far away from the would-be singularity, but contrarily to the latter has a very long throat which is capped off at the end (while the throat has in general infinite length for BPS black holes). It is also constrained to have the same charges of the would-be black hole. It is precisely at the bottom of the long throat that microstates can differ. As microstates are smooth solutions in Supergravity, they must have no localized sources and hence microstates fall in the class of supergravity solutions that arise from the phenomenon of geometric transition discussed in Chapter 2. The charges of a microstates derive by flux supported by nontrivial topological cycles at

the bottom of the microstate throat. The number and orientation of these bubble is allowed to vary while keeping the overall charges constant. In the fuzzball proposal, once an infalling object falls through the horizon scale it starts bouncing from microstate to microstate, hence making it extremely improbable for it to exit from the fuzzball. This simulates the fact that once something falls into the black hole horizon in General Relativity it will never come out again. Note that while this is physically impossible from the point of view of General Relativity, it is just extremely improbable from the point of view of the fuzzball.

Note that as the fuzzball proposal can be consistently formulated only in the context of String Theory, it offers a possible explanation of the entropy mystery only for specific classes of BPS black holes.

4.1.3 Instability of near-BPS microstates

Despite the success in constructing microstates for BPS black holes, the world of non-BPS non-extremal microstates remains quite unexplored. The few known exact solutions in the JMaRT class [48, 49, 50, 51, 52] and the Running-Bolt class [53, 54], though horizonless, do not have the right charges to correspond to a black hole with a classically-large horizon area.

In parallel to these efforts, it was argued in [44] that one can systematically obtain very large classes of microstate geometries for non-extremal black holes by placing a supertube [55] at metastable minimum inside the known BPS microstate geometries. The energy ΔM of this supertube then gives the mass above extremality of the solution. Although no exact solutions in this class are known, one can argue that the supertubes should backreact into a smooth solution[1], and hence one expects that there should exist a very large number of bubbled microstate geometries corresponding to near-extremal black holes. Since supertubes have charges opposite to those of the black hole, these bubbled geometries would have cycles that are wrapped both by positive and by negative fluxes, and this is exactly the structure that Gibbons and Warner have proven to be necessary if one is to replace non-extremal black holes by stationary horizonless black hole solitons [56, 57, 58].

Furthermore, since these microstate geometries have neither inner nor outer horizon, they should be thought of as resolving the singularity of the non-extremal black hole all the way to the outer horizon, which is *backwards in time* from the location of the singularity. This pattern of singularity resolution is rather extraordinary and, if confirmed by the construction of fully backreacted non-extremal microstate geometries, it would have important implications not only for black hole singularities but also for cosmological ones.

[1]For supersymmetric solutions it was shown that the Born-Infeld equations governing the supertube are equivalent to those ensuring smoothness and absence of closed timelike curves in the fully-backreacted solution [36].

There is another important difference between the non-extremal microstate geometries in the JMaRT and Running Bolt classes, and the near-extremal microstates constructed using anti-supertubes. The JMaRT geometry is unstable [59] (and so is the Runnning Bolt one [60]) and this instability, which comes from the existence of an ergoregion, can be matched precisely to the fact that the D1-D5-P CFT state dual to the JMaRT geometry is also unstable [61, 62, 63]. Furthermore, it has been argued that a similar ergoregion instability should be present in all non-extremal microstate geometries [64].

On the other hand, the near-extremal microstate geometries of [44] are obtained by placing probe anti-supertubes inside extremal bubbling geometries at metastable minima of their Hamiltonian, and hence these configurations could in principle be much longer lived than one expects for a typical near-extremal microstate by studying the D1-D5 CFT. Indeed, the near-extremal CFT states consist of a very large number of (supersymmetric) left-mover momentum modes and a much smaller number of supersymmetry-breaking right movers, and it seems very difficult to prepare states where the annihilation of these modes is suppressed such that the decay takes place over very long time scales.

In this chapter we resolve this tension by showing that the near-BPS microstate geometries that one obtains by placing metastable anti-supertubes inside long scaling solutions [44] can in fact lower their energy when the bubbles of the scaling solution move relative to each other. Hence, what appears to be a metastable configuration from the point of view of the action of a probe brane is in fact an unstable one if one takes into account the degrees of freedom corresponding to the motion of the bubbles.

We study a scaling microstate geometry that is constructed using seven collinear Gibbons-Hawking centers [21] as well as an anti-supertube probe. If one keeps the GH centers collinear, the supertube Hamiltonian will have both supersymmetric and metastable minima [43], corresponding respectively to microstate geometries for supersymmetric and non-extremal black holes. For the latter, the mass above extremality of the black hole, ΔM, is simply equal to the value of the Hamiltonian in the metastable minimum.

However, it is well known that supersymmetric solutions that are constructed using N GH centers have a $2N-2$-dimensional moduli space, that is parameterized by the solutions of the $N-1$ bubble (or integrability) equations that govern the inter-center distances [20, 19, 3]. Hence, the mass above extremality, ΔM, is in fact a function of the position in the moduli space. Thus, if one is to prove that the supertube minimum corresponds to a metastable black hole microstate, one must also show that ΔM has a minimum when the GH points are collinear, and does not decrease as one moves around the moduli space[2]. We show that it does.

[2]Things are even a bit more complicated: as the GH points move in the $2N-2$-dimensional space of solutions to the bubble equations the $SU(2)$ angular momentum of the BPS solution, J_L, changes and hence the solutions do not correspond to the same black hole. For fixed values of the charges and angular momenta the moduli space of microstates of the corresponding black hole is a constant-J_L slice of the $2N-2$ space of solutions to the bubble equations, and has therefore dimension $2N-5$.

Indeed, if one examines ΔM as a function of certain moduli space directions one finds that the collinear GH configuration corresponds to a saddle point, and ΔM can in fact decrease as some of the centers move off the axis. Our result implies that the instability is triggered by the motion of the bubbles threaded by flux. As the configuration moves away from the saddle point, the kinetic energy of the bubbles increases, and we expect this to result in gravitational radiation that will relax the system towards a supersymmetric minimum.

One can also estimate the time-scale characteristic to this instability, as well as the energy emission rate, as a function of the charges and mass of the solution as well as of the other parameters of the non-extremal microstate geometry. To compute the time-scale we estimate the energy of the configuration as a function of the tachyonic rotation angle in the GH base space of the solution, as well as the kinetic term corresponding to the motion in the moduli space. The latter calculation is performed by formally interpreting our solution as a multi-center four-dimensional solution whose constant in the Taub-NUT (D6 brane) harmonic function has been set to zero. We then argue that the kinetic term corresponding to the angular motion we consider is the same as the one obtained by replacing some of the centers of the bubbling solution with the corresponding black hole and black ring. This allows us to compute this term and to find its scaling with the length of the black hole microstate throat.

We also check whether the microstate decay channel we study is similar to the decay channel one expects for a typical microstate of a D1-D5-P near-extremal black hole, which was computed in [65] and nicely follows from Stephen's law in five dimensions. There are three quantities that one can compare: the emission rate, the frequency peak energy and the typical radius of the microstate [66]. By changing the parameters of the microstate solutions we scan over, we can get any two of these parameters to agree, but not the third. This indicates that the particular non-extremal microstate geometries that we are considering are not typical.

This is not at all unexpected: of all the microstates of the BPS black hole we have chosen to uplift to a non-BPS one only a particular one, corresponding to seven collinear GH centers with certain fluxes on them. Furthermore, the starting configuration is clearly not a typical representative of the microstate geometries of the BPS black hole - one can find even more complicated solutions with a GH base where the centers are not aligned, and we expect from [67] that the typical states that contribute to the entropy of this black hole come from superstrata excitations of solutions with a GH base, that depend on arbitrary functions of two variables. Hence, it is hard to expect generically that the uplift of the non-typical seven-center BPS microstate geometry will give us a typical non-BPS microstate geometry whose decay rate will match that of the black hole.

Our investigation has two important conclusions:

- Microstate geometries of non-extremal black holes are unstable, and therefore the

dynamics of these black holes should correspond to a chaotic motion of mutually-non-supersymmetric centers at a bottom of a black-hole like throat.

- There exists a new decay channel for antibranes in solutions with charge dissolved in fluxes. Normally one studies these antibranes by considering them as probes in a solution and examining their action while assuming that the solution remains unchanged. Our investigation shows that this approach can give misleading results, and in order to determine whether an antibrane is metastable or unstable one should examine its full interactions with the moduli of the underlying solution.

This chapter is organized as follows. In § 4.2 we review the construction of the near-BPS microstates found in [44] and give some physical interpretation. In § 4.3 we explicitly show that these near-BPS microstates are unstable along a direction in the moduli space. Then in § 4.4 we compute the energy emission rate for a decay along the channel corresponding to this direction. We then study how the emission rate and other quantities scale with the length of the throat and the charges of the solution. We also compare the microstate emission rate, emission frequency and radius to those corresponding to the typical states in the black hole thermodynamic ensemble. We present some future directions in § 4.5.

4.2 Near-extremal three-charge black hole microstates

4.2.1 Microstate geometries for BPS black holes with large horizon area

The smooth horizonless microstate geometry that has the same charges and supersymmetries of a five-dimensional three-charge BPS black hole and has a Gibbons-Hawking (GH) base space was presented in § 2.3 in the context of bubbled solution. Its metric is given by:

$$ds_{11}^2 = -(Z_1 Z_2 Z_3)^{-\frac{2}{3}}(dt+k)^2 + (Z_1 Z_2 Z_3)^{\frac{1}{3}} ds_4^2 + (Z_1 Z_2 Z_3)^{\frac{1}{3}} \sum_{I=1}^{3} \frac{dx_{3+2I}^2 + dx_{4+2I}^2}{Z_I} \quad (4.2)$$

where the Z_I are the warp factors corresponding to the three charges, k is the angular-momentum 1-form and ds_4^2 is the metric of the GH base:

$$ds_4^2 = V^{-1}(d\psi + A)^2 + V(dy_1^2 + dy_2^2 + dy_3^2) \quad (4.3)$$

All the quantities appearing in (4.2) and (4.3) are defined following the standard procedure [2, 3] detailed in § 2.3, so that:

- The microstate solution is completely smooth
- The five-dimensional subspace spanned by time and the GH space asymptotically becomes flat and minkowskian

The whole background is determined once one fixes the number N of GH centers, as well as the residues of the four harmonic functions V and K^I at these centers:

$$V = \sum_{i=1}^{N} \frac{v_i}{r_i} \qquad K^I = \sum_{i=1}^{N} \frac{k_i^I}{r_i} \qquad r_i = |\vec{y} - \vec{g}_i| \tag{4.4}$$

where $\vec{y} = (y_1, y_2, y_3)$ and $\vec{g}_i$ is the position of the i-th pole in the same subspace. The particular BPS microstate geometry we will study in this chapter has $N = 7$ GH centers, whose (v_i, k_i^I) parameters are symmetric with respect to the GH center in the middle[3]:

$$\begin{aligned}
&v_1 = 20 \qquad v_2 = -20 \qquad v_3 = -12 \qquad v_4 = 25 \\
&k_i^1 = \frac{5}{2}|v_i| \qquad k_i^2 = \hat{k}|v_i| \qquad k_i^3 = \frac{1}{3}|v_i| \qquad i = 3, 4 \\
&k_1^1 = 1375 \qquad k_1^2 = -1835/2 + 980\hat{k} \qquad k_1^3 = -8260/3 \\
&k_2^1 = 1325 \qquad k_2^2 = -1965/2 - 980\hat{k} \qquad k_2^3 = 8380/3 \\
&v_{8-i} = v_i \qquad k_{8-i}^I = k_i^I \qquad i = 1, 2, 3
\end{aligned} \tag{4.5}$$

where the meaning of $\hat{k}$ will become clear in a moment.
As explained in § 2.3, the distances r_{ij} between the GH centers are subject to $N-1$ *bubble equations* that need to be satisfied to prevent the existence of closed timelike curves:

$$\sum_{j=1\, j\neq i}^{N} \Pi_{ij}^{(1)} \Pi_{ij}^{(2)} \Pi_{ij}^{(3)} \frac{v_i v_j}{r_{ij}} = -v_i \sum_{I=1}^{3} \sum_{s=1}^{N} k_s^I + \sum_{I=1}^{3} k_i^I \qquad \text{with} \qquad \Pi_{ij}^I \equiv \left(\frac{k_j^I}{v_j} - \frac{k_i^I}{v_i} \right) \tag{4.6}$$

To solve (4.6) with the parameters (4.5) we first constrain all the GH centers to lie on the same axis. Given that the parameters in (4.5) are invariant under $i \to 8 - i$ for $i = 1, ...4$, the solution of (4.6) will give rise to a collinear configuration, shown in Figure 4.1, with

$$r_{ij} = r_{(8-i)(8-j)} \tag{4.7}$$

Hence, the collinear solution is determined completely by r_{12}, r_{23}, r_{34}.

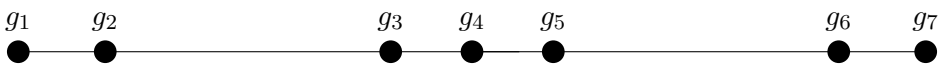

Figure 4.1: The collinear configuration of GH centers that we start from. Note that the distances between the satellites and the central blob are not on scale

[3]The value of k_1^3 given in [44] differs from the one we give here and in [66] because of a typo.

The family of collinear microstate geometries we consider is parameterized by $\hat{k}$, which controls the depth of our microstate. There is a critical value $\hat{k}_0$ at which the solution is singular[4], and changing $\hat{k}$ around this value gives rise to scaling solutions that have very small r_{ij} and hence a very long throat:

$$\hat{k} = \hat{k}_0 + \epsilon \qquad r_{ij} = \epsilon \overline{r}_{ij} + \mathcal{O}(\epsilon^2) \tag{4.8}$$

where the $\overline{r}_{ij}$ are determined by the fluxes on the two-cycles between the centers. As expected, in the scaling limit the ratios between the distances are fixed [20], and the physical distances between the GH centers become independent of the distance between these points in the GH base [21]. However, as ϵ approaches zero the length of the throat of the microstate geometry diverges as ϵ^{-1}.

We choose to work with a throat that is long-enough to describe the typical sector of the D1-D5-P black hole but not infinite, and we will fix the length of the throat for now by setting $\hat{k} = 3.1667$. In § 4.4.3 we will relax this condition and examine how the physics we find changes as $\hat{k}$ moves towards the critical value. We then use (4.5) to solve (4.6) and find

$$r_{12} = 3.58 \cdot 10^{-3} \quad r_{23} = 23.84 \quad r_{34} = 5.78 \cdot 10^{-3} \tag{4.9}$$

and the ratios

$$\frac{r_{23}}{r_{12}} \sim 6.7 \cdot 10^3 \quad \frac{r_{23}}{r_{34}} \sim 4.1 \cdot 10^3 \tag{4.10}$$

We discuss in § 4.2.2 the physical interpretation of these very large ratios.

The three electric charges of the solution and its $SU(2)$ angular momenta are (2.39):

$$Q_1 = 1.48 \cdot 10^5 \quad Q_2 = 1.20 \cdot 10^5 \quad Q_3 = 1.76 \cdot 10^5 \quad J_R = 1.018 \cdot 10^8 \quad J_L = 0 \tag{4.11}$$

As one can see from equation (2.41), J_L vanishes because of the Z_2 symmetry of our configuration (4.7). This solution represents a supersymmetric horizonless microstate of a BMPV black hole [68] with a classically large horizon area (and hence nonzero entropy) [21]. In the next section we illustrate some physical arguments that explain this conclusion.

4.2.2 Some physical properties of bubbled solutions

In [69] a smooth microstate was built for a maximally-spinning extremal horizonless BMPV black hole by taking a blob of GH centers ensuring that the (v_i, k_i^I) parameters are roughly of the same order. In the same paper it was shown that if one takes a huge number of

[4]For the curious, $\hat{k}_0 \approx 3.17975$.

centers and randomly assigns the (v_i, k_i^I) one inevitably ends up with a microstate of a maximally-spinning black hole.

On the other hand, in [19] it was shown that to build a bubbled solution for a maximally-spinning (zero-entropy) black ring it suffices to take a blob of GH centers (at least two) with zero total v-charge and a far-away GH center with $v = 1$. Such a solution can be obtained by choosing v_j approximatively of the same order, while taking $k_j^I \sim a$ for $j = 1, ...N-1$ and $k_j^I << a$ for $j = N_1$.

A crucial difference between these microstate solutions and the corresponding black holes and black rings is that the latter have an infinite AdS throat, while microstates have a finite throat that ends in smooth cap. There exists furthermore a limit in which the length of the throat can become infinite, and this scaling behavior (4.8) can be achieved for collinear solutions by tuning the v_j and the k_j^I [21], and for non-collinear solutions by changing the angles between the GH centers [66, 20].

Scaling solutions have also proved to be necessary ingredient for building microstates for BMPV black holes with *large* horizon area. This was done in [21] by merging a black ring blob with a black hole blob at its center. After a suitable choice of the black hole and black ring charges, this process can results in a microstate for a BMPV black hole with large horizon area.

We are now able to give a complete physical interpretation of the microstate of § 4.2. The parameters (4.5) are chosen so that centers g_1 and g_2 together with their counterparts g_6 and g_7 via (4.7) are far away from the central blob (4.10). The central blob $g_3 - g_4 - g_5$ has total GH charge one and hence represents a bubbled maximally-spinning black hole. The two satellites have zero GH charge, and represent two symmetric bubbled black rings. Because of the symmetry (4.7) the full solution has $J_1 = J_2 = J$, and furthermore one can check that $Q_1 Q_2 Q_2 > J^2$. Hence the solution represented in Figure 4.1 can be interpreted as a microstate of a BMPV black hole with a macroscopically large horizon area.

4.2.3 Adding Metastable Supertubes

To build a near-BPS microstate we add a supertube probe [55] to the BPS solution of § 4.2.1. If the supertube is at a supersymmetric minimum, the resulting microstate is still BPS. However, supertubes can also have metastable minima [43], and these give rise to microstate geometries of near-BPS black holes [44].
In the duality frame where the black hole has three M2 brane charges (4.2), a supertube is a tubular configuration of branes that has two types of M2 brane charges, q_1, q_2, as well as a dipole charge d_3 corresponding to an M5 brane that wraps the fiber of the

Gibbons-Hawking space [19]. The potential energy of a supertube is [43]:

$$\mathcal{H} = \frac{\sqrt{Z_1 Z_2 Z_3 V^{-1}}}{d_3 \rho^2} \sqrt{\left(\tilde{q}_1^2 + d_3^2 \frac{\rho^2}{Z_2^2}\right)\left(\tilde{q}_2^2 + d_3^2 \frac{\rho^2}{Z_1^2}\right)} + \frac{\mu \tilde{q}_1 \tilde{q}_2}{d_3 \rho^2} - \frac{\tilde{q}_1}{Z_1} - \frac{\tilde{q}_2}{Z_2} - \frac{d_3 \mu}{Z_1 Z_2} + q_1 + q_2 \tag{4.12}$$

where

$$\tilde{q}_1 \equiv q_1 + d_3(K^2 V^{-1} - \mu/Z_2), \quad \tilde{q}_2 \equiv q_2 + d_3(K^1 V^{-1} - \mu/Z_1) \tag{4.13}$$

and ρ is proportional to the size of the GH fiber at the location of the supertube

$$\rho^2 \equiv Z_1 Z_2 Z_3 V^{-1} - \mu^2 \tag{4.14}$$

The warp factors Z_I and the angular momentum parameter μ are defined in § 2.3, and V and K^I are the harmonic functions defined in (4.4). When the supertube is at a metastable point of the potential, $\mathcal{H} > q_1 + q_2$, and supersymmetry is broken. The total charges of the system are then given by the sum of the charges of the background and of the probe, while the total mass is

$$M_{tot} = \Delta M + \sum Q_{background} + q_{probe} \tag{4.15}$$

where ΔM is the value of $\mathcal{H} - (q_1 + q_2)$ at the metastable point. Even if the backreacted solution corresponding to this supertube has not been constructed explicitly, it is possible to argue that the resulting background is globally smooth in the duality frame where the charges of the black hole correspond to D1 branes, D5 branes and momentum.

As in [44], we consider a supertube whose charges are much smaller than those of the background, and whose physics can therefore be captured by the probe approximation:

$$(q_1, q_2, d_3) = (10, -50, 1) \tag{4.16}$$

The fact that q_2 and q_1 have opposite signs does not automatically imply that supersymmetry is broken [12]. A supertube with a given set of charges can have both BPS and metastable minima, and the parameters whose positivity ensures that supersymmetry is not broken are the $\tilde{q}_i$.

Let y_1 be the coordinate parameterizing the axis of Figure 4.1 centered in g_4. Given the symmetric arrangement of the GH points in § 4.2.1, $\mathcal{H}$ in (4.12) is invariant under $y_1 \to -y_1$. The probe potential has several Mexican-hat-type metastable minima, and we focus on the one in the proximity of g_6. The mass above extremality of this supertube is

$$\Delta M = \mathcal{H}(23.812, 0, 0) - (q_1 + q_2) \sim 0.04742 \tag{4.17}$$

It is important to stress that the existence of metastability does not depend on the parameter ϵ controlling the depth of the scaling BPS microstate geometry, because when the depth scales with ϵ as in (4.8) the probe potential (4.12) transforms as

$$\mathcal{H}(r'_{ij}) \to \epsilon \mathcal{H}(r_{ij}) + \mathcal{O}(\epsilon^2) \tag{4.18}$$

4.3 The instability of near-extremal microstates

In this section we show that the nearly-BPS microstates built in § 4.2.3 by using probe anti-supertubes are classically unstable.

We consider a microstate geometry with seven GH centers that have the v_i and k_i^I parameters as in (4.5). The location of the GH centers is constrained by the bubble equations (4.6) and by the requirement that J_L is zero, and hence the moduli space of the solutions is six-dimensional. For simplicity we examine a subset of this moduli space constrained by the symmetry (4.7), which automatically ensures that $J_L = 0$ and reduces the number of independent bubble equations from six to three. Furthermore, we will focus our discussion only on configurations where all the centers lie on the same plane[5]. The multicenter solutions that satisfy all these requirements can be parameterized by two coordinates (α, β), that are the angles shown in Figure 4.2.

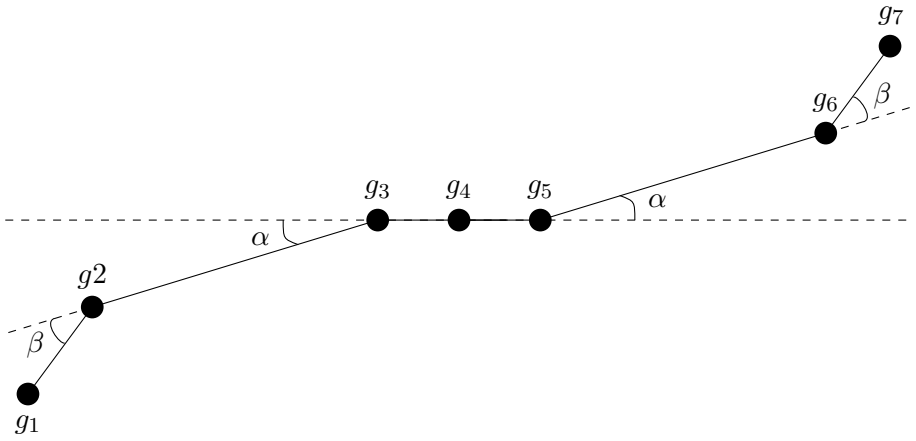

Figure 4.2: The parameterization for planar symmetric configurations with seven centers

As one changes these angles $(\alpha, \beta) \in [0, 2\pi] \times [0, \pi]$, the bubble equations (4.6) determining the inter-center distances are modified, and have to be solved again to determine the new values of the distances. In principle this way of parameterizing the solutions of the bubble equations can lead to singularities, as the bubbles can collapse for certain critical values of the angles, but this does not happen for the particular solution we consider.

It is not hard to see first that as one changes α and β the action of a probe supertube

[5]We have also analyzed the configurations where the centers are not on the same plane, but all the relevant physics is captured by the planar ones.

with charges (4.16) will continue having a metastable minimum in the vicinity of g_6 (or g_2). However, the exact value of the energy of the probe, which gives the mass above extremality, becomes a nontrivial function of the angles: $\Delta M(\alpha, \beta)$.

We analyzed $\Delta M(\alpha, \beta)$ numerically starting from the collinear configuration $(\alpha, \beta) = 0$. We found that keeping α fixed ΔM is monotonically increasing with $\beta \in [0, \pi]$ and this behavior does not depend on the choice of $\hat{k}$ for the scaling (4.8), as shown in Figure 4.3.

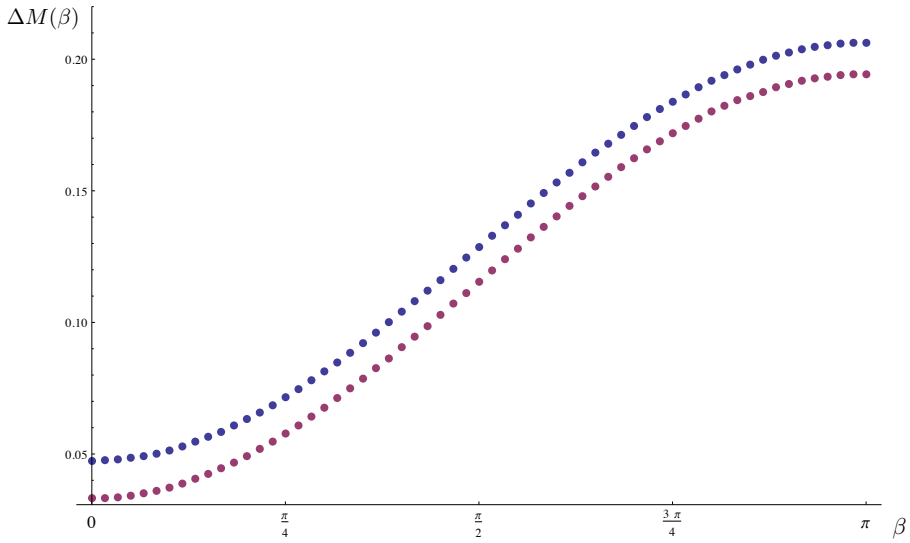

Figure 4.3: Plots of 60 values for ΔM in the interval $\beta \in [0, \pi]$ for $\alpha = 0$ in two different scaling regimes. The blue curve is obtained for $\hat{k} = 3.1667$, while the purple one is obtained for $\hat{k} = 3.175$, which corresponds to $\epsilon = 0.36$ in (4.8). For the sake of clarity, the values of the purple curves have been multiplied by 0.98 times the ratio of the two ΔM for the collinear configurations.

On the contrary, if one keeps β fixed and varies α, the mass of the anti-supertube $\Delta M(\alpha, \beta)$ decreases as α starts increasing. This behavior is again independent on the particular choice for $\hat{k}$ in (4.5), as shown in Figure 4.4.

This proves that the collinear near-BPS microstate configuration obtained in § 4.2 is classically unstable. Indeed, the initial microstate corresponds to $(\alpha, \beta) = 0$ for the parametrization of Figure 4.2 and Figure 4.4 shows that ΔM decreases when $\beta = 0$ and α starts increasing. The maximum relative difference in $\Delta M(\alpha, 0)$ is

$$\frac{\Delta M(0,0) - \Delta M(\pi/2, 0)}{\Delta M(0,0)} \sim 6.1 \cdot 10^{-4} \tag{4.19}$$

and in the scaling regime (4.18) this does not depend on the choice of $\hat{k}$.

Of course it is interesting to ask whether this configuration will settle into another metastable minimum somewhere in the moduli space, or simply will keep decaying until it reaches a BPS minimum. In the slice that we explored there appears to be a minimum

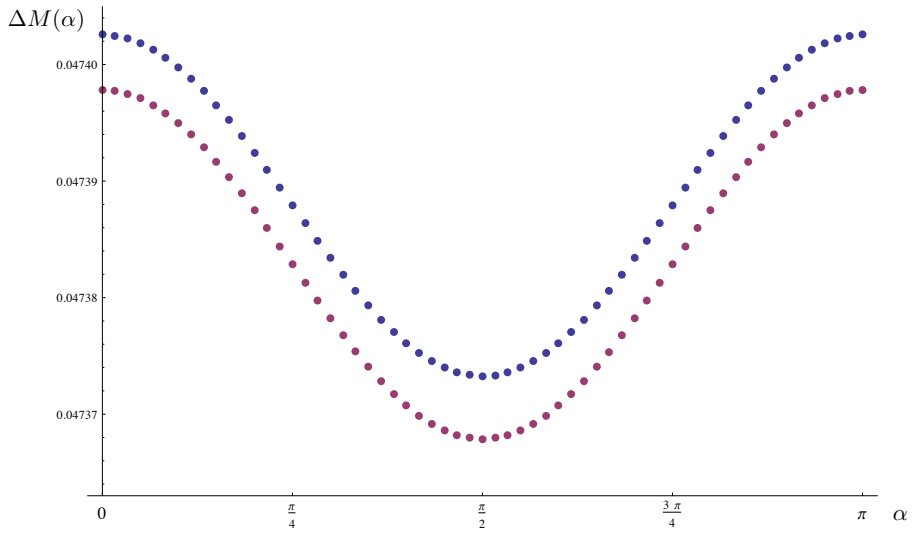

Figure 4.4: Plot of 60 values for ΔM in the interval $\alpha \in [0, \pi]$ for $\beta = 0$ in two different scaling regimes. The blue curve is obtained for $\hat{k} = 3.1667$, while the purple one is obtained for $\hat{k} = 3.175$, which corresponds to $\epsilon = 0.36$ in (4.8). The values of the purple curves have been multiplied by 0.98 times the ratio of the two ΔM for the collinear configurations in the two regimes.

when $\alpha = \pi/2$ and $\beta = 0$, but this does not imply that this minimum will be metastable. There could be other instability directions corresponding to other motions of the points in the moduli space.

To prove that there will never be any metastable minimum one should investigate the full 12-dimensional moduli space[6], which seems computationally tricky to perform, especially because not all solutions to the bubble equations are free of closed time-like curves. Furthermore, if we eliminate the constraint that the total J_L is zero, we can explicitly find a direction on the moduli space that leads to a scaling behavior, and as the configuration moves in that direction the energy of the anti-supertube approaches zero. Hence, we believe there is good reason to assume that metastable points in the moduli space are rare, if not altogether inexistent.

4.4 The emission rates of non-extremal microstates and their typicality

Figure 4.4 shows that the collinear near-BPS solution is unstable in the six dimensional moduli space of solutions to the bubble equations (4.6) with the symmetry (4.7). Classically, this instability would trigger a motion of the GH centers down the microstate throat and, in particular, Figure 4.4 represents the potential energy that governs this motion.

[6]The moduli space of N centers subject to the bubble equations and subtracting the center of mass motion is $2N - 2$ dimensional.

Quantum mechanically, this instability triggers a decay process towards extremality that causes the emission of radiation. From the thermodynamical point of view this is expected: a near-BPS black hole has a nonzero Hawking temperature and hence emits radiation according to (the five dimensional version of) Stephen's law. Our initial collinear near-BPS microstate would then decay into a series of different near-BPS microstates closer to extremality. We can interpret the symmetrical rotation in α of Figure 4.2 as a possible initial decay channel of the collinear microstate and using $\Delta M(\alpha)$ shown in Figure 4.4 we want to estimate the energy emitted per unit time Γ into this particular decay channel at the beginning of the decay cascade.

We consider the initial decay process from the collinear microstate to the state given by the configuration $\alpha = \pi/2, \beta = 0$ of Figure 4.2, which represents the minimum energy state in the slice considered in Figure 4.4. The emitted energy for this process is given by

$$\delta m \equiv \Delta M(\alpha = 0) - \Delta M(\alpha = \pi/2) \tag{4.20}$$

and is only a small fraction of the initial $\Delta M(0)$ - see (4.19). It is hence correct to say that $\alpha = \pi/2$ is only an intermediate state in the decay cascade that brings the microstate towards extremality.

To define an emission rate we need to know how much time the system needs to emit the energy δm. We suppose that this average time is of the same order of the characteristic time scale τ that, classically, governs the motion for small α as seen from an observer at infinity. Alternatively, τ can be seen as the necessary time to have a measurable displacement from the collinear configuration seen from infinity.

In order to find τ we need to estimate the kinetic and the potential energies corresponding to the classical motion of the GH centers in the moduli space of solutions to the bubble equations (4.6). We continue focusing on $\mathbf{Z}_2$ symmetric solutions (4.7), and we need to find the small-α expansion of the potential energy shown in Figure 4.4, as well as the small velocity expansion of the kinetic energy of the bubbles, $\frac{d^2E}{d\dot{\alpha}^2}$.

For small α, the mass above extremality behaves as

$$\Delta M(\alpha) = \Delta M_0 \left(1 - c_2\, \alpha^2\right) \tag{4.21}$$

where c_2 is a coefficient that can be found numerically and whose dependence of the charges of the solution and of the scaling parameters of the solution is discussed in detail in § 4.4.3.

The strategy for computing the kinetic term is much more involved. The few obvious guesses about how to do it, involving for example treating one of the GH centers as a probe in the background sourced by the others, do not give sensible answers. The essential reason is that the energy of a bubble does not come only from the GH centers but also from the fluxes wrapping this bubble, and to compute the total energy brought about by the slow

motion of the bubbles one has to compute the full energy of all the fluxes as well, and integrate the result over the full highly-warped spacetime.

Our strategy is to rather use the fact that some bubbles are much smaller than others, and therefore the collective motion of a certain small bubble has the same energy as the motion of the black ring that undergoes a geometric transition to form the small bubble. One can then "falsely compactify" the solution to a four-dimensional one, by adding a small constant in the harmonic function describing the Gibbons-Hawking base, and compute the kinetic energy corresponding to the motion of the black ring. The final result is clearly independent on the small constant we are adding, and hence does not change when taking this constant to zero and recovering the asymptotically 4+1 dimensional solution.

Hence, the strategy we use can be summarized in the following recipe:

1. We compactify the three-charge solution (4.2.1) to four dimensions along the fiber ψ by adding a constant to the V harmonic function.

2. We compute a Lagrangian for the motion in the α-direction excising GH centers g_1 and g_2 from the background and replacing them with a singular black ring having the same mass M_{br} and charges at the same distance $R \equiv r_{23}$ from the center, as explained in the physical interpretation of our solution in Appendix 4.2.2. The black ring in 4D is treated as a massive point particle that rotates in α in the background sourced by the other centers and under the effect of the potential in (4.21) generated by the anti-supertube probe closed to g_6.

3. We assume that the four-dimensional metric is not affected by the slow rotation in α, and hence that all the possible corrections to the background fields caused by this motion are negligible. In addition, the electromagnetic interactions between the black ring and the background can be neglected when the rotation is slow.

The first hypothesis helps to avoid useless computations as it allows to consider just point particles instead of extended objects. The supergravity solution (4.2.1) is asymptotically five-dimensional. The further compactification along ψ requires some caution. Indeed one needs to modify the asymptotic behavior of the GH space from $\mathbb{R}^4$ to $\mathbb{R}^3 \times S_1$ by introducing a constant δV in the function V in (4.4). The radius of the compactified S_1, $r \sim 1/\delta V^2$, can be thought of as a modulus of the solutions. In addition, one is also allowed to introduce constants δK^I in the definitions of the harmonic functions K^I in (4.4), which modify the bubble equations (4.6) - see [70] for more details. While all these moduli are completely arbitrary, they only specify the asymptotics of our solution and do not affect the computation we are interested in. The phenomenon that we want to study takes place deep into the black-hole-like throat and hence is not affected by the details of the asymptotic fields of the background. Therefore we can compactify to four dimensions with no risk of ambiguity.

The second hypothesis is really the key point of our computation. We have verified that taking away centers g_1 and g_2 from our system does not substantially modify the solution to the bubble equations (4.6). Using a hat to denote quantities computed without g_1 and g_2 we have $\widehat{r}_{56} \simeq r_{56} = r_{23}$, $\widehat{r}_{34} \simeq r_{34}$, up to corrections of order 0.1%. Most importantly, we verified numerically that the probe anti-supertube still has a metastable point close to g_6 and the behavior under rotation is similar to that of the complete system:

$$\Delta\widehat{M}(\alpha) = \Delta\widehat{M}_0(1 - \widehat{c}_2\alpha^2) \qquad \Delta\widehat{M}_0 \simeq \Delta M_0, \qquad \widehat{c}_2 \simeq \frac{c_2}{2} \tag{4.22}$$

where c_2 was introduced in (4.21)[7]. This means that we can excise the GH centers g_1 and g_2 from the whole solution and replace them by a BPS black ring whose charges are determined by the sum of the residues in the K, L and M harmonic functions of the points we excised. This is the inverse of the bubbling black ring transition described in [19], and it is not hard to check that the distance of the black ring from the central blob given by g_3, g_4 and g_5 is essentially the same as the original distance between the blob and the excised GH centers. Since the points g_6 and g_7 have not been excised, we can put the anti-supertube probe with charges (4.16) at the metastable location close to g_6.

Our strategy is to compute the kinetic term corresponding to the rotation of the black ring center in α (described in Figure 4.2), by treating the black ring center as a probe in the background sourced by the other GH centers.

Finally, the third hypothesis is reliable because α and its derivatives with respect to time are small and hence modifications to the four dimensional metric become higher-order corrections. Therefore we can safely use the four-dimensional metric generated by the collinear solution to estimate the kinetic term. Note that since the background is kept fixed to first order in α, the electromagnetic interactions between the point-like black ring and the background are negligible.

4.4.1 The decay time and the emission rate

We compactify the eleven-dimensional supergravity solution (4.2) on T_6 and ψ to a four-dimensional solution whose metric is

$$\begin{aligned} ds_4^2 &= J_4^{-\frac{1}{2}}(dt + \omega)^2 + J_4^{\frac{1}{2}}[dr^2 + r^2(d\alpha^2 + \sin^2\alpha\, d\phi^2)] \\ J_4 &= Z_1 Z_2 Z_3 V - \mu^2 V^2 \end{aligned} \tag{4.23}$$

[7]The factor in the relation between $\widehat{c}_2$ and c_2 comes from the fact that the energy reduction caused by the motion of the black ring alone is half of that caused by the movement of both the black ring and the bubbling black ring given by the points g_6 and g_7. Similarly, the kinetic energy corresponding to the motion of the black ring is half of that corresponding to the motion of both the black ring and the GH points g_6 and g_7.

and the four-dimensional dilaton is constant [3]. Note that the positivity of J_4 is one of the fundamental requirements for the construction of the solution [71], and comes from the absence of closed time-like curves in the eleven-dimensional geometry.

The GH centers g_1 and g_2 have been excised from the background (4.23) and we denote with a hat all the quantities computed using only the centers $g_3, ..., g_7$ with parameters as in (4.5). The black ring corresponds to a point-like particle at a distance

$$R = r_{23} = \hat{r}_{45} \tag{4.24}$$

from g_4 substituting g_1 and g_2 in Figure 4.1. Its mass M_{br} corresponds to the mass associated with g_1 and g_2 and is nothing but the mass of the black ring microstate that these centers represent, as explained in Appendix 4.2.2. The latter was found in [21]

$$M_{br} = Q^1_{br} + Q^2_{br} + Q^3_{br} \qquad Q^I_{br} = C^{IJK} d^J f^K \tag{4.25}$$

where we have introduced the parameters

$$d^I = 2\left(k^I_1 + k^I_2\right) \qquad f^I = 6k^I_0 + \left(1 + \frac{1}{v_1}\right) k^I_1 + \left(1 - \frac{1}{v_2}\right) k^I_2 \qquad k^I_0 = \frac{1}{3}\left(k^I_3 + k^I_4 + k^I_5\right) \tag{4.26}$$

If we then let the system rotate along α, the re-inserted point particle interacts with the potential (4.22). To compute the full Lagrangian we need to find the kinetic term corresponding to the slow motion of the black ring in the moduli space, and for this we can use the classical GR action:

$$S = -M_{br} \int \sqrt{-\hat{g}_{\mu\nu} \frac{dx^\nu}{dt} \frac{dx^\mu}{dt}} = -M_{br} \int \sqrt{\tilde{J}_4^{-\frac{1}{2}} - \tilde{J}_4^{\frac{1}{2}} R^2 \dot{\alpha}^2} \sim \int \frac{1}{2} M_{br} \tilde{J}_4^{\frac{3}{4}} R^2 \dot{\alpha}^2 + const \tag{4.27}$$

where we have used the time t measured by an observer at infinity to parameterize the worldline. Note that a tilde above J_4 means that this quantity is evaluated at the location of the black ring, namely at a distance R from the center g_4.

Thus, the full Lagrangian corresponding to the motion of the GH centers that triggers the decay of the metastable supertube

$$\mathcal{L} = \frac{1}{2} M_{br} \tilde{J}_4^{\frac{3}{4}} R^2 \dot{\alpha}^2 - \Delta \widehat{M}(\alpha) \tag{4.28}$$

and the associated equation of motion to first order in α is

$$M_{br} \tilde{J}_4^{\frac{3}{4}} R^2 \ddot{\alpha} - 2\widehat{c}_2 \Delta M_0 \alpha = 0 \tag{4.29}$$

Equation (4.22) allows us to approximate $2\widehat{c}_2 \sim c_2$ and hence the characteristic time scale

of this differential equation is

$$\tau = \sqrt{\frac{M_{br}\tilde{J}_4^{\frac{3}{4}}R^2}{\Delta M_0 c_2}} \tag{4.30}$$

This equation is the main result of this chapter. Since ΔM_0 parameterizes the initial energy of this solution above the BPS bound we see that the closer our solution is to the BPS bound the bigger τ is.

Using (4.20) and (4.30) following the arguments presented in § 4.4 we define the emission rate of our microstate in the α-channel to be

$$\Gamma = \frac{\delta m}{\tau} \tag{4.31}$$

In the next section we study how Γ scales under a scaling of the conserved charges Q_I and of the distances in the $\mathbb{R}^3$ base of the Gibbons-Hawking space underlying the BPS solution. These results will be used to check whether this particular kind of emission from the initial collinear microstate is typical in the thermodynamical ensemble.

4.4.2 Scaling properties of the α-emission rate

In this section we study how Γ behaves under two different types of scaling of the background. The results of this section will be used in the next one to compare Γ with the thermal emission rate found by the authors of [65] for a D1-D5-P non-extremal black hole and thus gain information about the typicality of the α-decay channel studied in the previous sections.

We are interested in two separate scalings that involve the parameters of our microstate. The first one corresponds to the scaling of the depth of the throat of our microstate (4.8) while keeping the charges and fluxes essentially fixed:

$$r_{ij} \to \epsilon\, r_{ij} \tag{4.32}$$

The second one corresponds to scaling all the magnetic fluxes in (4.5)

$$k \to \xi k \tag{4.33}$$

and modifies the charges and the mass as (2.39):

$$Q_I \to \xi^2 Q_I \qquad M \to \xi^2 M \tag{4.34}$$

Note that δM_0 is considered as a free parameter of the system and it does not scale. This quantity is the energy (4.17) brought about by placing an anti-supertube probe at metastable point close to g_6 and can be kept fixed while performing the scalings above by suitably tuning the anti-supertube charges (4.16). For the particular anti-supertube we are

using, we only need to tune the probe charge q_2 and keep q_1 and d_3 fixed as in (4.16). This is because the charge q_2 has opposite sign with respect to the corresponding background charge and it is responsible for supersymmetry breaking and metastability.

To study how τ in (4.30) scales with ϵ in (4.32) one can use equations (4.18) and (4.21) to deduce that c_2 in (4.30) does not transform, which is also shown in Figure 4.4. Then using the full construction of the solution presented in § 2.3 it is easy to determine that $\tilde{J}_4 \to \epsilon^{-3}\tilde{J}_4$, $R^2 \to \epsilon^2 R^2$ and hence

$$\tau \to \epsilon^{-\frac{1}{2}}\tau \tag{4.35}$$

As pointed out in [44], the physical importance of ϵ is to scale the (metric) length L_{MS} of the microstate throat as[8]

$$L_{MS} \to \epsilon^{-1} L_{MS} \tag{4.36}$$

Because of equations (4.35) and (4.36) we see that the decay time corresponding to the rotation α becomes longer as the length of the throat becomes longer; thus, the closer to BPS the configuration is the slower it decays.

To study how τ in (4.30) scales with ξ in (4.33) it is important to observe that after the scaling the bubble equations (4.6) are exactly solved by $r_{ij} \to \xi^2 r_{ij}$. Then it is easy to verify that

$$M_{br} \to \xi^2 M_{br} \qquad R^2 \to \xi^4 R^2 \qquad \tilde{J}_4 \to \xi^{-2}\tilde{J}_4 \tag{4.37}$$

Unlike for the ϵ-scaling, we could not evaluate analytically the scaling properties of c_2 in (4.30). To infer them numerically one can start from a ($\xi = 1$) solution with charges given in (4.11), and in order to keep ΔM_0 in (4.17) fixed while varying ξ one needs to change the q_2 charge of the anti-supertube probe in (4.16):

ξ	q_2
1	-50
1.2	-63.522
2	-117.92
3	-186.355
4	-254.958

By repeating for each value of ξ the evaluation that leads to the potential shown in Fig. 4.4, one finds that

$$c_2 \to \xi^{-\frac{1}{2}} c_2 \tag{4.38}$$

[8]The metric length of the microstate [44] is given by $L_{MS} = \int_{z_7}^{z_{neck}} V^{\frac{1}{2}} (Z_1 Z_2 Z_3)^{\frac{1}{6}} dz$, where z_{neck} is a suitable cutoff.

and therefore the overall scaling of τ with ξ under (4.33) is:

$$\tau \to \xi^{\frac{5}{2}}\tau \tag{4.39}$$

Finding the scaling properties of δm is much easier. This quantity does not scale with ϵ. Indeed, the probe hamiltonian (4.12) does scale with ϵ, as described in equation (4.18), but as we tune the probe charge to keep ΔM_0 constant it turns out that δm also remains constant. This does not happen for the ξ-scaling (4.33) and as there is no analytical formula for δm it is necessary to perform another numerical interpolation. Tuning the probe charge q_2 as before we find

$$\delta m \to \xi^{-0.8}\delta m \tag{4.40}$$

Finally, using the definition (4.31) with (4.35), (4.39) and (4.40) one determines the scaling properties of Γ under (4.32) and (4.33):

$$\Gamma \to \epsilon^{\frac{1}{2}}\Gamma \qquad \Gamma \to \xi^{-3.3}\Gamma \tag{4.41}$$

In the next section this result will be used to compare the emission rate Γ in the α-channel with the emission rate of the thermodynamical ensemble to check whether this decay is typical.

4.4.3 Typicality of the α-decay channel

In this section we want to compare the emission process of our microstate with the thermal emission of a near-BPS five-dimensional Reissner-Nordström black hole. In particular, we want to check whether the α channel emission has the features that one expects from thermodynamics.

We have three fundamental pieces of data about the radiation emission of the thermodynamical ensemble coming from general relativity and brane technology. The first is the computation [65] of the emission rate for a near-BPS three-charge five dimensional black hole in the D1-D5-P frame, where a tiny amount N_L of left-moving momentum is inserted on a string of length N_1N_5 with $N_R >> N_L$ right-moving momentum, so to break supersymmetry. The energy emission rate for closed strings was found to be

$$\Gamma_{th} \sim \sqrt{Q_1Q_2Q_3}T_H^5 \tag{4.42}$$

where T_H is the Hawking temperature of a five-dimensional Reissner-Nordström black hole computed from its surface gravity:

$$T_H \sim \frac{1}{R_e}\sqrt{\frac{\Delta M_0}{M}} \tag{4.43}$$

Here R_e and M are the horizon radius and mass of the black hole, and ΔM_0 is the mass above extremality, which is assumed to be much smaller than M. Given that the horizon area for this class of black holes is proportional to $A \propto \sqrt{Q_1 Q_2 Q_3}$ we see that (4.42) is simply Stephen's law in five dimensions.

The second piece of data for the comparison of energy emission rates is Wien's law, which follows from the five-dimensional version of Planck's law and has the same form in four and five dimensions:

$$\nu_{max,th} \sim T_H \tag{4.44}$$

where $\nu_{max,th}$ is the peak-frequency of energy emission from the ensemble and T_H is the black hole temperature (4.43).

The third and final piece of data is the difference ΔL between the depth of the microstate throat L_{ms} and the throat L_{bh} of the black hole corresponding to the microstate[9]. Since supersymmetric black holes have infinite L_{bh}, this comparison is meaningful only for non-supersymmetric black holes. In [44] it was shown that the for class of near-BPS microstates we discuss one can arrange L_{ms} to be arbitrarily larger or smaller than L_{bh}. However, we expect that typical microstate geometries of the black hole will have L_{ms} comparable to L_{bh}, and hence $\Delta L \approx 0$. In [44] ΔL was found to be

$$\Delta L = L_{bh} - L_{ms} = \rho_{neck} \ln\left(2\frac{\rho_{ms}}{\rho_{bh}}\right) \tag{4.45}$$

The parameter ρ_{ms} in (4.45) is given by

$$\rho_{ms} = 2\sqrt{R} \tag{4.46}$$

where R is the distance of the outermost GH center (4.24), while ρ_{bh} is given by:

$$\rho_{bh}^2 = \sqrt{\frac{8\Delta M}{\frac{1}{Q_1}+\frac{1}{Q_2}+\frac{1}{Q_3}}} \tag{4.47}$$

which is the horizon radius of the corresponding non-extremal black hole. The parameter ρ_{neck} in (4.45) corresponds to a certain cutoff needed to measure the throat lengths, but is irrelevant if when one imposes $\Delta L = 0$, which implies

$$\rho_{bh} = 2\rho_{ms} \tag{4.48}$$

The scaling properties of ρ_{ms} under (4.32) and (4.33) are easily found from the results of § 4.4.2:

$$\rho_{ms} \to \epsilon^{\frac{1}{2}} \rho_{ms} \qquad \rho_{ms} \to \xi \rho_{ms} \tag{4.49}$$

[9]This is a near-BPS five-dimensional Cvetič-Youm black hole [72].

It is straightforward to determine how (4.42), (4.43) and (4.47) scale with ξ under (4.34):

$$T_H \to \xi^{-2} T_H, \qquad \Gamma_{th} \to \xi^{-7} \Gamma_{th}, \qquad \rho_{bh} \to \xi^{\frac{1}{2}} \rho_{bh} \tag{4.50}$$

The thermal quantities do not scale with ϵ.

Given the three equations describing the thermal emission of the ensemble (4.42) and the size of the microstate, (4.44) and (4.48), we can argue that a given decay process of a microstate into a particular channel is typical if its Γ, $\nu_{\max}$ and ρ_{ms} match those given by these equations. The only missing information about our decay channel is ν_{max}. We can argue that the energy emitted during the decay of the nonextremal microstate geometry is given by the difference between the highest and the lowest values of the mass above extremality during the rotation in α:

$$\nu_{max} = \delta m \tag{4.51}$$

Given the scaling properties of our solutions (4.32), (4.33),(4.35), (4.39) and (4.49) we can start from the initial solution (with charges given in equation (4.11)) and check whether there is any value of ϵ and ξ (or alternatively of Q'_1, Q'_2, Q'_3 and ρ'_{ms}) for which the decay of our solutions matches the thermal decay:

$$\Gamma'_{th} = \Gamma' \qquad \nu'_{max,th} = \nu'_{max} \qquad \rho'_{bh} = 2\rho'_{ms} \tag{4.52}$$

Unfortunately, this is not possible, which implies that the solution we started from and the families of non-extremal microstate solutions obtained by scaling its depth and fluxes via (4.32) and (4.33) are not typical. This is not surprising - after all, we started from a very specific seven-center solution that has a lot of symmetry, and a very large ratio between certain inter-center distances, and we examined a non-extremal microstate geometry obtained by adding a certain type of anti-supertube to this solution. It would have been in fact much more surprising if this decay process had been thermal-like.

It is also possible to parameterizes the departure of the non-extremal microstate we consider from typicality by introducing a quantity, β, that can be thought of as modifying the estimation of τ of § 4.4[10]. If one multiplies τ by β in all the equations above, the system (4.52) can always be solved for some $\xi_{th}, \epsilon_{th}, \beta_{th}$. Plugging in the numbers we find that

$$\beta_{th} \sim 1.8 \cdot 10^5 \tag{4.53}$$

[10]The choice of multiplying τ is not arbitrary: we fully trust the assumptions that enter in the computation of τ of § 4.4, but given that we have not investigated the motion of the GH centers in the full six-dimensional moduli space, we do not know whether other decay directions exist where the decay time is faster or shorter. For example, if one would rather rotate the segment formed by the central points of the solutions, g_3, g_4 and g_5, the inertia momentum would be much smaller than the one corresponding to rotating the black ring centers, and hence the decay time would be much faster.

This therefore gives an estimate of the departure from typicality of the microstate we have considered. The final result $\beta_{th} >> 1$ has two possible implications that are not mutually exclusive. On one hand, it can imply that a typical microstate should have a Γ that is much smaller than the one of our emission process, or a much larger characteristic decay time τ.

This could be for example realized by considering non-extremal microstates that have more centers, and whose moment of inertia for the rotation in the direction that lowers the energy of the microstate is much bigger than in our solution. On the other hand (4.53) suggests also that the emitted energy δm should be much smaller than the one we found. This is not helped at all by considering microstate geometries that have more centers, because the potentials of these geometries will be generically less abrupt. Hence, to decrease the emitted energy one should rather consider creating non-extremal microstates by adding supertubes to BPS microstates with simple topology (like the superstrata of [67]). It would be interesting to investigate which of the two options is the best for producing more typical non-extremal microstate geometries.

4.5 Future developments

Given the results of the previous section, it becomes paramount to construct non-extremal microstate geometries that have a more typical decay. One way to do this is to build near-BPS microstates with more that seven centers, or whose centers are more evenly spaced as the ones in our solutions (which are at distances whose aspect ratio is of order 1000). Indeed, the seven-centers solution analyzed in this chapter represents somehow the minimal interesting model that one can build [21]. Furthermore, the moment of inertia corresponding to the motion that destabilizes our solution is very large as it corresponds to moving an entire bubbled black ring that has about one third of the total mass of the microstate. Finding a more sophisticated solution, though more involved, would allow us to look for analogous decay patterns that have a parametrically smaller moment of inertia or parametrically larger δm, such that and decay time that is fast-enough to be in the typical range.

From a more general perspective, our result confirms the intuition of [64], that most of the microstate solutions of non-extremal black holes should be unstable, and hence the dynamics of these black holes will display a chaotic behavior, corresponding to microstates being formed and immediately decaying into other microstates, which in their turn decay very fast. It would be interesting to see if our solutions can be used to shed light on some of the features of the chaotic behavior of non-extremal black holes discussed in [73].

It is also important to understand the physics of this instability in the decoupling limit. The Callan-Maldacena emission rate goes to zero in this limit, but there are other instabilities of supergravity solutions that do not [74, 75]. Our instability concerns the

dynamics deep down the throat of scaling solutions, and hence it is always present if one uses the time at the bottom of the throat. On the other hand, emission probabilities are computed using the time coordinate that is good at the asymptotically-flat infinity and in the scaling limit the relation between these two times becomes degenerate. Hence, in the scaling limit our emission rate becomes zero. Therefore, from this perspective our instability appears closer to the Callan-Maldacena one, and different from the ones in [74, 75], even though our instability would be set to zero by a qualitatively different process than the Callan-Maldacena one. There is a subtlety concerning the possible decoupling limits of our system: there are two of them. One is similar to the scaling limit, and corresponds to throwing away the constants in all the harmonic functions corresponding to the black hole charges, and obtaining a long throat that has an $AdS_2 \times S^3 \times T^6$ form in 11D supergravity. There is another decoupling limit, that one can only take in the duality frame where the charges of the black hole correspond to D1 branes, D5 branes and momentum, and which corresponds to throwing away the constant in the D1 and D5 harmonic functions but keeping the constant in the harmonic function corresponding to the momentum. This yields an asymptotically-$AdS_3 \times S^3 \times T^4$ geometry. We have not worked out what happens in this limit, but we expect that solutions are not affected by it, as happens for the instabilities of [74, 75]. A deeper analysis of the fate of our instability in the decoupling limit is hence needed to fully understand its nature.

Besides its implications for black hole physics, our result may also have important consequences for the program of uplifting AdS vacua obtained from generic flux compactifications to obtain de Sitter space in string theory. This will be the topic of the next chapter. There is a direct analogy between the uplift of AdS solutions to de Sitter by adding antibranes [14, 39] and the uplifting of BPS microstate geometries to microstates of non-BPS black holes by adding anti-supertubes [44]. In both constructions one used the action of the probe antibranes to argue that they have metastable vacua. However, our investigation reveals that the result of the probe calculation can be misleading, and that the metastable supertube can be in fact destabilized by the motion in the moduli space of the underlying geometry. However, unlike microstate geometries, flux compactifications usually come with all the moduli stabilized. Nevertheless, it is possible that even stabilized moduli can be destabilized, especially when their mass is very low. It would be interesting to understand whether this happens when investigating antibranes [39, 76, 77] in the Klebanov-Strassler warped deformed conifold solution [4].

CHAPTER 5

THE T-DUAL KLEBANOV-STRASSLER SOLUTION

5.1 de Sitter vacua in String Theory and infrared singularities

Recent observations together with theoretical developments in the field of cosmology indicate that our universe has a positive cosmological constant and hence asymptotes a de Sitter space. String Theory, the only known consistent theory of quantum gravity, has numerous compactifications to four and five dimensional Anti de Sitter spaces, while no straightforward compactification to de Sitter spaces has been realized. Finding compactifications with a small positive cosmological constant is an essential task for String Theory to be a predictable theory of Physics.

To date, the most well known procedure that uplifts AdS vacua to dS ones in String Theory is the KKLT mechanism [14]. This prescribes the insertion of antibranes in long warped throats of the compactification manifold, which ensures that the uplift of the cosmological constant does not destabilize the moduli. The antibrane then completely breaks supersymmetry and its presence allows to uplift the asymptotically AdS solution to dS. Needless to say, the uplifted dS vacuum is (meta)stable only if the antibrane is (meta)stable in the original flux compactification.

The most suitable framework where the KKLT uplift mechanism has been tested is given by the Klebanov-Strassler (KS) solution [4] presented in § 2.4. We remind that this is a smooth four-supercharge Type IIB solution with no brane sources and only fluxes threading a nontrivial topology. In particular, the ten-dimensional spacetime is divided into a warped four-dimensional Minkowski space and a six-dimensional internal space constituted by a deformed conifold. This is a cone over a base that topologically is equivalent

to an $S_2 \times S_3$, where the S_2 smoothly shrinks at the tip while the S_3 attains a finite radius and is threaded by constant fluxes. The KS solution is the model to study the validity of the KKLT uplift mechanism due to the fact that anti-D3 probe branes at the bottom of the KS throat have well-known metastable configurations [39].

However, recent investigations have shown that the fate of anti-D3 branes at the bottom of the KS throat is unclear. In [41, 76, 78, 79] their backreaction was taken into account and it was found that anti-D3 branes create a singularity in the solution. Furthermore, this singularity cannot be cloaked by a horizon [80, 81], which makes it problematic [82]. Analogous results for antibranes in highly warped throats were found in more general contexts [33, 83, 84, 85, 86], which might lead to the conclusion that the metastability of anti-D3 branes in KS is an artifact of the probe approximation [39].

On the other hand, it has been recently pointed out [87] that an analysis of the effective field theories of these probe branes should confirm the validity of their metastable configurations.

In this chapter we construct a consistent framework to test the stability of the antibranes in warped throats for a regime of parameters that has remained unexplored so far. Specifically, our aim is to construct the T-dual version of the KS solution, which is unknown to date[1]. The T-duality (see § 1.4) maps the radius of an S_1 isometry coordinate to its inverse, exchanging winding and momentum modes and giving access to the physics of a different region in the space of physical parameters. Such a new framework would then help solving the tension around the fate of antibranes in warped throats and the stability of the KKLT mechanism.

Two different pieces of information serve as guidance to construct the T-dual version of KS. On one side, the KS solution is the gravity dual of the $\mathcal{N} = 1$ cascading $SU(N + M) \times SU(N)$ gauge theory[2] and the corresponding Type IIA brane construction has been widely discussed in the literature [91, 92, 93, 94, 95, 96]. This construction involves $N+M$ D4 branes wrapping the four-dimensional Minkowski space and a compact direction, terminating on an NS5 brane. The latter also wraps a holomorphic curve [91].

On the other hand, the exact expression for the NS5 locus and its relation with the geometry of the deformed conifold is the second and most important clue we have. Indeed, it is general knowledge that a suitable T-duality of empty conifold geometries can give rise to solutions where an NS5 brane wraps a holomorphic locus [97, 98]. Qualitatively this happens when the $U(1)$ isometry chosen for the T-duality is fibered nontrivially over a base space and has a holomorphic locus of fixed points[3]. After a T-duality, this holomorphic

[1] Different T-dual versions are known [88, 89] for the Klebanov-Tseytlin singular theory [22], but none of these seems to be easily generalizable to KS and the results of [90] lack the mathematical rigor required for our purposes.

[2] Where $N = kM$ and k is an integer.

[3] More specifically, the locus of fixed points should just be composed of holomorphic branches, as for the singular conifold.

locus will be wrapped by NS5 branes. Recently, these kinds of T-dualities have been explicitly performed on the empty geometries of the singular [99], resolved and deformed conifolds [100] in a rigorous mathematical framework. In particular, as these NS5 branes arise from T-dualities of empty geometries, these techniques can still be applied to warped conifold geometries with nontrivial fluxes.

We start our analysis by showing that the isometry used in [100] and anticipated in [98] is not spoiled once one considers the full KS solution instead of the empty deformed conifold geometry. Unfortunately, even if we are granted that this isometry reproduces the desired components of the Type IIA brane engineering construction, the parameterization of this $U(1)$ in Type IIB is extremely involved. It is possible to have a clear picture of the isometry circle only on the three-sphere at the tip of the deformed conifold and the coordinates used to write the KS solution completely hide it.

To make progress we use the following strategy: As all the important physics to test the stability of antibranes is encoded in a region at the bottom of the KS warped throat, we focus on a small neighborhood of a particular point on the three-sphere at the tip, which we can refer to without loss of generality as the North Pole (NP). We choose this to be located on the fixed locus for our isometry. By introducing a small typical length we expand the KS solution in this neighborhood to a fixed order of precision. This allows to find a suitable set of coordinates that make the isometry of [100] manifest. At the same time the coordinates we introduce are easily related to the global topology of the deformed conifold. We explicitly check that by T-dualizing the empty geometry we reproduce the results of [100] expanded and written in the new NP coordinates, including the NS5 brane wrapping the desired holomorphic curve.

We then expand and T-dualize the full KS solution in the NP neighborhood. The expansion of the fields is realized by evaluating their squares contracted with the local KS metric. Since these scalar quantities are preserved under T-duality, this ensures no loss of physically relevant information in Type IIA. As the NP is mapped on the NS5 locus in type IIA we are able to reconstruct the physics close to this region, characterized by a blowing-up dilaton and B_2 NS-NS field. The same technique can be carried on at an arbitrary order of precision for the expansions.

To have a deeper insight of the KS physics and to test the stability of the antibranes, we then push our construction one step farther. We modify the KS solution by adding backreacted D3 branes localized at the NP. As this location belongs to the fixed locus of our isometry, the latter is not spoiled by the addition of the branes and thus we are able to reconstruct the corresponding T-dual solution using the same techniques as before. In particular, by expanding close to the NP, there is no need to solve the Laplace equation on the deformed conifold for the D3's, as we know that in our linearized metric the warp factor sourced by the branes will essentially coincide with that of D3 branes in flat space. In the resulting Type IIA solution we are able to see new interactions between the resulting

"background" NS5 brane and the added D4 branes.

This chapter is organized as follows. In § 5.2 we review the geometry of the deformed conifold and introduce three coordinate systems that are widely used in our analysis and geometrically describe the tip of the deformed conifold. In § 5.3 we describe the brane construction that one expects for the solution that is T-dual of KS, focusing on the NS5 locus and on the correct isometry for the T-duality. We then introduce the NP coordinates in § 5.4 and T-dualize the local empty geometry reproducing the same results as in [100]. In § 5.5 we expand the full KS solution close to the NP and explicitly write down its Type IIA T-dual solution. Some consistency tests are performed on the resulting solution. In § 5.6 we add backreacted D3 branes at the NP and apply the same procedure as before to reconstruct the corresponding T-dual solution. § 5.7 is dedicated to the discussion and outlook for our future work. In Appendix B we report some necessary computations to expand the KS solution in the NP neighborhood.

5.2 The geometry of the deformed conifold

In this section we briefly review the main features of the deformed conifold and introduce three coordinate systems that are of great importance for the subsequent analysis. We remind the reader that the KS solution was presented in § 2.4 and that its smooth metric (2.48) has a similar form to that of a standard D3 brane solution, having a deformed conifold as six-dimensional transverse space. A Ricci-flat metric for this manifold was already written in (2.46), together with a set of prime forms (2.44). Here the goal is to give a rigorous definition of what the deformed conifold is and find suitable coordinate sets to parameterize it.

The deformed conifold is a hypersurface in $\mathbb{C}^4$:

$$w_1^2 + w_2^2 + w_3^2 + w_4^2 = \varepsilon^2 \tag{5.1}$$

where $w_i \in \mathbb{C}$ and we assume $\varepsilon \in \mathbb{R}_{>0}$ with no loss of generality. We call the $w_i \in \mathbb{C}$ subject to the constraint (5.1) the *conifold coordinates*.
The deformed conifold is a cone over a $T^{1,1}$ base space, which was defined in § 2.4 as the coset:

$$T^{1,1} := \frac{SU(2) \times SU(2)}{U(1)} \tag{5.2}$$

The $T^{1,1}$ base is topologically equivalent to $S_2 \times S_3$, where only the S_2 shrinks at the tip of the cone so that deformed conifold has no singularities. These observations are easily proved in conifold coordinates. To study the base space of the deformed conifold one intersects (5.1) with a sphere of radius r in $\mathbb{C}^4$ defined as

$$|w_1|^2 + |w_2|^2 + |w_3|^2 + |w_4|^2 = r^2 \tag{5.3}$$

Writing each w_i as $w_i = a_i + ib_i$ one then gets the three following conditions that define the $T^{1,1}$ space in conifold coordinates:

$$\sum_{i=1}^{4} a_i^2 = \frac{r^2 + \varepsilon^2}{2} \tag{5.4}$$

$$\sum_{i=1}^{4} b_i^2 = \frac{r^2 - \varepsilon^2}{2} \tag{5.5}$$

$$\sum_{i=1}^{4} a_i \cdot b_i = 0 \tag{5.6}$$

which also require $r^2 \geq \varepsilon^2$. Equation (5.4) defines a three sphere S_3 that remains finite for $r = \varepsilon$, i.e. at the tip of the deformed confold. Equation (5.5) describes a two sphere S_2 fibered over the three sphere, where the fibration is specified by (5.6). Notice that the S_2 shrinks at the tip of the conifold. In [23] it was proved that $T^{1,1} = S_3 \times S_2$, namely that the fibration is trivial.

The most suitable coordinates to describe the brane content of the T-dual KS solution will be called *brane coordinates* and can be defined using the conifold ones. We introduce the matrix $\mathcal{W}$:

$$\mathcal{W} = \frac{1}{\sqrt{2}} w_i \, \sigma^i \tag{5.7}$$

where σ^i for $i = 1, 2, 3$ are the usual Pauli matrices and $\sigma^4 \equiv i\mathbf{1}$. The brane coordinates $(x, u, z_1, z_2) \in \mathbb{C}^4$ are defined by the entries of $\mathcal{W}$:

$$\mathcal{W} = \begin{pmatrix} z_1 & x \\ u & z_2 \end{pmatrix} = \frac{1}{\sqrt{2}} \begin{pmatrix} w_3 + iw_4 & w_1 - iw_2 \\ w_1 + iw_2 & -w_3 + iw_4 \end{pmatrix} \tag{5.8}$$

The definition of the deformed conifold (5.1) and the sphere in $\mathbb{C}^4$ (5.3) respectively become:

$$\det \mathcal{W} = -\frac{\varepsilon^2}{2} \quad \Rightarrow \quad z_1 z_2 - xu = -\frac{\varepsilon^2}{2} \tag{5.9}$$

$$\mathrm{Tr}(\mathcal{W}^\dagger \mathcal{W}) = r^2 \quad \Rightarrow \quad |x|^2 + |u|^2 + |z_1|^2 + |z_2|^2 = r^2 \tag{5.10}$$

We finally relate the brane coordinates to the *coset coordinates* that were used in § 2.4 to explicitly write the Klebanov-Strassler solution. This last set of coordinates is the one that is always used for computational purposes. In [23] the $T^{1,1}$ base space for the deformed conifold is defined as a coset manifold: Parameterizing each $SU(2)$ in (5.2) via Euler angles $(\phi_1, \theta_1, \psi_1)$ and $(\phi_2, \theta_2, \psi_2)$ as in [24] one can write a generic element in the coset as

$$e^{\frac{i}{2}\sigma_1 \phi_1} e^{\frac{i}{2}\sigma_2 \theta_1} e^{\frac{i}{2}\sigma'_1 \phi_2} e^{\frac{i}{2}\sigma'_2 \phi_2} e^{\frac{i}{2}(\sigma_3 + \sigma'_3)\psi} \tag{5.11}$$

where $\psi \equiv \psi_1 + \psi_2$ and σ_i σ_i' are two sets of Pauli matrices such that $[\sigma_i, \sigma_j'] = 0$. Given the coset parameterization (5.11) an element of the $U(1)$ quotient group is hence written as $e^{\frac{i}{2}(\sigma_3+\sigma_3')(\psi_1-\psi_2)}$. The radial coordinate τ is introduced via

$$r^2 = \varepsilon^2 \cosh \tau \tag{5.12}$$

where r is defined in (5.3), and hence the tip of the conifold is defined by $\tau = 0$. The coset coordinates allow to find the Ricci-flat Kähler metric in (2.46). One hence can relate brane coordinates to coset coordinates as follows [100]:

$$\begin{aligned}
x &= \frac{\varepsilon}{\sqrt{2}}\left(\cos\frac{\theta_1}{2}\cos\frac{\theta_2}{2}e^{\frac{1}{2}(\tau+i\psi)} - \sin\frac{\theta_1}{2}\sin\frac{\theta_2}{2}e^{-\frac{1}{2}(\tau+i\psi)}\right)e^{\frac{i}{2}(\phi_1+\phi_2)} \\
u &= \frac{\varepsilon}{\sqrt{2}}\left(-\sin\frac{\theta_1}{2}\sin\frac{\theta_2}{2}e^{\frac{1}{2}(\tau+i\psi)} + \cos\frac{\theta_1}{2}\cos\frac{\theta_2}{2}e^{-\frac{1}{2}(\tau+i\psi)}\right)e^{-\frac{i}{2}(\phi_1+\phi_2)} \\
z_1 &= -\frac{\varepsilon}{\sqrt{2}}\left(\cos\frac{\theta_1}{2}\sin\frac{\theta_2}{2}e^{\frac{1}{2}(\tau+i\psi)} + \sin\frac{\theta_1}{2}\cos\frac{\theta_2}{2}e^{-\frac{1}{2}(\tau+i\psi)}\right)e^{\frac{i}{2}(\phi_1-\phi_2)} \\
z_2 &= \frac{\varepsilon}{\sqrt{2}}\left(\sin\frac{\theta_1}{2}\cos\frac{\theta_2}{2}e^{\frac{1}{2}(\tau+i\psi)} + \cos\frac{\theta_1}{2}\sin\frac{\theta_2}{2}e^{-\frac{1}{2}(\tau+i\psi)}\right)e^{\frac{i}{2}(-\phi_1+\phi_2)}
\end{aligned} \tag{5.13}$$

5.3 The right isometry to T-dualize the Klebanov - Strassler solution

5.3.1 Brane content of a T-dualized KS solution

We would like to find an isometry in KS that, upon a T-duality, leads to a brane configuration that can be easily handled, as the one that realizes the gauge dual to KS in Type IIA supergravity [91]. To pursue this goal we hence apply an inverse-engineering process: starting from the expected brane content in Type IIA after the T-duality we are able to determine the main features of such isometry.

The Type IIA brane construction dual to the $\mathcal{N} = 1$ $SU(N+M) \times SU(N)$ theory consists of D4 branes wrapped on a circle and intersecting the two branches of an NS5 brane. The NS5 wraps a four-dimensional Minkowski space the holomorphic locus [101, 91]

$$z_1 z_2 = -\frac{\varepsilon^2}{2} \tag{5.14}$$

where we have defined $z_1 = x_4 + ix_5$ and $z_2 = x_8 + ix_9$. Away from the origin, namely for $|z_1|, |z_2| >> 0$, one can approximate $\varepsilon \simeq 0$ in (5.14) and hence consider the NS5 as two separate branes, the first one wrapping the directions x_4 and x_5 and located at $x_8 = x_9 = 0$ and vice-versa for the other. The coordinate x_6 parameterizes a circle wrapped by $N + M$ D4 branes, that also wrap the four-dimensional Minkowski space. The two NS5's intersect the compact direction x_6 in two distinct points. Among the D4

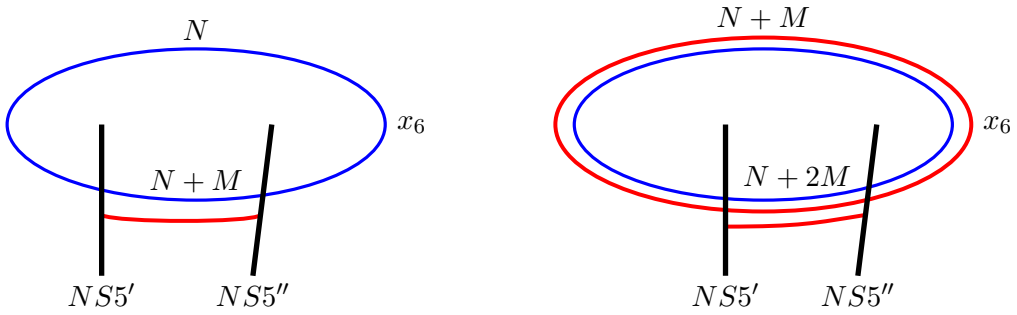

Figure 5.1: Brane configuration in the Type IIA dual to the (ultraviolet of the) $SU(N+M) \times SU(N)$ gauge theory. On the left there are N D4 branes wrapping the T-duality circle x_6 and M D4's stretched between the two NS5's for a fixed value of x_7. On the right the same configuration is represented for a higher value of x_7, where $NS5''$ has moved with respect to $NS5'$ spanning a full loop around the circle and pulling the M D4 branes. Now the dual theory has become $SU(N+M) \times SU(N+2M)$ and the crossing of the NS5's corresponds to the phase transition of Seiberg duality.

branes, only N of them wrap the whole x_6, while the remaining M wrap the same interval on x_6 delimited by the NS5 branes and terminate on them. This setup gives rise to a dual $\mathcal{N}=1$ $SU(N+M) \times SU(N)$ gauge theory. Furthermore, the intersections of the two NS5 branches on the circle x_6 depend on the remaining noncompact coordinate x_7: indeed the NS5 branches bend in this direction pulled by the D4. Therefore, while there are always M D4's between the two NS5's, the number of D4's wrapping the whole x_6 depends on how many times the NS5's have spiraled around it and hence depends on x_7. From the point of view of the dual theory the spiraling of the NS5's causes a cascade of Seiberg dualities [92] and x_7 qualitatively plays the role of the energy scale of the gauge theory. This mechanism along with the Type IIA brane construction is represented in Figure 5.1.

While the picture described so far is accurate in the ultraviolet where $|z_1|, |z_2| >> 1$ in (5.14), this is not so in the infrared, namely close to the origin of the coordinates. The chiral symmetry breaking that takes place in the infrared of the $SU(N+M) \times SU(N)$ theory is paralleled in the gravity dual by the joining of the two NS5 branches into a single holomorphic curve via the parameter ε. The smoothing of the brane locus due to quantum infrared physics is reminiscent of the geometric transition from the Klebanov-Tseytlin to the Klebanov-Strassler solution and as we will see this is not a coincidence.

The holomorphic locus expected for the NS5 (5.14) uniquely fixes the isometry that one has to use to T-dualize the KS solution, which is a common feature for conifold geometries. It is well known in the literature that only a suitable T-duality of empty conifold geometries can lead to NS5 brane configurations [98, 97]. Schematically, this is

made possible because the conifold geometries can be seen as nontrivial fibrations whose base spaces contains smooth loci where the fiber degenerates. Thus, choosing a $U(1)$ isometry on the fiber, the T-duality circle smoothly shrinks at the degeneration locus and hence blows up there in the T-dual solution, as is clear from Buscher's rules - see § 1.4. The T-duality hence gives a metric, dilaton and B_2 fields that blow up with the appropriate power on these loci, and $H_3 = dB_2$ measures an integer NS5 charge. This was rigorously shown for the empty singular conifold [99] and for the empty resolved and deformed conifolds[4] in [100]. In particular, the authors of [100] managed to get an NS5 wrapping precisely the locus (5.14), and the procedure makes use of the coordinates for the deformed conifold introduced in § 5.2. In brane coordinates, the deformed conifold is embedded in $\mathbb{C}^4$ via

$$z_1 z_2 - xu = -\frac{\varepsilon^2}{2} \tag{5.15}$$

The choice for the notation of (5.15) will be related to that of (5.14) in a moment. The brane coordinates describe the deformed conifold as a fibration, where the base space is a $\mathbb{C}^2$ parametrized by z_1, z_2, while the fiber is parametrized by either x or u. Indeed, two charts $\mathcal{U}_1 = \{x \neq 0\}$ and $\mathcal{U}_2 = \{u \neq 0\}$ are needed to cover the deformed conifold: in the following we will always assume that $x \neq 0$. The whole discussion can be rewritten for the other chart by simply replacing $x \leftrightarrow u$. The relationship between the brane coordinates and the coset ones of § 2.4 is presented in (5.13). For the deformed conifold note the existence of a $U(1)$ on the fiber of (5.15) that acts as

$$x \to e^{i\xi} x \qquad u \to e^{-i\xi} u \qquad \xi \in \mathbb{R} \tag{5.16}$$

Equation (5.16) is a symmetry for the conifold as written in (5.15) and it was proved in [100] that this an isometry for the conifold metric (2.46). The locus that is left invariant by (5.16) coincides precisely with (5.14) an gets wrapped by an NS5 in the T-dual solution. In [100] this was also confirmed by computing the integer NS5 brane charge with the NS-NS three-form field strength that one gets in Type IIA.

Incidentally, note that taking $\varepsilon = 0$ in (5.15) one obtains the defining equation for the singular conifold, which is the internal manifold of the Klebanov-Tseytlin solution [22]. Then T-dualizing along the same $U(1)$ as in (5.16) one ends up with two NS5 branes wrapping (5.14) with $\varepsilon = 0$. The Klebanov-Tseytlin and KS solutions essentially coincide in the ultraviolet and this happens also for the NS5 brane loci that one gets from a T-duality of their geometries. These two theories however differ in the infrared, where the Klebanov-Tseytlin solution is singular and the related NS5 locus remains composed by two separate branches. In KS, the chiral symmetry breaking is responsible for the puffing-up

[4] By empty deformed conifold here we mean a supergravity solution given by just the metric $ds^2 = dx^i dx^i + ds_6^2$ where ds_6^2 is as in (2.46). This is a valid supergravity solution as the deformed conifold is Ricci-flat.

of the S_3 at the tip, which in the T-dual solution is paralleled by the joining of the two NS5 branches into a single holomorphic curve.

The isometry (5.16) is the right one to obtain the NS5 configuration (5.14) expected from the brane construction dual to the $SU(N+M) \times SU(N)$ theory, starting from the empty deformed conifold. A priori it is not obvious that (5.16) remains an isometry for the full KS solution, but if it is we already know that a T-duality along it would give the NS5 configuration (5.14) that is required from the brane construction. The proof is presented in the next section.

5.3.2 The isometry for the T-duality of KS

In this section we prove that the transformation (5.16) performed on the brane coordinates (5.8) is an isometry for the KS solution of § 2.4, assuming that it is an isometry for the metric on the deformed conifold (2.46), which was shown in [100].

To prove that (5.16) is an isometry for the full KS background one must show that it leaves invariant all the other fields together with the warped metric. Observing that in the KS solution $F_5 = B_2 \wedge F_3$ and that F_3 and $H_3 = dB_2$ are related by the supersymmetry equations, one concludes that (5.16) is an isometry for the full KS solution if and only if it leaves B_2 in (2.50) and the warp factor $h(\tau)$ in (2.49) invariant.

From (5.8) only the conifold coordinates w_1 and w_2 depend on x and u and under (5.16) these transform as

$$\begin{aligned} w_1 = \frac{x+u}{\sqrt{2}} \quad &\longrightarrow \quad \frac{e^{i\xi}x + e^{-i\xi}u}{\sqrt{2}} \\ w_2 = -i\frac{u-x}{\sqrt{2}} \quad &\longrightarrow \quad -i\frac{e^{-i\xi}u + e^{i\xi}x}{\sqrt{2}} \end{aligned} \tag{5.17}$$

this is equivalent to

$$\begin{pmatrix} w_1 \\ w_2 \end{pmatrix} \longrightarrow \begin{pmatrix} \cos\xi & \sin\xi \\ -\sin\xi & \cos\xi \end{pmatrix} \begin{pmatrix} w_1 \\ w_2 \end{pmatrix} \tag{5.18}$$

This proves that w_1, w_2 are rotated by an angle ξ under (5.16) and hence this transformation belongs to the $SO(4)$ group that leaves the conifold invariant, as is clear from (5.1).

Working in conifold coordinates it is then easy to see from (5.12) and (5.3) that τ is invariant under (5.16). Consequently, all the functions in the KS solution (2.54) and the warp factor (2.49) are invariant under this transformation. In addition, as shown in [102], B_2 in (2.50) can be rewritten in conifold coordinates in an $SO(4)$-invariant form:

$$B_2 = g(\tau)\epsilon_{ijkl} w^i \bar{w}^{\bar{j}} dw^k \wedge d\bar{w}^{\bar{l}} \qquad\qquad g(\tau) = \frac{ig_s M\alpha'}{3\varepsilon^4} \frac{\tau\coth\tau - 1}{\sinh^2\tau} \tag{5.19}$$

and then a fortiori B_2 is invariant under (5.16). In the formula above $i, j, k = 1, 2, 3, 4$ and

τ is implicitly rewritten as a function of the w_i. This completes the proof that (5.16) is an isometry for the whole KS solution and as this is a $U(1)$ transformation it can be used to T-dualize this solution.

We have understood how to T-dualize the KS solution to a Type IIA one similar to that depicted in Figure 5.1, expected from the dual gauge theory. To be precise, a T-duality along (5.16) will result in a setup similar to that in Figure 5.1, but smeared along the T-duality circle, the equivalent of x_6 in the Figure. We will discuss in the next section how to perform this T-duality.

5.4 The North Pole expansion

In the previous section we found the isometry that allows to T-dualize the KS solution and obtain a similar brane configuration expected from the dual gauge theory, smeared along the T-duality direction. However, putting in practice this strategy proves to be most tricky. First of all, making the isometry (5.16) manifest in the KS solution requires a laborious change of coordinates on the deformed conifold. The transformation (5.16) can be identified with a shift in the complex phase of the brane coordinate x, when $x \neq 0$. Equation (5.13) shows the relationship between the brane coordinates of (5.15) and the coset coordinates used to write the KS solution in § 2.4. The phase of x written in coset coordinates is a highly nontrivial and ill-defined function. This is because one also has to deal with the $x = 0$ locus in (5.15), where the phase of u in (5.16) becomes the valid coordinate for the isometry instead. Secondly, it is quite hard to visualize the isometry circle (5.16) on the deformed conifold and we only have a clear picture of it on the S_3 at the tip - see Appendix 5.4.1. While the authors of [100] took care of these subtleties for the empty deformed conifold, this ends up in untreatable formulas if performed on the full KS solution that can hide the interesting physics encoded in Type IIA.

These difficulties are encountered if one attempts to T-dualize the KS solution as a whole, but might well be avoided if one compromises to reconstruct the T-dual solution of just a small region of the deformed conifold in the KS solution. This certainly does not invalidate the possibility to check the antibrane stability in Type IIA. Indeed, the stability of the antibrane should be checked close to the (image of the) tip of the deformed conifold and hence it suffices to choose a small region there.

We intend to realize the program of § 5.3.1 in the following way. We focus on a small region on the deformed conifold, requiring it to be a small neighborhood centered on a point on the S_3 at the tip that will be called the North Pole (NP). In the next section we explicitly study the tip of the deformed conifold using brane and coset coordinates. Then in the following section we will introduce a suitable coordinate set together with a typical characteristic length. By T-dualizing the empty deformed conifold metric expanded in the NP neighborhood using the isometry (5.16) we get an NS5 brane precisely wrapping the

(expansion of the) curve (5.14). Our local results are then compared with the globally-valid ones of [100]. In the next sections we expand the KS solution in the NP neighborhood and then T-dualize it to realize the program of § 5.3.1.

5.4.1 The tip of the deformed conifold

In order to understand what the NP coordinates should look like it is useful to analyze the geometry of the tip of the conifold. In this section we provide a suitable parameterization for the tip of the conifold, following [100]. The tip of the conifold is the $\tau = 0$ locus in coset coordinates, which corresponds to $r^2 = \varepsilon^2$ in (5.12). The metric (2.46) is finite as $K(\tau) \to \left(\frac{2}{3}\right)^{\frac{1}{3}}$ and the metric at the tip becomes:

$$d\Omega_3^2 = \frac{\varepsilon^{\frac{4}{3}}}{2}\left(\frac{2}{3}\right)^{\frac{1}{3}}\left[\frac{1}{2}(g^5)^2 + (g^3)^2 + (g^4)^2\right] \tag{5.20}$$

As expected from (5.4) this should be the round metric of the surviving S_3. This is can be proved defining as in [24]:

$$T = L_1\sigma_1 L_2^\dagger \sigma_1 \tag{5.21}$$

where L_1 and L_2 are matrices of the $SU(2)$ groups in (5.2) parametrized via Euler angles as in (5.11). One then has

$$\mathrm{Tr}(dT^\dagger dT) = \frac{1}{2}(g^5)^2 + (g^3)^2 + (g^4)^2 \tag{5.22}$$

and as T itself is an $SU(2)$ matrix the metric above represents the standard three-sphere metric. Then from (5.20) one reads that the squared radius of the S_3 at the tip is proportional to $\varepsilon^{\frac{4}{3}}$.

Note that the metric of the deformed conifold (2.46) is invariant under the $\mathbf{Z}_2$ symmetry that exchanges ϕ_1, θ_1 and ϕ_2, θ_2. Indeed, the coset coordinates depict the $T^{1,1}$ base as a symmetric S_1 fibration over $S_2 \times S_2$, where the fiber is parametrized by ψ, while (ϕ_i, θ_i) parametrize the two S_2. The coset coordinates are not suitable to describe this S_3. The matrix T introduced in (5.21) parameterizes precisely the $SU(2)$ to which the $T^{1,1}$ base degenerates at the tip of the conifold, which is symmetrically embedded in the coset (5.2). We then introduce the Euler angles $\zeta \in [0, \pi[$ and $\phi_w, \phi_x \in [0, 2\pi[$ to rewrite T as:

$$T = \begin{pmatrix} \cos\frac{\zeta}{2}e^{i\phi_x} & -\sin\frac{\zeta}{2}e^{-i\phi_w} \\ \sin\frac{\zeta}{2}e^{i\phi_w} & \cos\frac{\zeta}{2}e^{-i\phi_x} \end{pmatrix} \tag{5.23}$$

and comparing with (5.21) one gets

$$\begin{aligned}\cos^2\frac{\zeta}{2} &= \frac{1}{2}[1+\cos\theta_1\cos\theta_2-\cos\psi\sin\theta_1\sin\theta_2]\\ \phi_w &= \arctan\left[\frac{\sin\left(\frac{\theta_1-\theta_2}{2}\right)}{\sin\left(\frac{\theta_1+\theta_2}{2}\right)}\tan\frac{\psi}{2}\right]-\frac{1}{2}(\phi_1-\phi_2)\\ \phi_x &= \arctan\left[\frac{\cos\left(\frac{\theta_1-\theta_2}{2}\right)}{\cos\left(\frac{\theta_1+\theta_2}{2}\right)}\tan\frac{\psi}{2}\right]+\frac{1}{2}(\phi_1+\phi_2)\end{aligned} \tag{5.24}$$

while the metric (5.22) is given by

$$d\Omega_3^2 = \frac{d\zeta^2}{2}+2\sin^2\frac{\zeta}{2}d\phi_w^2+2\cos^2\frac{\zeta}{2}d\phi_x^2 \tag{5.25}$$

The coordinates (ζ,ϕ_w,ϕ_x) see the three sphere as a circle fibration over a disc, where the fiber is parameterized by ϕ_x and the base is parameterized by (ζ,ϕ_w). The fiber smoothly shrinks at the boundary of the disc so to give a smooth S_3.

The coordinates (5.24) allows to nicely parameterize the NS5 locus (5.14) at the tip of the conifold. For $\tau=0$ the coordinate ϕ_x in (5.24) is the phase of the brane coordinate x in (5.13) when rewritten as $x=|x|e^{i\phi_x}$. This means that it can be used to parametrize the isometry (5.16), i.e. it can be used as T-duality coordinate. Indeed, the coordinate β that we used for the T-duality around the NP basically coincides with ϕ_x plus a shift -see (5.31). Using (5.13) it is possible to rewrite the NS5 locus (5.14) in coset coordinates:

$$2+2\cos\theta_1\cos\theta_2-e^{-\tau+i\psi}(1+e^{2\tau+2i\psi})\sin\theta_1\sin\theta_2=0 \tag{5.26}$$

If one imposes $\tau=0$ in (5.26) and then uses (5.24) one gets

$$\cos^2\frac{\zeta}{2}=0 \tag{5.27}$$

which means that the NS5 for $\tau=0$ wraps the boundary of the disc $\zeta=\pi$ in Type IIA. Indeed, the component of the metric (5.25) for ϕ_x degenerates exactly on this locus in Type IIB.

5.4.2 Definition of the NP neighborhood

To construct the NP neighborhood we introduce a small parameter δ that will be used to linearize the KS background. We then define a new coordinate system suitable to both linearize the metric (2.46) and to make the isometry (5.16) manifest, which is performed in two steps. First of all, we redefine the coset coordinates of the deformed conifold in (2.46),

constraining some combinations of them to be of order δ [77]:

$$\begin{aligned} \alpha &= \frac{\theta_1+\theta_2}{2} & \beta &= \frac{\phi_1+\phi_2}{2} & \tilde{\tau} &= \frac{\tau}{2}\delta \\ \omega &= \frac{\phi_2-\phi_1}{2}\delta & \nu &= \left(\frac{\theta_1-\theta_2}{2}-\frac{\pi}{2}\right)\delta & \mu &= \frac{\pi-\psi}{2}\delta \end{aligned} \tag{5.28}$$

The tilde from $\tilde{\tau}$ will always be dropped, keeping in mind the rescaling of a factor of two. Secondly, ω, ν, μ in (5.28) are replaced with the following combinations:

$$\begin{aligned} r &= \sqrt{\mu^2\cos^2\alpha+\nu^2} \\ z &= \omega-\mu\sin\alpha \\ \sigma &= \arctan\left[\frac{-\nu}{\mu\cos\alpha}\right] \end{aligned} \tag{5.29}$$

The coordinates $\tau, \alpha, \beta, r, z, \sigma$ in (5.28) and (5.29) will be referred to as the NP coordinates. Note that these are composed by three angular coordinates α, β, σ and three radial coordinates of order δ, namely τ, r, z. The NP is located at $\tau = r = z = 0$ and hence lies on the S_3 at the tip of the conifold. To avoid clutter, the parameter δ will be suppressed in the formulas where it is not necessary, keeping in mind that only τ, r, z carry a power of δ. In addition, the base one-forms $d\tau, dr, dz$ will be considered of order δ, meaning that once one expresses these as functions of the coset coordinates they get multiplied by a factor of δ.

The conifold metric (2.46) expanded to lowest order in the NP coordinates then becomes:

$$ds_6^2 \simeq \varepsilon^{\frac{4}{3}}\left(\frac{2}{3}\right)^{\frac{1}{3}}\left[d\tau^2+\tau^2(d\alpha^2+\cos^2\alpha\, d\beta^2)+dr^2+dz^2+r^2\,(d\sigma+d\beta)^2\right] \tag{5.30}$$

Note that while each term in (5.30) is of order δ^2, the contraction of (5.30) with itself gives a scalar of order one. The metric (5.30) is not quite the metric of an $\mathbb{R}^6$, which can be recovered by adding β to the definition of σ in (5.29). The reason why it is necessary to write the metric (5.30) keeping the cross-term $d\sigma + d\beta$ is related to the shape of the NS5 locus in the NP neighborhood and will become clear in a moment.

The NP neighborhood is composed by two three-dimensional subspaces. The first one (spanned by τ, α and β) is written in spherical coordinates, while the second one is parameterized by cylindrical coordinates. These two subspaces have a direct connection with the topology of the deformed conifold. The two sphere that shrinks at $\tau = 0$ in (5.30) is *exactly* the S_2 that shrinks at the tip of the conifold, while the remaining subspace parameterizes the portion of the NP neighborhood that lies on the S_3.

The parameterization of the three-sphere (5.24) is useful also to justify the redefinition (5.29) that completes the NP expansion. Indeed plugging (5.28) and (5.29) into (5.24)

and expanding to lowest order in δ one gets

$$\cos^2\frac{\zeta}{2} \simeq r^2 \qquad \phi_w \simeq \frac{\pi}{2} + z \qquad \phi_x = \sigma + \beta \tag{5.31}$$

From (5.31) it is clear that the NP ($\tau = z = r = 0$) lies on the boundary of the base disc $\xi = \pi$ of the fibration (5.25). Inserting (5.29) into (5.25) and (5.31) one obtains the linearized flat metric in cylindrical coordinates of (5.30). Note that plugging (5.28) and (5.29) in (5.26) and expanding to lowest order one gets precisely (5.33)

To show that the NP expansion makes it easier to realize the program of § 5.3.1 it is useful to T-dualize the empty metric (5.30). Indeed (5.30) is the linearized metric on a small neighborhood of the empty deformed conifold and one can compare the local physics it exhibits with the globally-valid T-duality of [100]. The first step is to expand the brane coordinates of (5.15) using the NP ones. Equation (5.13) reports the coordinate change between brane and coset coordinate systems. Inserting (5.28) and (5.29) into (5.13) and expanding to lowest order one gets:

$$\begin{aligned}
x &\simeq \frac{\varepsilon}{\sqrt{2}}[r\cos\sigma + i(\tau\cos\alpha + r\sin\sigma)]e^{i\beta}\\
u &\simeq \frac{\varepsilon}{\sqrt{2}}[r\cos\sigma + i(\tau\cos\alpha - r\sin\sigma)]e^{-i\beta}\\
z_1 &\simeq \frac{\varepsilon}{\sqrt{2}}[z + i(1 - \tau\sin\alpha)]\\
z_2 &\simeq \frac{\varepsilon}{\sqrt{2}}[-z + i(1 + \tau\sin\alpha)]
\end{aligned} \tag{5.32}$$

One can observe two crucial facts from (5.32). First of all, x and u in (5.32) are of order δ, while z_1 and z_2 are of order one with corrections of order δ. The NP, that corresponds to $\tau = r = z = 0$, is precisely on the locus (5.14). Secondly, comparing (5.16) and (5.32) it is clear that β becomes the coordinate that parameterizes the T-duality circle, as it is a full angular coordinate in the definition (5.28).

We now rewrite the locus (5.14) in the NP coordinates. Note that inserting (5.32) into (5.15) one no longer obtains an equality, as (5.32) was obtained expanding to highest order in δ. Consequently, as (5.14) is satisfied at lowest order in the NP coordinates, to find the brane locus one has to also impose $x = u = 0$ to hold at lowest order as well. From (5.32) we get

$$x = u = 0 \quad \Longleftrightarrow \quad \cos\alpha = r = 0 \tag{5.33}$$

which is the locus that gets wrapped by an NS5 in Type IIA. The neighborhood around the NP parameterized by the coordinates used in (5.30) together with the NS5 locus is represented in Figure 5.2.

The T-duality along β of the empty geometry (5.30) confirms that (5.33) gets wrapped by an NS5 brane in Type IIA. Following Buscher's rules recalled in § 1.4, the metric (5.30)

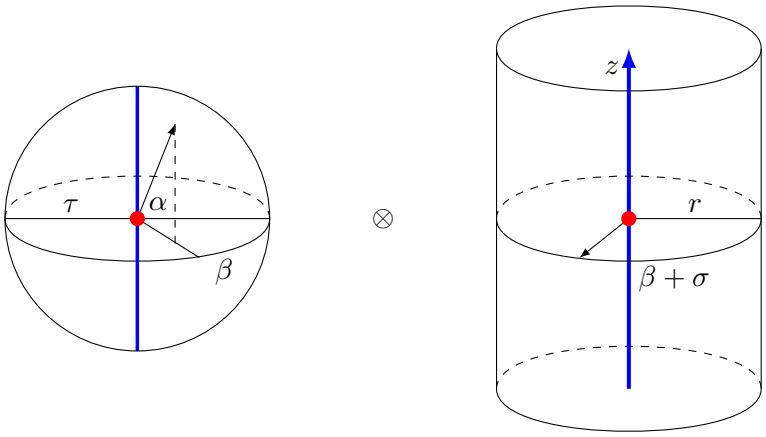

Figure 5.2: The NP neighborhood seen as a product of the collapsing S_2 at $\tau = 0$ and a cylinder that entirely lies on the S_3. The red dots represent the NP, while the blue lines represent the NS5 brane locus (5.33)

should be rewritten as:

$$ds_6^2 = \varepsilon^{\frac{4}{3}} \left(\frac{2}{3}\right)^{\frac{1}{3}} \left[(\tau^2 \cos^2\alpha + r^2) \left(d\beta + \frac{r^2}{\tau^2 \cos^2\alpha + r^2} \, d\sigma \right)^2 + d\tau^2 + \tau^2 \, d\alpha^2 + dr^2 + dz^2 + \frac{r^2 \tau^2 \cos^2\alpha}{\tau^2 \cos^2\alpha + r^2} \, d\sigma^2 \right] \tag{5.34}$$

and we define the quantity:

$$A_\sigma \, d\sigma = \frac{r^2}{\tau^2 \cos^2\alpha + r^2} \, d\sigma \tag{5.35}$$

Then a T-duality along β maps the NP neighborhood to a region in Type IIA, where the local metric is given by:

$$ds^2_{6,\,IIA} = \varepsilon^{\frac{4}{3}} \left(\frac{2}{3}\right)^{\frac{1}{3}} \left(d\tau^2 + \tau^2 \, d\alpha^2 + dr^2 + dz^2 + \frac{r^2 \tau^2 \cos^2\alpha}{\tau^2 \cos^2\alpha + r^2} \, d\sigma^2 \right) + \varepsilon^{-\frac{4}{3}} \left(\frac{2}{3}\right)^{-\frac{1}{3}} \frac{d\beta^2}{\tau^2 \cos^2\alpha + r^2} \tag{5.36}$$

In addition, in Type IIA one gets a nontrivial dilaton:

$$e^{2\Phi} = \varepsilon^{-\frac{4}{3}} \left(\frac{2}{3}\right)^{-\frac{1}{3}} \frac{1}{\tau^2 \cos^2\alpha + r^2} \tag{5.37}$$

and a nontrivial B_2 field:

$$B_2 = \frac{r^2}{\tau^2 \cos^2\alpha + r^2} \, d\sigma \wedge d\beta \tag{5.38}$$

The $g_{\beta\beta}$ component of (5.36), the dilaton (5.37) and B_2 in (5.38) blow up precisely on the

locus (5.33) as one would expect in a solution containing NS5 branes. We have also verified that (5.36), (5.37) and (5.38) represent the NP expansion of the corresponding quantities found in the analogous T-duality of the empty deformed conifold in [100]. In [100] it was also shown that the flux of $H_3 = dB_2$ found in Type IIA measures an integer NS5 charge. Qualitatively, this is also confirmed by the fact that B_2 in (5.38) does not contain any factor of ε, which is the only physically relevant constant of the empty geometry. It is important to stress that the shape of the NS5 brane in Type IIA is a feature of the T-duality along the particular isometry we chose and the manifold we are working with. Both these ingredients are still there in the KS solution and hence we expect also the same NS5 to appear in the T-dual version of this solution.

If (5.30) had been written exactly as an $\mathbb{R}^6$ metric the situation would be radically different. Indeed, a T-duality along β would not produce any B_2 field, while $g_{\beta\beta}$ and the dilaton in Type IIA would blow up on a locus that is different from (5.33), which verifies $u = x = 0$ in NP coordinates. The reason why the NP metric should be written as in (5.30) lies in the fact that the T-duality circle as defined in (5.16) wraps both the shrinking S_2 at the tip and the blown up S_3, as explained in § 5.4.1.

5.5 The Type IIA solution T-dual to KS

5.5.1 Expansion of the KS solution in the NP neighborhood

In this section we expand the KS solution reported in § 2.4 around the NP and rewrite it in the formalism of Buscher's rules of § 1.4 to ease the T-duality in β.

We expand the KS solution of § 2.4 starting from the metric (2.48). The deformed conifold metric (2.46) becomes as in (5.30) and is of order δ^2, while the Minkowski metric $dx^i dx^i$ on the first four coordinates remains untouched. Requiring to keep corrections up to order δ^2 in the metric determines how to expand the warp factor (2.49). In particular, one needs to truncate differently the expansions of $h^{-\frac{1}{2}}$ and $h^{\frac{1}{2}}$, which are then denoted with a hat:

$$\begin{aligned} \hat{h}^{-\frac{1}{2}} &= \frac{\varepsilon^{\frac{4}{3}}}{g_s M \alpha' 2^{\frac{1}{3}}} \left(\frac{1}{\sqrt{a_0}} - \frac{a_2 \tau^2}{2 a_0^{\frac{3}{2}}} \right) \\ \hat{h}^{\frac{1}{2}} &= g_s M \alpha' \varepsilon^{-\frac{4}{3}} 2^{\frac{1}{3}} \sqrt{a_0} \end{aligned} \tag{5.39}$$

where $a_0 \approx 0.71805$ was computed in [4] and $a_2 = -2^{\frac{8}{3}} \cdot 3^{-\frac{4}{3}}$ is computed in Appendix B. Note that in (5.39) $\hat{h}^{-\frac{1}{2}}$ was truncated at order δ^2, while $\hat{h}^{\frac{1}{2}}$ was truncated at order one, so that all the metric components contribute with terms up to order two. Indeed, the full expanded KS metric becomes

$$ds^2_{KS} = \hat{h}^{-\frac{1}{2}} dx^i dx^i + \hat{h}^{\frac{1}{2}} ds^2_6 \tag{5.40}$$

with ds_6^2 as in (5.30) and the warp factor as in (5.39). To perform a T-duality along β one rewrites ds_6^2 in (5.40) exactly as in (5.34) and defines the same quantity $A_\sigma d\sigma$ as in (5.35).

Now that the metric has been expanded one can proceed with the expansion of the KS RR and NS-NS field strengths. It is not possible to simply expand a field strength in power series and then just truncate it at some fixed order in δ, as this might lead to a loss of physically relevant information. To this purpose, we use a more reliable procedure that consists of two steps. Given an n-form field strength $F_{\mu_1\mu_2\ldots\mu_n}$ one computes its square $(F_n)^2$ defined as

$$(F_n)^2 = F_{\mu_1\mu_2\ldots\mu_n} g^{\mu_1\nu_1} g^{\mu_2\nu_2} \cdots g^{\mu_n\nu_n} F_{\nu_1\nu_2\ldots\nu_n} \tag{5.41}$$

where in (5.41) one has to use the expanded metric (5.40). Then one first truncates the power series expansion in δ of $(F_n)^2$ at a fixed order. Secondly, one expands $F_{\mu_1\mu_2\ldots\mu_n}$ in power series and keeps only the terms that contribute to the truncation of $(F_n)^2$. This criterion is mathematically accurate, as it based on the expansion of (5.41), which is a scalar. Most importantly, this criterion is also physically meaningful. The square of a field strength (5.41) is of the same order as (the square of) the flux that the field is carrying and this guarantees no loss of relevant information. Furthermore, the scalars built as in (5.41) are preserved under a T-duality together with their power series expansions. This means that if one expands the field strengths in Type IIB following the procedure described above then in Type IIA one automatically reconstructs the field strengths expanded with the very same criterion. Using this rule we can safely proceed to rewrite the KS fields in the NP coordinates of § 5.4.2. We choose to keep all the terms in the expansions of the KS field strengths that contribute to the lowest order term of the expansion of their square.

The expansion of the B_2 KS field in (2.50) rewritten directly in the formalism of Buscher's rules is given by

$$B_2 = B_{a\beta}\, dy^a \wedge (d\beta + A_\sigma\, d\sigma) + \widehat{B}_2 \tag{5.42}$$

where $A_\sigma\, d\sigma$ is as in (5.35) and

$$B_{a\beta}\, dy^a = \frac{2}{3} M g_s \alpha' \tau (\tau^2 \cos\alpha\, d\alpha - r \sin\alpha\, dr - r \cos\sigma \cos\alpha\, dz) \tag{5.43}$$

$$\begin{aligned} \widehat{B}_2 = &- \frac{2}{3} M g_s \alpha' \tau (r \cos\alpha \cos\sigma dz \wedge d\sigma + \cos\alpha \sin\sigma dz \wedge dr + r \sin\alpha dr \wedge d\sigma) \\ &- B_{a\beta} dy^a \wedge A_\sigma\, d\sigma \end{aligned} \tag{5.44}$$

It is useful to show how to count the factors of δ in B_2 and its square. According to the conventions of § 5.4.2, the coordinates τ, r, z along with $d\tau, dr, dz$ carry a factor of δ: consequently, all the terms appearing in (5.44) are of order δ^3. As B_2 has legs only along the deformed conifold, when one builds its square as in (5.41) one has to use the inverse expanded metric along the deformed conifold, which is of order δ^{-2}. Therefore $(B_2)^2$ is of

order δ^2, but the physically meaningful information is carried by $H_3 = dB_2$, whose square is of order one. Indeed, taking the differential of B_2 in (5.44) does not alter the order of magnitude of the single terms, which remains δ^3. Now H_3 has one more leg along the deformed conifold with respect to B_2 and hence $(H_3)^2$ receives an additional factor δ^{-2} from the expansion of the inverse metric on the conifold. The fact that H_3 is not irrelevant at the NP is expected from the discussion of the KS solution in § 2.4: as the flux of H_3 on the S_3 remains finite even at the tip then this form should be of order one close to the NP.

Using the conventions of Buscher's rules in § 1.4 we rewrite the expansion of F_3 in (2.51) as

$$F_3 = F_{3,\beta} \wedge (d\beta + A_\sigma \, d\sigma) + \widehat{F}_3 \tag{5.45}$$

where $A_\sigma d\sigma$ is as in (5.35). Then we find:

$$\begin{aligned} F_{3,\beta} = M\alpha' \Bigg(& -\frac{1}{3} r\tau \cos\sigma d\tau \wedge d\alpha + \frac{1}{3}\tau \cos\alpha \cos\sigma \sin\alpha d\tau \wedge dr + \frac{1}{3}\tau \cos^2\alpha d\tau \wedge dz \\ & -\frac{1}{3} r\tau \cos\alpha \sin\alpha \sin\sigma d\tau \wedge d\sigma + \frac{2}{3}\tau^2 \cos^2\alpha \cos\sigma d\alpha \wedge dr \\ & -\frac{2}{3}\tau^2 \cos\alpha \sin\alpha d\alpha \wedge dz - \frac{2}{3} r\tau^2 \cos^2\alpha \sin\sigma d\alpha \wedge d\sigma + 2r dr \wedge dz \Bigg) \end{aligned} \tag{5.46}$$

and

$$\begin{aligned} \widehat{F}_3 = & -\frac{1}{3} M\alpha' \tau \sin\sigma d\tau \wedge d\alpha \wedge dr - M\alpha' \frac{r\tau \cos\alpha}{3(r^2 + \tau^2 \cos^2\alpha)} \big(\tau^2 \cos\alpha \cos\sigma d\tau \wedge d\alpha \wedge d\sigma \\ & + r \cos\sigma \sin\alpha d\tau \wedge dr \wedge d\sigma + r \cos\alpha d\tau \wedge dz \wedge d\sigma + 2r\tau \cos\alpha \cos\sigma d\alpha \wedge dr \wedge d\sigma \\ & + 6r\tau \sin\alpha d\alpha \wedge dz \wedge d\sigma \big) \end{aligned} \tag{5.47}$$

The expansions of some wedge products among the base one-forms (2.44) are reported in Appendix B. Each term of (5.46) and (5.47) carries a factor δ^3, which implies that F_3^2 is of order one. This is again expected from the discussion at the end of § 2.4: as F_3 is constant and nonzero at the tip its square has to be of order one in the NP neighborhood.

The NP expansion of the self-dual RR five-form (2.52) is rewritten as

$$F_5 = F_{5,\beta} \wedge (d\beta + A_\sigma \, d\sigma) + \widehat{F}_5 \tag{5.48}$$

where

$$\begin{aligned} F_{5,\beta} &= -g_s M^2 (\alpha')^2 \frac{16\tau^3 r}{9} \cos\alpha \, d\alpha \wedge dr \wedge dz \wedge d\sigma \\ \widehat{F}_5 &= \frac{\varepsilon^{\frac{8}{3}}}{g_s^3 M^2 (\alpha')^2 a_0^2} \frac{4}{3^{\frac{4}{3}}} \tau \, dt \wedge dx^1 \wedge dx^2 \wedge dx^3 \wedge d\tau \end{aligned} \tag{5.49}$$

We stress that $\widehat{F}_5$ is just the expansion of the original $\star F_5$ in (2.52), as $F_{5,\beta} \wedge A_\sigma \, d\sigma = 0$. $(F_5)^2$ is of order δ^2 and then its flux is small. This is also expected from the physics of the KS solution: indeed the flux measured by F_5 on the $T^{1,1}$ space depends on τ and smoothly goes to zero at the tip.

5.5.2 The Type IIA solution dual to KS

The T-dual of the KS solution in the NP neighborhood is readily obtained from the results of § 5.5.1. Using the expansions for the warp factor 5.39 the full Type IIA metric at the NP is given by:

$$\begin{aligned} ds^2_{IIA} = & \frac{\varepsilon^{\frac{4}{3}}}{g_s M \alpha' 2^{\frac{1}{3}}} \left(\frac{1}{\sqrt{a_0}} - \frac{a_2 \tau^2}{2 a_0^{\frac{3}{2}}} \right) dx_i dx_i + \frac{3^{\frac{1}{3}} d\beta^2}{g_s M \alpha' 2^{\frac{2}{3}} \sqrt{a_0} (\tau^2 \cos^2\alpha + r^2)} \\ & + \frac{2^{\frac{4}{3}} 3^{\frac{1}{3}} \tau}{3\sqrt{a_0}(\tau^2 \cos^2\alpha + r^2)} \, d\beta \, (\tau^2 \cos\alpha \, d\alpha - r \sin\alpha \, dr - r \cos\sigma \cos\alpha \, dz) \\ & + g_s M \alpha' \sqrt{a_0} \frac{2^{\frac{2}{3}}}{3^{\frac{1}{3}}} \left(d\tau^2 + \tau^2 d\alpha^2 + dr^2 + dz^2 + \frac{r^2 \tau^2 \cos^2\alpha}{\tau^2 \cos^2\alpha + r^2} d\sigma^2 \right) \end{aligned} \tag{5.50}$$

while the Type IIA dilaton is nontrivial:

$$e^{2\Phi} = \frac{3^{\frac{1}{3}}}{g_s M \alpha' 2^{\frac{2}{3}} \sqrt{a_0} (\tau^2 \cos^2\alpha + r^2)} \tag{5.51}$$

The first and third lines in (5.50) together with the dilaton (5.51) are similar to the corresponding lines in (5.36) and the dilaton (5.37) that one gets by T-dualizing the empty geometry expanded around the NP. The fact that now we are T-dualizing the KS solution is signaled by the presence of the KS constants such as M and a_0 and by the τ^2-correction in the metric on the Minkowski space. The second line of (5.50) is completely new and contains cross-terms with β entirely coming from the nontrivial expansion of the KS B_2 field in (5.44). From (5.50) one can easily verify that $g_{\mu\nu} g^{\mu\nu}$ is still of order one, as expected. Note how the $g_{\beta\beta}$ component in (5.50) and the dilaton (5.69) blow up on the NS5 locus (5.33) with the appropriate power, as expected from § 5.5.1.

The same divergence appears for the Type IIA B_2 field:

$$\begin{aligned} B_{2,IIA} &= A_\sigma \, d\sigma \wedge d\beta + \widehat{B}_2 \\ &= \frac{r^2}{\tau^2 \cos^2\alpha + r^2} \, d\sigma \wedge d\beta + \widehat{B}_2 \end{aligned} \tag{5.52}$$

where $\widehat{B}_2$ is as in (5.44). The first term in (5.52) is the same as in (5.38) and arises just from the geometry. As in § (5.5.1) the square of $H_3 = dB_2$ is of order one.

The RR two-form field strength F_2 is:

$$F_2 = F_{3,\beta} \tag{5.53}$$

where $F_{3,\beta}$ is as in (5.46). The square of this flux computed as in (5.41) using (5.50) is of order δ^2.

According to Buscher's rules of § 1.4, the four-form field strength is given by:

$$F_4 = \widehat{F}_3 \wedge (d\beta + B_{a\beta}\, dy^a) + F_{5,\beta} \tag{5.54}$$

where $\widehat{F}_3$, $B_{a\beta}\, dy^a$ and $F_{5,\beta}$ are defined in (5.47), (5.43) and (5.49) respectively. Using the new metric (5.50) it turns out that $(\widehat{F}_3 \wedge d\beta)^2$ is of order δ^2, while $(\widehat{F}_3 \wedge B_{a\beta}\, dy^a)^2$ is of order δ^4 as well as $(F_{5,\beta})^2$. The lowest order component of F_4 in (5.54) is hence proportional to M, as one would expect for a four-form field-strength in the presence of smeared D4 branes.

The Type IIA RR sector also contains a six-form and an eight-form field strengths, that can be computed from the hodge duals of (5.54) and (5.53) respectively, keeping in mind that the star operator is defined using (5.50). We report here only the component of dC_5 with legs along the directions $0, 1, 2, 3, \tau, \beta$, which is important for the purposes of the next section:

$$dC_5|_{0123\tau\beta} = \frac{\varepsilon^{\frac{8}{3}}}{g_s^3 M^2 (\alpha')^2 a_0^2} \frac{4}{3^{\frac{4}{3}}} \tau\, dt \wedge dx^1 \wedge dx^2 \wedge dx^3 \wedge d\tau \wedge d\beta \tag{5.55}$$

The square of (5.55) is of order δ^4 and it is easy to verify that it comes from the hodge dual of the $F_{5,\beta}$ component in (5.54), whose square is also of order δ^4 as expected.

Check: a D4 probe brane feels zero force

In this section we show that a D4 probe brane wrapping t, x_1, x_2, x_3 and β feels no force in the Type IIA solution presented in § 5.5.2. This result is expected from the fact that a probe D3 wrapping the first four coordinates in KS does not break any supersymmetries and is hence in equilibrium regardless of its location on the deformed conifold. Our D4 probe in the Type IIA dual KS solution interacts only with the metric (5.68), the dilaton (5.69) and C_5 in (5.55). Denoting pullbacks on the D4 worldvolume with a tilde the probe action is (compare with (1.21)):

$$\mathcal{S} = -\int d^5\, \tilde{x}\, e^{-\widetilde{\Phi}} \sqrt{-\det \widetilde{g}_{\mu\nu}} + \int \widetilde{C}_5 \tag{5.56}$$

where the first integral is the Dirac - Born - Infeld action and the second one is the Wess-Zumino term. The potential $\widetilde{C}_5$ can be easily reconstructed by intrgrating (5.55):

$$\widetilde{C}_5 = \frac{\varepsilon^{\frac{8}{3}}}{g_s^3 M^2 (\alpha')^2 a_0^2} \frac{2}{3^{\frac{4}{3}}} \tilde{\tau}^2 \, d\tilde{t} \wedge d\tilde{x}^1 \wedge d\tilde{x}^2 \wedge d\tilde{x}^3 \wedge d\tilde{\beta} \tag{5.57}$$

In the Dirac-Born-Infeld part of the action (5.56) the dilaton (5.69) cancels $\tilde{g}_{\beta\beta}$ of (5.68) appearing in the determinant, so that the whole action is finite without divergences. The remaining of the integrand can be expanded in powers of δ up to highest corrections:

$$\sqrt{\left(1 - \frac{a_2 \tilde{\tau}^2}{2a_0}\right)^4} \simeq 1 - \frac{a_2 \tilde{\tau}^2}{a_0} \tag{5.58}$$

A quick check shows that (5.58) and (5.57) are of the same order in δ, so a cancellation in (5.56) is possible. Indeed, inserting (5.58) and (5.57) into (5.56) and restoring all the constants from § 5.5.2 including a_2 in (B.4) one has:

$$\mathcal{S} = -\int d^5\tilde{x} \, \frac{\varepsilon^{\frac{8}{3}}}{g_s^3 M^2 (\alpha')^2 a_0 2^{\frac{2}{3}}} \left(1 + \frac{2^{\frac{2}{3}} \tilde{\tau}^2}{3^{\frac{4}{3}} a_0}\right) + \int d^5\tilde{x} \, \frac{\varepsilon^{\frac{8}{3}}}{g_s^3 M^2 (\alpha')^2 a_0^2} \frac{2}{3^{\frac{4}{3}}} \tilde{\tau}^2 = const \tag{5.59}$$

which shows that our D4 probe does not feel any force in Type IIA KS, as expeted. Moreover, the fact that the τ-dependent part in (5.58) exactly cancels against (5.57) proves that the criterion used to expand the KS field strengths in § 5.5.1 is physically consistent with the expansion of the metric and its warp factors in (5.40).

5.6 Adding D3 branes to KS

In this section we want to push the T-duality procedure described in § 5.4.2 and § 5.5.1 one step forward. We modify the KS solution in § 2.4 by adding C D3 branes at the NP wrapping the Minkowski space of KS. These will backreact interacting with the KS fields and causing a singularity at the NP, giving rise to what will be referred to as the KS+D3 solution. This solution is static because the C D3 branes are perfectly stable at the NP, as shown for the T-dual solution in § 5.5.2. Applying the techniques described before we want to reconstruct the new T-dual version of the NP neighborhood. This operation is carried on to better understand the physics of the Type IIA dual solution to KS in view of testing the stability of the antibranes.

To perform the same procedure as in § 5.3.1 it is necessary to check that (5.16) remains an isometry after the backreaction of the C D3 branes at the NP. This is fundamental to insure the existence of a new Type IIA solution with the same NS5 wrapping the holomorphic curve (5.14). As proved in § 5.4.2, the NP lies on the locus (5.14), which is precisely the locus of fixed points on the deformed conifold under the isometry (5.16). Conse-

quently, the backreaction of the D3 branes placed at the NP cannot spoil this isometry, which is hence preserved globally. A new Type IIA KS+D4 background T-dualized along ξ in (5.16) exists and hence it is perfectly legitimate to reconstruct the T-dual version of only a small region, namely the NP neighborhood.

As the D3 branes at the NP do not break any supersymmetry it is easy to find an ansatz to include their backreaction on the KS solution. The KS+D3 solution can be seen as some kind of superposition between the KS solution and the solution that one would get by placing the D3 branes at the NP on the empty deformed conifold. Indeed, the metric ansatz is still as in (2.48), but the warp factor now becomes

$$h = h^{KS} + h^{D3} \tag{5.60}$$

where h^{KS} is the KS warp factor (2.49) and h^{D3} is the warp factor that one would get by placing only the D3 branes on the empty deformed conifold. In addition, the five-form field strength becomes:

$$F_5 = \mathcal{F}_5 + \star\mathcal{F}_5 \qquad\qquad \mathcal{F}_5 = d\left(h^{-1}\right) \wedge dt \wedge dx^1 \wedge dx^2 \wedge dx^3 \tag{5.61}$$

where the hodge star should be computed using (5.60). The rest of the solution is constituted by the remaining fields in KS, namely B_2 in (2.50) and F_3 in (2.51).

Finding h^{D3} in (5.60) is equivalent to solving the Laplace equation on the deformed conifold [103]. Now that the right ansatz for the KS+D3 solution has been found it is convenient to proceed to the next step, namely finding the expansion for h^{D3} around the NP. The deformed conifold metric becomes as in (5.30) which is an (almost) $\mathbb{R}^6$ metric. Therefore the lowest order expansion of h^{D3} in the NP just becomes the blowing up warp factor that one gets by putting some D3 branes in flat empty space, and it will be of order δ^{-4}, as confirmed by the analysis of [103]. The next-to-lowest order corrections will start at least from order one and originates from the fact that we are expanding the solution of a Laplace equation on the deformed conifold, hence they can possibly be of the same order as the terms in h^{KS} in (5.39). We choose to ignore these higher order correction coming from the D3 brane backreaction. On one side, we know that these corrections take care of themselves and do not really add interesting physics to the problem as long as one captures the D3 brane divergence. On the other side, the interaction between these corrections and those of the same order coming from KS give rise to negligible terms, as we are primarily interested in the interaction between the KS terms and the new D3 divergence. Hence, our h^{D3} is truncated at highest order, becoming:

$$h^{D3} = \varepsilon^{-\frac{8}{3}} \left(\frac{3}{2}\right)^{\frac{2}{3}} \frac{C}{R^4} \tag{5.62}$$

where we have defined $R = \sqrt{\tau^2 + r^2 + z^2}$ and we have taken into account the overall coefficient in (5.30). The KS+D3 warp factor (5.60) that we will consider is given by:

$$h = (g_s M \alpha')^2 \varepsilon^{-\frac{8}{3}} 2^{\frac{2}{3}} (a_0 + a_2 \tau^2) + \varepsilon^{-\frac{8}{3}} \left(\frac{3}{2}\right)^{\frac{2}{3}} \frac{C}{R^4} \tag{5.63}$$

The contribution coming from the D3 branes in (5.63) dominates over the KS ones, which can now be considered as corrections to the simple D3 brane solution. As in § 5.5.1, we have to expand the powers of the warp factor (5.63) differently so that all the coordinates contribute to the highest order in δ in the metric, taking into account that (5.30) is of order δ^2. We fix the highest order of expansion in the metric requiring it to comprise a τ-dependent contribution from the KS in the warp factor (5.63), which was essential for the stability of the D4 probes in § 5.5.2. This goal can be achieved if one expands $h^{\frac{1}{2}}$ and $h^{-\frac{1}{2}}$ as follows:

$$\begin{aligned} \hat{h}^{\frac{1}{2}} &= \left(\frac{3}{2}\right)^{\frac{1}{3}} \varepsilon^{-\frac{4}{3}} \frac{\sqrt{C}}{R^2} + \frac{(g_s M \alpha')^2}{\varepsilon^{\frac{4}{3}} 3^{\frac{1}{3}}} \frac{a_0 R^2}{\sqrt{C}} + \frac{(g_s M \alpha')^2}{\varepsilon^{\frac{4}{3}} 3^{\frac{1}{3}}} \frac{a_2 \tau^2 R^2}{\sqrt{C}} \\ \hat{h}^{-\frac{1}{2}} &= \left(\frac{2}{3}\right)^{\frac{1}{3}} \varepsilon^{\frac{4}{3}} \frac{R^2}{\sqrt{C}} - \frac{2^{\frac{2}{3}} (g_s M \alpha')^2 \varepsilon^{\frac{4}{3}}}{3} \frac{a_0 R^6}{C^{3/2}} \end{aligned} \tag{5.64}$$

Then the expanded metric of the KS+D3 solution becomes

$$ds^2_{KS+D3} = \hat{h}^{-\frac{1}{2}} dx^i dx^i + \hat{h}^{\frac{1}{2}} ds^2_6 \tag{5.65}$$

where ds^2_6 is as in (5.30). From (5.64) we get terms of order δ^2 and δ^6 from the Minkowski metric and terms of order 1, δ^4 and δ^6 from the expansion of the deformed conifold metric.

Now that we have expanded the KS+D3 metric we can proceed to the expansions of the field strengths. The criterion used for this purpose is the same as in § 5.5.1: one first expands the square of a field strength defined as in eq. (5.41) using (5.65) to highest order and then truncates the expansion of the field strength itself keeping only the terms that contribute to the square. As the metric we are dealing with now is different from that in 5.40, the orders of magnitude of the squares change, as one would expect given the fact that the D3 branes at the NP tend to hide the KS solution in the NP neighborhood.

The expansion of B_2 is the same as in (5.44), but now both $(B_2)^2$ and $(H_3)^2$ are of order δ^6. This is because the leading terms in the transverse metric are now of order one. Hence adding a leg to a form along a transverse direction does not change the order of magnitude of its square, while the differential of a form preserves the orders of magnitude of each term, as explained in § 5.5.1.

Similarly to B_2, also F_3 gets rewritten as (5.46) and (5.47), and its square is of order δ^6 as well. This is not the same for the expansion of F_5 in (5.61), as $(F_5)^2$ is now of order one. This is as expected, as F_5 measures also the D3 brane charge on a sphere surrounding

the NP, hence the flux of this form cannot be small. The component of $(F_5)^2$ that is of order one arises precisely from h^{D3} in (5.60) and if one truncated to this order the KS contribution to F_5 would be completely lost. To keep some reminiscence of the KS solution we expand $\mathcal{F}_5$ in (5.61) as follows:

$$\begin{aligned}\mathcal{F}_5 &= d\left[\left(\frac{2}{3}\right)^{\frac{2}{3}}\varepsilon^{\frac{8}{3}}\frac{R^4}{C} - \frac{4}{3^{\frac{4}{3}}}(g_sM\alpha')^2\varepsilon^{\frac{8}{3}}a_0\frac{R^8}{C^2}\right]\wedge dt\wedge dx^1\wedge dx^2\wedge dx^3 \\ &= \mathcal{F}_5^{D3} + \mathcal{F}_5^{KS+D3}\end{aligned} \tag{5.66}$$

where $\mathcal{F}_5^{D3}$ comes from the differential of the first term in the brackets and $\mathcal{F}_5^{D3+KS}$ comes from the second one. $\mathcal{F}_5^{D3}$ is purely due to the D3 branes, while $\mathcal{F}_5^{KS+D3}$ comes from the interaction between the KS solution and the branes. This can be qualitatively confirmed from the presence in $\mathcal{F}_5^{KS+D3}$ of some constants inherited from the KS solution, such as M or a_0. In addition, $(\mathcal{F}_5^{D3})^2$ is of order one, while the square of the second term is of order δ^8. In § 5.5.1 $(F_5)^2$ in (5.49) was of two orders higher than $(B_2)^2$ and $(F_3)^2$ and the same happens here for $(\mathcal{F}_5^{KS+D3})^2$ in (5.66). Even if the orders of magnitude of the fluxes due to the KS solution have changed, the relative differences are preserved.

To complete the expansion of F_5 we present the expression for $\star\mathcal{F}_5$:

$$\begin{aligned}\star\mathcal{F}_5 =& \varepsilon^{-\frac{8}{3}}\left(\frac{3}{2}\right)^{\frac{2}{3}}\frac{\tau^2\cos^2\alpha + 2r^2}{h^4\tau^4\cos^3\alpha}(\partial_\tau h\, dr\wedge dz - \partial_r h\, d\tau\wedge dz \\ &- \partial_z h\, d\tau\wedge dr)\wedge d\alpha\wedge d\beta\wedge d\sigma\end{aligned} \tag{5.67}$$

where h in (5.60) should be properly truncated so to get terms of the same order as in (5.66). For consistency, one should keep the two lowest order terms in the expansion of (5.67), whose squares are of order one and δ^8.

The T-duality in β of the new KS+D3 background is easily performed. The Type IIA metric close to the NP is given by

$$\begin{aligned}ds^2_{IIA,KS+D3} =& \hat{h}^{-\frac{1}{2}}\left[dx^i dx^i + \varepsilon^{\frac{4}{3}}\left(\frac{2}{3}\right)^{\frac{1}{3}}\frac{d\beta^2}{(\tau^2\cos^2\alpha + r^2)}\right] \\ &+ \hat{h}^{-\frac{1}{2}}\varepsilon^{\frac{4}{3}}\left(\frac{2}{3}\right)^{\frac{1}{3}}\frac{B_{a\beta}\,dy^a}{(\tau^2\cos^2\alpha + r^2)}d\beta \\ &+ \hat{h}^{\frac{1}{2}}\varepsilon^{\frac{4}{3}}\left(\frac{2}{3}\right)^{\frac{1}{3}}\left[d\tau^2 + \tau^2 d\alpha^2 + dr^2 + dz^2 + \frac{r^2\tau^2\cos^2\alpha}{\tau^2\cos^2\alpha + r^2}d\sigma^2\right]\end{aligned} \tag{5.68}$$

where the warp factors are expanded as in (5.64) and $B_{a\beta}\,dy^a$ is as in (5.44). As in § 5.5.2 the third line of the metric comes from the T-dualization of the deformed conifold, while the second line arises from the interaction between the KS B_2 and the geometry. The

Type IIA dilaton now becomes:

$$e^{2\Phi} = \varepsilon^{\frac{4}{3}} \left(\frac{2}{3}\right)^{\frac{1}{3}} \frac{\hat{h}^{-\frac{1}{2}}}{(\tau^2 \cos^2\alpha + r^2)} \tag{5.69}$$

which is clearly of order one. The NS-NS two-form B_2 is exactly the same as in (5.52):

$$B_{2,IIA} = \frac{r^2}{\tau^2 \cos^2\alpha + r^2} d\sigma \wedge d\beta + \widehat{B}_2 \tag{5.70}$$

with $\widehat{B}_2$ given by (5.44). The first term in (5.70) arises from $A_\sigma \, d\sigma \wedge d\beta$ where $A_\sigma \, d\sigma$ is defined in (5.35) and is a geometric feature of our T-duality in β of the metric (5.30). The square of this term with (5.68) is still of order one and the same applies metric structure for its differential H_3[5]. This together with the fact that B_2, the dilaton and the metric blow up on (5.33) indicate that this locus gets wrapped by NS5 branes even in the KS+D3 solution.

The RR sector of the Type IIA version of the new KS+D3 background comprises a two-form F_2 which is exactly the same as in (5.53), with $(F_2)^2 \sim \delta^6$. The four-form is now given by

$$F_4 = \widehat{F}_3 \wedge (d\beta + B_{a\beta} \, dy^a) + F_{5,\beta} \tag{5.71}$$

where $\widehat{F}_3$ and $B_{a\beta} \, dy^a$ are written in (5.47) and (5.43), while $F_{5,\beta}$ should be computed from (5.67). The lowest order contribution to F_4 is hidden in $F_{5,\beta}$ and its square is of order one: this represent the four-form field strength that one gets placing D4 branes in flat space. The next-to-lowest order contributions also come from $F_{5,\beta}$ and arise from the interactions between the KS solution and the D3 branes in Type IIB and their square is of order δ^8.

Finally, the RR sector of this solution also includes a six-form field strength and an eight-form field strength, which can be computed via the hodge duals of (5.71) and (5.53) respectively. In particular, the component of dC_5 with legs along the Minkowski space and one among the τ, r, z coordinates on the conifold together with β is easily computed from (5.66):

$$dC_5|_{0123\tau\beta} = (\mathcal{F}_5^{D3} + \mathcal{F}_5^{KS+D3}) \wedge d\beta \tag{5.72}$$

The Type IIA KS+D3 solution incorporates all the main features of the previous T-duality of KS in § 5.5.2, including the structure of the metric (5.68) and the NS5 branes wrapping the same locus. New features arise from the novel terms signaling the interaction between the D4 branes and the T-dual KS solution. As a test, one could perform the probe computation of § 5.5.2 using the metric (5.68) and the component of dC_5 in (5.72). However, the ansatz we used in (5.60) and (5.61) together with Buscher's rules guarantee

[5]Notice that in (5.68) the highest order components of the metric along the NP coordinates are of order one, hence even if H_3 has one more leg than B_2 their squares are of the same order.

that the D4 probe action is trivial. The cancellation in the D4 action (5.56) for the KS+D3 solution takes place at two different levels. Indeed, $\mathcal{F}_5^{D3} \wedge d\beta$ in (5.72) is canceled by the lowest order term in the DBI action arising from h^{D3} in (5.60). These terms come from the pure D3 brane background in Type IIB and their cancellation in Type IIA just states that a D4 probe is in equilibrium in a D4 brane background. Then, the next-to-leading order correction $\mathcal{F}_5^{KS+D3} \wedge d\beta$ in (5.72) is cancelled against the next-to-leading order term in the DBI action coming from h^{KS} in (5.60). This cancellation is physically more meaningful than the previous one, as it is due to terms in Type IIA arising from the interaction between the D3 localized branes and the KS solution.

5.7 Future developments

We reconstructed the Type IIA solution T-dual to the KS solution on a small region at the tip of the deformed conifold, choosing the correct isometry to obtain an NS5 brane wrapping a holomorphic curve in Type IIA. We discussed the choice of our isometry both from the point of view of the dual cascading four-dimensional gauge theory and from the geometric properties of the deformed conifold. This operation was made possible by finding a suitable set of coordinates for the North Pole expansion. In § 5.6 the same techniques were applied to T-dualize the solution constructed by adding D3 branes at the North Pole of the three-sphere at the bottom of the deformed conifold. On one hand, the North Pole expansion makes it easy to solve the Laplace equation for the D3's on the deformed conifold, as the leading order term in the expanded metric corresponds to the solution to the Laplace equation for D3 branes in flat space. On the other hand, the expansion makes it easy to identify the physics arising purely from the D4 branes in Type IIA and that coming from the interactions between the Type IIA T-dual solution to "empty" KS and the additional localized D4 branes.

The solutions dual to KS and KS+D3 constructed in this paper mark a first step towards testing the stability of antibranes in Type IIA. Adding an anti-D4 brane in the T-dual solution to KS of § 5.5.2 is the next step in this direction. It is difficult to find the full backreaction of the anti-D4 on the T-dual KS solution because of the supersymmetry breaking. However, we expect that the form of the T-dual solution to the KS+D3 one of § 5.6 could be used to get a better understanding about the backreaction of the anti-D4 and possibly to propose an ansatz. For instance, the backreaction of the anti-D4 should preserve the relative difference between the order of magnitudes of the squares of the fields arising from KS, as happens for a backreacted D4. In addition, the anti-D4 will not alter the divergencies of the dilaton, metric and B_2 near the Type IIA NS5 brane: as we have seen in § 5.6, the squares of these divergent terms have the same order of magnitude as in the T-dual solution of KS presented in § 5.5.2.

Another interesting possibility is to study the brane-antibrane interactions between

the backreacted D4 branes of the solution in § 5.6 and a probe anti-D4 brane. Clearly, the leading terms of the probe action would represent the attractive force exerted by the backreacted branes. The interesting physics would then be hidden in the subleading terms of this action. This would be the Type IIA correspondent of the interaction between the fields of the KS solution and the backreacted D3 branes in Type IIB. If the force exerted by the next-to-leading order terms were repulsive this would prove that anti-D4 branes at the bottom of the solution T-dual to KS are unstable. In particular, we expect the fields sourced by the NS5 brane in Type IIA to play a key role in the final results.

CHAPTER 6

FIVE-DIMENSIONAL NULL AND TIMELIKE SUPERSYMMETRIC GEOMETRIES

6.1 Review of five-dimensional supersymmetric solutions and their classification

6.1.1 Looking for solutions with mixed Killing vectors

Supersymmetric solutions of minimal Supergravity in five dimensions play an essential role in various areas of String Theory. For instance, they are fundamental to understand String Theory compactifications as well as the microscopic properties of black hole solutions. In addition, they are usually good toy models to understand the key properties and features of more complicated higher dimensional solutions. In fact, five-dimensional, pure, $\mathcal{N} = 1$ Supergravity is the perfect framework where to explore the geometry and topology of M-theory supersymmetric solutions [104].

The supersymmetric solutions of five-dimensional, pure, $\mathcal{N} = 1$ Supergravity were classified in [17] up to local isometries, while the local classification in the complete, matter-coupled, five-dimensional Supergravity was found in [105, 106, 107]. Locally, these solutions can be divided into two classes according to the causal character of the supersymmetric Killing vector field, namely the vector field given as a bilinear in terms of the Killing spinor[1]. The *time-like class* is characterized by a time-like Killing vector, while the *null class* is characterized by a null Killing vector[2]. In the time-like class, supersymmetry constrains the metric in such a way that it can be formally written in terms of a local

[1] To save unnecessary words, we will refer to the supersymmetric Killing vector as simply the Killing vector.

[2] It can be shown that the Killing vector cannot be spacelike.

Hyper-Kähler four-dimensional *base space*.

It is well-known that in the time-like class the Killing vector can become null at some loci of the four-dimensional Hyper-Kähler base manifold. Indeed, this is precisely what happens at the horizon of a black hole solution, or in the smooth five-dimensional solutions of [108] which will be considered in this chapter. A change in the causal character of the Killing vector is paralleled by a change of the supersymmetry conditions that the spinor satisfies. However, in all the solutions constructed so far this can happen only in some regions of codimension at most one of the space-time manifold, that are typically surfaces.

Our goal in this chapter is to construct five-dimensional solutions in minimal Supergravity whose Killing vector, which is generically time-like, becomes null at a point of the space-time manifold where all the derivatives of its norm vanish. The null condition is a closed condition, so if the norm of the spinor is a continuous function then the spinor can become null only on a closed subset of the manifold. Since all the derivatives of the norm vanish at the point where the Killing vector field becomes null, we conclude that the norm is not an analytic real function at this point, otherwise the Killing vector field would vanish on an open set, contradicting the fact that the null condition on the norm is a closed condition. Therefore, if we are able to construct a solution where the norm of the Killing vector field and all its derivatives vanish at some locus, we will know that the norm is not a real analytic function at those points. In either case, having a Killing vector whose norm has an infinite number of derivatives vanishing at a point is the closest scenario to having a null-spinor on an open set. These would be solutions that may mix, in a non-trivial way, the local classification that distinguishes between the time-like and the null classes. In this respect we consider smooth Supergravity solutions with a multi-center Gibbons-Hawking (GH) base manifold that asymptote to $AdS_3 \times S_2$. These can be generated from the compactification of eleven-dimensional Supergravity solutions on three tori with stabilized moduli and are essentially a modification of the three charge microstates introduced in § 2.3. The conditions that ensure smoothness were found in [19, 3] as these solutions represent microstate geometries for five-dimensional black holes. These solutions are uniquely determined once one fixes the poles and the residues of two harmonic functions V and K in the GH space. In particular, it is well known [108] that the related Killing vector is time-like almost everywhere, except for the loci where V is zero.

It is easy to give a physical interpretation for this phenomenon in the eleven-dimensional formalism: in the regions where the Killing vector is time-like the supersymmetry conditions are compatible with those of M2 branes wrapping one of the three tori. At the same time, on the surfaces where the Killing vector becomes null, the supersymmetry conditions become those required by M5 branes wrapping two of the three tori and the Gibbons-Hawking fiber (see § 2.3 for the detailed definitions). The transition between M2 brane-like supersymmetry and the M5-brane one can be of utmost importance for the construction of new microstate geometries for five-dimensional black holes that are not

electrically charged. This can be achieved by means of a new class of physical objects, the magnetubes, introduced in [108]. A magnetube has an M5 charge, which is magnetic in five dimensions, together with positive and negative M2 charges. The M2 charge density is allowed to smoothly vary along the M5-P common direction so that the net M2 charge is zero. The supersymmetry conditions are those for M5 branes along this direction and hence the positive and negative M2 charges do not interact and the whole magnetube is supersymmetric. This can lead to the construction of microstates for five-dimensional black holes with zero electric charges [109], such as the Schwarzschild ones. Finding a solution where the Killing vector becomes null at a point where its norm has an infinite number of vanishing derivatives can be relevant in this respect. Indeed, this solution would allow to construct new types of magnetubes, as the M5 brane charge is no longer constrained in the standard way. In addition, one could add different types of magnetubes in the same null region and study whether the counting of these types of configuration can partially reproduce the expectations from the black hole entropy.

To reach our goal it is hence necessary to construct a five-dimensional solution that asymptotes to $AdS_3 \times S_2$ where the harmonic function V vanishes at a point together with all its derivatives. This operation is in general impossible, unless one allows the number of poles to become infinite. We then adopt the following strategy. We arrange $2N$ poles on the same line in the GH space so that the function V defined in § 2.3 and all its derivatives up to order $2N-2$ vanish at the origin of the GH space. This constrains the residues of V at the poles to be determined by the distances d_i's between the poles and the origin. In the limit where N becomes infinite V and all its derivatives vanish at the origin, where the Killing vector becomes null.

The choice of the distances d_i's of the poles from the origin is the only degree of freedom left by our construction and the physical relevance of the solution given by the limit heavily depends on this. Indeed, a general requirement to determine whether the solution in the limit is physically meaningful is to demand it to asymptote to $AdS_3 \times S_2$, so that it still belongs to the original class of five-dimensional solutions. We give numerical evidence that there exists a distance distribution for the poles so that this condition is satisfied. At the same time, the residues of V remain finite in the limit, while all the poles collapse on two different points. This result motivates a future analysis about the behavior of the metric and the warp factor in the proximity of these two would-be essential singularities, that in fact might not be singularities at all. Indeed, considering the full backreaction what appears to be an essential singularity from the point of view of the three-dimensional base of the GH space will in fact give rise to smooth solutions [21, 66].

This chapter is organized as follows. In § 6.1.2 we present a general review about the supersymmetric structure of $\mathcal{N}=1$ five-dimensional Supergravity solutions, with emphasis on the distinction between time-like and null classes. In § 6.2 we recall the construction of smooth five-dimensional solutions with a Gibbons-Hawking base that asymptote to

$AdS_3 \times S_2$ and prove that the associated Killing vector becomes null when V vanishes. In § 6.3.1 we show that by suitably arranging $2N$ GH centers on a line it is possible to have V as well as all its derivatives up to order $2N-2$ vanish at the origin. In § 6.3.2 we consider the limit where N becomes infinite, so that all the derivatives of the norm of the Killing vector vanish at the origin. In particular, we numerically show that it is possible to arrange the distances between the GH centers so that the limit solution still asymptotes to $AdS_3 \times S_2$. In § 6.4 we underline the physical properties of the limit solution and state some future work. Additional details are presented in the Appendix [**GP: arrange references**]. In particular, in Appendix C.1 we prove that the residues of V attain a finite value in the limit, while in Appendix C.2 we briefly describe an alternative construction that does not lead to a physically relevant limit solution.

6.1.2 The supersymmetric solutions of $\mathcal{N}=1$ five-dimensional Supergravity

In this section we review the structure of the supersymmetric solutions of five-dimensional $\mathcal{N}=1$ pure Supergravity. Although the theory under scrutiny here seems to be relatively simple, the structure of its supersymmetric solutions is remarkably rich. This fact can be traced back to the particular form of the Killing spinor equation, which is relatively involved[3] but also to the quaternionic structure of the spinor bundle of the solutions.

We will focus exclusively on bosonic solutions. The bosonic matter content of five-dimensional, pure, $\mathcal{N}=1$ Supergravity consists of a Lorentzian, oriented, spin manifold (M_5, g_5) together with a connection A on principal $U(1)$-bundle $P \to M_5$ over M_5. The bosonic part of the action is given by[4]:

$$\mathcal{S} = \int_{M_5} \left\{ R - \frac{1}{4}|F|^2 + \frac{1}{12\sqrt{3}} F \wedge F \wedge A \right\} \tag{6.1}$$

The equations of motion of the theory are given by:

$$\begin{aligned} g(u,v) + \frac{1}{2}\left(< F(u), F(v) > - \frac{1}{4} g(u,v) < F, F > \right) &= 0 \qquad u, v \in \mathfrak{X}(M_5) \\ d * F + \frac{1}{4\sqrt{3}} F \wedge F &= 0 \qquad \alpha \in \mathbb{R}^* \end{aligned} \tag{6.2}$$

where F is the curvature associated to A and $< \cdot, \cdot >$ denotes the inner product on forms induced by g. A pair (g_5, A) satisfying equations (6.2) is said to be a bosonic solution of the theory.

[3] In particular, it is not the *lift* to the spin bundle of a metric connection.

[4] In this section we preferred to use the notation typical of the supergravity literature. This might slightly differ from those used for instance in Chapter 1 and Chapter 4 as it tends to be more mathematically-oriented. Despite the differences, we believe that the supergravity language should not be so mysterious and on the other side think that translating this section into the microstate formalism would be inappropriate.

Let $Cl(M_5, g_5)$ denote the bundle of real Clifford algebras over (M_5, g_5), isomorphic as a bundle of, unital, associative algebras to the Kähler-Atiyah bundle $(\Lambda T^* M_5, \diamond)$, see references [110, 111, 112] for a detailed account of this formalism. Let us assume in addition that there exists a bundle of real Clifford modules S over M_5 with representation homomorphism denoted by:

$$\gamma \colon (\Lambda T^* M_5, \diamond) \to (End(S), \circ) \tag{6.3}$$

where $(End(S), \circ)$ denotes the unital, associative, algebra of endormophisms of S. In Lorentzian signature in five dimensions, γ is neither surjective nor injective [112], and S is a rank-eight bundle of real Clifford modules, which remains irreducible as a spinor bundle for $Spin(1,4)$. The commutant subbundle Σ of the Kähler-Atiyah bundle inside the endomorphisms of S is of quaternionic type. This implies that on every open set $U \subset M_5$ there exists a local triplet $J^i, i = 1,2,3$, of almost complex structures satsfying the algebra of the imaginary quaternions. Notice however that these almost-complex structures do not exist globally and thus Σ_γ is in general not topologically trivial. This is already a hints that the supersymmetric solutions of the theory may have very subtle non-trivial properties at the global level.

Since $Cl(M_5, g_5)$ is non-simple, there are two inequivalent Clifford modules S, distinguished by the value of the volume element $\gamma(\nu)$ inside $End(S)$:

$$\gamma(\nu) = s_\gamma \, Id \qquad s_\gamma \in \{1, -1\} \tag{6.4}$$

We will take the $s_\gamma = 1$ in the following. The bundle of Clifford modules S can be endowed with a symmetric admissible bilinear $\mathcal{B}$, that is of utmost importance in order to write a spinor as a polyform. A bosonic solution (g_5, A) is said to be supersymmetric if there exists a globally defined spinor $\epsilon \in \Gamma(S)$ satisfying:

$$\nabla_u \epsilon - \frac{1}{8\sqrt{3}} \, u^\flat \wedge F \cdot \epsilon + \frac{1}{2\sqrt{3}} \, \iota_u F \cdot \epsilon = 0 \qquad \forall u \in \mathfrak{X}(M_5) \tag{6.5}$$

A pair (g_5, A) for which there exists a globally defined spinor $\epsilon \in \Gamma(S)$ satisfying (6.5) is said to be a *supersymmetric configuration*. Using the results of references [112, 113], we conclude that a spinor in five Lorentzian dimensions is equivalent a polyform:

$$E \in \Omega^\bullet(M_5) \tag{6.6}$$

satisfying the *generalized Fierz relations*[5]. The polyform E can be written in terms of a function Z, the supersymmetric Killing vector p and a triplet of two-forms Φ^s depending only on the coordinates of the base space. In turn, these can be locally written in terms of

[5]These relations are not always equivalent to the standard Fierz relations appearing in the physics literature. See reference [114] for more details.

the admissible bilinear form $\mathcal{B}$ and the local triplet of almost-complex structures J^i, local sections of Σ which exist precisely because Σ is of quaternionic type. The local expressions of Z, p and Φ^s in terms of a local frame are:

$$Z^{-1} = \mathcal{B}_0(\epsilon, \epsilon) \qquad p_a = \mathcal{B}_0(\epsilon, \gamma_a \epsilon) \qquad \Phi^i_{ab} = \mathcal{B}(\epsilon, J^i \circ \gamma_{ab} \epsilon) \tag{6.7}$$

The Killing spinor equation (6.5) translates into a set of differential conditions for Z, p and Φ^i. In reference [17] the most general local form of a supersymmetric solution of five-dimensional pure, $\mathcal{N} = 1$ Supergravity was obtained[6]. The supersymmetric solutions can be divided in two classes: the *time-like class* is characterized by a time-like Killing vector p, while the *null class* is characterized by a null Killing vector. Notice that this classification is local and that the two classes can overlap. From the Fierz algebra one gets:

$$g_5(p, p) = -Z^{-2} \tag{6.8}$$

and hence p cannot be space-like. The local form of the solution in each class is as follows:

- **Null class**. There exist local coordinates u, v, x^s with $s = 1, 2, 3$ such that the metric can be written as:

$$ds^2 = -Z^{-1} du(dv + H\, du + \omega) + Z^2 \delta_{rs} dx^r dx^s \tag{6.9}$$

  where Z, H are v-independent functions and ω is a v-independent one-form, all of them satisfying particular differential equations on the transverse three-dimensional space.

- **Time-like class** There exist local coordinates t, x^i, $i = 1, \ldots, 4$, such that the metric can be written as:

$$ds^2 = -Z^{-2}(dt + \omega)^2 + Z^{-1} g_{ij} dx^i dx^j \tag{6.10}$$

  where Z is t-independent and ω is a t-independent one-form. The symbol g_{ij} denotes a four-dimensional euclidean metric, which has to be Hyper-Kähler. In fact, it can be shown that the triplet Φ^s of two forms is the corresponding Hyper-Kähler structure. Therefore, time-like solutions are amenable to be locally written in terms of a four-dimensional Riemannian manifold, making the problem of obtaining these solutions a problem in Riemannian geometry and suggesting that the moduli-space problem of time-like solutions is well-defined.

[6] See also reference [106] for the most general local form of the supersymmetric solutions of $\mathcal{N} = 1$ five-dimensional Supergravity coupled to vectors and hypers.

Once the local form of the solution has been found, in principle one can obtain the global solution by a maximally analytic extension of the space-time, which is a very non-trivial procedure that has to be done on a case by case basis. In the analytic extension, the fields of the solution can potentially change some of their properties which were holding on the original local set.

As an example of this global phenomenon, one can analyze the *chirality* of supersymmetry spinor ϵ as one moves on the space-time manifold. There is no notion of chirality in five dimensions, an it has to be imported from the four-dimensional language. Given the structure of the time-like class of supersymmetric solutions, amenable to be written in terms of a four-dimensional, *transverse* space, together with the fact that the spinor does not depend on the time coordinate, one can study ϵ as a Clifford module in four euclidean dimensions. Notice that ϵ remains irreducible as a $Cl(4)$ module, but is not irreducible anymore as a representation of $Spin(4)$. The Clifford module is still of quaternionic type, and seeing ϵ as a Clifford-module for $Cl(4)$ it can be decomposed as follows:

$$\epsilon = \epsilon_+ \oplus \epsilon_- \tag{6.11}$$

where $\epsilon_\pm$ are $Spin(4)$ spinors of positive and negative chirality, namely inequivalent irreps. of $Spin(4)$. Now, ϵ is parallel under a generalized connection on the spinor bundle S given by the Killing spinor equation. In other words, the Killing spinor equation (6.5) can be rewritten as:

$$D_v\epsilon = 0\,, \qquad \forall\, v \in \mathfrak{X}(M_5) \tag{6.12}$$

where $D\colon \Gamma(S) \to \Gamma(S)\otimes\Omega^1(M_5)$ is a connection on the spinor bundle. Therefore, if ϵ is non-zero at one point it will be non-zero everywhere. However, this does not imply that the individual components $\epsilon_\pm$ must remain non-zero at every point: they can indeed vanish at a locus in M_5, as long as they do not vanish simultaneously.

On a similar vein, one can consider the global properties of the Killing vector field p, which concern the main analysis of this chapter. Supersymmetric solutions of five-dimensional, pure, $\mathcal{N}=1$ Supergravity are characterized in terms of a polyform E satisfying some differential equations that can be succinctly written as follows:

$$D^{Ad}\, E = 0 \tag{6.13}$$

where D^{Ad} is the connection on the Kähler-Atiyah bundle induced by the *supersymmetric* connection [110]:

$$D_u \equiv \nabla_u - \frac{1}{8\sqrt{3}}\, u^\flat \wedge F + \frac{1}{2\sqrt{3}}\, \iota_u F \qquad \forall u \in \mathfrak{X}(M_5) \tag{6.14}$$

We then see that E is parallel under the connection D^{Ad}, and therefore if it is non-zero at

one point (which holds by assumption), it will be non-zero everywhere. However, this does not imply that the vector field p or its norm is parallel under any connection. Therefore, it is in principle possible that the norm of p becomes null at some locus in M_5.

Inspired then by these results, we want to explore if the following phenomenon may happen in five-dimensional, pure $\mathcal{N} = 1$ Supergravity: we want to check if there are supersymmetric solutions of this theory having a Killing vector whose norm has an infinite number of vanishing derivatives at its null locus in M_5, and is generically time-like on its complement. In the next sections we explicitly construct a family of these solutions.

6.2 Five-dimensional $\mathcal{N} = 1$ smooth solutions asymptotic to $AdS_3 \times S_2$

6.2.1 Constructing the family of solutions

In this section we review the class of five-dimensional solutions in minimal Supergravity we will be concerned with. These are nothing but the familiar microstate geometries already studied in § 2.3 compactified on the three-tori so that they become five-dimensional solutions. Although this compactification is quite a straightforward operation (the three tori in (2.22) can be considered as "spectator" coordinates), some modifications are needed to change the asymptotic behavior of these solutions. The microstates studied in § 2.3 and thoroughly analyzed in Chapter 4 asymptote flat space, while here we want them to asymptote to $AdS_3 \times S_2$. It turns out that for this condition to hold it suffices to suitably turn on constant terms in the harmonic functions that are the building blocks of this family of solutions, as will explained below.

We want to work with smooth $\mathcal{N} = 1$ solutions that asymptote to $AdS_3 \times S_2$ and have a Gibbons-Hawking (GH) space as four-dimensional Hyper-Kähler base. As we will show at the end of this section, these solutions admit a Killing vector that is time-like almost everywhere, except for some codimension one loci where it becomes null. This fact is crucial for the construction described in the following sections that leads to a solution where the norm of the Killing vector vanishes at a point of the GH space together with an infinite number of derivatives.

The conditions that ensure the smoothness of the class of $\mathcal{N} = 1$ five-dimensional solutions we review here were first found in [2, 3], while we follow the conventions of [115, 116] to impose the solutions to asymptote to $AdS_3 \times S_2$. As the Killing vector is time-like almost everywhere the metric can be written in the standard form of the time-like class (6.10):

$$ds_5^2 = -Z^{-2}(dt + \omega)^2 + Z\, g_{ij} dx^i dx^j \tag{6.15}$$

$$A = -Z^{-1}(dt + \omega) + V^{-1} K\, (d\psi + \omega_0) + \xi \tag{6.16}$$

The solution above has been obtained from (2.22) by just eliminating the three tori and fixing the parameters $k_i^I = k_i$ so that $Z_1 = Z_2 = Z_3 = Z$ in (2.22). Additional modifications to adjust the asymptotic behavior will become clear in the following.

A in (6.16) is the potential one-form and $g_{ij}dx^i dx^j$ is a Gibbons Hawking metric:

$$g_{ij}dx^i dx^j = V^{-1}(d\psi + \omega_0)^2 + V\delta_{ab}dx^a dx^b \tag{6.17}$$

with $a, b = 1, 2, 3$ and the GH fiber ψ has period 4π. The functions in (6.15), (6.16) and (6.17) are defined on the three-dimensional space spanned by $x = (x^1, x^2, x^3)$ in the GH space. In particular, V in (6.16) and (6.17) is a harmonic function

$$V = \sum_{i=1}^{N} \frac{v_i}{r_i} \qquad r_i = |x - g_i| \tag{6.18}$$

where g_i is the location of the i-th pole (GH center). The one-form ω_0 in (6.17) is related to V via $d\omega_0 = \star dV$, where the Hodge star is constructed using the euclidean $\mathbb{R}^3$ metric. By imposing $v_i \in \mathbb{Z}$, the poles of V become orbifold singularities for the metric (6.17) (which are benign in String Theory) of the form $S_3/\mathbb{Z}^{|v_i|}$. One has to impose also $\sum_i v_i = 0$ so that the metric asymptotes to $AdS_3 \times S_2$[7].

The function Z in (6.15) and (6.16) is expressed as a combination of V together with two additional harmonic functions K and L:

$$Z = L + \frac{K^2}{V} \tag{6.19}$$

Requiring Z to be smooth everywhere constrains K and L to have the same poles as V in (6.18) and uniquely fixes the residues of L once those of K have been specified[8] - see § 2.3:

$$K = \sum_{i=1}^{N} \frac{k_i}{r_i} \qquad L = -\sum_{j=1}^{N} \frac{k_j^2}{v_j}\frac{1}{r_j} \tag{6.20}$$

The one-form ξ in (6.16) is then defined by $d\xi = -\star dK$, where the Hodge star is again defined using a flat $\mathbb{R}^3$ metric. The BPS solution for the angular momentum one-form ω in (6.15) is written as[9]:

$$\omega = S(d\psi + \omega_0) + \zeta \tag{6.21}$$

[7] In [2, 3] these solutions are built to be microstates for a class of five-dimensional three-charge black holes, and hence they asymptote to flat space. This is achieved by requiring $\sum_i v_i = 1$.

[8] In [2, 3] it was necessary to add a constant $+1$ to L so that Z is nicely behaved at infinity for an asymptotically-flat metric. As our solutions are asymptotic to $AdS_3 \times S_2$ there is no such requirement for Z.

[9] Note that the momentum form is conventionally called ω in Supergravity language and k in microstate language, which is employed in § 2.3 and Chapter 4.

with S given by[10]:

$$S = \frac{K^3}{V^2} + \frac{3KL}{2V} + M \tag{6.22}$$

where M is another harmonic function that has the same poles as V in (6.18). Its residues are fixed by those of V and K so that S is finite and smooth everywhere:

$$M = m_0 + \frac{1}{2}\sum_{i=1}^{N} \frac{k_i^3}{v_i^2}\frac{1}{r_i} \tag{6.23}$$

The nonzero constant m_0 in (6.23) determines the radius of the asymptotically $AdS_3 \times S_2$ metric (6.15). Finally, ζ in (6.21) is given given by

$$\star d\zeta = VdM - MdV + \frac{3}{2}(KdL - LdK) \tag{6.24}$$

Some constraints have to be satisfied to prevent the existence of closed time-like curves. First of all, from (6.15) it easy to see that one has to require S in (6.22) to vanish at each GH center. This imposes $N-1$ independent conditions known as *bubble equations* that involve the residues v_i and k_i together with the inter-center distances r_{ij}[11]:

$$\sum_{\substack{j=1\\ j\neq i}}^{N} \left(\frac{k_j}{v_j} - \frac{k_i}{v_i}\right)^3 \frac{v_i v_j}{r_{ij}} + v_i\, m_0 = 0 \qquad\qquad i = 1, ..., N-1 \tag{6.25}$$

Secondly, to avoid closed time-like curves the following inequalities must hold everywhere in the GH base space:

$$Z^3 V - S^2 V^2 > 0 \qquad\qquad ZV > 0 \tag{6.26}$$

Therefore, to completely determine one of these solutions one has to fix m_0 in (6.23) and the number of GH centers N. Secondly, one specifies the residues v_i, k_i and the inter-center distances r_{ij} so that (6.25) are satisfied. There is no general prescription known to satisfy (6.26) and these two conditions have to be checked a posteriori.

It is useful to show that the metric (6.15) asymptotes to $AdS_3 \times S_2$. We parameterize the $\mathbb{R}^3$ base of the GH space with spherical coordinates r, θ, ϕ and define the following quantities:

$$Q = \sum_{i=1}^{N} k_i \qquad\qquad J = \left|\sum_{i=1}^{N} v_i \cdot g_i\right| \qquad\qquad P = \sum_{j=1}^{N} \frac{k_j^2}{v_j} \tag{6.27}$$

[10] We stress that S here is nothing but the function μ of § 2.3: however, as greek letters in this section are reserved to define the $AdS_3 \times S_2$ coordinates we preferred to redefine this quantity.

[11] The bubble equations (6.25) are slightly different from those in (2.36): this is due to the different asymptotic behavior of the two solutions.

By introducing the coordinates [115]:

$$\eta = Q \log \frac{r}{Q} \qquad \tau = t \qquad \sigma = 2m_0\psi - t \tag{6.28}$$

the metric (6.15) and potential (6.16) asymptotically become

$$ds^2 \simeq d\eta^2 + \frac{1}{4m_0} e^{\frac{\eta}{Q}} (-d\tau^2 + d\sigma^2) + Q^2 \left(d\theta^2 + \sin^2\theta (d\phi + \tilde{\omega}_0)^2\right) \tag{6.29}$$

$$A \simeq Q \cos\theta \, (d\phi + \tilde{\omega}_0) + -\frac{3P}{2Qm_0} \, (d\sigma + d\tau) \tag{6.30}$$

where we have defined

$$\tilde{\omega}_0 = \frac{J}{2Q^3}(d\tau - d\sigma) \tag{6.31}$$

Equation (6.29) shows that the metric of these solutions asymptotes to $AdS_3 \times S_2$. In addition, from (6.29) it is clear that one should impose Q in (6.27) to be positive.

Note that the asymptotic behavior of these solution (6.29) and (6.30) is uniquely determined once the quantities in (6.27) have been fixed.

6.2.2 From time-like to null Killing vector

The $\mathcal{N}=1$ five-dimensional Supergravity solutions reviewed in § 6.2 have a Killing vector p that is time-like almost everywhere and that in the coordinates of (6.15) is simply written as $\frac{\partial}{\partial t}$. As recalled in § 6.1.2, it is locally defined by the Killing spinor through a bilinear form $\mathcal{B}$, which for the metric (6.15) simply becomes:

$$p_a = \mathcal{B}_0(\epsilon, \gamma_a \epsilon) = \bar{\epsilon}\, \gamma_a \epsilon \tag{6.32}$$

while (6.26) allows to rewrite (6.8) as follows:

$$g_5(p,p) = -Z^{-2} = -(ZV)^{-2} \, V^2 \tag{6.33}$$

Therefore in our class of solutions the Killing vector is time-like everywhere except for the $V=0$ loci, where it becomes null. This peculiarity belongs to the class of solution reviewed in § 6.2 and the reason why the time-like Killing vector can become null at some loci lies in the fact that the GH metric (6.17) is ambipolar. Indeed, its signature can pass from $(-,-,-,-)$ to $(+,+,+,+)$ and the surfaces $V=0$ mark the borders between the two signatures. This does not affect neither the physical validity of the Supergravity solutions of § 6.2 nor their smoothness, as it can be shown [71] that the full metric (6.15) has lorentzian signature everywhere.

To better understand how these solutions can switch from the time-like class to the null one it is useful to analyze what happens to the Killing spinor ϵ as one approaches the

$V = 0$ loci [108]. The standard frames for the metric (6.15) are given by:

$$e^0 = Z^{-1}(dt + \omega) \qquad e^1 = (ZV)^{\frac{1}{2}} V^{-1}(d\psi + \omega_0) \qquad e^{i+1} = (ZV)^{\frac{1}{2}} dx^i \tag{6.34}$$

and it was shown in [17] that if e^0 is written as in (6.34) then the Killing spinor satisfies

$$\gamma^0 \epsilon = \epsilon \tag{6.35}$$

in the frame indices defined by (6.34). This is indeed the prototypical spinor equation for time-like solutions. However, the frames e^0 and e^1 in (6.34) become singular as V approaches zero and (6.35) does not hold in these regions. In particular, one can see from (6.33) that

$$\epsilon^\dagger \epsilon = \bar{\epsilon} \gamma^0 \epsilon = Z^{-1} = (ZV)^{-1} V \tag{6.36}$$

which shows that the norm of ϵ vanishes in the $V = 0$ loci. To understand what happens in these regions one has to define a completely regular set of frames, which is made possible by simply replacing e^0 and e^1 in (6.34) with:

$$\begin{aligned} \hat{e}^0 &= \frac{1}{2}(V + V^{-1})\, e^0 + \frac{1}{2}(V - V^{-1})\, e^1 \\ \hat{e}^1 &= \frac{1}{2}(V - V^{-1})\, e^0 + \frac{1}{2}(V + V^{-1})\, e^1 \end{aligned} \tag{6.37}$$

Note that the regular set of frames is related to the original one (6.34) simply by a boost, with boost parameter χ defined by

$$\cosh \chi = \frac{1}{2}(|V| + |V|^{-1}) \qquad\qquad \sinh \chi = \frac{1}{2}(|V| - |V|^{-1}) \tag{6.38}$$

and clearly the boost parameter becomes infinite when $V = 0$. The Killing spinor in the regular set of frames $\hat{\epsilon}$ is hence related to the original one ϵ by

$$\hat{\epsilon} = e^{\frac{\chi}{2}\gamma^{01}} \epsilon = \frac{1}{2}|V|^{\frac{1}{2}}(1 + \gamma^{01})\epsilon + \frac{1}{2}|V|^{-\frac{1}{2}}(1 - \gamma^{01})\epsilon \tag{6.39}$$

where the frame indices are again defined by (6.34). From (6.36) one can see that the magnitude of ϵ in the original frame vanishes as $|V^{\frac{1}{2}}|$ and then from (6.39) one concludes that on the $V = 0$ loci the spinor ϵ satisfies

$$\gamma^{01} \epsilon = -\epsilon \tag{6.40}$$

which is nothing but the prototypical spinor equation for the null class of five-dimensional solutions.

As V in (6.18) is a harmonic function, these loci are two-dimensional surfaces in the GH space [108], hence the Killing vector cannot become null on an open set of the five-

dimensional space-time manifold. The closest condition to having a null Killing vector on an open set is to have it vanish at a point together with all its derivatives. This result can be achieved if one compromises to consider a solution of the kind reviewed in § 6.2 with an infinite number of GH centers. Indeed, in the next section we show that by suitably arranging a solution with $2N$ GH centers V and all its derivatives up to order $2N-2$ can be set to zero at a point. In the limit where N becomes infinite V and all its derivatives vanish at a point of the GH space. Consequently, all derivatives of the norm of the Killing vector of the limit solution vanish at the origin. Since the null condition is a closed condition, we conclude that the norm of the Killing vector field is not a real analytic function at the origin.

6.3 Five-dimensional null and timelike supersymmetric geometries

6.3.1 Our construction

In this section we show how to arrange a smooth solution of the class reviewed in § 6.2 with $2N$ GH centers so that all the derivatives of V up to order $2N-2$ vanish at a point, which we fix to be the origin of the GH space.

We consider a solution with $2N$ GH centers located on the same axis, parameterized by the coordinate x in the GH base space. The full solution (6.15) then has cylindrical symmetry with respect to this axis and the angular coordinate can be ignored. Focusing on a plane containing the axis, the orthogonal direction is parameterized with y. We dispose N GH centers on the semi-axis $x \geq 0$, labeled by $i = 1, ...N$, while the remaining N centers are arranged on $x < 0$ and labeled by $i = -1, -2, ... - N$. Denoting the distance of the $i-$th center from the origin with d_i, we constrain the residues v_i's and k_i's of (6.18), (6.20) and the d_i's to satisfy the following conditions:

$$v_{-i} = -v_i \qquad k_{-i} = k_i \qquad d_{-i} = d_i \qquad i = 1, ...N \tag{6.41}$$

In addition, for the semi-axis $x > 0$ we require the sign of the v_i's to be alternating:

$$v_i = (-1)^{i+1}|v_i| \qquad i = 1, ...N \tag{6.42}$$

As a consequence of (6.41) the quantity P defined in (6.27) is identically zero. In addition, because of (6.41) and (6.42), only N equations (6.25) among the initial $2N-1$ remain independent, as the equation for i is equivalent to that for $-i$.

This configuration ensures that V in (6.18) and some of its derivatives vanish at the

origin $x = y = 0$. In particular, by introducing the notation

$$(m, n) \equiv \left. \frac{\partial^{m+n} V}{\partial x^m \partial y^n} \right|_{x=y=0} \tag{6.43}$$

one can observe the following simplifications:

- $(2s, n) = 0 \ \forall s, n$,
- $(2s + 1, 2p + 1) = 0 \ \forall s, p$,
- (m, n) and (s, p) are multiples of each other provided that $m + n = s + p$.

Therefore, after fixing the number of GH centers to be $2N$ and requiring (6.41) and (6.42) to hold, one can annihilate the $N - 1$ nonzero derivatives at the origin of the form $(1, 2s)$ with $s = 0, ...N - 2$. Indeed, defining the ratios $\xi_i = v_i/v_1$ and $\delta_i = d_i/d_1$, these $N - 1$ constraints completely fix the $N - 1$ ξ_i's as functions of the δ_i's, so that all the derivatives up to order $2N - 2$ are zero at the origin. For instance, in a solution with $2N = 8$ GH centers one is free to assign the three ratios of the distances δ_i's and then the three ξ_i's are determined to annihilate the nontrivial derivatives $(1, 0)$, $(1, 2)$ and $(1, 4)$. As a result, V and all its derivatives up to order six are zero at the origin.

Without loss of generality we fix

$$v_1 = 1 \qquad\qquad d_1 = 1 \tag{6.44}$$

so that the v_i's can be directly expressed as functions of the d_i's. There are two such expressions, depending on whether the GH centers g_i with $|i| > 1$ are added externally with respect to g_1 and g_{-1}, namely choosing $d_i > d_j$ for $i > j$, or internally, satisfying $d_j < d_i$ for $j > i$. We adopt this second convention, as the numerical investigations for the limit $N \to \infty$ give evidence that this is the physically sensible option, presenting the formula we get from the first option in Appendix C.2.

Therefore, after fixing N one arranges the first two centers $g_{\pm 1}$ on the line by means of (6.44). The remaining centers are then progressively added in the intervals $]0, 1[$ and $]-1, 0[$ according to (6.41) and (6.42). We are left free to assign the distances subject to the requirement $d_i < d_j < 1$ for $i > j$, while the v_i's remain fixed to annihilate all the derivatives of V up to order $2N - 2$ at the origin:

$$|v_i| = d_i^{2N-2} \prod_{\substack{j=2 \\ j \neq i}}^{N} \frac{1 - d_j^2}{|d_i^2 - d_j^2|} \qquad\qquad i = 1, ...N \tag{6.45}$$

and their sign is determined according to (6.42).

To completely determine a five-dimensional solution of the class reviewed in § 6.2, also N parameters k_i's for $i = 1, ...N$ have to be determined. These parameters are fixed by

numerically solving the N remaining independent equations (6.25) while requiring $Q > 0$ in (6.27).

To summarize, after fixing N, one disposes the centers symmetrically with respect to the origin according to (6.41) and (6.42) and fixes the N distances d_i's subject to $0 < d_i < d_j < 1$ for $i > j$. The v_i's are determined by (6.45) and the k_i's are determined by solving the N independent bubble equations (6.25). Once the v_i's and k_i's have been found, the whole five-dimensional solution can be written according to § 6.2.

The N bubble equations have to be solved numerically once m_0 and the distances d_i's have been fixed. We studied the behavior of these solutions for many different distance distributions d_i, progressively increasing N. Our numerical analysis indicates that among the many possible real solutions for the k_i's, there is always one where the k_i's are all positive. We observed that this is the only option to systematically satisfy $VZ > 0$ everywhere in (6.26), as we verified numerically that if some of the k_i's are negative the function VZ can become negative close to some of the GH centers. This kind of analysis was repeated for many different distance distributions d_i using (6.45) and also adding the GH centers externally with respect to $g_{\pm 1}$ using (C.6) in Appendix C.2. As changing the value of m_0 in (6.25) just scales the values for the k_i's, we fix $m_0 = -1$ in our numerical analysis, keeping in mind that our results are valid for any nonzero m_0.

We found that the second constraint in (6.26) is also satisfied if one requires the k_i's to be positive for different distributions of distances and different N, although we lack a rigorous generalization to arbitrary N.

6.3.2 Analysis of the solutions in the limit of infinite centers

In this section we analyze the limit $N \to \infty$ applied to the construction of § 6.3.1. In this limit all the derivatives of V vanish at the origin. For finite N the construction of § 6.3.1 leads to valid, smooth Supergravity solutions of the class reviewed in § 6.2. However, the situation is different for $N \to \infty$, as one gets a solution with an infinite numbers of poles. Depending on the chosen distribution for the d_i's, the GH centers can accumulate towards single points or in finite intervals, but one cannot say a priori whether this invalidates the smoothness of the solution in the limit without a thorough analysis of the metric (6.15) in the limit $N \to \infty$.

Two more general issues can compromise the physical relevance of the limit solution for $N \to \infty$. First of all, the constraint $Z^3V - S^2V^2 > 0$ should be checked for every N. We verified that for a wide range of distributions of the d_i's and for different values of N this condition is valid and it seems reasonable to assume that it still holds in the infinite limit. Secondly, it is natural to require that the limit solution still asymptotes to $AdS_3 \times S_2$, and hence that its metric and potential can be rewritten as in (6.29) and (6.30) at infinity. In particular, this means that J and Q in (6.27) have to remain finite for $N \to \infty$[12]. As the

[12]We remind the reader that because of (6.41) P in (6.27) is identically zero in our construction.

sign of the v_i's is alternating according to (6.41) and (6.42) and as we are accumulating the poles within finite intervals, it is easy to find a distance distribution for the poles such that J in (6.27) goes to zero in the limit.

On the other hand, it is tricky to find a distribution for the d_i's so that the parameter Q in (6.27) does not grow indefinitely with N. As remarked at the end of § 6.3.1, for each finite N the k_i's are determined by numerically solving N bubble equations (6.25) and selecting the only solution where they all have the same sign. For this reason Q in (6.27) can easily grow to become infinite with growing N.

For N large enough there seems to be a correlation between how the v_i's -determined via (6.45)- and the k_i's behave with N. We observed that an exponential growth for the v_i's is paralleled by an exponential growth of Q in (6.27), which we want to avoid.

We found a distribution for the d_i's so that the v_i's attain a finite limit for $N \to \infty$ that can lead to a finite Q as well. For fixed N we assign the distances d_i's according to:

$$d_i = 1 - \frac{(i-1)^\alpha}{N^\beta} \qquad i = 1, ...N \tag{6.46}$$

with $0 < \alpha < \beta$. In Appendix C.1 we show that for each fixed i, $|v_i|$ given by (6.45) with (6.46) is finite in the limit provided that $\beta > 1$. Note that (6.46) satisfies $0 < d_i < d_j \leq 1$ for $i > j$ and that in the limit $N \to \infty$ all the GH centers collapse on the fixed g_1 and g_{-1} at unitary distance from the origin. This does not automatically imply that the limit solution becomes singular without a thorough analysis of the full metric (6.15) in the limit.

It is important to stress that with the distribution (6.46) the GH centers do not accumulate at the origin and hence the function V in (6.18) becomes constant and in fact it has an infinite number of vanishing derivatives in the limit. The configuration for the GH centers obtained with a distance distribution of the kind (6.46) is represented in Figure 6.1.

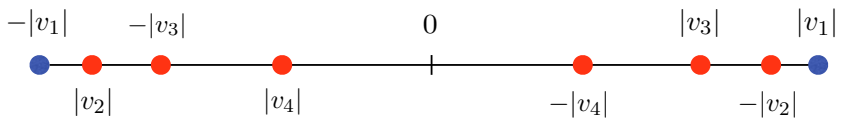

Figure 6.1: The configuration of GH centers obtained with the distance distribution (6.46). The blue dots represent the centers $g_{\pm 1}$, whose position has been fixed in (6.44). The red dots represent the other GH centers, whose positions and v_i's are determined by (6.41) and (6.42).

We analyzed the behavior of Q and J in (6.27) as a function of N for different values of α and β in (6.46), up to $N = 300$[13]. The quantity J in (6.27) rapidly goes to zero

[13]Note the solution obtained for $N = 300$ has 600 GH centers in total. The related value of Q is hence

as N increases, while the behavior of Q is more subtle. We noted that for $\beta - \alpha > 1$ in (6.46) the bigger $\beta - \alpha$ is the faster $Q(N)$ goes to zero for $N \to \infty$. For $\beta - \alpha < 1$ we have not found a clear connection between this quantity and the behavior of $Q(N)$ at infinity. For instance, $Q(N)$ goes to infinity for $\beta = 2.05$ and $\alpha = 1.9$, while it goes to zero for $\beta = 2.05$ and $\alpha = 2$ - see Figure 6.2. This indicates that there exists some value $\tilde{\alpha}$ with $1.99 < \tilde{\alpha} < 2$ such that $Q(N)$ asymptotes to a constant. The related solution hence asymptotes to $AdS_3 \times S_2$ and the norm of the Killing vector has an infinite number of vanishing derivatives at the origin.

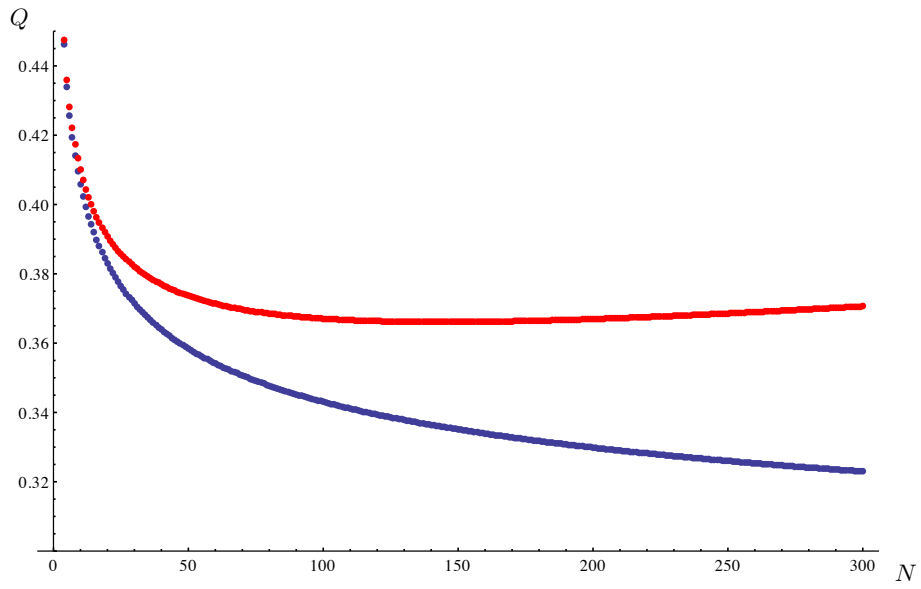

Figure 6.2: Numerical analysis for $Q(N)$ up to $N = 300$ for two different regimes. The red dots were obtained choosing $\beta = 2.05$ and $\alpha = 1.99$ in (6.46) and $Q(N)$ is divergent. The blue dots were obtained for $\beta = 2.05$ and $\alpha = 2$ and $Q(N)$ asymptotes to zero.

The asymptotic behavior of $Q(N)$ for $150 \leq N \leq 300$ for the two distance distributions studied in Figure 6.2 is modeled by

$$Q(N) \sim \frac{N^a}{c\, N^b + d} \tag{6.47}$$

where the parameters a, b, c, d can be estimated numerically. The fact that $Q(N)$ for large N behaves as in (6.47) is a general feature of the distance distribution (6.46). In particular, for the values of α and β of Figure 6.2 we find the following values for a, b, c, d in (6.47):

	a	b	c	d	$a-b$
$\alpha = 1.99$	1.83	1.79	3.51	-724.011	0.04
$\alpha = 2$	1.59	1.64	2.35	-44.12	-0.05

determined by numerically solving 300 bubble equations (6.25), each of them consisting of 600 terms.

It is interesting to study how the v_i's determined by (6.45) with the distance distribution (6.46) evolve with N. From Figure 6.3 we see that for fixed N the v_i's of the last GH centers are small compared to the v_i's to the first one. In addition, each v_i slowly grows with N but remains finite in the limit, as proved in Appendix C.1 for the distance distribution (6.46).

A similar analysis can be performed to study the trend of the k_i's, numerically determined by solving the bubble equations (6.25) - see Figure 6.4. For a given N the k_i's of the last centers -namely the ones closest to the origin- are small compared to those of the most external centers. Each k_i decreases with N and limits to zero for $N \to \infty$ so that the conserved charge Q in (6.27) can remain finite in the limit.

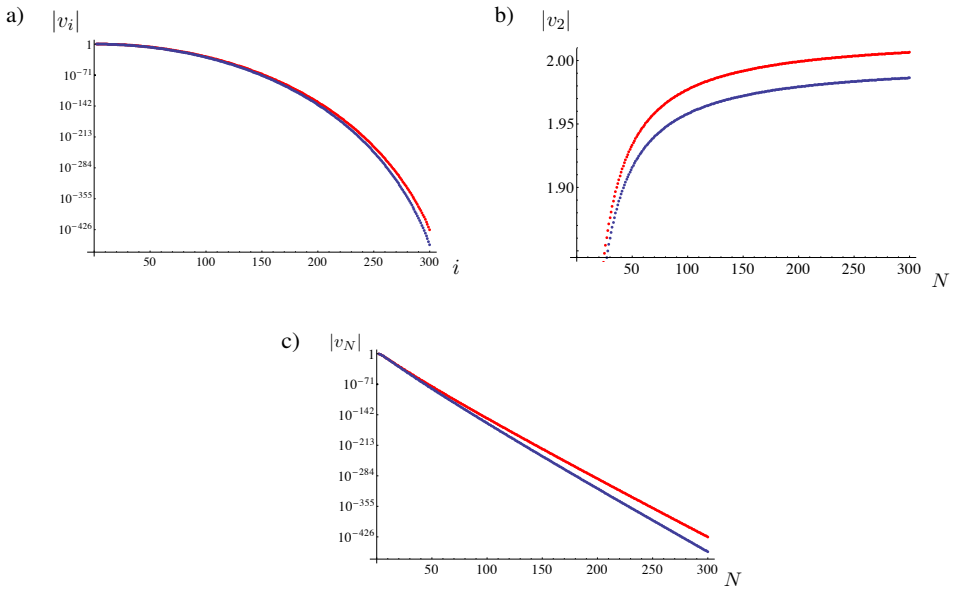

Figure 6.3: Numerical analysis for the v_i's determined with (6.46) and (6.45) for $\alpha = 1.99$, $\beta = 2.05$ (red) and for $\alpha = 2$, $\beta = 2.05$ (blue). **a)** Representation of the v_i's for the solutions with $N = 300$. **b)** Trend of $|v_2|$ as a function of N up to $N = 300$. The trends of all the other v_i's for fixed i are similar. **c)** Trend of $|v_N|$ for the last-added GH center, as a function of N up to $N = 300$.

6.4 Future developments

We have shown the existence of five-dimensional Supergravity solutions such that the Killing vector together with an infinite number of derivatives vanish at a point in the base space. Since the null condition is a closed condition, this implies that the norm of the Killing vector is not a real analytic function at this point. This was achieved by considering the infinite limit for the number of centers in a class of smooth solutions with a

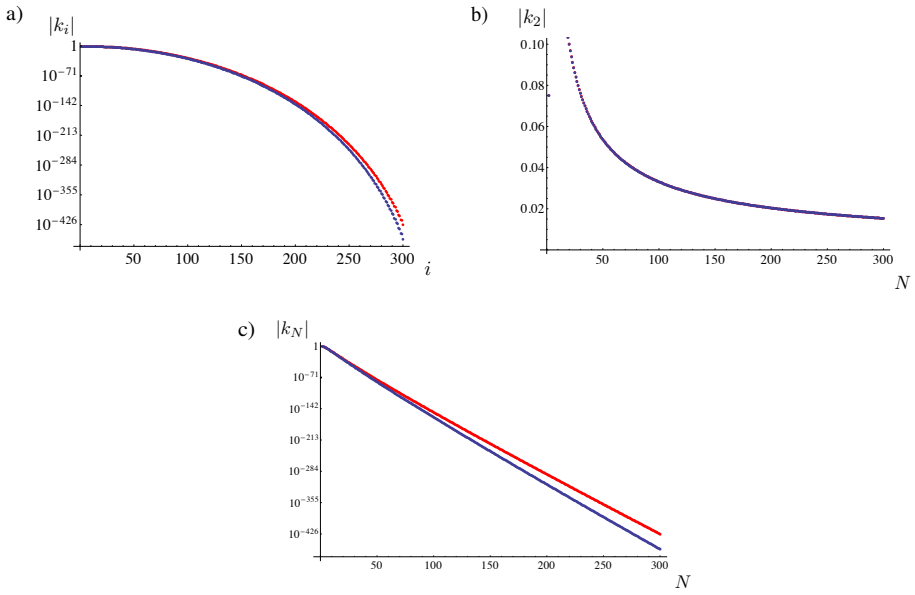

Figure 6.4: Numerical analysis for the k_i's determined by solving the bubble equations (6.25) computed with the distance distribution (6.46) for $\alpha = 1.99$, $\beta = 2.05$ (red) and for $\alpha = 2$, $\beta = 2.05$ (blue). **a)** Representation of the k_i's for the solutions with $N = 300$. **b)** Trend of $|k_2|$ as a function of N up to $N = 300$. The trends of all the other k_i's for fixed i are similar. **c)** Trend of k_N for the last-added GH center, as a function of N up to $N = 300$.

Gibbons-Hawking base that asymptote to $AdS_3 \times S_2$. By suitably tuning the distances of the poles before taking the limit, we gave evidence that the limit solution still asymptotes to $AdS_3 \times S_2$ and that its charges are finite.

It is important to stress that while our construction is valid in Supergravity, it is not necessarily so in String Theory. Indeed, in § 6.3.1 we stressed that the residues of V should be integers, so that the Gibbons-Hawking space looks like an $S^3/\mathbb{Z}^{|v_i|}$ close to a center. In addition, also the residues of K in (6.20) should be constrained to be integers. This is because one can define numerous two-cycles by fibering the coordinate ψ in (6.17) between two centers and the differential of $A+Z^{-1}(dt+\omega)$ in (6.16) measures fluxes on these cycles that depend on the ratios k_i/v_i. The usual quantization conditions require these fluxes to be semi-integers. In the infinite limit analyzed in § 6.3.2 one a priori cannot say that the v_i's and the k_i's are integers, although this does not seem impossible. It would be interesting to study whether there exist other distance distributions different from (6.46) so that also this requirement is satisfied.

It is also useful to analyze what happens in this class of solutions when the GH centers collide, as for the infinite limit with the distance distribution (6.46). In [71] a physical interpretation for this phenomenon was given seeing these five-dimensional solutions as black hole microstates. Indeed, one can compute the metric distance between the most

external GH center and a suitable cutoff far away in the Gibbons-Hawking space, which can be seen as the length of the would-be black hole throat in this language. This quantity is always finite for the solutions of § 6.2, but can grow indefinitely once one moves the GH centers close together. As in the limit solution of § 6.3.2 all the centers collapse on two points, this fact can be interpreted as the would-be black hole throat becoming infinite.

Finally, the collapse of all the centers to two points does not automatically give rise to singularities in the metric. Indeed it was shown in [21, 66] that what appears to be an essential singularity from the point of view of the three-dimensional base of the GH space can in fact give rise to a smooth solution once the full backreaction is taken into account. To verify the validity of this statement for our solutions it would be necessary to analyze the behavior of the function Z in (6.15) close to $g_{\pm 1}$ in the infinite limit. This operation is highly nontrivial and we suspect that it might also not be well defined, as the limit for $N \to \infty$ might not commute with the limit $r \to g_{\pm 1}$. We plan to carry a full mathematical analysis of the properties of the limit solution in future work.

ACKNOWLEDGMENTS

I wish to thank my supervisor, Iosif Bena, for his support, help and advice during this three years. Without him this work would have never been possible.
Secondly, I would like to express my gratitude to the whole String Theory group at IPhT (permanents, postdocs and graduate students) for constantly providing a stimulating environment.
As it would be impossible to list all the people that contributed to my formation or to my work I will only explicitly mention those that concretely helped to made progress, collaborators in primis: Stefano Massai, Andrea Puhm, Carlos Shahbazi, David Turton, Nick Warner.

APPENDIX A

ADDITIONAL DETAILS ON SUPERSYMMETRY BREAKING IN THE LIN-LUNIN-MALDACENA SOLUTION

A.1 1/2 BPS geometries in type IIB supergravity

We present here the original form of the LLM solution. The LLM type IIB solutions [1] correspond to states of $\mathcal{N}=4$ SYM theory on $R\times S_3$. They preserve 16 supercharges and have an $SO(4)\times SO(4)\times R$ bosonic symmetry, hence they contain two three-spheres S_3, $\tilde{S}_3$ and a Killing vector. The metric and five-form flux compatible with such symmetries are:

$$ds^2 = g_{\mu\nu}dx^\mu dx^\nu + e^{H+G}d\Omega_3^2 + e^{H-G}d\tilde{\Omega}_3^2 \tag{A.1}$$

$$F_5 = F_{\mu\nu}dx^\mu\wedge dx^\nu\wedge d\Omega_3^2 + \tilde{F}_{\mu\nu}dx^\mu\wedge dx^\nu\wedge d\tilde{\Omega}_3^2 \tag{A.2}$$

where $\mu,\nu=0,...,3$ and $d\Omega_3^2$, $d\tilde{\Omega}_3^2$ denote the metric on the three-spheres[1]. The dilaton and axion are assumed to be constant and the three-form field strengths are set to zero. Requiring that the above ansatz preserves the Killing spinor equations yields the following solution for the metric:

$$ds^2 = -h^{-2}(dt+V_idx^i)^2 + h^2(dy^2+dx^idx^i) + ye^Gd\Omega_3^2 + ye^{-G}d\tilde{\Omega}_3^2 \tag{A.3}$$

[1]The LLM function H in (A.1) should not be confused with the warp factor H in (2.1).

where $i = 1, 2$ and the functions h, G, V are determined by a single function z:

$$h^{-2} = 2y \cosh G \quad G = \text{arctanh}(2z) \tag{A.4}$$

$$y\partial_y V_i = \epsilon_{ij}\partial_j z \quad y(\partial_i V_j - \partial_j V_i) = \epsilon_{ij}\partial_y z \tag{A.5}$$

The five form flux is given by the two forms F, $\tilde{F}$ as follows:

$$\begin{aligned} F &= dB_t \wedge (dt + V) + B_t dV + d\hat{B} \\ \tilde{F} &= d\tilde{B}_t \wedge (dt + V) + \tilde{B}_t dV + d\hat{\tilde{B}} \end{aligned} \tag{A.6}$$

where we defined

$$B_t = -\frac{1}{4}y^2 e^{2G} \quad d\hat{B} = -\frac{1}{4}y^3 \star_3 dA \quad A = \frac{z + \frac{1}{2}}{y^2} \tag{A.7}$$

$$\tilde{B}_t = -\frac{1}{4}y^2 e^{-2G} \quad d\hat{\tilde{B}} = -\frac{1}{4}y^3 \star_3 d\tilde{A} \quad \tilde{A} = \frac{z - \frac{1}{2}}{y^2} \tag{A.8}$$

and the Hodge star $\star_3$ is referred to the flat space spanned by y, x_1, x_2.

The full solution is determined in terms of a single master function z that obeys a linear equation:

$$\partial_i\partial_i z + y\partial_y\left(\frac{\partial_y z}{y}\right) = 0 \tag{A.9}$$

The geometry described by this background is similar to that discussed in § 2.2: y is the product of the radii of the three-spheres S_3 and $\tilde{S}_3$. The geometry is smooth if $z = \pm\frac{1}{2}$ on the $y = 0$ plane spanned by x_1 and x_2. On this plane S_3 and $\tilde{S}_3$ shrink to a point in $z = -1/2$ and $z = 1/2$ regions respectively, while both of them shrink on the boundaries of these regions. To represent a general solution one just needs to specify the black and white regions on the $y = 0$ plane according to $z = \pm 1/2$: see Figure A.1 for an example.

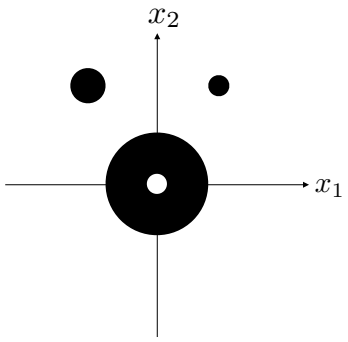

Figure A.1: A general type IIB solution is defined by boundary values of z in the $y = 0$ plane spanned by (x_1, x_2), depicted as black and white droplets.

A.2 Bubbling geometries in IIA supergravity

We now T-dualize the IIB solution (A.1) along x_1. We assume that $V_2 = 0$ and that V_1 and z do not depend on x_1. In the following we will drop the indices of V_1 and x_2 for convenience and rename $x_1 = \omega_1$. In the IIA frame the metric and the fluxes become[2]

$$ds^2_{IIA} = H^{-1}(-dt^2 + d\omega_1^2) + h^2(dy^2 + dx^2) + ye^G d\Omega_3^2 + ye^{-G} d\tilde{\Omega}_3^2 \tag{A.10}$$

$$B_2 = -H^{-1}h^{-2}V dt \wedge d\omega_1 \tag{A.11}$$

$$F_4 = \left[d(y^2 e^{2G}V) - y^3 \star_2 dA\right] \wedge d\Omega_3 + \left[d(y^2 e^{-2G}V) - y^3 \star_2 d\tilde{A}\right] \wedge d\tilde{\Omega}_3 \tag{A.12}$$

where we defined the warp factor H as:

$$H = e^{-2\Phi} = h^2 - V^2 h^{-2} \tag{A.13}$$

The six-form field strength F_6 is given by $F_6 = \star F_4$[3]. Explicitly we obtain:

$$\begin{aligned} \star F_4 = {} & H^{-1}e^{3G} dt \wedge d\omega_1 \wedge \left[\star_2\, d(y^2 e^{-2G}V) + y^3 d\tilde{A}\right] \wedge d\Omega_3 \\ & - H^{-1}e^{-3G} dt \wedge d\omega_1 \wedge \left[\star_2\, d(y^2 e^{2G}V) + y^3 dA\right] \wedge d\tilde{\Omega}_3 \end{aligned} \tag{A.14}$$

It is useful to obtain explicit expressions for the RR gauge potentials C_3 and C_5. We define

$$C_3 = c_3(x,y)\, d\Omega_3 + \tilde{c}_3(x,y)\, d\tilde{\Omega}_3 \tag{A.15}$$

$$C_5 = dt \wedge d\omega_1 \wedge \left[c_5(x,y)\, d\Omega_3 + \tilde{c}_5(x,y)\, d\tilde{\Omega}_3\right] \tag{A.16}$$

Since $C_1 = 0$ we have $F_4 = dC_3$. It is useful to define $\gamma_3 = c_3 - x - y^2 e^{2G}V + c$, where c is an integration constant that corresponds to the gauge choice for C_3 discussed in § 3.4.5. The equation for C_3 along the S_3 becomes

$$d\gamma_3 = -\left(y^3 \star_2 dA + dx\right) \tag{A.17}$$

which in components reads:

$$\begin{aligned} \partial_y \gamma_3 &= y\partial_x z \\ \partial_x \gamma_3 &= 2z - y\partial_y z \end{aligned} \tag{A.18}$$

[2]Note that the solution for the four-form field strength (D.1) as given in [1] is incorrect. Consequently, also the solution for the four-form flux G_4 of the gravity dual of the mass-deformed M2 brane theory as stated in (2.35) of [1] is incorrect. The correct form of G_4 is given in (2.2). In both (2.2) and (A.12) we dropped a factor 1/4 due to different conventions for the volume forms on the spheres with respect to [1].

[3]In our conventions $\star F_4 = F_6 = dC_5 + H_3 \wedge C_3$.

and a similar result holds for $\tilde{S}_3$. We stress that the only condition to integrate the potential C_3 is to solve the *linear* system (A.18). With the explicit form for z and V in the multi-strips solution (2.10)-(2.11) it is easy to find an analytic solution, whose general form

$$\gamma_3(x,y) = \sum_{i=1}^{2n+1} (-1)^{i+1} \gamma_3^0(x - x^{(i)}, y) \tag{A.19}$$

is obtained by superpositions of the plane wave solution:

$$\gamma_3^0(x,y) = \frac{2x^2 + y^2}{2\sqrt{x^2+y^2}} \tag{A.20}$$

To integrate $\tilde{c}_3$ one can use a similar technique. Defining $\tilde{\gamma}_3 = \tilde{c}_3 + x - y^2 e^{-2G} V + \tilde{c}$ it is straightforward to verify that $\tilde{\gamma_3}$ satisfies the differential equation (A.17) and hence apart from irrelevant constants $\tilde{\gamma}_3 = \gamma_3$.

The equations for C_5 are obtained from the gauge-invariant improved field strength $F_6 = dC_5 + H_3 \wedge C_3$. Defining $\gamma_5 = c_5 - c_3 H^{-1} h^{-2} V$ the equation for the part of C_5 along S_3 becomes

$$d\gamma_5 = H^{-1} \left[-h^{-2} V \left(d(y^2 e^{2G} V) - y^3 \star_2 dA \right) + e^{3G} \left(\star_2 d(y^2 e^{-2G} V) + y^3 d\tilde{A} \right) \right] \tag{A.21}$$

which remarkably can be solved in closed form:

$$\gamma_5 = \frac{2y^2}{1 - 2z(x,y)} - y^2 \tag{A.22}$$

To find $\tilde{c}_5$ one proceeds with a similar technique: defining $\tilde{\gamma}_5 = \tilde{c}_5 - \tilde{c}_3 H^{-1} h^{-2} V$ one can integrate $\tilde{\gamma}_5$:

$$\tilde{\gamma}_5 = \frac{2y^2}{1 + 2z(x,y)} - y^2 \tag{A.23}$$

We stress that the only condition to integrate the RR potentials is to solve the linear equation (A.17).

A.3 Solution in the limit $y \to 0$

In the following we report the formulas for the $y \to 0$ limit, keeping in mind that the background (A.10)-(A.12) is not singular. While the limit has to be performed distinguishing between white and black strips, it can be shown that V defined in (A.5) and γ_3 defined in (A.19) are well defined even for $y = 0$, regardless of the particular strip considered. The Hamiltonian (3.13) for the M5 brane probe is continuous for $y \to 0$ even at the boundaries $x^{(i)}$ of the strips.

A.3.1 White strips $z = 1/2$

On white strips S_3 remains at a finite-size, while $\tilde{S}_3$ shrinks to a point. Using the equation (A.4):

$$z = \frac{1}{2}\tanh G \tag{A.24}$$

one gets $e^G \to \infty$ in this limit as well as the expansion

$$z \simeq 1/2 - e^{-2G} \simeq 1/2 - y^2\zeta_+^2(x) \tag{A.25}$$

where $\zeta_+(x)$ is given by

$$\zeta_+(x) = -\lim_{y\to 0}\frac{1}{\sqrt{2}}\frac{\partial_y z}{\sqrt{1-2z}} \tag{A.26}$$

$\zeta_+(x)$ is the primary function that allows to compute all the other fields in this limit, notice also that $\zeta_+(x)$ is positive. Restricting to multi-strip solutions (2.10)-(2.11), $\zeta_+(x)$ is given by

$$\zeta_+(x) = \frac{1}{2}\sqrt{\sum_{i=1}^{2s+1}(-1)^{i+1}\frac{|x-x^{(i)}|}{(x-x^{(i)})^3}} \tag{A.27}$$

All the fields in the white strip limit will be marked with + subscript. For the metric functions and NS potential we get:

$$h_+(x) = \sqrt{\zeta_+(x)} \qquad H_+(x) = \zeta_+(x) - \frac{V_+^2(x)}{\zeta_+(x)} \qquad B_+(x) = -\frac{V_+(x)}{\zeta_+^2(x) - V_+^2(x)} \tag{A.28}$$

The RR potentials on the finite S_3 become

$$c_3^+(x) = \frac{V_+(x)}{\zeta_+^2(x)} + \gamma_3^+(x) + x + c \qquad c_5^+(x) = -c_3^+(x)B_+(x) + \frac{1}{\zeta_+^2(x)} \tag{A.29}$$

where

$$\gamma_3^+(x) = \sum_{i=1}^{2s+1}(-1)^{i+1}|x-x^{(i)}| \tag{A.30}$$

The RR potentials on the shrunk $\tilde{S}_3$ become

$$\tilde{c}_3^+(x) = \gamma_3^+(x) - x + \tilde{c} \qquad \tilde{c}_5^+ = -\tilde{c}_3^+ B_+(x) \tag{A.31}$$

The Hamiltonian (3.13) for the probe wrapping S_3 becomes:

$$\mathcal{H}(x) = H_+^{-1}(x)\sqrt{\frac{H^+(x)}{\zeta_+^3(x)} + \left[p - c_3^+(x)\right]^2} - pB_+(x) - c_5^+(x) \tag{A.32}$$

A.3.2 Black strips $z = -1/2$

On black strips S_3 shrinks to a point, while $\tilde{S}_3$ keeps a finite radius. Proceeding as in the previous section we now have the expansion

$$z \simeq -1/2 + e^{2G} \simeq -1/2 + y^2\zeta_-^2(x)$$

where $\zeta_-(x)$ is positive and defined by

$$\zeta_-(x) = \lim_{y\to 0} \frac{1}{\sqrt{2}} \frac{\partial_y z}{\sqrt{1+2z}} \tag{A.33}$$

Restricting to multi-strip solutions (2.10)-(2.11), ζ_- is given by

$$\zeta_-(x) = \frac{1}{2}\sqrt{-\sum_{i=1}^{2s+1}(-1)^{i+1}\frac{|x-x^{(i)}|}{(x-x^{(i)})^3}} \tag{A.34}$$

As in the previous section all the fields can be rewritten in terms of V and ζ_-. We use the subscript $-$ to indicate that these expressions are valid in the limit $z \to -1/2$. We get for the metric functions and NS potential

$$h_-(x) = \sqrt{\zeta_-(x)} \qquad H_-(x) = \zeta_-(x) - \frac{V_-^2(x)}{\zeta_-(x)} \qquad B_-(x) = \frac{-V_-(x)}{\zeta_-^2(x) - V_-^2(x)} \tag{A.35}$$

The RR potentials on the shrinking S_3 become

$$c_3^-(x) = \gamma_3^-(x) + x + c \qquad c_5^- = -c_3^-(x)B_-(x) \tag{A.36}$$

where $\gamma_3^-(x) = \gamma_3^+(x)$. $c_{3-}(x)$ turns out to be locally constant and given by twice the total width of the finite-size white strips to the left of x.
The RR potentials on the finite $\tilde{S}_3$ become

$$\tilde{c}_3^-(x) = \frac{V_-(x)}{\zeta_-^2(x)} + \gamma_3^-(x) - x + \tilde{c} \qquad \tilde{c}_5^-(x) = -\tilde{c}_3^-(x)B_-(x) + \frac{1}{\zeta_-^2(x)} \tag{A.37}$$

We have used the same notation even for V, but clearly $V_- = V_+$.
The Hamiltonian (3.13) for the probe wrapping the shrinking S_3 is simplified to

$$\mathcal{H}_-(x) = \frac{1}{\zeta_-^2(x) - V_-^2(x)}\left[\zeta_-(x)|p - c_3^-(x)| + V_-(x)\left[p - c_3^-(x)\right]\right] \tag{A.38}$$

While the Hamiltonian (3.13) for a probe wrapping the finite $\tilde{S}_3$ becomes

$$\mathcal{H}^{\tilde{S}_3}(x)_- = H_-^{-1}(x)\sqrt{\frac{H^-(x)}{\zeta_-^3(x)}\left[p - \tilde{c}_3^-(x)\right]^2} - pB_-(x) - \tilde{c}_5^-(x) \tag{A.39}$$

A.4 Relation to the Bena-Warner solutions

In this section we provide a dictionary that relates the M-theory LLM solution presented in § 2.2 to the solution of Bena and Warner (BW) in [28]. The BW metric is written as

$$ds_{11}^2 = 16L^4 e^{2B_0}(-dt^2 + d\omega_1^2 + d\omega_2^2) + e^{2B_2 - B_0}(du^2 + dv^2) + \frac{1}{4}e^{2B_3 - B_0}u^2\sigma_i\sigma_i + \frac{1}{4}e^{-2B_3 - B_0}v^2\tau_i\tau_i \tag{A.40}$$

where B_0, B_2, B_3 are functions of u and v only and σ_i and τ_i are left-infariant 1-forms that parameterize the two three-spheres. Identifying

$$\frac{1}{4}\sigma_i\sigma_i = d\Omega_3 \qquad \frac{1}{4}\tau_i\tau_i = d\tilde{\Omega}_3 \tag{A.41}$$

and comparing (A.40) with (A.10) one gets:

$$\begin{aligned} 4u^2L^2e^{2B_3} &= ye^G \\ 4v^2L^2e^{-2B_3} &= ye^{-G} \\ 4uvL^2 &= y \\ 2L^2(u^2 - v^2) &= x \\ \frac{1}{64L^6}e^{-3B_0} &= H \end{aligned} \tag{A.42}$$

and hence

$$4L^2u^2 = x + \sqrt{x^2 + y^2} \qquad 4L^2v^2 = -x + \sqrt{x^2 + y^2} \tag{A.43}$$

In BW the background fields are determined once one fixes a master function $g(u, v)$, analogous to $z(y, x)$ in our Type IIA background, which satisfies the linear equation

$$\frac{\partial^2 g}{\partial u^2} + \frac{\partial^2 g}{\partial v^2} - \frac{1}{u}\frac{\partial g}{\partial u} - \frac{1}{v}\frac{\partial g}{\partial v} = 0 \tag{A.44}$$

Using (A.43) it is possible to rewrite g in the (y, x) coordinates. Considering that

$$z = \frac{1}{2}\frac{e^{2G} - 1}{e^{2G} + 1} \tag{A.45}$$

and using (A.42) one gets:

$$z = -2\partial_x g + z_0 \tag{A.46}$$

where $z_0 = \frac{x}{2\sqrt{x^2+y^2}}$ is the usual half-filled plane solution. One can indeed check that with this identification equation (2.7) for z is equivalent to the master equation (A.44).
The background of [28] that preserves 16 supercharges also depends on the constant β. The latter is related to the mass deformation on the dual M2 theory and for $\beta \to 0$

the background reduces to the standard Coulomb Branch of M2 branes only. The IIA background derived from [1] has a fixed value $\beta = 1/4$ and hence also the mass-deformation is fixed.

APPENDIX B

SOME EXPANSIONS IN THE NORTH POLE NEIGHBORHOOD

We report in this section some necessary computations to expand the KS solution in the neighborhood of the NP. After rewriting the deformed conifold metric around the NP in (5.30), it is necessary to expand the KS warp factor, defined as:

$$h(\tau) = (g_s M\alpha')^2 \varepsilon^{-\frac{8}{3}} 2^{\frac{2}{3}} I(\tau) \qquad I(\tau) = \int_\tau^\infty dx \, \frac{x \coth x - 1}{\sinh^2 x} (\sinh 2x - 2x)^{\frac{1}{3}} \tag{B.1}$$

The function $I(\tau)$ is even and close to the NP for τ of order δ it behaves as[1]:

$$I(\tau) = a_0 + a_2 \tau^2 + \mathcal{O}(\tau^4) \tag{B.2}$$

with $a_0 \approx 0.71805$ was computed in [4]. To compute a_2 one expands:

$$a_2 \tau^2 \simeq I(\tau) - I(0) \simeq -\int_0^\tau \frac{2^{\frac{2}{3}}}{3^{\frac{4}{3}}} x \, dx \tag{B.3}$$

where the integrand of (B.1) has been expanded for x small. One then easily gets:

$$a_2 = -2 \left(\frac{2}{9}\right)^{\frac{2}{3}} \tag{B.4}$$

[1] We are using here $\tilde{\tau}$ of (5.28), dropping the twiddle and taking care of the factor of two

The expansion of the other functions of τ in (2.54) is much easier[2]:

$$\begin{aligned} f(\tau) &\simeq \frac{2}{3}\tau^3 & k(\tau) &\simeq \frac{2}{3}\tau \\ F(\tau) &\simeq \frac{\tau^2}{3} & \ell(\tau) &\simeq \frac{8}{9}\tau^3 \\ K(\tau) &\simeq \left(\frac{2}{3}\right)^{\frac{1}{3}} & \frac{\ell(\tau)}{K^2\sinh^2\tau} &\simeq \left(\frac{2}{3}\right)^{\frac{1}{3}}\frac{\tau}{3} \end{aligned} \tag{B.5}$$

The next step is to expand the base one-forms of the deformed conifold (2.44) around the NP using (5.28). The expansion is carried on up to order δ:

$$\begin{aligned} g^1/\sqrt{2} &\simeq -\cos\alpha\, d\beta + r\frac{\cos\sigma}{\cos\alpha}d\alpha \\ g^2/\sqrt{2} &\simeq d\alpha + r\cos\sigma\, d\beta \\ g^3/\sqrt{2} &\simeq \cos\alpha\, dz + \sin\alpha\,[\cos\sigma\, dr - r\sin\sigma(d\beta + d\sigma)] \\ g^4/\sqrt{2} &\simeq -r\cos\sigma\,(d\beta + d\sigma) - \sin\sigma\, dr \\ g^5 &\simeq 2\sin\alpha\, dz - 2\cos\alpha\,[\cos\sigma\, dr - r\sin\sigma(d\beta + d\sigma)] \end{aligned} \tag{B.6}$$

Note that only g^1 and g^2 are of order one in the δ-expansion, while all the other forms are of order δ. Indeed, these two-forms are defined on the angles of the sphere (and cylinder) in the coordinate system of (5.28).

Finally, to expand the RR and NS-NS fields around the NP one needs to expand the wedge products of the base one-forms on the conifold. We report here some nontrivial ones, that can be derived using (B.6):

$$\begin{aligned} g^1 \wedge g^3 &\simeq 2\cos\alpha\,(\cos\alpha\, dz + \sin\alpha\cos\sigma\, dr - r\sin\alpha\sin\sigma d\sigma) \wedge d\beta \\ g^2 \wedge g^4 &\simeq -2[r\cos\sigma(d\beta + d\sigma) + \sin\sigma\, dr] \wedge d\alpha \\ g^5 \wedge g^3 \wedge g^4 &\simeq 4r\,[dr \wedge dz \wedge (d\beta + d\sigma)] \\ g^5 \wedge g^1 \wedge g^2 &\simeq 4\cos\alpha\,(\sin\alpha\, dz - \cos\alpha\cos\sigma\, dr - r\cos\alpha\sin\sigma d\sigma) \wedge d\alpha \wedge d\beta \end{aligned} \tag{B.7}$$

The sign of a wedge product depends on the orientation chosen for the coordinates. Here and in every NP expansion we have always used the following ordering: $\tau, \alpha, \beta, r, z, \sigma$.

[2]Here as before we are expanding substituting $\tau = 2\tilde{\tau}$ as prescribed in (5.28) and then we remove the twiddle

APPENDIX C

ADDITIONAL DETAILS ABOUT HYBRID TIMELIKE AND SPACELIKE FIVE-DIMENSIONAL GEOMETRIES

C.1 Proof of convergence of the v_i's for $N \to \infty$

In this section we prove that each v_i determined with (6.45) with distance distribution d_i given by (6.46) with $0 < \alpha < \beta$ is finite in the $N \to \infty$ limit, namely that

$$\lim_{N\to\infty} |v_i| = \lim_{N\to\infty} d_i^{2N-2} \prod_{\substack{j=2 \\ j\neq i}}^{N} \frac{1-d_j^2}{|d_i^2 - d_j^2|} \qquad \text{with} \qquad d_s = 1 - \frac{(s-1)^\alpha}{N^\beta} \tag{C.1}$$

is finite for each fixed i.

As the logarithm is a monotonic bijection between $\mathbb{R}_+$ and $\mathbb{R}$, the $|v_i|$'s are finite if and only if $\log|v_i|$ remains finite, namely if

$$\lim_{N\to\infty} \log|v_i| = \lim_{N\to\infty} (2N-2)\log d_i + \sum_{\substack{j=2 \\ j\neq i}}^{N} \log\left(\frac{1-d_j^2}{|d_i^2 - d_j^2|}\right) \tag{C.2}$$

is finite. The first term on the rhs of (C.2) for sufficiently large N becomes:

$$(2N-2)\log d_i = (2N-2)\log\left(1 - \frac{(i-1)^\alpha}{N^\beta}\right) \sim -2(i-1)^\alpha N^{1-\beta} \tag{C.3}$$

and hence goes to zero provided that $\beta > 1$. The sum in (C.2) for large N can be rewritten

as:

$$\sum_{\substack{j=2\\j\neq i}}^{N} \log(j-1)^{\alpha} - \log|(j-1)^{\alpha} - (i-1)^{\alpha}| = -\sum_{\substack{j=2\\j\neq i}}^{N} \log\left|1 - \frac{(i-1)^{\alpha}}{(j-1)^{\alpha}}\right| \tag{C.4}$$

and then for $j >> i$ the asymptotic part of this sum becomes

$$(i-1)^{\alpha} \sum_{j>>i}^{N} (j-1)^{-\alpha} \sim \frac{(i-1)^{\alpha}}{\alpha} N^{-\alpha-1} + const \tag{C.5}$$

which is finite provided that $\alpha > -1$. Therefore the limit (C.1) with $0 < \alpha < \beta$ is finite for each fixed i provided that $\beta > 1$.

C.2 An alternative construction

The distance distribution (6.46) is the only one we have found that gives rise to a physically sensible solution in the limit $N \to \infty$ for the construction of Section 6.3.1. As mentioned in Section 6.3.1, after fixing the centers $g_{\pm 1}$ with (6.44) one can add the other centers externally with respect to these two, namely choosing $d_i > d_j > 1$ for $i > j > 1$. Then arranging the $2N$ centers on a line imposing (6.41) and (6.42) and requiring the derivatives of V up to order $2N-2$ to vanish at the origin uniquely fixes the v_i's as functions of the d_i's:

$$|v_i| = (1+d_i)^{2N-2} \prod_{\substack{j=1\\j\neq i}}^{N} \frac{d_j(2+d_j)}{|d_i(2+d_i) - d_j(2+d_j)|} \tag{C.6}$$

and the sign of each v_i is determined according to (6.42). We studied the solution in the limit for $N \to \infty$ using different distance distributions d_i's. For instance, one can arrange the centers to be equally spaced on the axis, to accumulate close to a point or within an interval or to reach infinite distance with different spacings. We always find that $Q \to \infty$ for $N \to \infty$. The same happens inserting the GH centers internally using (6.45) with distance distributions different from (6.46). We believe that the reason for this lies on the fact that each $|v_i|$ grows exponentially when one adds more and more centers. The distance distribution (6.46) with (6.45) is the only we have found that keeps the v_i's finite in the limit, as shown in Figure 6.3.

BIBLIOGRAPHY

[1] H. Lin, O. Lunin, and J. M. Maldacena, *Bubbling AdS space and 1/2 BPS geometries*, *JHEP* **10** (2004) 025, [hep-th/0409174].

[2] I. Bena and N. P. Warner, *One ring to rule them all ... and in the darkness bind them?*, *Adv. Theor. Math. Phys.* **9** (2005) 667–701, [hep-th/0408106].

[3] P. Berglund, E. G. Gimon, and T. S. Levi, *Supergravity microstates for BPS black holes and black rings*, *JHEP* **06** (2006) 007, [hep-th/0505167].

[4] I. R. Klebanov and M. J. Strassler, *Supergravity and a confining gauge theory: Duality cascades and chi SB resolution of naked singularities*, *JHEP* **08** (2000) 052, [hep-th/0007191].

[5] E. Cremmer, B. Julia, and J. Scherk, *Supergravity Theory in Eleven-Dimensions*, *Phys. Lett.* **B76** (1978) 409–412.

[6] J. P. Gauntlett, *Intersecting branes*, in *Dualities in gauge and string theories. Proceedings, APCTP Winter School, Sorak Mountain Resort, Seoul, Sokcho, Korea, February 17-28, 1997*, 1997. hep-th/9705011.

[7] J. Polchinski, *String theory. Vol. 1: An introduction to the bosonic string.* Cambridge University Press, 2007.

[8] J. Polchinski, *String theory. Vol. 2: Superstring theory and beyond.* Cambridge University Press, 2007.

[9] A. W. Peet, *TASI lectures on black holes in string theory*, in *Strings, branes and gravity. Proceedings, Theoretical Advanced Study Institute, TASI'99, Boulder, USA, May 31-June 25, 1999*, pp. 353–433, 2000. hep-th/0008241.

[10] R. Gopakumar and C. Vafa, *On the gauge theory / geometry correspondence*, *Adv. Theor. Math. Phys.* **3** (1999) 1415–1443, [hep-th/9811131].

[11] C. Vafa, *Superstrings and topological strings at large N*, *J. Math. Phys.* **42** (2001) 2798–2817, [hep-th/0008142].

[12] S. Massai, G. Pasini, and A. Puhm, *Metastability in Bubbling AdS Space*, *JHEP* **02** (2015) 138, [arXiv:1407.6007].

[13] I. Bena and G. Pasini, *Instabilities of microstate geometries with antibranes*, *JHEP* **04** (2016) 181, [arXiv:1511.0189].

[14] S. Kachru, R. Kallosh, A. D. Linde, and S. P. Trivedi, *De Sitter vacua in string theory*, *Phys. Rev.* **D68** (2003) 046005, [hep-th/0301240].

[15] G. Pasini, *Type IIA Klebanov-Strassler: the hard way*, *JHEP* **03** (2016) 178, [arXiv:1511.0668].

[16] G. Pasini and C. S. Shahbazi, *Five-dimensional null and time-like supersymmetric geometries*, *Class. Quant. Grav.* **33** (2016), no. 17 175003, [arXiv:1512.0221].

[17] J. P. Gauntlett, J. B. Gutowski, C. M. Hull, S. Pakis, and H. S. Reall, *All supersymmetric solutions of minimal supergravity in five- dimensions*, *Class. Quant. Grav.* **20** (2003) 4587–4634, [hep-th/0209114].

[18] S. Cheon, H.-C. Kim, and S. Kim, *Holography of mass-deformed M2-branes*, arXiv:1101.1101.

[19] I. Bena and N. P. Warner, *Bubbling supertubes and foaming black holes*, *Phys. Rev.* **D74** (2006) 066001, [hep-th/0505166].

[20] B. Bates and F. Denef, *Exact solutions for supersymmetric stationary black hole composites*, *JHEP* **11** (2011) 127, [hep-th/0304094].

[21] I. Bena, C.-W. Wang, and N. P. Warner, *Mergers and typical black hole microstates*, *JHEP* **11** (2006) 042, [hep-th/0608217].

[22] I. R. Klebanov and A. A. Tseytlin, *Gravity duals of supersymmetric SU(N) x SU(N+M) gauge theories*, *Nucl. Phys.* **B578** (2000) 123–138, [hep-th/0002159].

[23] P. Candelas and X. C. de la Ossa, *Comments on Conifolds*, *Nucl. Phys.* **B342** (1990) 246–268.

[24] R. Minasian and D. Tsimpis, *On the geometry of nontrivially embedded branes*, *Nucl. Phys.* **B572** (2000) 499–513, [hep-th/9911042].

[25] N. Seiberg, *Electric - magnetic duality in supersymmetric nonAbelian gauge theories*, *Nucl. Phys.* **B435** (1995) 129–146, [hep-th/9411149].

[26] I. Bena, *The M theory dual of a three-dimensional theory with reduced supersymmetry*, *Phys.Rev.* **D62** (2000) 126006, [hep-th/0004142].

[27] J. Polchinski and M. J. Strassler, *The String dual of a confining four-dimensional gauge theory*, hep-th/0003136.

[28] I. Bena and N. P. Warner, *A Harmonic family of dielectric flow solutions with maximal supersymmetry*, *JHEP* **0412** (2004) 021, [hep-th/0406145].

[29] C. P. Herzog, "String Tensions and Three Dimensional Confining Gauge Theories." Phys.Rev. D66 (2002) 065009, 2002.

[30] I. R. Klebanov and S. S. Pufu, *M-Branes and Metastable States*, *JHEP* **1108** (2011) 035, [arXiv:1006.3587].

[31] A. Hashimoto, *Comments on domain walls in holographic duals of mass deformed conformal field theories*, *JHEP* **1107** (2011) 031, [arXiv:1105.3687].

[32] P. Pasti, D. P. Sorokin, and M. Tonin, *Covariant action for a D = 11 five-brane with the chiral field*, *Phys.Lett.* **B398** (1997) 41–46, [hep-th/9701037].

[33] I. Bena, M. Grana, S. Kuperstein, and S. Massai, *Tachyonic Anti-M2 Branes*, *JHEP* **06** (2014) 173, [arXiv:1402.2294].

[34] D. Z. Freedman and J. A. Minahan, *Finite temperature effects in the supergravity dual of the N=1* gauge theory*, *JHEP* **0101** (2001) 036, [hep-th/0007250].

[35] M. Taylor, *Anomalies, counterterms and the N=0 Polchinski-Strassler solutions*, hep-th/0103162.

[36] I. Bena, N. Bobev, C. Ruef, and N. P. Warner, *Supertubes in Bubbling Backgrounds: Born-Infeld Meets Supergravity*, *JHEP* **07** (2009) 106, [arXiv:0812.2942].

[37] I. Bena, A. Puhm, O. Vasilakis, and N. P. Warner, *Almost BPS but still not renormalized*, *JHEP* **1309** (2013) 062, [arXiv:1303.0841].

[38] R. C. Myers, *Dielectric branes*, *JHEP* **9912** (1999) 022, [hep-th/9910053].

[39] S. Kachru, J. Pearson, and H. L. Verlinde, *Brane / flux annihilation and the string dual of a nonsupersymmetric field theory*, *JHEP* **06** (2002) 021, [hep-th/0112197].

[40] V. Borokhov and S. S. Gubser, *Nonsupersymmetric deformations of the dual of a confining gauge theory*, *JHEP* **0305** (2003) 034, [hep-th/0206098].

[41] I. Bena, G. Giecold, M. Grana, N. Halmagyi, and S. Massai, *The backreaction of anti-D3 branes on the Klebanov-Strassler geometry*, *JHEP* **06** (2013) 060, [arXiv:1106.6165].

[42] I. Bena, M. Grana, S. Kuperstein, and S. Massai, *Polchinski-Strassler does not uplift Klebanov-Strassler*, *JHEP* **1309** (2013) 142, [arXiv:1212.4828].

[43] I. Bena, A. Puhm, and B. Vercnocke, *Metastable Supertubes and non-extremal Black Hole Microstates*, *JHEP* **04** (2012) 100, [arXiv:1109.5180].

[44] I. Bena, A. Puhm, and B. Vercnocke, *Non-extremal Black Hole Microstates: Fuzzballs of Fire or Fuzzballs of Fuzz ?*, *JHEP* **12** (2012) 014, [arXiv:1208.3468].

[45] A. Strominger and C. Vafa, *Microscopic origin of the Bekenstein-Hawking entropy*, *Phys. Lett.* **B379** (1996) 99–104, [hep-th/9601029].

[46] S. D. Mathur, *The Fuzzball proposal for black holes: An Elementary review*, *Fortsch.Phys.* **53** (2005) 793–827, [hep-th/0502050].

[47] K. Skenderis and M. Taylor, *The fuzzball proposal for black holes*, *Phys.Rept.* **467** (2008) 117–171, [arXiv:0804.0552].

[48] V. Jejjala, O. Madden, S. F. Ross, and G. Titchener, *Non-supersymmetric smooth geometries and D1-D5-P bound states*, *Phys. Rev.* **D71** (2005) 124030, [hep-th/0504181].

[49] S. Giusto, S. F. Ross, and A. Saxena, *Non-supersymmetric microstates of the D1-D5-KK system*, *JHEP* **12** (2007) 065, [arXiv:0708.3845].

[50] J. H. Al-Alawi and S. F. Ross, *Spectral Flow of the Non-Supersymmetric Microstates of the D1-D5-KK System*, *JHEP* **10** (2009) 082, [arXiv:0908.0417].

[51] S. Banerjee, B. D. Chowdhury, B. Vercnocke, and A. Virmani, *Non-supersymmetric Microstates of the MSW System*, *JHEP* **05** (2014) 011, [arXiv:1402.4212].

[52] G. Bossard and S. Katmadas, *Floating JMaRT*, *JHEP* **04** (2015) 067, [arXiv:1412.5217].

[53] I. Bena, S. Giusto, C. Ruef, and N. P. Warner, *A (Running) Bolt for New Reasons*, *JHEP* **11** (2009) 089, [arXiv:0909.2559].

[54] G. Bossard and S. Katmadas, *A bubbling bolt*, *JHEP* **07** (2014) 118, [arXiv:1405.4325].

[55] D. Mateos and P. K. Townsend, *Supertubes*, *Phys. Rev. Lett.* **87** (2001) 011602, [hep-th/0103030].

[56] G. W. Gibbons and N. P. Warner, *Global structure of five-dimensional fuzzballs*, *Class. Quant. Grav.* **31** (2014) 025016, [arXiv:1305.0957].

[57] P. A. Haas, *Smarr's Formula in Eleven-Dimensional Supergravity*, arXiv:1405.3708.

[58] P. de Lange, D. R. Mayerson, and B. Vercnocke, *Structure of Six-Dimensional Microstate Geometries*, *JHEP* **09** (2015) 075, [arXiv:1504.0798].

[59] V. Cardoso, O. J. C. Dias, J. L. Hovdebo, and R. C. Myers, *Instability of non-supersymmetric smooth geometries*, *Phys. Rev.* **D73** (2006) 064031, [hep-th/0512277].

[60] S. G. Avery. Private communication.

[61] B. D. Chowdhury and S. D. Mathur, *Radiation from the non-extremal fuzzball*, *Class. Quant. Grav.* **25** (2008) 135005, [arXiv:0711.4817].

[62] S. G. Avery, B. D. Chowdhury, and S. D. Mathur, *Emission from the D1D5 CFT*, *JHEP* **10** (2009) 065, [arXiv:0906.2015].

[63] B. Chakrabarty, D. Turton, and A. Virmani, *Holographic description of non-supersymmetric orbifolded D1-D5-P solutions*, *JHEP* **11** (2015) 063, [arXiv:1508.0123].

[64] B. D. Chowdhury and S. D. Mathur, *Non-extremal fuzzballs and ergoregion emission*, *Class. Quant. Grav.* **26** (2009) 035006, [arXiv:0810.2951].

[65] C. G. Callan and J. M. Maldacena, *D-brane approach to black hole quantum mechanics*, *Nucl. Phys.* **B472** (1996) 591–610, [hep-th/9602043].

[66] I. Bena, C.-W. Wang, and N. P. Warner, *Plumbing the Abyss: Black ring microstates*, *JHEP* **07** (2008) 019, [arXiv:0706.3786].

[67] I. Bena, M. Shigemori, and N. P. Warner, *Black-Hole Entropy from Supergravity Superstrata States*, *JHEP* **10** (2014) 140, [arXiv:1406.4506].

[68] J. C. Breckenridge, R. C. Myers, A. W. Peet, and C. Vafa, *D-branes and spinning black holes*, *Phys. Lett.* **B391** (1997) 93–98, [hep-th/9602065].

[69] I. Bena, C.-W. Wang, and N. P. Warner, *The Foaming three-charge black hole*, *Phys. Rev.* **D75** (2007) 124026, [hep-th/0604110].

[70] V. Balasubramanian, E. G. Gimon, and T. S. Levi, *Four Dimensional Black Hole Microstates: From D-branes to Spacetime Foam*, *JHEP* **01** (2008) 056, [hep-th/0606118].

[71] I. Bena and N. P. Warner, *Black holes, black rings and their microstates*, *Lect. Notes Phys.* **755** (2008) 1–92, [hep-th/0701216].

[72] M. Cvetic and D. Youm, *General rotating five-dimensional black holes of toroidally compactified heterotic string*, *Nucl. Phys.* **B476** (1996) 118–132, [hep-th/9603100].

[73] S. H. Shenker and D. Stanford, *Black holes and the butterfly effect*, *JHEP* **03** (2014) 067, [arXiv:1306.0622].

[74] I. Bena, B. D. Chowdhury, J. de Boer, S. El-Showk, and M. Shigemori, *Moulting Black Holes*, *JHEP* **03** (2012) 094, [arXiv:1108.0411].

[75] B. D. Chowdhury and B. Vercnocke, *New instability of non-extremal black holes: spitting out supertubes*, *JHEP* **02** (2012) 116, [arXiv:1110.5641].

[76] I. Bena, M. Grana, and N. Halmagyi, *On the Existence of Meta-stable Vacua in Klebanov-Strassler*, *JHEP* **09** (2010) 087, [arXiv:0912.3519].

[77] I. Bena, M. Grana, S. Kuperstein, and S. Massai, *Giant Tachyons in the Landscape*, *JHEP* **02** (2015) 146, [arXiv:1410.7776].

[78] I. Bena, M. Grana, S. Kuperstein, and S. Massai, *Anti-D3 Branes: Singular to the bitter end*, *Phys. Rev.* **D87** (2013), no. 10 106010, [arXiv:1206.6369].

[79] I. Bena, G. Giecold, M. Grana, N. Halmagyi, and S. Massai, *On Metastable Vacua and the Warped Deformed Conifold: Analytic Results*, *Class. Quant. Grav.* **30** (2013) 015003, [arXiv:1102.2403].

[80] I. Bena, A. Buchel, and O. J. C. Dias, *Horizons cannot save the Landscape*, *Phys. Rev.* **D87** (2013), no. 6 063012, [arXiv:1212.5162].

[81] J. Blaback, U. H. Danielsson, D. Junghans, T. Van Riet, and S. C. Vargas, *Localised anti-branes in non-compact throats at zero and finite T*, *JHEP* **02** (2015) 018, [arXiv:1409.0534].

[82] S. S. Gubser, *Curvature singularities: The Good, the bad, and the naked*, *Adv. Theor. Math. Phys.* **4** (2000) 679–745, [hep-th/0002160].

[83] J. Blaback, U. H. Danielsson, D. Junghans, T. Van Riet, T. Wrase, and M. Zagermann, *Smeared versus localised sources in flux compactifications*, *JHEP* **12** (2010) 043, [arXiv:1009.1877].

[84] J. Blaback, U. H. Danielsson, D. Junghans, T. Van Riet, T. Wrase, and M. Zagermann, *The problematic backreaction of SUSY-breaking branes*, *JHEP* **08** (2011) 105, [arXiv:1105.4879].

[85] D. Cohen-Maldonado, J. Diaz, T. Van Riet, and B. Vercnocke, *Observations on fluxes near anti-branes*, arXiv:1507.0102.

[86] U. H. Danielsson and T. Van Riet, *Fatal attraction: more on decaying anti-branes*, *JHEP* **03** (2015) 087, [arXiv:1410.8476].

[87] B. Michel, E. Mintun, J. Polchinski, A. Puhm, and P. Saad, *Remarks on brane and antibrane dynamics*, *JHEP* **09** (2015) 021, [arXiv:1412.5702].

[88] R. Minasian and D. Tsimpis, *Hopf reductions, fluxes and branes*, *Nucl. Phys.* **B613** (2001) 127–146, [hep-th/0106266].

[89] K. Dasgupta, K.-h. Oh, J. Park, and R. Tatar, *Geometric transition versus cascading solution*, *JHEP* **01** (2002) 031, [hep-th/0110050].

[90] K. Ohta and T. Yokono, *Deformation of conifold and intersecting branes*, *JHEP* **02** (2000) 023, [hep-th/9912266].

[91] D. Kutasov and A. Wissanji, *IIA Perspective On Cascading Gauge Theory*, *JHEP* **09** (2012) 080, [arXiv:1206.0747].

[92] S. Elitzur, A. Giveon, and D. Kutasov, *Branes and N=1 duality in string theory*, *Phys. Lett.* **B400** (1997) 269–274, [hep-th/9702014].

[93] A. Giveon and D. Kutasov, *Brane dynamics and gauge theory*, *Rev. Mod. Phys.* **71** (1999) 983–1084, [hep-th/9802067].

[94] K. Dasgupta and S. Mukhi, *Brane constructions, fractional branes and Anti-de Sitter domain walls*, *JHEP* **07** (1999) 008, [hep-th/9904131].

[95] K. Dasgupta and S. Mukhi, *Brane constructions, conifolds and M theory*, *Nucl. Phys.* **B551** (1999) 204–228, [hep-th/9811139].

[96] S. S. Gubser and I. R. Klebanov, *Baryons and domain walls in an N=1 superconformal gauge theory*, *Phys. Rev.* **D58** (1998) 125025, [hep-th/9808075].

[97] M. Bershadsky, C. Vafa, and V. Sadov, *D strings on D manifolds*, *Nucl. Phys.* **B463** (1996) 398–414, [hep-th/9510225].

[98] A. M. Uranga, *Brane configurations for branes at conifolds*, *JHEP* **01** (1999) 022, [hep-th/9811004].

[99] J. McOrist and A. B. Royston, *Relating Conifold Geometries to NS5-branes*, *Nucl. Phys.* **B849** (2011) 573–609, [arXiv:1101.3552].

[100] J. McOrist and A. B. Royston, *T-dualising the Deformed and Resolved Conifold*, *Class. Quant. Grav.* **29** (2012) 055014, [arXiv:1107.5895].

[101] E. Witten, *Branes and the dynamics of QCD*, *Nucl. Phys. Proc. Suppl.* **68** (1998) 216–239.

[102] C. P. Herzog, I. R. Klebanov, and P. Ouyang, *Remarks on the warped deformed conifold*, in *Modern Trends in String Theory: 2nd Lisbon School on g Theory Superstrings Lisbon, Portugal, July 13-17, 2001*, 2001. hep-th/0108101.

[103] C. Krishnan and S. Kuperstein, *The Mesonic Branch of the Deformed Conifold*, *JHEP* **05** (2008) 072, [arXiv:0802.3674].

[104] S. Mizoguchi and N. Ohta, *More on the similarity between D = 5 simple supergravity and M theory*, *Phys. Lett.* **B441** (1998) 123–132, [hep-th/9807111].

[105] J. P. Gauntlett and J. B. Gutowski, *All supersymmetric solutions of minimal gauged supergravity in five-dimensions*, *Phys.Rev.* **D68** (2003) 105009, [hep-th/0304064].

[106] J. Bellorin, P. Meessen, and T. Ortin, *All the supersymmetric solutions of N=1,d=5 ungauged supergravity*, *JHEP* **0701** (2007) 020, [hep-th/0610196].

[107] J. Bellorin and T. Ortin, *Characterization of all the supersymmetric solutions of gauged N=1, d=5 supergravity*, *JHEP* **08** (2007) 096, [arXiv:0705.2567].

[108] I. Bena, S. F. Ross, and N. P. Warner, *On the Oscillation of Species*, *JHEP* **09** (2014) 113, [arXiv:1312.3635].

[109] S. D. Mathur and D. Turton, *Oscillating supertubes and neutral rotating black hole microstates*, *JHEP* **04** (2014) 072, [arXiv:1310.1354].

[110] C.-I. Lazaroiu, E.-M. Babalic, and I.-A. Coman, *Geometric algebra techniques in flux compactifications (I)*, arXiv:1212.6766.

[111] C.-I. Lazaroiu and E.-M. Babalic, *Geometric algebra techniques in flux compactifications (II)*, *JHEP* **06** (2013) 054, [arXiv:1212.6918].

[112] C. I. Lazaroiu, E. M. Babalic, and I. A. Coman, *The geometric algebra of Fierz identities in arbitrary dimensions and signatures*, *JHEP* **09** (2013) 156, [arXiv:1304.4403].

[113] C. L. M. Babalic and C. S. Shahbazi, *The reconstruction theorem for generalized constrained killing pinors*, *In preparation* (2015).

[114] C. L. M. Babalic and C. S. Shahbazi, *Pin foliations on four-manifolds*, *In preparation* (2015).

[115] J. de Boer, F. Denef, S. El-Showk, I. Messamah, and D. Van den Bleeken, *Black hole bound states in AdS(3) x S**2*, *JHEP* **11** (2008) 050, [arXiv:0802.2257].

[116] I. Bena, N. Bobev, S. Giusto, C. Ruef, and N. P. Warner, *An Infinite-Dimensional Family of Black-Hole Microstate Geometries*, *JHEP* **03** (2011) 022, [arXiv:1006.3497]. [Erratum: JHEP04,059(2011)].

université PARIS-SACLAY
ÉCOLE DOCTORALE
Physique en île-de-France (EDPIF)

Title : Black holes and bubbled solutions in String Theory

Keywords : black holes, String Theory, smooth solutions, supergravity, microstates

Abstract : There exist many smooth solutions in String Theory characterized by a nontrivial topology threaded by fluxes and no localized sources. In this thesis we analyze some of the most important bubbled solutions along with the different purposes they are studied for.
Some smooth, eleven-dimensional solutions can be interpreted as BPS black hole microstates in the context of the Fuzzball proposal. One can promote these to be microstates for near-BPS black holes by placing probe supertubes at a metastable minimum inside these solutions. We show that these minima can lower their energy when the bubbles move in certain directions in the moduli space, which implies that these near-BPS microstates are in fact unstable. The decay of these solutions corresponds to Hawking radiation and we compare the emission rate and frequency to those of the corresponding black hole.
By modifying the asymptotic behavior of these microstates one could be able to construct microstates for five-dimensional BPS black rings with no electric charge. To do so one needs to find a new supergravity solution in five-dimensions whose Killing vector switches from timelike to null in some open regions. We construct explicit examples where the norm of the supersymmetric Killing vector is a real not-everywhere analytic function such that all its derivatives vanish at a point where the Killing vector becomes null.
In the Lin-Lunin-Maldacena solution we find a supersymmetry-breaking mechanism similar to that used for near-BPS microstates. We analyze the potential energy of M2 probes polarized into M5 brane shells. When the charges of the probe are parallel to those of the solution we find stable configurations, while when the charges are opposite we find metastable states that break supersymmetry and analyze the decay process to supersymmetric configurations.
We analyze also the Klebanov-Strassler solution and construct its T-dual in Type IIA. This is done by just reconstructing the solution expanded on a small region of the deformed conifold, after a thorough analysis to choose the most suitable isometry. Our construction is the first step in a program to test the stability of antibranes in Type IIA backgrounds.

Titre : Trous noirs et solutions régulières en Théorie des Cordes

Mots clefs : trous noirs, Théorie des Cordes, solutions régulières, supergravité, microétats

Résumé : Il existe des nombreuses solutions lisses dans le domaine de la thèorie des cordes, caractérisées par une topologie non triviale (bulles) et sans sources localisées. Dans cette thèse nous analysons quelques-unes parmi les solutions les plus importantes avec les différents objectifs pour lesquels ils sont étudiées.
Des solutions lisses en onze dimensions peuvent être interprétées comme microétats BPS de trous noirs dans le cadre de la *Fuzzball proposal*. On peut promouvoir ces microétats à être quasi-BPS en plaçant de supertubes dans un minimum métastable à l'intérieur de ces solutions. Nous montrons que ces minima peuvent abaisser leur énergie lorsque les bulles se déplacent dans certaines directions dans l'espace des modules, ce qui implique que ces microétats quasi-BPS sont en fait instables. L'énergie dissipée par ces solutions correspond au rayonnement Hawking et on compare le taux d'émission et la fréquence à celles du trou noir correspondant.
En modifiant la géométrie asymptotique de ces microétats on pourrait construire des microétats pour des trous noirs BPS sans charge électrique en cinq dimensions. Il faut donc trouver une nouvelle solution de supergravité en cinq dimensions dont la norme du vecteur de Killing passe de positive à nulle dans certaines régions. Nous construisons des exemples explicites où la norme du vecteur de Killing supersymétrique est une fonction réelle non-analytique telle que tous ses dérivés sont nulles à un point où le vecteur de Killing devient nul.
Dans la solution de Lin-Lunin-Maldacena on trouve un mécanisme pour briser la supersymétrie similaire à celui utilisé pour les microétats quasi-BPS. Nous analysons l'énergie potentielle des branes M2 polarisées en branes M5. Lorsque les charges des branes M2 sont parallèles à ceux de la solution, nous trouvons des configurations stables. Lorsque les charges des branes M2 ne sont pas parallèles, nous trouvons des états métastables qui brisent la supersymétrie et nous analysons le processus de rayonnement d'énergie.
Nous analysons aussi la solution de Klebanov-Strassler et construisons sa version T-duale dans la supergravité de type IIA. Pour cela une analyse approfondie est nécessaire pour choisir l'isométrie la plus appropriée. Notre construction est la première étape d'un programme pour tester la stabilité des antibranes dans la supergravité de type IIA.

Université Paris-Saclay
Espace Technologique / Immeuble Discovery
Route de l'Orme aux Merisiers RD 128 / 91190 Saint-Aubin, France